ҚАЗАҚСТАН РЕСПУБЛИКАСЫ
ҒЫЛЫМ ЖӘНЕ ЖОҒАРЫ БІЛІМ МИНИСТРЛІГІ
SATBAYEV UNIVERSITY
МЕТАЛЛУРГИЯ ЖӘНЕ КЕН БАЙЫТУ ИНСТИТУТЫ

ISSN 2616-6445 (Online)
ISSN 2224-5243 (Print)
DOI 10.31643/2018/166445

Минералдық шикізаттарды кешенді пайдалану

1(340)

Комплексное Использование Минерального Сырья

Complex Use of Mineral Resources

ҚАҢТАР-НАУРЫЗ 2027
JANUARY – MARCH 2027
ЯНВАРЬ - МАРТ 2027

ЖЫЛЫНА 4 РЕТ ШЫҒАДЫ
QUARTERLY JOURNAL
ВЫХОДИТ 4 РАЗА В ГОД

ЖУРНАЛ 1978 ЖЫЛДАН БАСТАП ШЫҒАДЫ
JOURNAL HAS BEEN PUBLISHING SINCE 1978
ЖУРНАЛ ИЗДАЕТСЯ С 1978 ГОДА

АЛМАТЫ - 2027

Редакция мекен жайы:
«Металлургия және кен байыту институты» АҚ
050010, Қазақстан Республикасы, Алматы қ., Шевченко к-сі, Уәлиханов к-нің қиылысы, 29/133,
Fax. +7 (727) 298-45-03, Tel. +7-(727) 298-45-02, +7 (727) 298-45-19
E mail: journal@kims-imio.kz, product-service@kims-imio.kz
http://kims-imio.com/index.php/main

«Минералдық шикізаттарды кешенді пайдалану» журналы ғылыми жұмыстардың негізгі нәтижелерін жариялау үшін Қазақстан Республикасы Білім және ғылым министірлігінің Білім және ғылым сапасын қамтамасыз ету комитеті ұсынған ғылыми басылымдар тізіміне енгізілген.
Меншік иесі: «Металлургия және кен байыту институты» АҚ

Журнал Қазақстан Республикасының Ақпарат және коммуникация министрлігінің Байланыс, ақпараттандыру және бұқаралық ақпарат құралдары саласындағы мемлекеттік бақылау комитетінде қайта тіркелген

2016 ж. 18 қазандағы № 16180-Ж Куәлігі

Address:
"Institute of Metallurgy and Ore Beneficiation" JSC
29/133 Shevchenko Street, corner of Ch. Valikhanov Street, Almaty, 050010, Kazakhstan
Fax. +7 (727) 298-45-03, Tel. +7-(727) 298-45-02, +7 (727) 298-45-19
E mail: journal@kims-imio.kz, product-service@kims-imio.kz
http://kims-imio.com/index.php/main

The Journal "Complex Use of Mineral Resources" is included in the List of publications recommended by the Committee for Control in the Sphere of Education and Science of the Ministry of Education and Science of the Republic of Kazakhstan for the publication of the main results of scientific activities.
Owner: "Institute of Metallurgy and Ore Beneficiation" JSC

The Journal was re-registered by the Committee for State Control in the Sphere of Communication, Information and Mass Media of the Ministry of Information and Communication of the Republic of Kazakhstan.

Certificate № 16180-Ж since October 18, 2016

Адрес редакции:
АО «Институт металлургии и обогащения»
050010, Республика Казахстан, г. Алматы, ул. Шевченко, уг. ул. Валиханова, 29/133,
Fax. +7 (727) 298-45-03, Tel. +7 (727) 298-45-02, +7 (727) 298-45-19
E mail: journal@kims-imio.kz, product-service@kims-imio.kz
http://kims-imio.com/index.php/main

Журнал «Комплексное использование минерального сырья» включен в Перечень изданий, рекомендуемых Комитетом по контролю в сфере образования и науки Министерства образования и науки Республики Казахстан для публикации основных результатов научной деятельности.
Собственник: АО «Институт металлургии и обогащения»

Журнал перерегистрирован в Комитете государственного контроля в области связи, информатизации и средств массовой информации
Министерства информации и коммуникации Республики Казахстан
Свидетельство № 16180-Ж от 18 октября 2016 г.

Crossref
DOI: 10.31643/2027/6445.01
Engineering and Technology
IRSTI 67.09.33

Influence of additives and temperature regime on the setting kinetics and strength of foamed concrete

Sartaev D.T., *Orynbekov Y.S., Baisarieva A.M., Uxikbayeva D.A.

LLP International Educational Corporation, Almaty, Kazakhstan

** Corresponding author email: orynbekov.savenergy@gmail.com*

Received: *March 19, 2025*
Peer-reviewed: *April 2, 2025*
Accepted: *August 25, 2025*

ABSTRACT
The article presents the results of the development of the physico-mechanical characteristics of fast-setting lightweight concrete. Based on the obtained data, it was concluded that the use of metal cassette molds in foam concrete technology is ineffective. Their turnover can be increased by heating the floor in the workshop and insulating the sides and surfaces of the molds. However, the high cost of energy carriers increases the material's production cost and reduces its competitiveness. At ambient temperatures below 16 °C, it is advisable to use insulated wooden molds, which help retain the heat released during cement hydration. The optimal mold dimensions (1.2 × 1.25 × 0.5 m and 1.2 × 1.25 × 0.6 m) were selected based on cutting technology capabilities. The formation of large monolithic masses is associated with the risk of cracks and even structural rupture due to uneven heat distribution. To maintain the initial mix temperature within 22 – 25 °C, the molding mixture should be prepared using water heated to 30 °C. In insulated wooden molds, the formed material retains a temperature of at least 18 – 20 °C before the onset of hydration. Then, due to the exothermic reaction of cement, the temperature remains stable until demolding. Improvements in natural-setting foam concrete technology have demonstrated the feasibility of introducing a chemically active siliceous component into the mixture. This component binds free $Ca(OH)_2$ released during alite hydration, contributing to long-term strength development. *Research objective* – The development of effective methods to accelerate the early-stage hardening of foamed concrete by studying the influence of electrolyte additives and surfactants on the setting and hardening processes of cement paste. *The novelty of work* lies in establishing patterns in the formation of physical and mechanical properties of foamed concrete with accelerated initial hardening, taking into account its porous structure, and the characteristics of the hardening process.

Keywords: Foam concrete, fast-hardening, lightweight concrete, additives, temperature, ash, waste.

Information about authors:

Sartaev D.T. *Candidate of technical sciences, Associate research professor, LLP International Educational Corporation, 50043, Ryskulbekov str. 28, Almaty, Kazakhstan. Email: sartayev.dake@gmail.com; ORCID ID: https://orcid.org/0000-0002-2817-0955*

Orynbekov Y.S. *Candidate of technical sciences, Associate research professor, LLP International Educational Corporation, 50043, Ryskulbekov str. 28, Almaty, Kazakhstan. Email: orynbekov.savenergy@gmail.com; ORCID ID: https://orcid.org/0000-0003-2131-6293*

Baisarieva A.M. *Associate professor, LLP International Educational Corporation, 50043, Ryskulbekov str. 28, Almaty, Kazakhstan. Email: abajsarieva@mail.ru; ORCID ID: https://orcid.org/0000-0002-7473-8820*

Uxikbayeva D.A. *Master of Technical Sciences, Tutor, LLP International Educational Corporation, 50043, Ryskulbekov str. 28, Almaty, Kazakhstan. Email: dayana.uxikbayeva@mail.ru; ORCID ID: https://orcid.org/0009-0006-3189-933X*

Introduction

Rapid-hardening foamed concrete is a promising building material that combines low destiny, high thermal insulation properties, and accelerated strength development [[1], [2], [3], [4], [5], [6]].

These characteristics make it highly sought for the construction of enclosing structures, thermal insulation layers, and prefabricated elements [[7], [8], [9], [10], [11]].

This study is dedicated to the analysis of key physical and mechanical characteristics of foamed concrete with accelerated initial hardening, the identification of patterns in their formation, and the development of recommendations for optimizing the composition to improve the strength and thermal insulation properties of the material [[3], [12], [13], [14], [15]]. Special attention is given to the composition of raw materials, porous structure, and the hydration processes of cement stone [[11], [16], [17]].

This study focuses on analyzing the key physical and mechanical characteristics of fast-setting lightweight foam concrete, identifying patterns in their formation, and developing recommendations for optimizing the composition to improve strength and thermal insulation properties [[12], [13], [14], [15]].

Foam concrete production has shown growth trend, and it is widely used for wall construction alongside ceramic bricks, aerated concrete, and hollow blocks made of heavy concrete [[18], [19], [20], [21], [22], [23]]. However, the overall production volume of foam concrete blocks remains significantly lower compared to aerated concrete and ceramic bricks. One of the main limiting factors is the low productivity of foam concrete block production lines due to the turnaround time of the molds. A considerable amount of time is required for foam concrete to gain sufficient strength for demolding [[6], [18], [19], [20], [21], [22]].

The analysis of scientific and technical literature has shown that research on accelerating the hardening of foam concrete is being conducted in two main directions:

- the first involves the setting and hardening time of the cement binder [[23], [24], [25]];

- the second focuses on the use of technological methods and additives directly during the concrete preparation process [[7], [9], [26], [27]].

In concrete technology, including foam concrete, the most commonly used method for accelerating hardening is the introduction of chemical additives. However, unlike heavy concrete, foam concrete has less dense structure and is saturated with water and surfactant molecules from the foaming agents. There are no universal and reliable recommendations for ensuring the accelerated hardening of foam-cement system [[11], [17]]. Conventional additives, such as superplasticizers and calcium chloride, which effectively reduce water demand and speed up hardening in traditional concrete, either do not work in foam concrete or even reduce its strength (as in the case superplasticizers) or fail to produce any significant practical results.

Research objective: The development of effective methods to accelerate the early-stage hardening of foamed concrete by studying the influence of electrolyte additives and surfactants on the setting and hardening processes of cement paste.

The novelty of work lies in establishing patterns in the formation of physical and mechanical properties of foamed concrete with accelerated initial hardening, taking into account its porous structure, and the characteristics of the hardening process.

Experimental part

Materials. In the research, the following raw materials were used:

- portland cements of grade CEM I 32.5N from manufacturers Heidelberg (Ust – Kamenogorsk) and Standard Cement и Standard Cement (Shymkent), produced at cement plants and complying with the requirements of GOST 10178 – 85;

- quartz-feldspar sand from the Kapchagay deposit (Almaty region), with a fineness modulus of 1.48, a silica (SiO_2) content of 37 %, feldspar content of 60.1 %, mica content of 1 %, dust and clay particle content of 1.9 %;

- fly ash from Almaty TPP (thermal power plant), with a SiO_2 content of 88 %;

- synthetic foaming agent FA-2000 (ПВ-2000);

- chemical additives, including sodium nitrate, sodium sulfate, sodium chloride, sodium carbonate, potassium sulfate, potassium chloride, potassium carbonate, potassium nitrate, calcium chloride, and sodium silicate solution. All additives complied with the requirements of the relevant standards.

The study was conducted mainly using standard research methods.

Methods. According to the working hypothesis, the introduction of individual additives was first tested, followed by complex hardening accelerators for concrete. The effectiveness of the additives was initially evaluated using dense cement paste, meaning that the additives were dissolved in mixing water, and the resulting salt solution was mixed with cement until a paste of normal consistency was obtained. The setting time was determined in accordance with GOST 310.10. Standard methods for determining the physical and mechanical properties of binders and concrete were used in the study.

Compressive strength determination according to GOST 25485 – 2019 and GOST 10180 – 2012:

The essence of the method – determination of concrete compressive strength consists in measuring the minimum force that destroys specially prepared control samples of concrete measuring 100 x 100 x 100 mm under static loading at a constant load increase rate, followed by

calculating the stress at these forces in accordance with GOST 10180 – 2012.

After placing the sample on the support plates of the testing machine or additional steel plates, the upper plate of the testing machine is aligned with the top surface of the sample so that their planes are fully in contact. The sample is loaded until failure at a constant rate of load increase (0.6 ± 0.2) MPa/s.

The methods of preparing the foamed concrete mixture includes:

- dry mixing: Cement, sand, and ash are mixed for 3 – 5 minutes until a homogeneous dry mixture is obtained;

- foam preparation: Stable foam based on PB-2000 is prepared at a pressure of 0.4 – 0.6 MPa from a 3 – 5 % aqueous solution and air. The expansion ratio is regulated by the component ratio and pressure.

- addition of water and chemicals: Water with additives (0.1 – 5 % of the cement weight) is mixed until homogeneous. The amount of water is calculated based on the workability of the mixture and the water-cement ratio;

- mixing with foam: The liquid solution is added to the dry mix and mixed for 3 – 5 minutes until a uniform mass is obtained;

- casting: The mixture is poured into greased molds without sudden impacts. Light vibration is acceptable.

- curing: Molds are kept at 20 ± 2 °C and humidity ≥ 90 % for 28 days. It is important to maintain high humidity during the first 1-2 days. At low temperatures, heating or accelerators are used.

Main equipment for the experiments:

- laboratory scales (accuracy up to 0.01 g);

- measuring glassware (graduated cylinders, beakers);

- mixer for cement paste preparation;

- consistency meter (Vicat apparatus) for setting time determination;

- laboratory spatula for mixing.

For mixture preparation, the raw materials were dried in a drying oven at a temperature of 100 - 110 °C.

Results and Discussion

According to the working hypothesis, the introduction of individual additives was first tested, followed by complex hardening accelerators for concrete. The effectiveness of the additives was evaluated at the initial stage using dense cement paste. Specifically, the additives were dissolved in mixing water, and the resulting salt solution was mixed with cement until a paste of normal consistency was obtained. The foaming agent was not used in these experiments.

When using portland cement grade CEM I 32.5N in the initial additive – free cement paste, the initial setting time is 2 hours 20 minutes, and the final setting time is 4 hours 20 minutes, which meets the regulatory requirements and indicates a moderate rate of hydration processes at the early stages of hardening.

The test results (Figures 1 a, b) demonstrated the high efficiency of additives containing sulfate ions, as well as sodium and potassium nitrites, in accelerating the setting time of cement paste.

When 1 %, 2 %, and 6 % Na_2SO_4, were introduced, the initial setting time was reduced from 2 hours 20 minutes to 12 minutes, 6 minutes, and 8 minutes, respectively, while the final setting time decreased from 4 hours 20 minutes to 57 minutes, 32 minutes and 22 minutes, respectively. The addition of 1 – 2 % potassium sulfate showed a more moderate effect on setting times compared to the same amount of sodium sulfate, However, at higher K_2SO_4 concentrations, the mixture rapidly thickened and set almost immediately. The effect of $Al_2(SO_4)_3$ was found to be similar to that of potassium sulfate solution when introduced into the cement paste.

Experimental data indicated a moderate effect of sodium, potassium, and calcium chloride salts on cement setting times (Figure 2a). The influence of sodium and potassium nitrites was intermediate between that of sulfate and chlorides (Figure 2a).

A significant reduction in setting time was observed when potassium carbonates were introduced into the cement (Figure 2b, Table 1). With 0.5 % potassium carbonate (potash) and 1 % sodium carbonate (soda), the setting times were as follows: initial setting - 3 minutes (potash), 1 minute (soda); final setting: 5 minutes (both). Further increases in dosage became impractical, as the cement began to set immediately during mixing with potassium and sodium carbonate salt solutions.

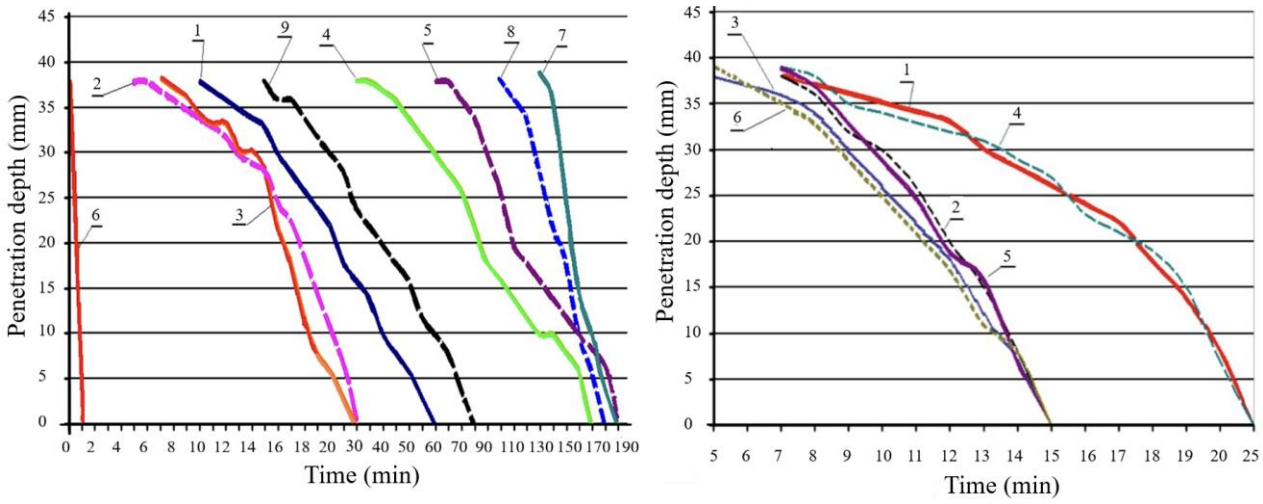

a) b)

a) Additive content: №1 – 3. Na_2SO_4. respectively 1; 2; 6 %. №4 – 6 K_2SO_4 respectively 1; 2; 6 %.
№7-9 $Al_2(SO_4)_3$ respectively 1; 2; 6 %.
b) Additive content: №1 – 3 Na_2NO_2 respectively 1; 2; 6 %.
№4 – 6 K_2NO_2 respectively 1; 2; 6 %; $Al_2(SO_4)$ respectively 1; 2; 6 %.

Figure 1 – Setting times of cement paste with sulfate and nitrite additives

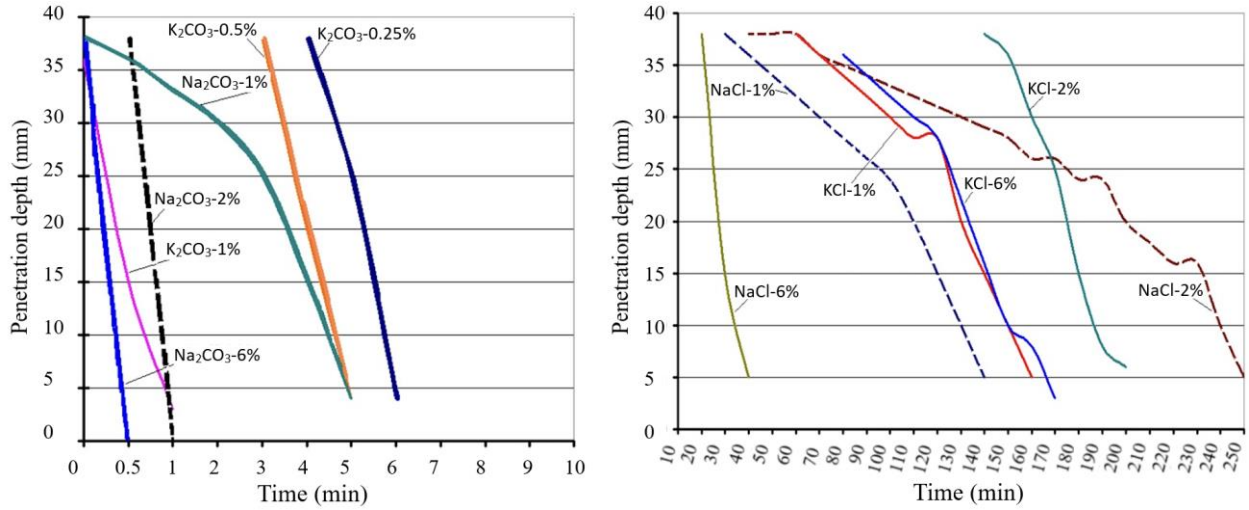

a) b)

Figure 2 – Setting time of cement paste with various additives

Thus, based on the experimental data, the high efficiency of electrolyte additives and the possibility of controlling the setting time of cement binders by adjusting the type and dosage of additives have been established.

Since foam concrete necessarily contains foaming surfaces – active agents (surfactants) that form a dense layer on the surface of hydrating cement particles, thereby slowing down the setting and hardening process, it was important to determine the effect of setting accelerators in the presence of surfactants.

The surfactant dosage in the study was set at 0.25 – 0.5 % of the cement mass, which corresponds to the actual consumption of foaming agents in the production of foam concrete with bulk density of 500 – 1200 kg/m^3. At the initial stage of the experiments, the effect of additives was assessed in dense cement paste, meaning that an electrolyte solution and surfactant were added to the mixing water and stirred with cement until a paste of normal consistency was obtained. Further tests were conducted in accordance with GOST 310.10.

Experimental methods, which data presented in Figure 3 (a, b) – 4 (a, b), have shown that the addition of a foaming agent in combination with most additives does not result in a significant negative effect, such as a prolonged setting time of the cement paste.

Table 1 – Effect of potassium and sodium carbonate additives on cement paste setting time

Additive	Additive content. % by cement mass	Setting time (t – min.)	
		initial	final
With additives	—	2 – 20	4 – 20
Potash (K_2CO_3)	0.25	0 – 0.4	0 – 0.6
Potash (K_2CO_3)	0.5	0 – 0.3	0 – 0.5
Potash (K_2CO_3)	1.0	0 – 0.0	0 – 0.1
Potash (K_2CO_3)	2.0	0 – 0.0	0 – 0.0
Soda (Na_2CO_3)	1.0	0 – 0.1	0 – 0.5
Soda (Na_2CO_3)	2.0	0 – 0.0	0 – 0.1
Soda (Na_2CO_3)	6.0	0 – 0.0	0 – 0.0

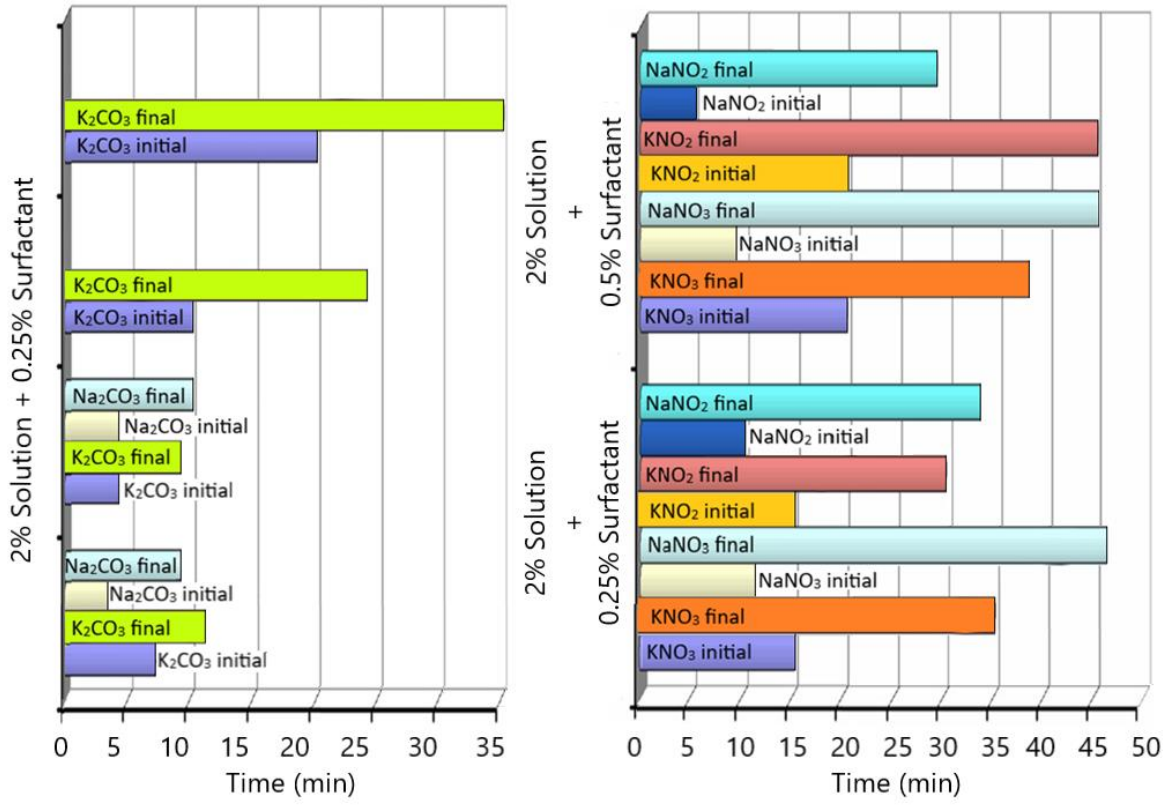

Figure 3 – Setting time of cement paste with nitrate, carbonate additives, and surfactant

When a foaming surfactant was introduced into solutions containing sodium sulfate, sodium and potassium carbonate, sodium nitrite and nitrate, and potassium nitrite and nitrate, the setting times remained relatively short: initial setting time 3 – 20 minutes, final setting time 9 – 46 minutes. However, the setting time increased, when the surfactant was used together with potassium and aluminum sulfate, and potassium, sodium, and calcium chlorides. In this case: initial setting time ranged from 55 minutes to 4 hours, final setting time ranged from 2 hours 50 minutes to 5 hours.

Thus, based on the study results, it was concluded that in dense cement paste, most electrolyte additives in the presence of a foaming surfactant effectively accelerate cement setting. However, in real foam concrete production, the cement paste is in a less dense state. Moreover, the water-to-cement ratio (W/C) in foam concrete is typically higher than the W/C ratio of the same cement paste or cement – silica slurry.

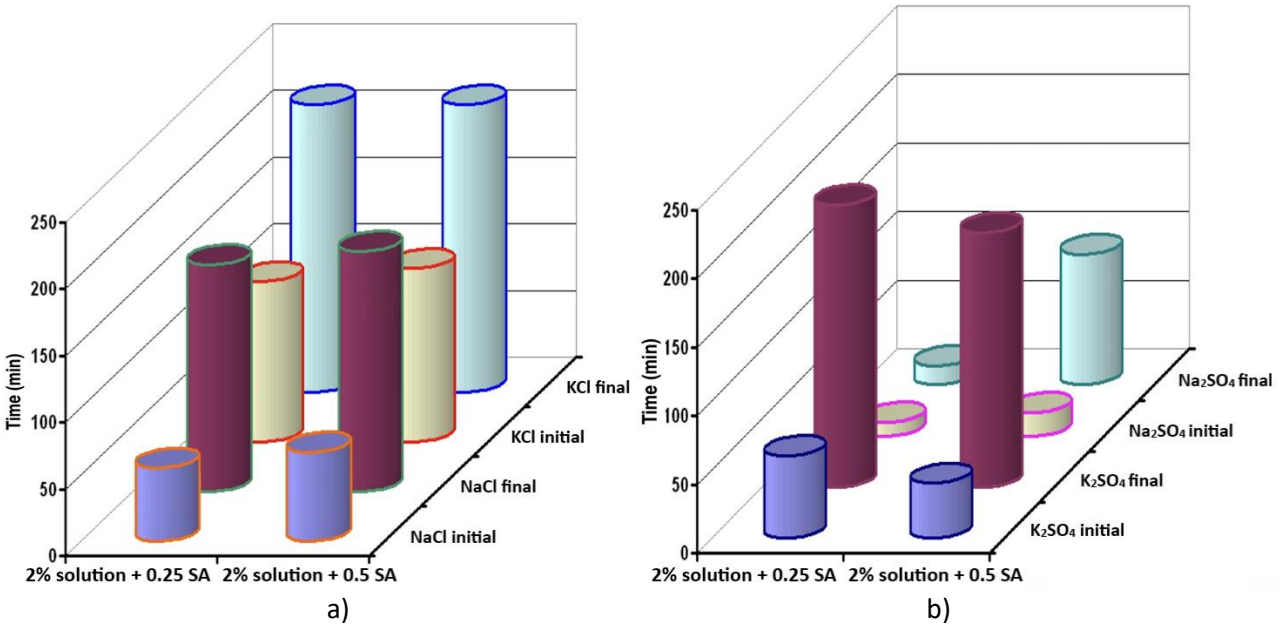

Figure 4 - Setting times of cement paste with chloride, sulfate, and surfactant additives

Therefore, the final assessment of the effectiveness of setting and hardening accelerators can only be made by preparing foamed cement paste and testing the physical properties of the mixture and the physico-mechanical characteristics of the hardened paste.

In the study, the kinetics of strength development of the hardened material and the chemical compatibility of additives with surfactants in an alkaline environment were selected as the controlled parameters to evaluate the effect of additives in production of porous systems. At the same time, the absence of standardized testing method for determining the setting time of foamed cement paste was taken into account.

The experiments revealed the chemical incompatibility of certain foam concrete mixture components during hardening, including sodium carbonate, potassium and sodium nitrites, and potassium and sodium sulfates. This incompatibility manifested as coagulation of the mixture, uncontrolled gas formation, and foam sedimentation. Ultimately leading to the formation of a material with large irregular pores, a loose surface, efflorescence, and low strength. Therefore, this group of additives was excluded from further experiments. When studying the effect of additives on the acceleration of foam concrete hardening, it is crucial from a technological perspective to assess both the setting rate and the hardening rate of the system. Rapid setting is necessary for structural stabilization of the foam concrete during the mixing of the cement-silica slurry with foam and the subsequent shaping of the molded mass. Meanwhile, accelerated hardening ensures the rapid development of early strength, which is essential for demolding the material. At the same time, the final strength of the foam concrete with additives must not be lower than that of foam concrete without additives.

The setting time of foamed cement paste was determined by measuring the temperature change of the foam-cement mixture, while hardening was assessed by testing the strength at different curing ages. The study (Figure 5) established that during foaming of cement paste, the previously observed effects of electrolyte additives on setting time are largely neutralized. The initial heat release from cement hydration, when combined with electrolytes and a foaming agent, begins approximately 2 hours after mixing the binder with an aqueous solution of surfactant and respective salt, while the final setting time occurs within 12 – 14 hours.

To accelerate the setting rate of foamed cementitious mass, a combination of two electrolyte additives along with a surfactant was tested. According to the working hypothesis, CaC_2 was expected to accelerate the hardening of foam concrete, while potassium carbonate (K_2CO_3) would promote rapid setting by reacting with calcium sulfate dihydrate (gypsum), a natural setting retardant in Portland cement.

The results (Figure 5, Table 2) confirmed the validity of this hypothesis and revealed new trends in the hardening kinetics of foam concrete with hardening accelerators (Figure 6).

Foam concrete without additives with a bulk density 600 kg/m^3 reaches demolding strength only after 12 hours. In contrast, with electrolyte additives, the demolding time is reduced by half, and within 24 hours, the strength exceeds that of additive – free foam concrete by more than 1.5 times.

The most significant effect was observed when chloride salts were combined with potassium carbonate (potash) or sodium silicate solution. In this case: foam concrete could be demolded after 2 hours, after 4 – 6 hours, compressive strength reached 0.27 – 0.41 MPa.

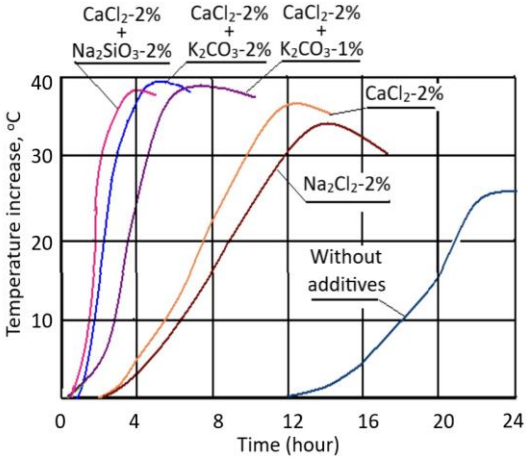

Figure 5 – Temperature change in cement paste with hardening accelerators

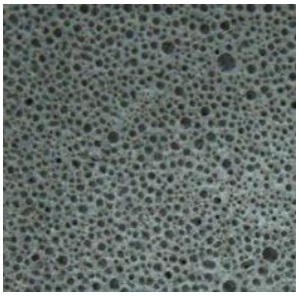

Figure 6 – Structure of foamed concrete

Table 2 – Effect of electrolyte additives on the hardening time of foam concrete with an average density of 600 kg/m^3

Additive		Compressive strength. MPa. After										
Name	Dosage %	2h	4h	6h	8h	12h	24h	2d	3d	7d	14d	28d
—	—	HP	HP	HP	HP	HP	0.13	0.23	0.46	0.62	1.09	1.7
$CaCl_2$	2	HP	HP	HP	HP	0.12	0.21	0.3	0.48	0.74	1.5	2.9
$NaCl_2$	2	HP	HP	HP	HP	0.11	0.18	0.28	0.51	0.98	1.26	2.23
$CaCl_2 + K_2CO_3$	2+1	HP	0.09	0.17	0.18	0.21	0.29	0.42	0.55	0.92	1.4	2.8
$CaCl_2 + K_2CO_3$	2+2	0.13	0.27	0.38	0.41	0.47	0.51	0.55	0.72	1.2	1.6	2.7
$NaCl + K_2CO_3$	2+1	HP	0.06	0.15	0.16	0.19	0.25	0.38	0.57	0.8	1.1	2.7
$NaCl + K_2CO_3$	2+2	0.11	0.28	0.36	0.37	0.42	0.48	0.52	0.66	0.95	1.3	2.6
$CaCl_2 + Na_2SiO_3$	2+2	0.14	0.29	0.41	0.43	0.52	0.55	0.57	0.78	1.34	1.72	3.1
Note – NR – not possible to demold, the sample collapses upon demolding												

After 6 hours, the rate of strength gains significantly slowed down and by 3 days, the compressive strength of all samples (with and without additives) became comparable.

The most noteworthy aspect is the hardening of kinetics between 7 and 28 days.

Calculations based on experimental data (Table 3) indicate that by 7 days heavy concrete reaches 60 % of its design strength, foam concrete (with and without additives) reaches 25 % to 44.4 % of their final strength. Between 7 and 14 days, the strength of heavy concrete increases from 65 % to 80 % (1.23 times), while from 14 to 28 days, it further rises from 80 % to 100 % (1.25 times). In contrast, foam concrete strength increases from 51.7 % to 100 % over the 14 – 28 day period, showing a significantly higher by 1.93 times rate. After 28 days, the strength of foam concrete reaches 1.7 MPa, corresponding to class M15. The addition of individual calcium and sodium chloride salts further optimized the time required to reach final strength.

Table 3 - Strength development kinetics of heavy concrete and foam concrete

Material	**Additive**		**Strength growth. %. Days**				
	Name	**Dosage**	**1**	**3**	**7**	**14**	**28**
Heavy concrete	-	-	-	33	65	80	100
Foam concrete			7.6	27.0	36.5	64.1	100
	$CaCl_2$	2	7.2	16.5	25.5	51.7	100
	$CaCl_2$+K_2CO_3	2+2	18.6	24.8	44.4	59.2	100
	$CaCl_2$+Na_2SiO_3	2+2	17.7	25.1	43.2	55.5	100

Table 4 - Effect of ambient temperature on the strength development of foam concrete with an average density of 600 kg/m^3

Ambient temperature (^{0}C)	**Additive**		**Compressive strength. MPa, after**						
	Name	**Dosage, %**	**0.5 day**	**1 day**	**2 days**	**3 days**	**7 days**	**14 days**	**28 days**
14 – 16	—	—	NR	NR	0.07	0.16	0.35	0.62	1.3
	$CaCl_2$	2	NR	0.09	0.15	0.26	0.42	0.85	2.2
	$CaCl_2$ + K_2CO_3	2+2	0.08	0.32	0.36	0.47	0.84	0.88	2.5
18 – 20	—	—	NR	0.13	0.23	0.46	0.62	1.09	1.7
	$CaCl_2$	2	0.12	0.21	0.3	0.48	0.74	1.5	2.9
	$CaCl_2$ + K_2CO_3	2+2	0.47	0.51	0.55	0.72	1.2	1.6	2.7
23 – 25	—	—	NR	0.11	0.23	0.47	0.67	1.12	1.8
	$CaCl_2$	2	0.13	0.26	0.32	0.49	0.69	1.52	3.0
	$CaCl_2$ + K_2CO_3	2+2	0.18	0.52	0.58	0.75	1.3	1.7	2.8
28 – 30	—	—	NR	0.14	0.25	0.48	0.68	1.11	1.9
	$CaCl_2$	2	0.12	0.23	0.31	0.52	0.70	1.58	2.8
	$CaCl_2$ + K_2CO_3	2+2	0.15	0.49	0.61	0.83	1.4	1.75	2.85

The findings suggest that in foam concrete, the retardation effect of cement hydration persists for up to 7 days, even in the presence of setting accelerators.

After the specified period, the density of the adsorbed layer of surfactant (SA) molecules on the surface of hydrating clinker minerals in cement significantly decreases, leading to accelerated hardening of foam concrete. The reduction in the density of the adsorbed SA layer is caused by a sharp increase in the surface area of hydration products.

One of the disadvantages of natural curing foam concrete technology is the slow strength development at temperatures between + 10 and + 16 °C. These temperatures are most typical during the autumn-spring period in the southern regions of Kazakhstan, while in northern regions, ambient temperatures drop even lower.

As a result, foam concrete production is essentially limited to the summer months.

Since foam concrete is molded in metal forms, the heat generated during cement hydration is rapidly dissipated into the environment due to the high thermal conductivity of steel (λ_{st} = 45 W/(m °C)) through the walls and bottom of the mold. Consequently, foam concrete hardens at ambient temperature. Moreover, nighttime temperatures are typically 5 – 10 °C lower than daytime temperatures, further slowing the hardening process.

Experimental studies (Table 4) revealed a significant decrease in the rate of strength development in foam concrete, both without additives and with electrolyte additives, as the ambient temperature decreased from 8 – 20 °C to 14 – 16 °C.

Foam concrete without additives reached an acceptable strength only after 3 days (Rc = 0.16 MPa), foam concrete with $CaCl_2$ reached 0.26 MPa, foam concrete with $CaCl_2$ combined with potassium carbonate (K_2CO_3) reached 0.47 MPa. At 14 – 16 °C, foam concrete with the optimal additive dosage could be demolded after 12 hours, but it achieved guaranteed strength only after 24 hours of curing.

Conclusions

Based on experimental data, the following comparative and quantitative conclusions can be drawn about the influence of various electrolyte additives and temperature on the setting times and strength characteristics of foamed concrete:

- without additives, the initial setting time of cement paste is 2 h 20 min, final setting – 4h 20 min;

- with 1 % Na_2SO_4, initial setting time is reduced to 12 min, final to 57 min (reduction of more that 4 times);

- with 0.5 % K_2CO_3, initial – 3 minal. Final – 5 min, which shows a 20-fold acceleration.

Compatibility with surfactants:

- with the addition of surfactants, most additives retain the accelerating effect with initial setting from 3 to 20 min, final – 9 to 46 min, but combinations with potassium sulfate and chloride extend the initial setting up to 4 hours, indicating chemical incompatibility.

Demolding strength (after 4-6 h):

- without additives, foamed concrete does not reach the required strength;

- with $CaCl_2$ + K_2CO_3 (2 + 2 %) the strength is 0.27 – 0.41 MPa, allowing the demolding time to be halved.

Strength after 28 days:

- without additives – 1.7 MPa (M15);

- with $CaCl_2$ + Na_2SiO_3 – 3.1 MPa, an increase of 82%.

Temperature regime:

- at 14 – 16°C, foamed concrete without additives reaches 0.16 MPa in 3 days;

- with $CaCl_2$ + K_2CO_3 – strength after 1 day is 0.47 MPa, nearly 3 times faster;

- at 28 – 30 °C, the strength of foamed concrete with additives reaches 2.85 MPa, which is 67 % higher than the base level.

Strength kinetics – by day 7, foamed concrete with additives reach up 44.4 % of the design strength, and by day 28 – 100 % or more.

In comparison, conventional concrete gains from 60 % to 100 % strength during the same period, but foamed concrete with additives shows an almost 2-fold increase in strength gain rate during the 14 – 28 day phase (1.93x).

Conflicts of interest. On behalf of all the authors, the correspondent author declares that there is no conflict of interest.

CRediT author statement: **D. Sartaev, Y. Orynbekov:** Conceptualization, Visualization, Project administration, Funding acquisition; **D. Sartaev, Y. Orynbekov, A. Baisarieva, D. Uxikbayeva:** Methodology, Writing – original draft preparation; **A. Baisarieva, D. Uxikbayeva:** Software; **Y. Orynbekov:** Formal analysis;

All authors have read and agreed to the published version of the manuscript.

Cite this article as: Sartaev DT, Orynbekov YS, Baisarieva AM, Uxikbayeva DA. Influence of additives and temperature regime on the setting kinetics and strength of foamed concrete. Kompleksnoe Ispolzovanie Mineralnogo Syra = Complex Use of Mineral Resources. 2027; 340(1):5-16. https://doi.org/10.31643/2027/6445.01

Қоспалар мен температуралық режимнің көбік бетонының қатаю кинетикасы мен беріктігіне әсері

Сартаев Д.Т., Орынбеков Е.С., Байсариева А.М., Уксикбаева Д.А.

Халықаралық Білім Беру Корпорациясы ЖШС, Алматы, Қазақстан

Мақала келді: *19 наурыз 2025*
Сараптамадан өтті: *2 сәуір 2025*
Қабылданды: *25 тамыз 2025*

ТҮЙІНДЕМЕ

Мақалада тез қататын жеңіл бетонның физикалық-механикалық сипаттамаларын әзірлеу нәтижелері ұсынылған. Алынған мәліметтер негізінде көбік бетон технологиясында металл кассета қалыптарын қолданудың тиімсіздігі туралы қорытынды жасалды. Олардың айналымын цехтағы еденді жылыту және қалыптардың бүйірлері мен беттерін оқшаулау арқылы арттыруға болады. Алайда, энергия тасымалдаушылардың құны жоғары болғандықтан материалдың өзіндік құнын арттырады және оның бәсекеге қабілеттілігін төмендетеді. Қоршаған ортаның температурасы 16°С-тан төмен болғанда цемент ылғалданған кезде пайда болатын жылуды сақтауға көмектесетін оқшауланған ағаш қалыптарды қолданған жөн. Кесудің технологиялық мүмкіндіктерін ескере отырып, пішіндердің оңтайлы өлшемдері (1.2 × 1.25 × 0.5 м және 1.2 × 1.25 × 0.6 м) таңдалады. Жылудың біркелкі бөлінбеуіне байланысты ірі монолитті массивтерді қалыптау құрылымның жарылуы және тіпті жыртылу қаупін тудырады. Қоспаның бастапқы температурасын 22 – 25°С диапазонында ұстау үшін қалыптау массасын 30°С дейін қыздырылған суды пайдаланып дайындау керек. Жылытылған ағаш қалыптарда қалыпталған материал ылғалдандыру басталғанға дейін температураны кемінде 18 – 20 °С сақтайды. Содан кейін цементтің экзотермиялық реакциясы арқылы температура қалыптан шыққанға дейін тұрақты болып қалады. Көбік бетонының табиғи қатаю технологиясын жетілдіру қоспаның құрамына химиялық белсенді кремний диоксиді компонентін енгізудің орындылығын көрсетті. Ол алитті ылғалдандырған кезде бөлінетін бос $Ca(OH)_2$ байланыстырады, бұл ұзақ қатаю кезеңінде беріктік жиынтығына ықпал етеді. Зерттеудің мақсаты – Электролиттік қоспалар мен беттік-белсенді заттардың цемент езіндісінің қатаю процестеріне әсерін зерттеу арқылы көбікті бетонның бастапқы кезеңдердегі қатаюын жеделдетудің тиімді тәсілдерін әзірлеу. Жұмыстың жаңалығы – көбік бетонның кеуекті құрылымын, құрамдас бөліктерінің құрамын және қатаю процесінің ерекшеліктерін ескере отырып, жеделдетілген бастапқы қатаю кезеңімен көбік бетонның физикалық-механикалық қасиеттерінің қалыптасу заңдылықтарын анықтау.

Түйін сөздер: Көбік бетон, тез қататын, жеңіл бетон, қоспалар, температура, күл, қалдық.

Авторлар туралы ақпарат:

Сартаев Д.Т. *Техника ғылымдарының кандидаты, қауымдастырылған профессор – зерттеуші, Халықаралық білім беру корпорациясы ЖШС, 50043, Рысқұлбеков көшесі, 28, Алматы, Қазақстан. Email: sartayev.dake@gmail.com; ORCID ID: https://orcid.org/0000-0002-2817-0955*

Орынбеков Е.С. *Техника ғылымдарының кандидаты, қауымдастырылған профессор – зерттеуші, Халықаралық білім беру корпорациясы ЖШС, 50043, Рысқұлбеков көшесі, 28, Алматы, Қазақстан. Email: orynbekov.savenergy@gmail.com; ORCID ID: https://orcid.org/0000-0003-2131-6293*

Байсариева А.М. *Қауымдастырылған профессор, Халықаралық білім беру корпорациясы ЖШС, 50043, Рысқұлбеков көшесі, 28, Алматы, Қазақстан. Email: abajsarieva@mail.ru; ORCID ID: https://orcid.org/0000-0002-7473-8820*

Уксикбаева Д.А. *Техника ғылымдарының магистрі, тьютор, Халықаралық білім беру корпорациясы ЖШС, 50043, Рысқұлбеков көшесі, 28, Алматы, Қазақстан. Email: dayana.uxikbayeva@mail.ru; ORCID ID: https://orcid.org/0009-0006-3189-933X*

Влияние добавок и температурного режима на кинетику схватывания и прочность пенобетона

Сартаев Д.Т., Орынбеков Е.С., Байсариева А.М., Уксикбаева Д.А.

ТОО Международная образовательная корпорация, Алматы, Казахстан

Поступила: *19 марта 2025*
Рецензирование: *2 апреля 2025*
Принята в печать: *25 августа 2025*

АННОТАЦИЯ
Статья представляет результаты разработки физико-механических характеристик быстротвердеющего лёгкого бетона. На основании полученных данных сделан вывод о неэффективности использования металлических кассетных форм в технологии пенобетона. Их оборот можно увеличить за счёт подогрева пола в цехе и изоляции боковин и поверхности форм. Однако высокая стоимость энергоносителей повышает себестоимость материала и снижает его конкурентоспособность. При температуре окружающей среды ниже 16 °C целесообразно использовать утеплённые деревянные формы, которые помогают сохранять тепло, выделяемое при гидратации цемента. Оптимальные размеры форм (1.2 × 1.25 × 0.5 м и 1.2 × 1.25 × 0.6 м) выбраны с учётом технологических возможностей резки. Формование крупных монолитных массивов сопряжено с риском появления трещин и даже разрывов структуры из-за неравномерного распределения тепла. Для поддержания начальной температуры смеси в пределах 22–25 °C формовочную массу следует готовить с использованием воды, подогретой до 30 °C. Затем, за счёт экзотермической реакции цемента, температура остаётся стабильной до момента расформовки. Совершенствование технологии естественного твердения пенобетона показало целесообразность введения в состав смеси химически активного кремнеземистого компонента. Он связывает свободный $Ca(OH)_2$, выделяемый при гидратации алита, что способствует набору прочности на длительных сроках твердения. *Цель исследования* Разработка эффективных способов ускорения твердения пенобетона на ранних этапах путём исследования влияния электролитных добавок и поверхностно-активных веществ на процессы схватывания и твердения цементного теста. *Новизна работы* заключается в установлении закономерностей формирования физико-механических свойств пенобетона с ускоренным сроком начального твердения, с учётом его пористой структуры, состава компонентов и особенностей процесса твердения.

Ключевые слова: пенобетон, быстротвердеющий, легкий бетон, добавки, температура, зола, отход.

Информация об авторах:

Сартаев Д.Т. *Кандидат технических наук, Ассоциированный профессор-исследователь, ТОО Международная образовательная корпорация, 50043, ул. Рыскулбекова, 28, Алматы, Казахстан. Email: sartayev.dake@gmail.com; ORCID ID: https://orcid.org/0000-0002-2817-0955*

Орынбеков Е.С. *Кандидат технических наук, Ассоциированный профессор-исследователь, ТОО Международная образовательная корпорация, 50043, ул. Рыскулбекова, 28, Алматы, Казахстан. Email: orynbekov.savenergy@gmail.com; ORCID ID: https://orcid.org/0000-0003-2131-6293*

Байсариева А.М. *Ассоциированный профессор, ТОО Международная образовательная корпорация, 50043, ул. Рыскулбекова, 28, Алматы, Казахстан. Email: abajsarieva@mail.ru; ORCID ID: https://orcid.org/0000-0002-7473-8820*

Уксикбаева Д.А. *Магистр технических наук, тьютор, ТОО Международная образовательная корпорация, 50043, ул. Рыскулбекова, 28, Алматы, Казахстан. Email: dayana.uxikbayeva@mail.ru; ORCID ID: https://orcid.org/0009-0006-3189-933X*

References

[1] Chica L, Alzate A. Cellular concrete review: New trends for application in construction. Constr. Build. Mater. 2019; 200:637-647. https://doi.org/10.1016/j.conbuildmat.2018.12.136

[2] Zhou G, Su RKL. A Review on Durability of Foam Concrete. Buildings. 2023; 13:1880. https://doi.org/10.3390/buildings13071880

[3] Raj A, Sathyan D, Mini K. Physical and functional characteristics of foam concrete: A review. Constr. Build. Mater. 2019; 221:787-799. https://doi.org/10.1016/j.conbuildmat.2019.06.052

[4] Zhang S, Qi X, Guo S, Zhang L, Ren J. A systematic research on foamed concrete: The effects of foam content, fly ash, slag, silica fume and water-to-binder ratio. Construction and Building Materials. 2022; 339:127683. https://doi.org/10.1016/j.conbuildmat.2022.127683

[5] Amran YM, Farzadnia N, Ali AA. Properties and applications of foamed concrete; a review. Construction and Building Materials. 2015; 101:990-1005. https://doi.org/10.1016/j.conbuildmat.2015.10.112

[6] Jones M, McCarthy A. Preliminary views on the potential of foamed concrete as a structural material. Magazine of Concrete Research. 2005; 57:21-31. https://doi.org/10.1680/macr.2005.57.1.21

[7] Lukpanov R, Dyussembinov D, Yenkebayev S, Yenkebayeva A, Tkach E. Additive for improving the quality of foam concrete made on the basis of micro silica and quicklime. Kompleksnoe Ispolzovanie Mineralnogo Syra = Complex Use of Mineral Resources. 2022; 323(4):30-37. https://doi.org/10.31643/2022/6445.37

[8] Ramamurthy K, Kunhanandan Nambiar EK. A classification of studies on properties of foam concrete. Cement and Concrete Composites. 2009; 31(6):388-396. https://doi.org/10.1016/j.cemconcomp.2009.04.006

[9] Dyussembinov D, Lukpanov R, Altynbekova A, Zhantlesova Z, & Awwad T. Effect of soapstock in the composition of modified additive for improving strength characteristics of concrete structures. Kompleksnoe Ispolzovanie Mineralnogo Syra = Complex Use of Mineral Resources. 2024; 334(3):37-50. https://doi.org/10.31643/2025/6445.26

[10] Kunhanandan Nambiar EK, Ramamurthy K. Influence of filler type on the properties of foam concrete. Cement and Concrete Composites. 2006; 28(5):475-480. https://doi.org/10.1016/j.cemconcomp.2005.12.001

[11] Hilal AA, Thom NH, Dawson AR. On void structure and strength of foamed concrete made without-with additives. Construction and Building Materials. 2015; 85:157-164. https://doi.org/10.1016/j.conbuildmat.2015.03.093

[12] She W, Du Y, Zhao G, Feng P, Zhang Y, Cao X. Influence of coarse fly ash on the performance of foam concrete and its application in high-speed railway roadbeds. Construction and Building Materials. 2018; 170:153-166. https://doi.org/10.1016/j.conbuildmat.2018.02.207

[13] Shang X, Qu N, Li J. Development and functional characteristics of novel foam concrete. Construction and Building Materials. 2022; 324:126666. https://doi.org/10.1016/j.conbuildmat.2022.126666

[14] Mydin MAO, Wang Y. Mechanical properties of foamed concrete exposed to high temperatures. Construction and Building Materials. 2012; 26:638-654. https://doi.org/10.1016/j.conbuildmat.2011.06.067

[15] Tan X, Chen W, Wang J, Yang D, Qi X, Ma Y, Wang X, Ma S, Li C. Influence of high temperature on the residual physical and mechanical properties of foamed concrete. Construction and Building Materials. 2017; 135:203-211. https://doi.org/10.1016/j.conbuildmat.2016.12.223

[16] Gencel O, Bilir T, Bademler Z, Ozbakkaloglu T. A detailed review on foam concrete composites: Ingredients, properties, and microstructure. Appl. Sci. 2022; 12:5752. https://doi.org/10.3390/app12115752

[17] Gong J, Zhang W. The effects of pozzolanic powder on foam concrete pore structure and frost resistance. Construction and Building Materials. 2019; 208:135-143. https://doi.org/10.1016/j.conbuildmat.2019.02.021

[18] Kocí V, Cerný R. Directly foamed geopolymers: A review of recent studies. Cement and Concrete Composites. 2022; 130:104530. https://doi.org/10.1016/j.cemconcomp.2022.104530

[19] Lukpanov R, Dyussembinov D, Altynbekova A, Yenkebayev S, & Awwad T. Optimal concentration of post-alcohol bard and microsilica in cement-sand mixtures determination. Kompleksnoe Ispolzovanie Mineralnogo Syra = Complex Use of Mineral Resources. 2023; 330(3):92-103. https://doi.org/10.31643/2024/6445.33

[20] Dhasindrakrishna K, Pasupathy K, Ramakrishnan S, Sanjayan J. Rheology and elevated temperature performance of geopolymer foam concrete with varying PVA fibre dosage. Materials Letters. 2022; 328:133122. https://doi.org/10.1016/j.matlet.2022.133122

[21] Zhang Z, Provis JL, Reid A, Wang H. Geopolymer foam concrete: An emerging material for sustainable construction. Construction and Building Materials. 2014; 56:113-127. https://doi.org/10.1016/j.conbuildmat.2014.01.081

[22] Dhasindrakrishna K, Pasupathy K, Ramakrishnan S, Sanjayan J. Progress, current thinking and challenges in geopolymer foam concrete technology. Cem. Concr. Compos. 2021; 116:103886. https://doi.org/10.1016/j.cemconcomp.2020.103886

[23] Xi X, Jiang S, Yin C, Wu Z. Experimental investigation on cement-based foam developed to prevent spontaneous combustion of coal by plugging air leakage. 2021; 301:121091. https://doi.org/10.1016/j.fuel.2021.121091

[24] Li T, Wang Z, Zhou T, He Y, Huang F. Preparation and properties of magnesium phosphate cement foam concrete with H_2O_2 as foaming agent. Construction and Building Materials. 2019; 205:566-573. https://doi.org/10.1016/j.conbuildmat.2019.02.022

[25] Tikalsky PJ, Pospisil J, MacDonald W. A method for assessment of the freeze–thaw resistance of preformed foam cellular concrete. Cement and Concrete Research. 2004; 34:889-893. https://doi.org/10.1016/j.cemconres.2003.11.005

[26] Dyussembinov D, Altynbekova A, Yenkebayev S, Zhumagulova A. Investigation of Effect of Proposed Two-Stage Foam Injection Method and Modified Additive on Workability of Foam Concrete. Materials. 2024; 17(9). https://doi.org/10.3390/ma17092024

[27] Plank J, Sakai E, Miao CW, Yu C, Hong JX. Chemical admixtures—Chemistry, applications and their impact on concrete microstructure and durability. Cement and Concrete Research. 2015; 78:81-99. https://doi.org/10.1016/j.cemconres.2015.05.016

Crossref

DOI: 10.31643/2027/6445.02
Engineering and Technology
IRSTI 61.31.35

The effect of halite mineral impurities on the technological parameters of the sodium chloride production process

***Urazkeldiyeva D.A., Kadirbayeva A.A.**

M. Auezov South Kazakhstan Research University, Shymkent, Kazakhstan

** Corresponding author email: urazkeldieva.97@list.ru*

Received: *July 27, 2025*
Peer-reviewed: *August 20, 2025*
Accepted: *August 27, 2025*

ABSTRACT

This paper shows the findings of a detailed investigation of the natural halite from the Bakhyt-Tany deposit. The mineral's composition is sodium chloride with the addition of calcium sulfate, magnesium salts, and some other matters, including a residue of less than 2% insoluble residue. Elemental assaying indicates the occurrence of elements like Ca, Mg, Al, Si, Fe, and Pb, which points to the occurrence of clay and some sulfate impurities. To understand how impurities are distributed in different sizes, a sample was classified using a sieve with a mesh of 0.2 mm. It was discovered that less than twenty per cent of the salt mass is a fine fraction (d < 0.2 mm), where up to 3.4% of insoluble impurities are found, and in the coarse fraction (d > 0.2 mm), this value is less than 1.8%. A mathematical model developed showed that the fine fraction and the total amount of the residue insoluble are directly related, which supports its use for estimating contamination and evaluating the effectiveness of the processes of desalination. Moreover, the generated 3D model revealed that temperature and humidity, in addition to raising the concentration of insoluble impurities, also increase the concentration of such impurities in the fine fraction even more. The results obtained also support the need for the pre-purification of halite before its use in food and other technological applications, and support the statement of the fractionation and desalination based purification process for halite.

Keywords: halite, sodium chloride, mineral impurities, colloidal particles, recrystallization, purification.

Information about authors:

Dilbar Urazkeldiyeva Abdikhmidovna
PhD doctoral student, The Higher School of Chemical Engineering and Biotechnology, M. Auezov South Kazakhstan Research University, Shymkent, Kazakhstan. Email: urazkeldieva.97@list.ru; ORCID ID: https://orcid.org/0000-0001-7825-6995

Kadirbayeva Almagul Akkopeykyzy
Candidate of technical sciences, Assistant Professor, The Higher School of Chemical Engineering and Biotechnology, M. Auezov South Kazakhstan Research University, Shymkent, Kazakhstan. Email: diac_2003@mail.ru, ORCID ID: https://orcid.org/0000-0003-0702-1114

Introduction

Sodium chloride is produced on the basis of halite minerals extracted by mining; brines are obtained by in-situ leaching or processing of solid sediments of salt lakes, which is the most cost-effective method. The Republic of Kazakhstan is regarded as one of the most mineral-rich countries in Central Asia with regard to salt minerals. The latest data indicates that the number of salt lakes in Kazakhstan exceeds 2,500, with an annual production of sodium chloride that surpasses 1 million tons. Notably, more than 80% of this production is concentrated within the Kyzylorda region. It is estimated that approximately 40% of the global production of table salt is exported [[1], [2], [3], [4], [5]].

The rich reserves of salt deposits in the Sarysu region could be of industrial importance to the Zhambyl Oblast region. The reserves are estimated at 45 million tons, and only one of the nearby deposits, Majdekenkol, has about 10 million tons. There are 22 salt deposits in the Zhambyl district. They are located at a considerable distance from each other and spread over a vast territory from the foothill plain of the Karatau Range in the south to the valley of the Shu River in the north [[6], [7]].

Exploration works were carried out at four sites: Aydyn, Yunkikol, Tuzkol and Maidegenkol.

On the lake "Koibagar", salt deposits consist of two layers. The upper layer with seam thickness from 1 to 3.4 m contains mainly mineral halite (NaCl), the lower layer with ore thickness from 0.3 to 2 m contains the following minerals: halite (NaCl), tenardite, astrakhanite, glauberite, espomite and gypsum. Lakes Isteken and Kokalegel are sulphate lakes, varying in thickness from 0.2 to 1.4 m and containing the following minerals: halite (NaCl),

tenardite (Na_2SO_4), myrobilite, astrachanite, glauberite and gypsum. In all explored deposits, the content of insoluble waste is concentrated in the range of 2-6% [[3], [8], [10]].

In terms of its technical characteristics, it is the opinion of experts that the percentage of water-insoluble substances, potassium ions, magnesium and sulphate, in both food products and technical salt, is below the permissible standards. The sodium chloride content of the composition is found to be 98.6%, which has been demonstrated to have a positive effect on quality [[8], [9]].

A significant presence of colloidal and mineral impurities has been identified in the composition of Halite ores. Such additives include sulfates, carbonates, silt and other substances of organic origin, which greatly interfere with the production of pure sodium chloride [[10], [11], [12]].

During the purification process of ore from impurities, colloidal particles function not only as mechanical impurities but also facilitate the destruction of the crystal structure through adsorption processes, accumulating on the crystal surface and thereby impeding the process [13]. The presence of colloidal particles has been demonstrated to have a number of effects on the process of crystallisation. These include the slowing down of crystal growth, the increase of the energy barrier at the start of crystallisation, and the formation of micropore effects [[14], [15]].

The mineral additives most frequently employed include kaolinite and montmorillonite, which are characterised by their silty composition, in addition to calcium and magnesium sulfates and carbonates, and heavy metals [16].

The movement and distribution of colloidal particles within a sodium chloride solution flow are contingent on environmental conditions, thereby exerting a substantial influence on the optimal parameters of solution purification. In the presence of salt gradients, the rate and direction of colloid migration are contingent on temperature and contact time, thereby affecting the efficiency of impurity separation [17]. For instance, at elevated temperatures, diffusiophoretic processes are enhanced, thus facilitating faster migration of particles to the interface. Concurrently, the optimal residence time is such that the maximum concentration of particles is achieved in the target zone. Consequently, the selection of temperature and duration in NaCl purification systems utilising colloids must consider the kinetics of their movement, thereby achieving a balance between the purification speed and the degree of contaminants removed [[18], [19]].

A recent study published on Phys.org demonstrates that salt gradients can effectively control the direction of motion of colloidal particles in microfluidic systems through a combination of diffusiophoresis and diffusioosmosis [20]. Researchers at Yale University have discovered that even a minor variation in salt concentration can induce focusing and redirection of colloids, obviating the necessity for external fields. This finding offers a promising outlook for the development of passive and energy-efficient systems for liquid purification and targeted delivery of substances in medicine and the environment [[19], [20]].

There are also studies on the purification of solutions from colloidal particles using membranes and electrocoagulation. Bharti et al. [21] presented a comprehensive review of electrocoagulation as a universal method for purifying wastewater and natural water from colloidal ions, organic substances, and turbidity. The authors showed that electrocoagulation provides a high degree of removal of dispersed particles due to the formation of hydroxide flocs, which makes it promising for the preliminary purification of mineral raw materials. Aouni et al. and Moneer et al. focused on the combination of electrocoagulation with membrane processes such as ultrafiltration and reverse osmosis. It has been shown that hybrid schemes can significantly reduce membrane fouling and ensure effective removal of colloids, increasing the stability of seawater desalination processes. The authors showed that such hybrid systems provide improved selectivity and efficiency in the removal of impurities, including finely dispersed colloids, which is particularly important in the preparation of complex brines and wastewater for further processing [[22], [23]].

While modern methods of sodium chloride purification by evaporation, recrystallization, filtration, and even sedimentation work wonders, they all have one thing in common: dealing with colloidal and mineral impurities remains a challenge. As an example, evaporation can be energy intensive, especially when heating to overcome colloids stabilizing the solution.

Recrystallization poses a challenge when the solution has a lot of clay particles. These clay particles adsorb onto the crystals, disrupting the shape, disturb, and purity of the crystals [[23],[24]].

The filtration method does not work well with stable colloidal systems, especially if the particles in

the colloidal solution are not likely to aggregate into larger structures.

Time and, at the same time, very sensitive to external influence such as pH, ionic strength, and, if the solution has a lot of contaminants, they may not be as effective [[20], [25]].

In this particular case, studying the behavior of colloidal particles in saturated sodium chloride solutions and developing effective colloidal particle removal strategies are very relevant. One example is the removal of colloidal impurities before crystallization, a process known as desliming. Desliming (deslammation) is a technological process for removing finely dispersed particles (particles typically < 10–20 μm in size) from mineral raw materials or ore pulp.

Improving the desliming process directly translates into purification. This desliming process improves the final purity while reducing energy consumption and preventing excessive waste. The purpose of the work is to evaluate the influence of the fractional composition and external conditions on the distribution of impurities in halite to optimize the purification scheme.

Experimental part

For this article, a sample of natural halite was used, which was taken from the Bakhyt-Tany deposit. The initial material was first dried at room temperature for 24 hours, after which it was mechanically crushed to obtain fractions of different particle size distribution. To determine the distribution of impurities into fractions, the sample was separated by dry sieving through a sieve with a mesh diameter of 0.2 mm. Thus, two fractions were separated: coarse (f > 0.2 mm) and fine (d < 0.2 mm). To accurately separate and sort the material by size, a vertically oscillating laboratory sieve shaker Analysette 3 PRO (FRITSCH) was used. Samples of about 50 g were subjected to wet sieving for approximately 45 minutes, with the vibration amplitude set to 1–2 mm.

The analysis of raw materials and products was conducted using a combination of spectral microscopy, X-ray analysis, and differential thermal studies. Elemental analysis (elemental composition) was performed using X-ray fluorescence spectroscopy on an INCA Energy 450 energy dispersive microanalysis system mounted on a JSM 6610 LV scanning electron microscope, JEOL, Japan. A scanning electron microscope JSM 6610 LV, JEOL, Japan was used to study the microstructure of the samples. Differential thermal analysis (DTA) was carried out on a Q-1500D derivatograph at a heating rate of 10 °C/min in an air atmosphere.

To determine the moisture content, the sample was pre-weighed in analytical scales and dried at 100 ^{0}C in a desiccator. Drying time 6 hours, interval 30 minutes. Chemical analysis was performed according to GOST R 51574-2000 [26].

The discussion of the results

The halite sample came from the Bakhyt Tany deposit (Fig.1). The salt exhibits the typical cubic crystal habit. However, it is distinguished by a grayish-beige color with significant dark inclusions. This is a raw natural substance with contaminants, likely clay and organic matter. Some salt will crumble into a fine powder when rubbed, suggesting the presence of colloidal particles. These characteristics explain the reasons for a preliminary treatment and the refined steps that might be required in the further treatment of the sample. The sample's chemical composition is shown in Table 1 (Fig.2) below.

Figure 1 - The halite sample from the Bakhyt Tany deposit

According to the elemental analysis of the mineral, it can be said that the salt composition is dominated by sodium and chlorine; there are also such elements as silicon, calcium, magnesium and aluminium, which confirm the presence of clay colloidal impurities. Such impurities are usually in a

dispersed form and negatively affect the process of crystallization, and so they are very poorly filtered. This, in turn, harms the purification parameters

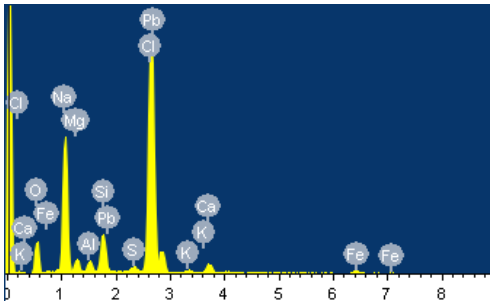

Figure 2 - Elemental composition of halite mineral of the Bakyt-Tany deposit

Table 1 - Elemental composition of halite mineral of Bakyt-Tany deposit, %

Element	Mass %
O	19.61
Na	25.40
Mg	2.36
Al	1.57
Si	4.97
S	0.54
Cl	39.46
K	0.64
Ca	2.21
Fe	1.12
Pb	2.11
Total	100.00

The results of thermal analysis of the natural salt mineral of the Bakhyt-Tany deposit are shown in Figure 3.

Figure 3 - The following report presents the DTA results of the natural sodium salt of the Bakhyt Tany deposit

The DTA of the salt sample from the natural mineral of the Bakhyt-Tany deposit is characterised by three endo effects and three exo effects. During the preliminary heating stage, two non-intensive endothermic effects have been identified at temperatures of 330°C and 560°C. These effects are attributed to the removal of moisture from the crystal structure of sodium and calcium chloride minerals. The intensive endothermic effect in the region of 820-830°C is indicative of the melting of sodium chloride. Endo effects in the region of 470°C and 685°C are associated with the burnout of a small amount of organic sulfur-containing magnesium compounds.

The data obtained has revealed that the natural sodium salt of the Bakhyt Tany deposit contains a high concentration of sodium chloride, with only a minor presence of impurities. It is reasonable to hypothesise that the natural sodium salt obtained at the Bakhyt Tany deposit has the potential to be utilised as a raw material in the production of table salt and soda ash. The calcium sulfate and other silicate compounds contained within insoluble precipitates have the potential to be utilised in the production of construction materials.

According to the results of the study, it was found that the mass fraction of moisture in halite samples ranges from 0.6% to 1.0%. These values are typical for natural materials stored under standard conditions and not subjected to additional drying. Based on the results of the chemical analysis, the approximate salt composition of the studied mineral was calculated. The base is sodium chloride (NaCl), the proportion of which reaches 88.4% of the total mass. In addition, the sample contains impurities in the form of calcium sulfate ($CaSO_4$) — about 2.5%, magnesium sulfate ($MgSO_4$) — 0.18%, and magnesium chloride ($MgCl_2$) — 0.37%. The presence of such impurities significantly affects the quality of salt and its suitability for various types of processing. In particular, the mineral contains up to 2% of the mass fraction of an insoluble residue, which makes it impossible to use it directly in the food industry without a preliminary stage of desalination — the removal of fine and colloidal impurities. Such a level of contamination can not only worsen the organoleptic properties of salt but also affect the technological parameters of crystallisation and filtration during processing. The analysis showed that the insoluble residue has a complex nature and consists of two main phases. The first is a clay mass, represented by finely dispersed insoluble components of natural origin. The second is clearly distinguishable transparent crystals of calcium sulfate, resistant to dissolution in water and prone to precipitation. For a more detailed study of the composition of the insoluble residue, an elemental

analysis using X-ray fluorescence spectroscopy was performed. Micrographs, as well as data on the elemental composition of the insoluble residue obtained during the study of halite from the Bakhyt-Tany deposit, are shown in Tables 2 and 3, and also shown in Figures 4 and 5.

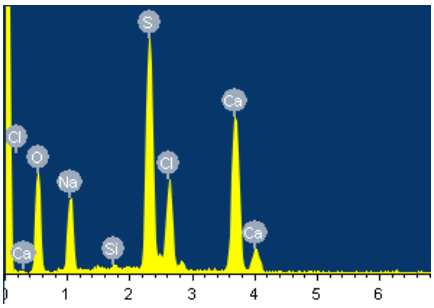

Figure 4 - Elemental composition of crystalline phase of insoluble precipitate of sodium salt mineral of Bakhyt-Tany deposit

The main peaks correspond to Na and Cl, which confirm the presence of halite (NaCl). Additional peaks of S and Ca indicate the occurrence of $CaSO_4$ phases. Minor Si and O peaks are attributed to traces of clay impurities. In Fig.5, besides the dominant Na and Cl peaks, significant signals of Si, Al, Mg, K, and Fe were observed, which are typical of clay minerals such as kaolinite and montmorillonite. The presence of Ca and Ti also supports the association with mineral impurities of terrigenous origin.

Table 2 - Elemental composition of the crystalline phase of the insoluble residue of the mineral of the Bakhyt-Tany deposit, %

Element	Mass %
O	41.34
Na	10.87
Si	0.28
S	18.49
Cl	8.85
Ca	20.16
Total	100.00

The presence of calcium sulfate in halite is of particular importance. On the one hand, $caso_4$ is an undesirable impurity: in the production of soda, it increases the formation of scale in evaporators and reduces the efficiency of the process, and in edible salt, it affects the purity requirements. On the other hand, calcium sulfate is a valuable raw material. Recent research [[27], [28]] highlights its widespread use in building materials, ceramics, soil-improving agents, and asphalt composites. Thus, the removal of $caso_4$ from halite not only improves the quality of salt but also opens up opportunities for processing and reuse of this byproduct in other industries.

The data obtained allowed not only to identify the composition of impurities, but also to understand their distribution inside the material. In order to study the distribution of insoluble impurities by size fractions, the salt sample was pre-crushed and fractionated using a laboratory sieve with a diameter of 0.2 mm. According to the results of sieving, it was found that up to 20% of the total mass of salt is a fine fraction with a particle size of less than 0.2 mm. It contains up to 3.4% of the mass fraction of the insoluble residue, the main part of which is the clay component.

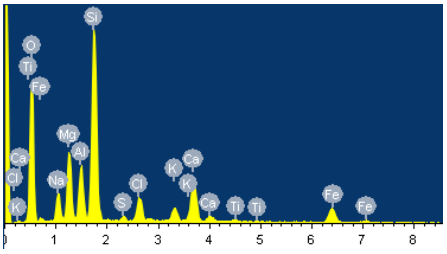

Figure 5 - Elemental composition of the clay phase of the insoluble residue of the sodium salt mineral of Bakhyt-Tany deposit

Table 3 - Elemental composition of the clay phase of the insoluble residue of the mineral of the Bakhyt-Tany deposit, %

Element	Mass %
O	44.64
Na	4.86
Mg	7.79
Al	5.58
Si	19.36
S	0.53
Cl	3.15
K	1.94
Ca	6.27
Ti	0.37
Fe	5.52
Total	100.00

This confirms the tendency of fine impurities to pass into small fractions during grinding and enrichment. The remaining 80% of the mass is accounted for by a large fraction (particles d > 0.2 mm), where the insoluble residue content is much lower — about 1.8%. In this case, calcium sulfate crystals predominate, forming in the salt structure in the form of dense transparent inclusions. Thus, the data obtained allow us to conclude that a

comprehensive purification scheme for this halite is necessary, including not only mechanical fractionation and filtration, but also methods aimed at the effective removal of clay and sulfate impurities. Accounting for the distribution of salt by fractions can be useful in designing the technological process of salt processing for food or technical purposes. However, it was found that simple dry sieving is not sufficient to remove the mucous fraction. This may be because colloidal particles are bound to calcium sulphate crystals, forming dense inclusions in the salt matrix. Therefore, the authors conducted additional experiments on mucus removal using a saturated NaCl solution [29]. The results of the experiments showed that the optimal ratio of solid to liquid substances is 1:3, which ensures the most effective removal of clay and colloidal impurities with minimal NaCl losses.

Figure 6 shows the model dependence of the insoluble residue content in the fine salt fraction on temperature and humidity. The graph clearly demonstrates that with an increase in both parameters, both temperature and humidity, an increase in the amount of insoluble impurities is observed.

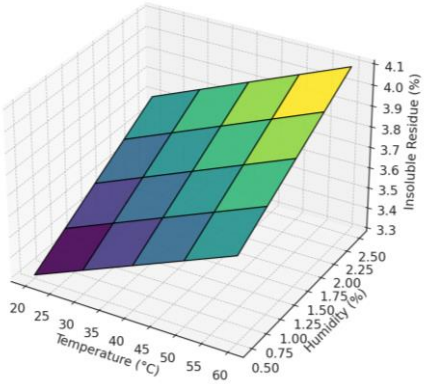

Figure 6 - Simulated 3D Dependence of Insoluble Residue (%) on Temperature(^{0}C) and Humidity (%)

This is because at higher temperatures, degradation and desorption processes are activated, contributing to the release of impurities fixed on crystals, and increased humidity increases the migration of clay and colloidal particles into solution, where they are more difficult to remove. This trend is especially relevant for the storage and processing of natural halite containing up to 2-3% insoluble impurities. The growth of these indicators in conditions of high humidity and temperature requires an adjustment of the cleaning process, for example, an increase in the settling time, the dose of coagulant, or the choice of another method of pre—desalination. Thus, the obtained model makes it possible to evaluate the behavior of impurities under changing external conditions and can be used in designing or optimizing the salt preparation scheme for processing.

Conclusions

The results of the study showed that up to 20% of salt mass goes to the fine fraction, and up to 80% of salt mass remains on the sieve in the coarse fraction. The fine fraction, d<0.2 mm, contains up to 3.4 wt.% of insoluble residue, and most of the clay residue passes into this fraction. The coarse fraction, d>0.2 mm, contains up to 1.8 wt. % of insoluble residue, and the main mass of insoluble residue consists of calcium sulfate crystals.

The compiled mathematical model confirmed a direct correlation between the increase in the fraction of fine fraction and the increase in the total content of insoluble impurities. Based on the fractional composition, it is possible to evaluate the products, which allows optimising the desliming technology.

On the other hand, a model of the effect of temperature and humidity as external factors on the behaviour of impurities was studied. It was demonstrated on a 3D plot that as the mentioned factors increase, the fraction of insoluble residue, especially its fine fraction, increases towards the insoluble residue. This needs to be taken into account in long-term and short-term salt operations to minimise impurities or improve performance.

It was also shown that simple dry sieving is not sufficient for the removal of fine clay and colloidal impurities, since colloidal particles are often associated with calcium sulfate crystals. Effective desliming was achieved only when using a saturated NaCl solution, where the optimal solid-to-liquid ratio was determined experimentally as 1:3.

In general, the work showed that from this deposit, it is necessary to pre-treat the finished halite with the use of fractionation, desliming, and further with the introduction of thermal or chemical after-treatment.

CRediT author statement: **D. Urazkeldiyeva**: Methodology, formal analysis, investigation, Data writing, Original draft preparation, writing–review

and editing; **A. Kadirbayeva:** Data curation, Reviewing and Editing.

Conflicts of Interest. On behalf of all authors, the corresponding author declares that there is no conflict of interest.

Funding: This research was funded by the intramural grant "Zhas Galym" of M. Auezov South Kazakhstan Research University, Grant No. ЮКУ2024-005.

Cite this article as: Urazkeldiyeva DA, Kadirbayeva AA. The effect of halite mineral impurities on the technological parameters of the sodium chloride production process. Kompleksnoe Ispolzovanie Mineralnogo Syra = Complex Use of Mineral Resources. 2027; 340(1):17-25. https://doi.org/10.31643/2027/6445.02

Натрий хлоридін алу процесінің технологиялық параметрлеріне галиттің минералды қоспаларының әсері

Уразкелдиева Д.А., Кадирбаева А.А.

М. Әуезов атындағы Оңтүстік Қазақстан Зерттеу Университеті, Шымкент, Қазақстан

Мақалада келді: *27 шілде 2025*
Сараптамадан өтті: *20 тамыз 2025*
Қабылданды: *27 тамыз 2025*

ТҮЙІНДЕМЕ

Мақалада Бақыт-Таны кен орнынан алынған табиғи галитті кешенді зерттеу нәтижелері келтірілген. Құрамы бойынша бұл минерал – кальций сульфаты, магний тұздары және кейбір басқа заттар қосылған натрий хлоридінен, оның ішінде 2%-дан аз ерімейтін қалдықтардан тұрады. Элементтік талдау нәтижесінде Ca, Mg, Al, Si, Fe және Pb сияқты элементтердің болатыны анықталды, бұл саз балшық пен кейбір сульфатты қоспалардың бар екенін көрсетеді. Әр түрлі өлшемдегі қоспалардың қалай таралатынын анықтау үшін үлгі 0,2 мм ұяшықты елеуіш арқылы фракцияларға бөлінді. Зерттеу нәтижесінде тұз массасының 20 %-дан азы d < 0,2 мм болатын ұсақ фракцияны құрайтыны анықталды, ал бұл фракцияда ерімейтін қалдықтың мөлшері 3,4 %-ға дейін жетеді. Ал ірі фракцияда (d > 0,2 мм) бұл көрсеткіш 1,8 %-дан аспайды. Құрастырылған математикалық модель ұсақ фракцияның мөлшері мен ерімейтін қалдықтың жалпы мөлшері арасында тікелей байланыс бар екенін көрсетті. Бұл модель тұздың ластану деңгейін бағалау және тазалау процесінің тиімділігін болжау үшін пайдаланылуы мүмкін. Сонымен қатар, жасалған үш өлшемді модель температура мен ылғалдылықтың артуы тек ерімейтін қоспалардың концентрациясын жоғарылатып қана қоймай, олардың ұсақ фракцияда жинақталуын да күшейтетінін көрсетті. Зерттеу нәтижелері галитті тағам өндірісінде және басқа да технологиялық мақсаттарда қолданбас бұрын алдын ала тазалау қажет болатынын көрсетті және тазалау процесінің фракциялау мен тұзсыздандыруға негізделген тиімді концепциясын қолдайды.

Түйін сөздер: галит, тазалығы жоғары натрий хлориді, минералды қоспалар, коллоидтық бөлшектер, қайта кристалдану, тазарту.

Авторлар туралы ақпарат:

Уразкелдиева Дилбар Абдихамидовна
PhD докторант, Химиялық инженерия және биотехнология жоғарғы мектебі, М. Әуезов атындағы Оңтүстік Қазақстан зерттеу университеті, Шымкент, Қазақстан. E-mail: urazkeldieva.97@list.ru; ORCID ID: https://orcid.org/0000-0001-7825-6995

Қадірбаева Алмагүл Ақкөпейқызы
Техника ғылымдарының кандидаты, қауымдастырылған профессор, Химиялық инженерия және биотехнология жоғарғы мектебі, М. Әуезов атындағы Оңтүстік Қазақстан зерттеу университеті, Шымкент, Қазақстан. E-mail: diac_2003@mail.ru; ORCID ID: https://orcid.org/0000-0003-0702-1114

Влияние минеральных примесей галита на технологические параметры процесса получения хлорида натрия

Уразкелдиева Д.А., Кадирбаева А.А.

Южно-Казахстанский Исследовательский Университет имени М. Ауезова, Шымкент, Казахстан

Поступила: *27 июля 2025*
Рецензирование: *20 августа 2025*
Принята в печать: *27 августа 2025*

АННОТАЦИЯ

В данной статье представлены результаты детального исследования природного галита с месторождения Бахыт-Таны. По составу минерал представляет собой хлорид натрия с добавлением сульфата кальция, солей магния и некоторых других веществ, в том числе менее 2% нерастворимого остатка. Элементный анализ показывает наличие таких элементов, как Ca, Mg, Al, Si, Fe и Pb, что указывает на наличие примесей глины и некоторых сульфатов. Чтобы понять, как распределяются примеси разного размера, образец был

	классифицирован с помощью сита с ячейкой 0,2 мм. Было обнаружено, что менее двадцати процентов массы соли составляет мелкая фракция (d < 0,2 мм), в которой содержится до 3,4% нерастворимых примесей, а в крупной фракции (d > 0,2 мм) это значение составляет менее 1,8%. Разработанная математическая модель показала, что мелкодисперсная фракция и общее количество нерастворимого осадка находятся в прямой зависимости, что позволяет использовать ее для оценки загрязнения и эффективности процессов опреснения. Более того, созданная 3D-модель показала, что температура и влажность не только повышают концентрацию нерастворимых примесей, но и еще больше увеличивают концентрацию таких примесей в мелкой фракции. Полученные результаты также подтверждают необходимость предварительной очистки галита перед его использованием в пищевой промышленности и других технологических применениях и подтверждают концепцию процесса очистки галита, основанного на фракционировании и опреснении.
	Ключевые слова: галит, хлорид натрия высокой чистоты, минеральные примеси, коллоидные частицы, перекристаллизация, очистка.
Уразкелдиева Дилбар Абдихамидовна	***Информация об авторах:*** *PhD докторант, Высшая школа химической инженерии и биотехнологии, Южно-Казахстанский исследовательский университет имени М. Ауезова, Шымкент, Казахстан. E-mail: urazkeldieva.97@list.ru; ORCID ID: https://orcid.org/0000-0001-7825-6995*
Кадирбаева Алмагул Аккопейкызы	*Кандидат технических наук, ассоцированный профессор, Высшая школа химической инженерий и биотехнологии, Южно-Казахстанский исследовательский университет имени М. Ауезова, Шымкент, Казахстан. E-mail: diac_2003@mail.ru; ORCID ID: https://orcid.org/0000-0003-0702-1114*

References

[1] Kadirbaeva AA. Mineral raw materials of Kazakhstan [Qazaqstannyń mıneraldy shıkizattary]. For students and undergraduates of the Specialty - Chemical Technology of inorganic substances. Manual. Shymkent: SKU M. Auezov. 2017, 112. (in Kazakh).

[2] Posokhov EV. Mineralnye bogatsva soliyonyh oziyor Kazakhstana [Mineral wealth of the salt lakes of Kazakhstan]. Alma-Ata. 2009. (in Russ).

[3] Urazkeldiyeva D, Kadirbayeva A. Overview Of Sodium Mineral Ores In South Kazakhstan. Proceedings of the international scientific and practical conference dedicated to the 80th anniversary of the SKU named after M. Auezov. 2023, 24-27.

[4] Bishimbayev VK, Amreev DD, Kapsalyamov BA, Gapparova KM, Sarsenov A. Analız rynka súlfata natrıa ı ıssledovanıe vozmojnostı ego polýchenıa ız súlfatnıkov mestorojdenıa Jaksykylysh [Analysis of the sodium sulfate market and study of the possibility of its production from sulfate rocks of the Zhaksykylysh deposit]. Bulletin of Science of Southern Kazakhstan. 2019; 1(5):58-65. (in Russ).

[5] Desyatov AV, Kruchinina NE, Novikov SV. Deep processing of mineralized mine waters to produce crystalline sodium sulfate. [Glubokaya pererabotka mineralizovannykh shakhtnykh vod s polucheniem kristallicheskogo sul'fata natriya]. Advances in chemistry and chemical technology. 2016; XXX(9):96-99. (in Russ.).

[6] Kadirbayeva AA, Kaldybayeva G, Iskakova T, Raiymbekov EB. As tuzynyng kuramyn zhane ony tazalaudy zertteu [Study of the composition of table salt and its purification]. Bulletin Of KazNTU, 2017; 3(121):605-609. (in Kazakh).

[7] Baitureev AA. Ecology. Educational post for practical training. Taraz: University of Taraz. 2002.

[8] Baitureev AM. Processing and drying in table salt production [Pererabotka i sushka v proizvodstve povarennoi soli]. Taraz: Taraz University. Educational post for practical training. 2005. (in Russ).

[9] Cyran K, et al. The Influence of Impurities and Fabrics on Mechanical Properties of Rock Salt for Underground Storage in Salt Caverns. Archives of Mining Sciences. 2021; 66(2):155-179. https://doi.org/10.24425/ams.2021.13745

[10] Sangwal K, & Zaniewska G. Influence of Impurities on the Etching of NaCl Crystals. Journal of Materials Science. 1984; 19:1131-1144. https://doi.org/10.1007/BF01120022

[11] Al-Jibbouri S, & Ulrich J. The Influence of Impurities on the Crystallization Kinetics of Sodium Chloride. Crystal Research and Technology. 2001; 36(12):1365-1375. https://doi.org/10.1002/1521-4079(200112)36:12<1365::AID-CRAT1365>3.0.CO;2

[12] Smith JA, & Jones PL. Mineralogy and Microstructure of Halite Deposits: Impacts of Impurities on Crystallization and Processing. Journal of Geological Sciences. 2023; 79(4):342-355. https://doi.org/10.1007/s10040-023-01234-5

[13] Adnan Chakra, Christina Puijk, Goran T. Vladisavljević, Cécile Cottin-Bizonne, Christophe Pirat, Guido Bolognesi. Surface chemistry-based continuous separation of colloidal particles via diffusiophoresis and diffusioosmosis. Journal of Colloid and Interface Science. 2025; 693:137577. https://doi.org/10.48550/arXiv.2412.00246

[14] Singh K, Kumar A, & Dey S. Reversible Trapping of Colloids in Microgrooved Channels via Diffusiophoresis under Steady-State Solute Gradients. Phys. Rev. Lett. 2020. https://doi.org/10.48550/arXiv.2007.11114

[15] Alonso-Matilla R, Bricteux L, & Guazzelli É. Diffusiophoretic Transport of Colloids in Porous Media. *arxiv preprint*, arXiv:2411.14712. 2024. https://doi.org/10.48550/arXiv.2411.14712

[16] Abécassis B, Cottin-Bizonne C, Ybert C, & Bocquet L. How a Pinch of Salt Can Tune Chaotic Mixing of Colloids in Microchannels. *arXiv preprint*, arXiv:1403.6390. 2014. https://doi.org/10.48550/arXiv.1403.6390

[17] Linnikov OD, Malinkina TI, & Zhuk NA. The Influence of Impurities on Crystallization Kinetics of Sodium Chloride. Crystal Research and Technology. 2006; 41(10):966-972. https://doi.org/10.1002/crat.200510653

[18] Flatt RJ, Caruso F, Sanchez AMA, Scherer GW. Chemomechanics of salt damage in stone Nat. Commun. 2014; 5:5823. https://doi.org/10.1038/ncomms5823

[19] Steiger M. Crystal growth in porous materials - II: Influence of crystal size on the crystallization pressure. J. Cryst. Growth. 2005; 282(3-4):470- 481. https://doi.org/10.1016/j.jcrysgro.2005.05.008

[20] Haoyu Liu et al. Diffusioosmotic Reversal of Colloidal Focusing Direction in a Microfluidic T-Junction. Physical Review Letters. 2025. https://doi.org/10.1103/PhysRevLett.134.098201

[21] Mukesh Bharti, Pranjal P Das, Mihir K Purkait. A review on the treatment of water and wastewater by electrocoagulation process: Advances and emerging applications. Journal of Environmental Chemical Engineering. 2023; 11(6):111558. https://doi.org/10.1016/j.jece.2023.111558

[22] Aouni A, Tounakti R, Ait Ahmed B, Hafiane A. Hybrid electrochemical/membrane couplings processes for enhancing seawater pretreatment and desalination. Water Environment Research. 2024. https://doi.org/10.1002/wer.10979

[23] Abeer A Moneer. The potential of hybrid electrocoagulation-membrane separation processes for performance enhancement and membrane fouling mitigation: A review. Egyptian Journal of Aquatic Research. 2023; 49(3):269-282. https://doi.org/10.1016/j.ejar.2023.08.007

[24] Shen Y, Linnow K, Steiger M. Crystallization behavior and damage potential of Na_2SO_4 –NaCl mixtures in porous building materials. Cryst. Growth Des. 2020; 20(9):5974-5985. https://doi.org/10.1021/acs.cgd.0c00671

[25] Zhang H, Li Y, Chen J, & Wang X. Thermal coagulation–flocculation for enhanced removal of stable colloidal impurities from saline solutions. Journal of Colloid and Interface Science. 2023; 643:1128-1136. https://doi.org/10.1016/j.jcis.2023.06.052

[26] GOST P 51574-2000. Common salt. Test methods. Publishing House of Standards. Moscow. (in Russ).

[27] Li X, Zhang Y, Wang H, Liu J, & Chen Z. Review of the state of impurity occurrences and utilization of calcium sulfate. Minerals. 2023; 13(7):987. https://doi.org/10.3390/min13070987

[28] Xie Z, Liu Y, Zhang L, & Huang P. Application of the industrial by-product gypsum in building materials: sources, properties and utilization prospects. Construction and Building Materials. 2024; 405.

[29] Kadirbayeva A, Urazkeldiyeva D, Minakouski A, Seitmagzimova G, Koshkarbayeva S, Tukhtaev H. The Development of A Technology for the Purification of Sodium Chloride by Removing Impurities Using the Phosphate Method. Open Chem Eng J. 2025; 19:e18741231373719. http://dx.doi.org/10.2174/0118741231373719250430111944

Crossref

DOI: 10.31643/2027/6445.03
Engineering and Technology

Development of environmentally sustainable cement compositions based on processed ceramic waste

[1] Abdullaev M.Ch., [1] Khomidov F.G., [2*] Jumaniyozov Kh.P., [2] Yakubov Y.Kh.

[1] Institute of General and Inorganic Chemistry of the Academy of Sciences of Uzbekistan, Tashkent
[2] Urgench State University named after Abu Rayhon Beruni, Urgench, Uzbekistan

** Corresponding author email: azamat.x@urdu.uz*

Received: *June 21, 2025*
Peer-reviewed: *July 28, 2025*
Accepted: *August 26, 2025*

ABSTRACT

One of the major challenges in the modern construction materials industry is the development of environmentally sustainable, energy-efficient, and economically viable materials. This study investigates the production of composite cement compositions by partially replacing Portland cement clinker with recycled ceramic brick waste (CBW). The primary objective is to reduce carbon dioxide (CO_2) emissions during cement manufacturing by utilising secondary raw materials with pozzolanic and filler properties. The experimental program encompasses a comprehensive analysis of the chemical, mineralogical, and structural characteristics of CBW, as well as its impact on the hydration process and the mechanical properties of cement composites. The clinker was partially replaced with CBW at 15% and 20% by mass in the binder component. Mechanical strength tests (flexural and compressive) were conducted at 2, 7, and 28 days of curing. Additionally, phase composition was analysed by X-ray diffraction (XRD), and microstructural development was evaluated using scanning electron microscopy (SEM). The results show that replacing clinker with CBW improves the microstructural compactness of the hardened matrix and ensures comparable mechanical performance after 28 days. A Life Cycle Assessment (LCA) confirmed that this approach can reduce CO_2 emissions by approximately 15–25% compared to conventional cement. The scientific novelty lies in the combined pozzolanic and micro-filler role of CBW, enabling its use as a supplementary cementitious material in low-carbon binder systems. The findings support the development of sustainable technologies for the cement industry and promote the circular economy through the utilisation of industrial waste.

Keywords: Clinker replacement, CO_2 emission reduction, ceramic brick waste, pozzolanic activity, supplementary cementitious materials, microstructure.

Information about authors:

Abdullaev Muslimbek Chori o'g'li — *PhD student, Institute of General and Inorganic Chemistry of the Academy of Sciences of Uzbekistan, 77 Mirzo Ulugbek Street, 100170, Tashkent. Email: abdullayev.bro.prof@gmail.com; ORCID ID: https://orcid.org/0009-0002-8192-7897*

Khomidov Fakhriddin Gafurovich — *PhD, Senior Research Fellow, Institute of General and Inorganic Chemistry of the Academy of Sciences of Uzbekistan, 77 Mirzo Ulugbek Street, 100170, Tashkent. Email: faha0101@mail.ru; ORCID ID: https://orcid.org/0000-0002-9110-351X*

Jumaniyozov Khurmatbek Palvannazirovich — *PhD, Associate Professor, Faculty of Chemical Technology, Urgench State University named after Abu Rayhon Beruni, Urgench, H. Olimjon Street 14, 220100, Uzbekistan. Email: hurmatbek.jumaniyozov@gmail.com; ORCID ID: https://orcid.org/0000-0001-6235-1365*

Yakubov Yusufboy Khasan o'g'li — *PhD student, Urgench State University named after Abu Rayhon Beruni, Urgench, H. Olimjon Street 14, 220100, Uzbekistan. Email: yyoqubov97@gmail.com; ORCID ID: https://orcid.org/0000-0003-3852-3141*

Introduction

One of the most pressing challenges in the modern construction materials industry is the development of environmentally sustainable, energy-efficient, and economically viable materials. Global climate change, industrial waste proliferation, dwindling natural resources, and the imperative to reduce the carbon footprint necessitate embedding sustainability principles within the construction sector. In particular, reducing carbon dioxide (CO_2) emissions and increasing the use of recycled raw materials in production processes have attracted significant scientific and practical attention.

Extensive research has demonstrated that partial replacement of cement with industrial by-products—such as fly ash, ground granulated blast-furnace slag, silica fume, metakaolin, and recycled ceramic waste—can lead to substantial CO_2 reduction and performance improvements. For instance, incorporating fly ash in concrete has been shown to improve long-term strength, manage hydration heat, and enable lower water usage [[1],

[2], [3]]. Moreover, life cycle assessment (LCA) studies indicate that these SCMs can reduce CO_2 emissions by 15–25%, consistent with findings from recycled aggregate systems [4].

The cement industry is crucial in this regard, as global cement production amounts to over 4 billion tons per year, contributing around 8% of anthropogenic CO_2 emissions [5]. Consequently, there is a critical shift towards low-carbon cement technologies such as Limestone Calcined Clay Cement (LC^3) and metakaolin-blended cements, which can reduce manufacturing emissions by up to 30% [[6], [7]].

Ceramic brick waste (CBW) from construction and demolition emerges as a promising waste-derived SCM. Due to its high firing temperature, crystalline structure, and mechanical stability, CBW contains reactive SiO_2 and Al_2O_3—key components of pozzolanic behavior—enabling its use in hydraulic cementitious systems and promoting the formation of strength-bearing hydration products [[8], [9], [10]]. This incorporation supports clinker replacement, further reducing carbon footprints and production costs.

Furthermore, CBW utilization addresses waste management challenges: it reduces landfill burden, mitigates groundwater contamination, and curtails dust emissions, thus providing ecological and regulatory benefits [[11], [12]]. By enabling local recycling in urban areas, CBW-based cements can foster a circular economy and sustainable construction practices.

Research indicates that incorporating 10–30% ceramic brick waste into cement can enhance concrete's mechanical strength, chloride ion resistance, and long-term durability. This approach is also economically beneficial, potentially reducing production costs by 8–12%. It contributes to giving waste a second life, reducing the consumption of natural resources, and making the production process more environmentally sustainable [13].

Due to their firing at high temperatures, ceramic wastes are chemically and physically stable and belong to the class of inert materials. They contain silicon dioxide (SiO_2) and aluminum oxide (Al_2O_3), which exhibit pozzolanic properties, enabling their use as active mineral additives in cement compositions [[14], [15]]. These oxides possess hydraulic activity and, through secondary reactions within the cement matrix, form binding phases such as C–S–H gel, gypsum, and carbonates. As a result, the demand for conventional clinker is reduced, which significantly lowers both CO_2 emissions and the production cost of cement.

Numerous studies have investigated the use of industrial by-products such as fly ash, slag, silica fume, and metakaolin as supplementary cementitious materials (SCMs) to reduce clinker consumption and CO_2 emissions. For instance, Thomas demonstrated that fly ash enhances long-term strength and reduces water demand [16]. Dhandapani et al. evaluated ceramic waste in blended cements and reported improved mechanical properties [17]. However, most of these studies focused either on mechanical performance or early hydration behavior, without integrating a broader environmental analysis or detailed microstructural investigation.

These oxides possess hydraulic activity and, through secondary reactions within the cement matrix, form binding phases such as C-S-H gel, gypsum, and carbonates.

As a result, the demand for conventional clinker is reduced, which significantly lowers both CO_2 emissions and the production cost of cement.

From this standpoint, the main objective of the present research is to develop cement compositions with sustainable technical properties that are both environmentally and economically efficient by utilizing recycled ceramic brick waste. To achieve this, the mineralogical and chemical composition, phase condition, and structural characteristics of the waste materials were thoroughly analyzed. Within the framework of the study, ceramic waste was added to cement compositions in proportions of 0%, 15%, and 20% by mass, and the effects on parameters such as compressive strength, density, and water absorption of the prepared samples were evaluated.

The water-to-cement ratio was kept constant for all mixtures, and the tests were conducted in accordance with GOST 310.3–76, GOST 30744–2001, and GOST 310.4–81 standards [18].

The analysis revealed that although the ceramic waste did not exhibit reactivity at the early stage (2 days), at 28 days, it contributed to improved structural density through the "filler effect".

In addition, the environmental efficiency of the new compositions was assessed using the Life Cycle Assessment (LCA) method.

Experimental results demonstrated that the use of ceramic waste can reduce CO_2 emissions by 15–25%. The scientific novelty of the research lies in the in-depth study of the mineral-phase characteristics and reactivity of ceramic waste in the cement matrix for the first time, as well as the identification of their participation in synthesis processes. This makes it possible to utilize waste as a secondary raw material,

reduce the need for landfilling, and minimize environmental impact.

Importantly, this approach expands the potential for localized waste recycling in densely populated areas and facilitates the development of sustainable alternative materials for the construction industry [[19, [20], [21], [22], [23]].

Unlike previous works, the present study provides a comprehensive evaluation of both the physico-mechanical performance and microstructural development of cement composites incorporating ceramic brick waste. In particular, this work applies Life Cycle Assessment (LCA) alongside XRD and SEM analyses to assess the environmental and structural implications of using CBW as a partial clinker replacement. Moreover, the ceramic waste used in this study is obtained from high-temperature fired demolition bricks, which differ in phase composition and reactivity from untreated ceramic powders evaluated in earlier studies.

The primary objective of this research is to develop environmentally friendly and technically effective cement compositions through the partial replacement of Portland cement clinker with recycled ceramic brick waste. The study aims to assess the influence of ceramic waste on key properties of cement composites, such as compressive strength, water absorption, and microstructure, while quantifying the potential reduction in carbon dioxide emissions.

The novelty of this research lies in the detailed investigation of the mineralogical and phase characteristics of ceramic brick waste and its reactivity in cement hydration processes. Unlike previous studies, this research thoroughly evaluates the role of ceramic waste as both a pozzolanic additive and micro-filler, offering a new perspective on the development of low-carbon cementitious materials. Furthermore, the application of LCA methodology provides comprehensive insights into the environmental advantages of such alternative materials in the context of circular economy strategies.

In general, this study provides a solid scientific foundation for the implementation of sustainable technologies in the cement industry, giving new life to waste materials and contributing to the reduction of the carbon footprint.

Experimental part

The experimental program involved the preparation, characterization, and mechanical evaluation of cement-based composite specimens modified with ceramic brick waste (CBW). Standard prismatic samples with dimensions of 4 × 4 × 16 cm were prepared using a cement-to-sand ratio of 1:3. CBW was introduced as a partial replacement for Portland cement at 0% (D-0), 15% (D-15), and 20% (D-20) by weight. All mixes were prepared with a constant water-to-cement (W/C) ratio of 2.25 to maintain uniform consistency across compositions.

The ceramic brick waste was obtained from the Yangiyo‘l Brick Factory and ground to a particle size distribution with a median diameter (D_{50}) of approximately 42 μm, as determined by laser diffraction analysis. Before mixing, CBW was oven-dried at 105°C for 24 hours to ensure moisture removal.

The setting time of the fresh mortar was measured according to GOST 310.3–76 using a Vicat apparatus. Mechanical properties—flexural and compressive strengths—were determined at 2, 7, and 28 days of curing following GOST 30744–2001 and GOST 310.4–81, respectively. The tests were conducted using a CONTROLS MCC 8.5 universal testing machine (Italy) at a constant loading rate of 2.4 kN/s.

Mineralogical analysis of 28-day cured specimens was performed using X-ray diffraction (XRD) on a Bruker D8 Advance diffractometer (Germany) with CuKα radiation (λ = 1.5406 Å), operated at 40 kV and 40 mA. Scanning was carried out over a 2θ range of 5° to 60° with a step size of 0.02° and a counting time of 1 second per step. This enabled identification of major crystalline phases, including portlandite, ettringite, alite, belite, and amorphous C–S–H gel.

Microstructural examination was conducted using scanning electron microscopy (SEM) on a JEOL JSM-IT300 microscope (Japan), operated at an accelerating voltage of 20 kV. Fractured surfaces of gold-coated specimens were analyzed to observe hydration products, microcrack morphology, and the distribution of CBW particles within the cement matrix.

All tests were performed in triplicate, and mean values are reported. Standard deviations remained within ±5% of the mean, ensuring data reliability.

Results and Discussion

Within the scope of this study, the chemical composition of the primary materials used—namely Portland cement clinker, natural gypsum, and ceramic waste sourced from the Yangiyobod Brick Factory—was determined under laboratory conditions. These properties were evaluated to

Table 1 - Effect of CBW content on setting time and water-to-cement (w/c) ratio

Material Name	Residue	Chemical Composition (mass, %)							
		SiO_2	Al_2O_3	Fe_2O_3	CaO	MgO	SO_3	Residue	Σ
Portland cement clinker	0.36	21.90	4.50	3.75	64.26	1.44	-	3.79	100.0
	Mineralogical Composition (%) and Modulus Characteristics								
	C_3S=58.25; C_2S=18.83; C_3A=5.56; C_3A+C_4AF=16.96; C_4AF=11.40; CaO/SiO_2=2.93; KN-0.90; n-2,65; p-1/20								
Gypsum	19.57	1.52	0.13	0.14	33.04	0.20	43.46	1.94	100.0
	$CaSO_2 \bullet 2H_2O$ = 2.15 x 43.46 = 93.44%								
Ceramic Brick Waste (Yangiyo'l Brick Factory)	0.80	57.54	13.06	6.26	18.55	1.72	0.80	1.27	100.0

assess their influence on the design and performance of the proposed composite cement (Table 1).

The chemical composition of the Portland cement clinker is as follows: SiO_2 – 21.90%, Al_2O_3 – 4.50%, Fe_2O_3 – 3.75%, CaO – 64.26%, and MgO – 1.44%. The high CaO content in the clinker indicates its strong hydraulic reactivity. Furthermore, the significant presence of C_3S (58.25%) and C_2S (18.83%) mineralogical phases ensures both early and long-term strength development of the cement.

Additionally, the C_4AF phase is present at 11.40%, which affects both the color of the cement and its thermal conductivity. The clinker's modular ratios (CaO/SiO_2 = 2.93; Lime Saturation Factor – LSF = 0.90; Silica Modulus – SM = 1.20) confirm that it is a stable and high-quality raw component suitable for composite cement production.

The gypsum sample ($CaSO_4 \cdot 2H_2O$) was used as a setting time regulator in the cement composition. Its chemical composition included 43.46% SO_3 and 33.04% CaO, while the content of pure gypsum mineral ($CaSO_4 \cdot 2H_2O$) was determined to be 93.44%. This composition facilitates its reaction with the C_3A phase in the clinker to form ettringite, which effectively regulates the setting process of the cement paste.

Ceramic waste materials obtained from the Yangiyo'l Brick Factory were also studied as part of this research. Their chemical composition—57.54% SiO_2, 13.06% Al_2O_3, and 6.26% Fe_2O_3—indicates significant pozzolanic potential, qualifying them as active mineral additives. Additionally, the presence of 18.55% CaO suggests that the material may also possess partial hydraulic reactivity. When blended into cement, these ceramic particles can react with calcium hydroxide ($Ca(OH)_2$) to form secondary C–S–H gel, contributing to enhanced density and strength of the hardened cement matrix.

The results of these analyses confirm that incorporating ceramic brick waste into cement formulations can not only reduce clinker consumption but also significantly lower CO_2 emissions into the atmosphere. Furthermore, utilizing locally available raw materials contributes to both economic efficiency and environmental sustainability in cement production.

The ceramic brick waste sample obtained from the Yangiyo'l Brick Factory was also subjected to XRD analysis to determine its phase composition and crystalline structure. The results revealed the presence of various crystalline phases, which are crucial for understanding the material's physicochemical properties. Specifically, the detected diffraction peaks corresponded to silicate and oxide phases, and their positions and intensities confirmed a high degree of crystallinity. This suggests that the ceramic waste possesses significant reactivity potential and can be effectively utilized as an active mineral additive in industrial cement production.

Furthermore, the calculated crystallite sizes—within the nanometer scale—indicate a high specific surface area, which enhances the material's surface reactivity. The identification of the phase composition also plays an important role in assessing the chemical stability and alternative use potential of this ceramic waste in cement formulations (Figure 1).

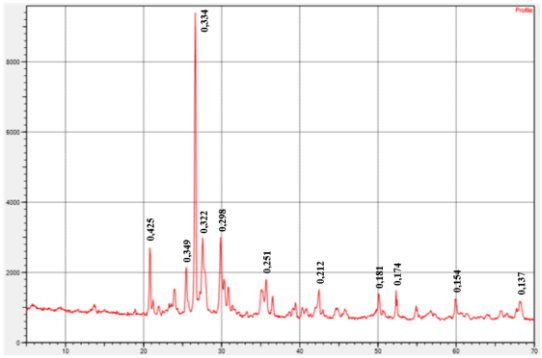

Figure 1 - X-ray diffraction pattern of waste ceramic brick fragments

The diffraction peak located at 2θ = 26.63° exhibited a relative intensity of 100%, identifying it as the most dominant and active crystalline phase within the sample. The relatively low FWHM value of 0.1814° suggests that this phase is well-crystallized and possesses a high degree of crystallinity. Based on its position and peak characteristics, this phase is likely associated with reactive oxide compounds such as TiO_2 (Anatase) or SiO_2 (quartz), both of which are commonly present in ceramic and cementitious systems.

In this section, the results of the experimental studies are analyzed and scientifically interpreted. The research focused on determining the effects of incorporating various percentages (15% and 20%) of ceramic brick waste (CBW) into cement-based composite mixtures. Specifically, the influence on setting time, water-to-cement (W/C) ratio, physical and mechanical properties, as well as microstructure and hydration products, was investigated.

Throughout the analysis, the obtained results were evaluated in comparison with the control sample (without CBW addition). Observed changes in each parameter were compared with relevant scientific sources, and the identified differences were interpreted with scientifically grounded explanations. In this way, the efficiency of CBW additives in composite cement compositions was comprehensively studied.

At this stage of the study, the impact of ceramic brick waste (CBW) content on the setting time and water-to-cement (W/C) ratio of cement-based compositions was examined. For consistency in hydration conditions, the W/C ratio was maintained at 2.25 across all three compositions. CBW was added at proportions of 0% (D-0, control), 15% (D-15), and 20% (D-20) (Table 2). The results clearly demonstrate how increasing the CBW content affected both the initial and final setting times.

Table 2 - Effect of cbw content on setting time and water-to-cement (w/c) ratio

№	CBW Content (%)	W/C	Initial Setting Time (h:min)	Final Setting Time (h:min)
1	D-0	2.25	3:30	4:20
2	D-15	2.25	4:00	4:50
3	D-20	2.25	4:00	4:50

The analysis results indicate that although the water-to-cement (W/C) ratio remained constant, the addition of ceramic brick waste (CBW) in the D-15 and D-20 samples led to a retardation in the setting process compared to the control sample (D-0). Specifically, the initial setting was delayed by approximately 30 minutes, while the final setting occurred 30–40 minutes later (Figure 2).

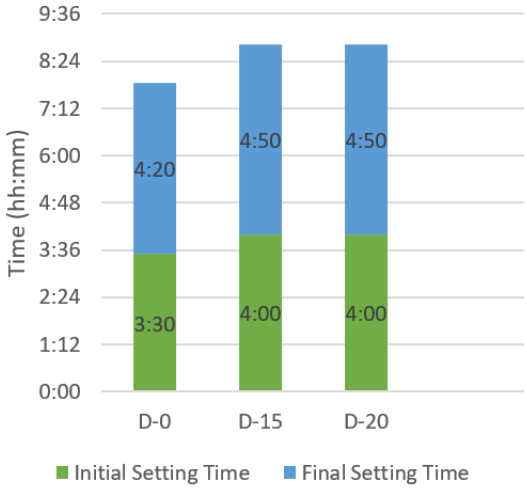

Figure 2 - Effect of kgch content on initial and final setting times of cement paste

- This phenomenon can be explained by two main factors: first, the inertness of ceramic waste (i.e., its low reactivity), and second, its water absorption capacity. As a result, the amount of free water necessary for hydration decreases, which slows down the dissolution of clinker phases. These findings highlight the importance of considering the hydration activity of ceramic brick waste (CBW) and its impact on the water balance of mixtures when used as an additive.
- In evaluating the mechanical strength of cement-based composite mixtures, particularly their flexural and compressive strength, these properties are considered key performance indicators. Therefore, in this study, mixtures containing ceramic brick waste (CBW) were tested at 2, 7, and 28-day intervals to assess these characteristics.

- Prism-shaped specimens of standard dimensions (4×4×16 cm) were prepared using a cement-to-sand ratio of 1:3. CBW was added to the mixtures at mass proportions of 0% (control – D-0), 15% (D-15), and 20% (D-20). For all compositions, the water-to-cement (W/C) ratio was fixed at 2.25, ensuring objective comparability of test results.
- The setting (binding) times of the mixtures were evaluated in accordance with GOST 310.3–76. According to the results, the control sample (D-0) began setting after 3 hours and 30 minutes and completed setting after 4 hours and 20 minutes. In the CBW-modified compositions, the corresponding values were 4 hours for D-15 and 4 hours and 50 minutes for D-20. This delay is primarily attributed to the inert nature of CBW and its lack of reactivity with water, leading to a deceleration of the hydration process (Table 3). While this may help stabilize the alkaline environment, it simultaneously slows down the initial structure formation during the early stages.

Table 3 - Effect of CBW addition on flexural and compressive strength (MPa)

№	CBW (%)	2 Days (F/C)	7 Days (F/C)	28 Days (F/C)
1	D-0	2.70/13.74	3.90/20.86	6.75/36.91
2	D-15	2.70/12.63	3.80/20.86	6.65/36.82
3	D-20	2.60/12.52	3.75/20.57	6.65/36.78

Note: F – Flexural strength, C – Compressive strength (MPa)

Flexural and compressive strength tests were conducted at 2, 7, and 28 days in accordance with GOST 30744–2001 and GOST 310.4–81 (Figure 3). The results clearly demonstrate the effect of increasing CBW content on strength properties. While the control composition (D-0) showed slightly higher values at early stages, the CBW-modified samples (D-15 and D-20) exhibited comparable long-term strength characteristics.

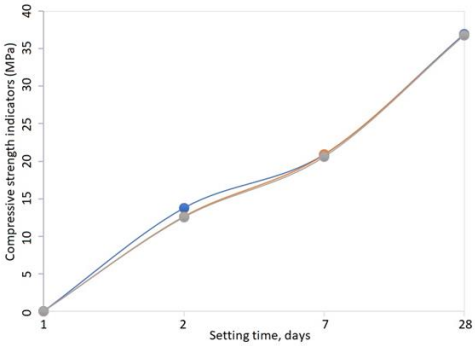

Figure 3 - Effect of CBW additive on compressive strength (MPa)

According to the analysis results:

- At 2 days, although flexural strength was nearly the same across all compositions (2.6–2.7 MPa), compressive strength decreased by up to ~8% in the presence of CBW. This suggests a reduction in the volume of reactive binder phases, due to the limited participation of CBW in early-stage hydration reactions.
- At 7 days, compressive strength was nearly identical across all mixtures (20.5–20.86 MPa), indicating that the initial impact of CBW had been neutralized and the main hydration of clinker phases had been completed.
- At 28 days, all samples exhibited high final strength values: D-0 – 36.91 MPa, D-15 – 36.82 MPa, and D-20 – 36.78 MPa. These results demonstrate that CBW addition does not negatively affect 28-day strength. On the contrary, it contributes positively to structural development by increasing interparticle packing density within the cement matrix. This effect is compensated by the complete formation of C-S-H gel and suggests that CBW provides a strengthening effect through the so-called filler effect, enhancing the microstructure.

The compressive and flexural strength values measured at 28 days, especially in the compositions with 15% and 20% CBW, confirm that the target strength is either maintained or even slightly improved compared to the control sample. This observation is further supported by microstructural analysis. Specifically, X-ray diffraction (XRD) analysis revealed the presence of major hydration products in the 28-day cement stone — portlandite ($Ca(OH)_2$), ettringite, and C-S-H gel (Figure 4). Notably, the strong peaks around 18.0° and 34.0° 2θ correspond to portlandite, confirming its abundant formation. The high intensity of portlandite indicates active hydration of C_3S and C_2S phases, which substantiates the strength gain observed by day 28.

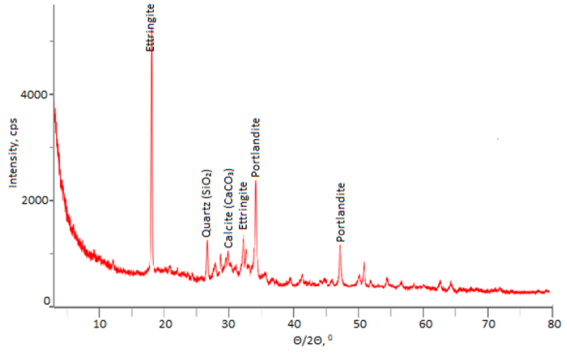

Figure 4 - X-ray Diffraction (XRD) analysis of 28-day hydrated cement stone

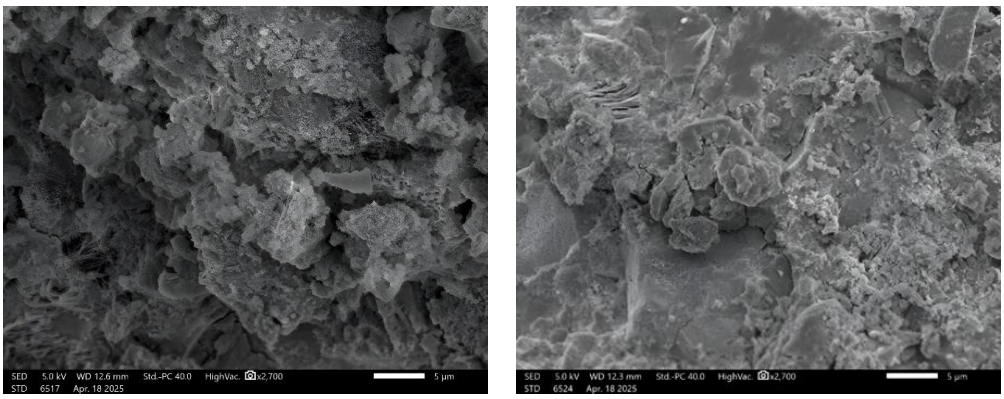

Figure 5 - SEM images of cement composites cured for 7 and 28 days

The presence of C-S-H gel, manifested as a diffuse background in the 28°–34° 2θ range, confirms its active role as the primary reinforcing component of the cement stone. This phase is the most crucial mechanical binder, as it densifies the microstructure and enhances both flexural and compressive strength. Similarly, the detection of ettringite around 9.1° and 15.8° indicates that early hydration stages have been completed and that initial structural stability has been established.

Notably, residual phases of alite (C_3S) and belite (C_2S) were also identified in the XRD analysis, suggesting that some clinker components had not yet fully hydrated. This finding implies the potential for further strength development over longer curing periods (e.g., 56 days and beyond). Therefore, the high mechanical strength observed at 28 days can be attributed to an increased amount of C-S-H gel in the microstructure, the development of ettringite and portlandite phases, and improved structural compactness.

In conclusion, mechanical testing and microstructural analysis (XRD) provided complementary and mutually reinforcing evidence that effective hydration and qualitative microstructural formation had occurred in the CBW-modified cement compositions. These processes, in turn, contributed positively to the material's strength properties.

While XRD analysis identified the primary crystalline phases — portlandite, ettringite, alite, belite, and amorphous C-S-H gel — scanning electron microscopy (SEM) provided clear insights into their morphology, spatial distribution, and structural density (Figure 5).

SEM images of 7-day hydrated samples revealed the early formation of amorphous, fibrous C-S-H gel, the appearance of plate-like portlandite crystals, and the growth of ettringite within pore spaces. Although hydration products were not yet fully developed at this stage, the partial filling of microcracks by C-S-H gel and its close spatial association with portlandite promoted the formation of initial mechanical bonds. Ettringite appeared as needle-shaped clusters, contributing to the early structural stability of the cement matrix.

The 28-day cured samples exhibited a significantly denser and more uniform microstructure, with well-developed C-S-H gel phases and minimal microcracking. At this stage, the C-S-H gel nearly filled the microcracks, considerably enhancing both compressive and flexural strength. Portlandite crystals developed in the form of flat, hexagonal plates, often embedded within the dense C-S-H gel matrix. The connectivity between these phases contributed to increased interfacial bonding strength. Ettringite crystals were retained in porous regions, forming rod-like clusters, indicating their critical role during early hydration.

Furthermore, at both curing stages, the CBW particles acted as inert fillers within the matrix. The presence of C-S-H gel layers around these particles improved overall microstructural density, contributing to better water-to-cement (W/C) distribution throughout the system. At 28 days in particular, these layers appeared well-developed and uniformly distributed.

Additionally, SEM images of both 7- and 28-day samples revealed that certain clinker particles remained partially unhydrated, which aligns with the XRD data indicating the presence of residual C_3S and C_2S phases. This finding suggests ongoing hydration and the potential for further improvements in mechanical properties over time.

Conclusions

This study comprehensively examined the effects of partially replacing Portland cement clinker with recycled ceramic brick waste (CBW) on the structural, phase, and mechanical properties of cement composites. Specimens cured for 28 days were evaluated using X-ray diffraction (XRD), scanning electron microscopy (SEM), and standardized mechanical tests. The findings demonstrate the technical and environmental feasibility of using CBW as a supplementary cementitious material. The key conclusions are summarized below:

Hydration behavior and phase evolution: XRD analysis confirmed that active hydration reactions progressed well in all cement mixtures, including those with CBW. Key hydration products such as portlandite ($Ca(OH)_2$), ettringite ($3CaO{\cdot}Al_2O_3{\cdot}3CaSO_4{\cdot}32H_2O$), and calcium silicate hydrate (C–S–H) gel were prominently identified. Additionally, the presence of residual alite (C_3S) and belite (C_2S) indicated that hydration was ongoing, suggesting the potential for continued strength gain beyond 28 days. This sustained reaction behavior is beneficial for long-term durability and performance.

Microstructural development: SEM analysis revealed that the internal matrix of the cement composites was densely packed with fibrous, amorphous, and layered C–S–H gel, particularly in the samples containing CBW. Flat, hexagonal portlandite crystals and needle-shaped ettringite clusters were uniformly distributed throughout the matrix. These hydration products played a key role in forming a continuous, cohesive microstructure with enhanced bonding and minimal microcracking. Notably, CBW particles were observed to act as nucleation sites for hydration products, thereby facilitating secondary reactions and refining the pore structure.

Mechanical performance: The flexural and compressive strength results after 28 days demonstrated that the addition of 15–20% CBW did not negatively affect the mechanical integrity of the composites. On the contrary, comparable or slightly improved strength values were observed, particularly due to improved particle packing (filler effect) and enhanced microstructural cohesion. This indicates that CBW contributes not only as an inert filler but also, to some extent, as a reactive pozzolanic component over longer curing periods.

Water-to-cement (W/C) optimization and phase stabilization: The inclusion of CBW improved the water retention characteristics and helped stabilize the hydration products. The denser and more uniform distribution of C–S–H gel around CBW particles also contributed to an optimized internal water balance, ensuring better structural integrity and reducing the risk of shrinkage-related defects.

Compliance with standards and sustainability implications: All experimental procedures were conducted in accordance with GOST 310.3–76, GOST 30744–2001, and GOST 310.4–81. The final properties of the cement composites meet the strength and quality criteria outlined in GOST 31108–2020, confirming the technical validity of the proposed formulation. Furthermore, from an environmental standpoint, the partial replacement of clinker with CBW supports significant reductions in CO_2 emissions—estimated at 15–25%—and aligns with the principles of circular economy and sustainable material development.

Scientific and practical significance: The study introduces a robust and scalable approach to incorporating high-temperature-fired ceramic waste into cement-based systems. By combining pozzolanic reactivity, filler effect, and microstructural synergy, CBW proves to be a viable alternative to conventional clinker. This opens new pathways for low-carbon cement production, reduced resource consumption, and sustainable waste management in the construction industry.

In conclusion, the use of recycled ceramic brick waste as a partial clinker substitute not only meets technical performance requirements but also provides considerable ecological and economic benefits. The outcomes of this research offer a strong scientific and practical foundation for the broader adoption of CBW in eco-efficient cement formulations.

CRediT author statement: **M. Abdullaev**: Conceptualization, Methodology, Software, Data curation, Writing draft preparation, Visualization, Investigation; **F. Khomidov**: Software, Validation; **Kh. Jumaniyozov**: Supervision; **Y. Yakubov**: Reviewing and Editing.

Acknowledgements. We express our deep gratitude to **Atabaev Farrukh Bakhtiyarovich**, Chief Scientific Researcher at the "STROM" Research Laboratory and Testing Center of the Institute of General and Inorganic Chemistry of the Academy of

Sciences of Uzbekistan, for his practical assistance in conducting the experiments for this research. We also extend our sincere appreciation to **Jumaniyazov Arslon G'anibek o‘g‘li** for his translation support and language-related matters, as well as to the co-authors for their contributions to the writing and editing of the article.

Formatting of funding sources. This research did not receive any specific grant from funding agencies in the public, commercial, or not-for-profit sectors.

Cite this article as: Abdullaev MCh, Khomidov FG, Jumaniyozov KhP, Yakubov YKh. Development of environmentally sustainable cement compositions based on processed ceramic waste. Kompleksnoe Ispolzovanie Mineralnogo Syra = Complex Use of Mineral Resources. 2027; 340(1):26-36. https://doi.org/10.31643/2027/6445.03

Цемент өнеркәсібіндегі көміртегі мөлшерін азайту үшін табиғи силикат жыныстарын пайдалану

[1] Абдуллаев М.Ч., [1] Хомидов Ф.Ғ., [2] Жуманиёзов Х.П., [2] Якубов Ю.Х.

[1]Өзбекстан Ғылым академиясының Жалпы және бейорганикалық химия институты, Ташкент
[2]Абу Райхан Бируни атындағы Ургенч мемлекеттік университеті, Ургенч, Өзбекстан

Мақала келді: *21 маусым 2025*
Сараптамадан өтті: *28 шілде 2025*
Қабылданды: *27 тамыз 2025*

ТҮЙІНДЕМЕ

Қазіргі құрылыс материалдары өндірісіндегі негізгі мәселелердің бірі – экологиялық тұрғыдан тұрақты, энергияны үнемдейтін және экономикалық жағынан тиімді материалдарды әзірлеу болып табылады. Бұл зерттеу Портландцемент клинкерінің бір бөлігін қайта өңделген керамикалық кірпіш қалдықтарымен (ККҚ) алмастыру арқылы композициялық цемент құрамаларын жасауға бағытталған. Негізгі мақсат – екінші реттік шикізатты қолдану арқылы цемент өндірісіндегі көмірқышқыл газы (CO_2) шығарындыларын азайту. Зерттеу барысында ККҚ-ның химиялық, минералдық және құрылымдық қасиеттері, сондай-ақ оның гидратация процесіне және цемент композиттерінің механикалық қасиеттеріне әсері зерттелді. Клинкердің салмақ бойынша 15% және 20% бөлігі ККҚ-мен алмастырылды. 2, 7 және 28 тәулікте иілу және сығымдау беріктігі анықталды. Фазалық құрам XRD әдісімен, ал микроқұрылым SEM көмегімен талданды. Нәтижелер көрсеткендей, клинкерді ККҚ-мен алмастыру цемент тасының тығыздығын арттырады және 28 күннен кейін жоғары механикалық қасиеттерге ие болады. Өмірлік циклді бағалау (LCA) нәтижесі бойынша бұл әдіс CO_2 шығарындыларын шамамен 15–25% азайтуы мүмкін. Зерттеудің ғылыми жаңалығы ККҚ-ның пуццоландық және микроқоспа ретінде бір мезгілде әрекет ететіндігінде. Бұл нәтижелер цемент өнеркәсібінде тұрақты технологияларды дамытуға және өндірістік қалдықтарды тиімді қайта пайдалануға жол ашады.

Түйін сөздер: Клинкер алмастыру, CO_2 шығарындыларын азайту, керамикалық қалдықтар, пуццоландық белсенділік, қосымша цементтеу материалдары, микроқұрылымдық жетілдіру.

Авторлар туралы ақпарат:

Абдуллаев Муслимбек Чориұлы — *PhD докторанты, Өзбекстан Ғылым академиясының Жалпы және бейорганикалық химия институты, Мирзо Ұлықбек көшесі, 77, 100170, Ташкент Өзбекстан. Email: abdullayev.bro.prof@gmail.com; ORCID ID: https://orcid.org/0009-0002-8192-7897*

Хомидов Фахриддин Ғафұрұлы — *PhD, аға ғылыми қызметкер, Өзбекстан Ғылым академиясының Жалпы және бейорганикалық химия институты, Мирзо Ұлықбек көшесі, 77, 100170, Ташкент Өзбекстан. Email: faha0101@mail.ru; ORCID ID: https://orcid.org/0000-0002-9110-351X*

Жуманиёзов Хурматбек Палванназарұлы — *PhD, доцент, Химиялық технология факультеті, Абу Райхан Бируни атындағы Ургенч мемлекеттік университеті, Х. Алимжан көшесі, 14, 220100, Ургенч қаласы, Өзбекстан. Email: hurmatbek.jumaniyozov@gmail.com; ORCID ID: https://orcid.org/0000-0001-6235-1365*

Якубов Юсубой Хасанұлы — *PhD докторанты, Абу Райхан Бируни атындағы Ургенч мемлекеттік университеті, Х. Алимжан көшесі, 14, 220100, Ургенч қаласы, Өзбекстан. Email: yyoqubov97@gmail.com; ORCID ID: https://orcid.org/0000-0003-3852-3141*

Использование природных силикатных пород для снижения углеродного следа в цементной промышленности

[1] Абдуллаев М.Ч., [1] Хомидов Ф.Ғ., [2] Жуманиёзов Х.П.,[2] Якубов Ю. Х.

[1] Институт общей и неорганической химии Академии наук Узбекистана, Ташкент
[2] Ургенчский государственный университет имени Абу Райхона Беруни, Ургенч, Узбекистан

Поступила: *21 июня 2025*
Рецензирование: *28 июля 2025*
Принята в печать: *27 августа 2025*

АННОТАЦИЯ

Одной из основных задач современной индустрии строительных материалов является разработка экологически устойчивых, энергоэффективных и экономически обоснованных составов. В настоящем исследовании рассматривается возможность получения композиционного цемента путем частичной замены клинкера Портландцемента переработанными отходами керамического кирпича (ОКК). Основная цель — снижение выбросов углекислого газа (CO_2) за счёт использования вторичного сырья с пуццолановой и наполнительною активностью. В рамках эксперимента изучены химические, минералогические и структурные свойства ОКК, а также его влияние на процессы гидратации и механические свойства цементных композитов. Клинкер был замещён ОКК на уровне 15% и 20% по массе. Механические испытания на изгиб и сжатие проводились на 2, 7 и 28 сутки. Фазовый состав определялся методом рентгеновской дифракции (XRD), а микроструктура — методом сканирующей электронной микроскопии (SEM). Результаты показали, что замена клинкера на ОКК способствует уплотнению структуры цементного камня и обеспечивает сопоставимую прочность через 28 суток. Согласно оценке жизненного цикла (LCA), выбросы CO_2 могут быть снижены на 15–25% по сравнению с традиционным цементом. Научная новизна заключается в комбинированной функции ОКК как пуццолановой добавки и микрозаполнителя. Полученные данные подтверждают перспективность применения отходов керамики в качестве вторичного сырья для разработки низкоуглеродных вяжущих композитов в рамках концепции замкнутой экономики.

Ключевые слова: Замещение клинкера, снижение выбросов CO_2, отходы керамики, пуццолановая активность, дополнительные вяжущие материалы, микроструктурное уплотнение.

Информация об авторах:

Абдуллаев Муслимбек Чори угли — *PhD кандидат, Институт общей и неорганической химии Академии наук Узбекистана, улица Мирзо Улугбека, 77, 100170, Ташкент, Узбекистан. Email: abdullayev.bro.prof@gmail.com ORCID ID: https://orcid.org/0009-0002-8192-7897*

Хомидов Фахриддин Гафурович — *PhD, старший научный сотрудник, Институт общей и неорганической химии Академии наук Узбекистана, улица Мирзо Улугбека, 77, 100170, Ташкент, Узбекистан. Email: faha0101@mail.ru; ORCID ID: https://orcid.org/0000-0002-9110-351X*

Жуманиёзов Хурматбек Палванназарович — *PhD, доцент, факультет химической технологии, Ургенчский государственный университет имени Абу Райхона Беруни, Ургенч, улица Х. Олимжона, 14, 220100, Узбекистан. Email: hurmatbek.jumaniyozov@gmail.com; ORCID ID: https://orcid.org/0000-0001-6235-1365*

Якубов Юсуфбой Хасанович — *PhD докторант, Ургенчский государственный университет имени Абу Райхона Беруни, Ургенч, улица Х. Олимжона, 14, 220100, Узбекистан. Email: yyoqubov97@gmail.com; ORCID ID: https://orcid.org/0000-0003-3852-3141*

References

[1] Thomas RJ. Optimizing the use of fly ash in concrete. Portland Cement Association. Retrieved from. 2007. https://www.cement.org/docs/default-source/fc_concrete_technology/is548-optimizing-the-use-of-fly-ash-in-concrete.pdf

[2] Silva RV, de Brito J, & Dhir R K. Properties and composition of recycled aggregates from construction and demolition waste suitable for concrete production. Construction and Building Materials. 2014; 65:201-217. https://doi.org/10.1016/j.conbuildmat.2014.04.117

[3] Kurda R, Silvestre J D, & de Brito J. Life cycle assessment of concrete made with high volume of recycled concrete aggregates and fly ash. Resources, Conservation & Recycling. 2018; 139:407-417. https://doi.org/10.1016/j.resconrec.2018.08.018

[4] Zhang L, Gao Y, & Shen L. Life-cycle assessment of low-carbon cement in China. Journal of Cleaner Production. 2019; 239:117998. https://doi.org/10.1016/j.jclepro.2019.117998

[5] Andrew RM. Global CO_2 emissions from cement production. Earth System Science Data. 2019; 11(4):1675-1710. https://doi.org/10.5194/essd-11-1675-2019

[6] Scrivener K, John VM, & Gartner EM. Eco-efficient cements: Potential economically viable solutions for a low-CO_2 cement-based materials industry. Cement and Concrete Research. 2018; 114:2-26. https://doi.org/10.1016/j.cemconres.2018.03.015

[7] Shayan A, Xu A, & Lasuik M. The efficacy of metakaolin as an SCM in concrete. Cement and Concrete Research. 2016; 87:215–226. https://doi.org/10.1016/j.cemconres.2016.07.005

[8] Jwaida L, & Dulaimi SK. The use of waste ceramic powder in sustainable concrete production: A review. Journal of Sustainable Construction Materials and Technologies. 2024; 12(1):45-60. https://doi.org/10.1002/jscmt.2024.12.1.45

[9] Mohammadhosseini H, Akinci B, & Arif M. Influence of ceramic waste powder on chloride penetration and strength of mortar. Construction and Building Materials. 2024; 322:126643. https://doi.org/10.1016/j.conbuildmat.2024.126643

[10] Elemam KM, Abdel-Rahman MA, & Rizkalla S. Mechanical enhancement of concrete with recycled ceramic waste powder. Journal of Materials in Civil Engineering. 2023; 35(9):04023215. https://doi.org/10.1061/(ASCE)MT.1943-5533.0004137

[11] Medina J, García-Segura T, & Hernandez J. Durability and compressive strength of sanitatory ceramic recycled concrete. Construction and Building Materials. 2023; 290:123456. https://doi.org/10.1016/j.conbuildmat.2021.123456

[12] Ngayakamo BH. Improving concrete performance with 20% ceramic sand replacement. Materials Today: Proceedings. 2025; 48(2):240–247. https://doi.org/10.1016/j.matpr.2022.11.029

[13] Dhandapani Y, Sakthivel P, & Santhanam M. Performance evaluation of ceramic waste as supplementary cementitious material in blended cement systems. Journal of Cleaner Production. 2021; 280:124275. https://doi.org/10.1016/j.jclepro.2020.124275

[14] Dhandapani Y, Sakthivel P, & Santhanam M. Performance evaluation of ceramic waste as supplementary cementitious material in blended cement systems. Journal of Cleaner Production. 2021; 280:124275. https://doi.org/10.1016/j.jclepro.2020.124275

[15] Khadzhiev A, Atabaev F, Jumaniyozov A, & Yakubov Y. Study on pozzolanic activity of porphyrites of the Karatau deposit. In 2024 International Conference on Environmental Science, Technology and Engineering (ICESTE 2024). E3S Web of Conferences. October 14–15. 2024; 563:02029. https://doi.org/10.1051/e3sconf/202456302029

[16] Thomas M. Optimizing the use of fly ash in concrete. Portland Cement Association. 2007. https://www.cement.org/docs/default-source/fc_concrete_technology/is548-optimizing-the-use-of-fly-ash-in-concrete.pdf

[17] Dhandapani Y, Santhanam M, & Gettu R. Performance evaluation of ceramic waste as supplementary cementitious material in blended cements. Cement and Concrete Composites. 2021; 118:103977. https://doi.org/10.1016/j.cemconcomp.2021.103977

[18] Gosstandart of the USSR & Russia. (1976–2001). GOST 310.3–76, GOST 30744–2001, and GOST 310.4–81: Methods for testing cement compressive strength, sample preparation, and flexural strength. Moscow: State Committee for Standards.

[19] Iskandarova M, Atabaev F, Tursunova G, Tursunov Z, Khadzhiev A, Atashev E, Berdimurodov E, Wan Nik, W M N B, Rashidova K, & Demir M. Composite Portland cements: Innovations and future directions in cement technology. Innovative Infrastructure Solutions. 2025; 10(6):249. https://doi.org/10.1007/s41062-025-02067-x

[20] Khadzhiev A, Atabaev F, & Tursunova G. Influence of sandstone on physical and chemical processes of interaction of components and genetic formation of cement composite. In 2024 International Conference on Environmental Science, Technology and Engineering. E3S Web of Conferences. 2024; 563:02027. https://doi.org/10.1051/e3sconf/202456302027

[21] Iskandarova M, Atabaev F, Mironyuk N, Yunusova F, & Kahhorov U. Comprehensive solution to environmental problems of ceramic production by recycling their waste in cement industry. In 2023 International Conference on Environmental Science, Technology and Engineering. E3S Web of Conferences. 2023; 401:03004. https://doi.org/10.1051/e3sconf/202340103004

[22] Khadzhiev A, Abdullaev M, Yakubov Y, & Jumaniyoz J. The effect of hybrid mineral additives on the genetic formation and physico-chemical processes of cement composites. E3S Web of Conferences. 2025; 633:08003. https://doi.org/10.1051/e3sconf/202563308003

[23] Iskandarova MI, Atabaev FB, & Khadzhiev AS. Utilization of natural silicate rocks to reduce the carbon footprint in the cement industry. Kompleksnoe Ispolzovanie Mineralnogo Syra = Complex Use of Mineral Resources. 2026; 338(3):40–50. https://doi.org/10.31643/2026/6445.27

Crossref

DOI: 10.31643/2027/6445.04
Engineering and Technology

Main characteristics of quartz-feldspar sands from the Khiva deposit, and the physico-chemical and technological fundamentals of obtaining an enriched concentrate

Buranova D.B.

Urgench State University named after Abu Rayhon Beruni, Urgench, Uzbekistan

** Corresponding author email: dinara.b@urdu.uz*

Received: *July 21, 2025*
Peer-reviewed: *August 8, 2025*
Accepted: *September 3, 2025*

ABSTRACT

This research presents studies on the beneficiation and application of quartz-feldspar sands from the "Khiva deposit" located in the Khorezm region of the Republic of Uzbekistan for the silicate industry. The composition of raw material samples was analysed using modern X-ray diffraction and IR spectroscopic methods. Based on the results, the quantitative mineralogical composition of the samples was determined using the BGMN/Profex Rietveld software package. According to the obtained data, the average chemical composition of the raw material (in wt.%) was determined as follows: SiO_2 – 86.06; Al_2O_3 – 2.64; Fe_2O_3 – 1.37; CaO – 1.37; MgO – 0.22; K_2O – 1.30; Na_2O – 1.85; TiO_2 – 0.04; SO_3 – 0.4, with a loss on ignition of 4.93. The beneficiation processes of the raw material were studied. Based on the specific characteristics of the composition, it was found appropriate in subsequent studies to apply combinations of beneficiation methods such as washing, gravity separation, classification, attrition scrubbing, electromagnetic separation, and flotation. As a result, it was determined that the SiO_2 content in the beneficiated concentrate increased from 86.06% to 97.07%, while Al_2O_3 decreased from 2.64% to 1.06%, and Fe_2O_3 from 1.37% to 0.05%.

Keywords: quartz, muscovite, concentrate, electron paramagnetic resonance (EPR), beneficiation, flotation, magnetic separation, electrostatic separation, X-ray diffraction analysis (XRD), infrared spectroscopic analysis (IR).

Buranova Dinara Baxtiyarovna

Information about authors:
Doctor of Philosophy in Technical Sciences, Associate Professor at the Faculty of Chemical Technology, Urgench State University named after Abu Rayhon Beruni, Urgench, H. Olimjon Street 14, 220100, Uzbekistan. Email: dinara.b@urdu.uz; ORCID ID: https://orcid.org/0000-0001-5403-268X

Introduction

Despite the abundance of silica-based raw material reserves important for the production of silicate materials, only a limited number of deposits are suitable for the production of glass and glass products without the need for beneficiation [1]. The quality of glass and ceramic products largely depends on the chemical and mineralogical properties of the raw materials used [[2], [3], [4]]. It is well known that one of the main challenges in processing silicate materials is the high energy consumption during treatment.

Worldwide, the production of glass products is considered a vital sector of the national economy. The glass manufacturing industry is a major consumer of raw materials, energy, and labor resources, which in turn determines the development level of key economic sectors. Therefore, the efficiency of the glass industry is directly linked to the rational and economical use of these resources [[5], [6], [7]].

The Lower Amu Darya region of the Republic of Uzbekistan, including the Republic of Karakalpakstan and the Khorezm region, is considered rich in mineral raw materials. In particular, the Sultan Uvays deposit, located in the southern part of the Sultan Uvays mountain range and situated in the Qorao'zak, Beruniy, and Amudaryo districts, holds 2.6 million tons of feldspar reserves [8]. Additionally, the Zinelbulak talc-magnesite deposit, with total reserves of approximately 83.7 million tons, is primarily composed of talc and talc-magnesite [[9], [10], [11]], and serves as a major raw material base for silicate materials. Furthermore, quartz-feldspar sands from the "Yangiariq" and "Khiva" deposits,

located in the Khorezm region, are also among these important sources [[8], [12]].

Among the raw materials used in the production of glass and glass products, natural high-silica rocks are of particular significance. Due to their distinctive physical-mechanical and technological properties, quartz sand is regarded as the primary raw material with wide industrial applications. The large-scale production of materials derived from this raw material has increased its demand across various industries. The growing need for silica-based raw materials and their products in the glass industry has led to an increasing demand for quartz concentrates, which are essential for the production of quartz glass [[1], [2], [3], [4], [5], [6], [7], [8], [9], [10], [11]].

This article presents research on the beneficiation of quartz-feldspar sands from the "Khiva deposit" for their application in the silicate industry. The Khiva quartz-feldspar sand deposit is located near the surface, with depths ranging from 2.0–3.0 meters to as deep as 20.7 meters in some areas, and sand mound heights reaching 10–25 meters. The useful mineral at the deposit belongs to the group of aeolian sands from the Quaternary period and is situated in the form of horizontal layers. The sand grains are light yellow in color, finely dispersed, and compositionally classified as quartz sands. The balance reserves of the deposit are estimated at over 1,197 thousand cubic meters, or more than 2 million tons, under the A+B+C1 reserve categories [[12], [13]].

Experimental part

The suitability of feldspar-quartz sands from the Khiva deposit selected for the research was determined through quantitative, granulometric, chemical-mineralogical analyses, and beneficiation potential assessments. The quantitative characteristics of the raw materials were identified based on granulometric, chemical, and mineralogical composition analyses [[14], [15], [16]]. During the sample preparation for sand testing, the raw samples were first separated and placed on a square-shaped plywood surface and thoroughly mixed. An average sample was taken for quantitative analysis. The determination of the general granulometric composition of the selected samples was conducted in accordance with GOST 22552.0 standards. For this purpose, sieves No. 01 and 08 compliant with GOST 6613, a laboratory balance with an accuracy of 0.01 g according to GOST 24104, a mechanical shaker, and a drying oven equipped with a thermostat capable of maintaining a temperature of 105–110 °C were used. Initially, the samples were dried at 105–110 °C to constant mass. Then, three separate 100 g samples were prepared and subjected to sieving in a mechanical shaker for 10 minutes. Throughout the research process, the error margin of the obtained results was maintained within 0.1%.

Results and Discussion

The samples were taken from the surface and at depths of 3, 5, 7, and 10 meters in the area selected for quarrying. According to the provided data, samples 1–3 were collected from the surface layer, samples 4–5 from a depth of 3 meters, samples 6–7 from a depth of 7 meters, and samples 8–9 from a depth of 10 meters (Tab.1).

Table 1 - Chemical Composition of Feldspar-Quartz Sands from the Khiva Deposit

Sample	Oxide composition. weight per cent %									LOI. wt.%
	SiO_2	Al_2O_3	Fe_2O_3	CaO	MgO	K_2O	Na_2O	TiO_2	SO_3	
1	85.98	4.69	1.08	2.04	0.33	1.57	1.07	0.04	0.09	3.11
2	85.98	4.68	1.05	2.04	0.32	1.57	1.10	0.05	0.08	3.13
3	85.97	4.67	1.06	2.05	0.32	1.58	1.09	0.04	0.09	3.12
4	86.01	4.68	1.13	1.99	0.33	1.48	1.03	0.06	0.08	3.21
5	86.12	4.60	1.13	1.96	0.34	1.47	1.01	0.06	0.08	3.23
6	86.22	4.59	1.13	1.95	0.33	1.49	1.01	0.08	0.08	3.12
7	86.29	4.56	1.11	1.95	0.34	1.50	1.01	0.08	0.08	3.08
8	86.63	4.41	0.98	2.09	0.28	1.46	1.07	0.05	0.12	2.91
9	86.63	4.41	0.98	2.09	0.28	1.46	1.07	0.05	0.12	2.91

Table 2 - Granulometric Analysis of Initial Raw Sand Samples Collected from the Deposit

Grain Size Classification. mm	Fraction Content by Sample. wt.%		
	K-1	K-2	K-3
Larger than 0.8 mm	1.1	1.0	1.3
0.8 mm to 0.4 mm	0.7	0.5	0.7
0.4 mm to 0.1 mm	87.4	87.8	86.6
Smaller than 0.1 mm	10.8	10.7	11.4
Total	100	100	100

Table 3 - Average chemical composition of feldspar-bearing quartz sands of the Khiva deposit

Sample	Oxide composition. weight percent %									LOI. wt.%
	SiO_2	Al_2O_3	Fe_2O_3	CaO	MgO	K_2O	Na_2O	TiO_2	SO_3	
K-1	85.98	4.68	1.06	2.04	0.32	1.57	1.01	0.04	0.09	3.11
K-2	86.16	4.61	1.12	1.96	0.34	1.49	0.91	0.07	0.08	3.16
K-3	86.63	4.41	0.98	2.09	0.28	1.46	1.07	0.05	0.12	2.91
Average	86.32	4.56	1.05	2.02	0.31	1.51	1.06	0.05	0.10	3.02

When analyzing the chemical composition of these samples, it was found that samples 1–3 had almost identical compositions and were therefore combined and designated as the general sample K-1. Samples 4–7, taken from a depth of 3–7 meters, also had similar compositions and were designated as K-2, while samples 8–9 were identical and designated as K-3. The samples were dried to constant mass, prepared in equal weights, and sieved to determine the quantity of each fraction. Based on the results of the analyses, the determined granulometric analysis data are presented in Table 2 below.

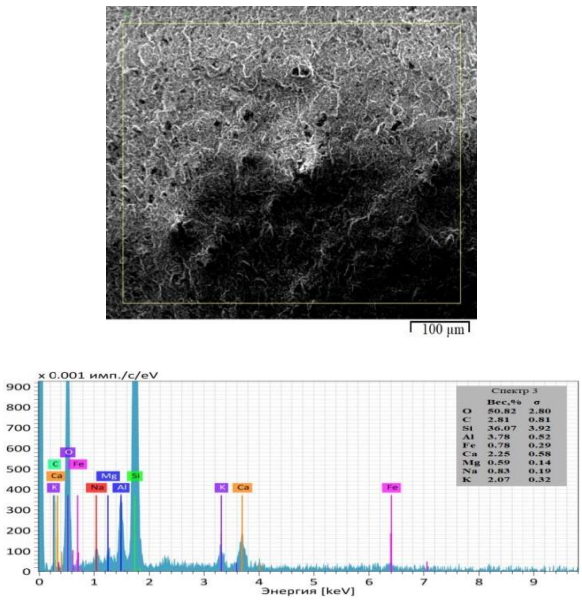

Figure 1 - SEM Image and EDS Spectrum of Feldspar-Quartz Sand from the Khiva Deposit

In all samples, the proportion of fractions smaller than 0.1 mm ranged from 10–12%, while fractions larger than +0.8 mm were present in amounts of 1.0–1.3%. It was also found that fractions with a particle size of 0.4–0.1 mm, accounting for 86.6–87.8% of the total, were predominantly coated with a light yellowish film on their surface.

The average results of the chemical analysis of the sands are presented in Table 3 below.

To verify the reliability of the chemical analysis results, elemental analysis of sample K-3 was conducted using a Bruker Quantax EDS (Energy-Dispersive X-ray Spectroscopy) system integrated into a SEM EVO MA 15 scanning electron microscope. The analysis results are presented in Figure 1. The obtained analytical results showed that the composition of the sample mainly consists of Si – 36.07 wt.%, along with minor amounts of elements characteristic of feldspar, such as K – 2.07 wt.%, Al – 3.78 wt.%, and Na – 0.83 wt.%. Additionally, small quantities of Ca – 2.25 wt.% and C – 2.81 wt.% were detected, indicating the presence of a minor amount of calcite mineral in the composition. To further determine the composition of these raw material samples, modern physico-chemical methods were applied, including X-ray diffraction (XRD) and infrared (IR) spectroscopic analyses (see Figure 2) [[17], [18], [19], [20], [21], [22], [23], [24]].

In the X-ray diffraction pattern, the strongest and most intense peaks were observed at d-spacings of 3.24 Å, 3.34 Å, and 4.25 Å, which correspond to α-quartz. Peaks at 3.03 Å, 2.57 Å, and 2.28 Å were

attributed to feldspar; the 3.57 Å peak corresponds to hydromica, while the 3.18 Å peak is associated with biotite. Additionally, weaker intensity peaks at 10.51 Å, 7.10 Å, and 6.47 Å indicate the presence of chlorites, and peaks at 3.85 Å, 3.03 Å, 2.89 Å, and 2.28 Å correspond to calcite. Iron-bearing minerals such as hematite were mainly detected at 3.66 Å, 2.28 Å, and 1.45 Å.

Infrared spectroscopic (IR) analysis was also carried out on the same sample. According to the results, the presence of the –OH functional group was identified by stretching vibrations at 3368 cm^{-1}. No deformation vibrations were observed in this region, which indicates the absence of physically adsorbed water and suggests that the raw material is highly dehydrated.

The non-bridging Si–O bond was identified through stretching vibrations at 876 cm^{-1} and 1007 cm^{-1}, while bridging Si–O–Si bonds were confirmed by deformation vibrations at 459 cm^{-1}, 777 cm^{-1}, and 694 cm^{-1}. Bridging Si–O–Al bonds were observed through vibrations at 1434 cm^{-1}. Additionally, absorption bands at 591 cm^{-1} and 526 cm^{-1} correspond to sodium (Na) and potassium (K) feldspars, respectively. These findings confirm the presence of albite and microcline, as indicated in the XRD analysis.

The IR spectroscopic analysis theoretically supports and scientifically validates the results of the X-ray diffraction analysis.

Based on the preliminary studies conducted, it was determined that enrichment of these quartz sands is necessary for producing colorless and transparent glass enamel frits from this raw material. Therefore, in the subsequent stages of research, beneficiation processes were carried out on feldspar-bearing quartz sands from the Khiva deposit. According to X-ray diffraction (XRD) and infrared (IR) spectroscopic analyses, the Khiva quartz sand contains small amounts of chlorite, muscovite, microcline, limonite, hematite, and calcite. The physico-chemical properties of the mineral phases identified in the sample are summarized in Table 4.

The effects of gravity separation, classification, and flotation processes on increasing the silica (SiO_2) content of feldspar-bearing quartz sand samples from the Khiva deposit were studied under laboratory conditions (Table 5). The low efficiency of these beneficiation processes is due to the presence of 5–10 wt% brown, black, and light reddish iron-bearing mineral impurities, as well as the high content of iron oxides in the fine-dispersed clay fractions (50–65 wt%) and their presence on the surfaces of quartz grains (10–20%). In addition, according to mineralogical and petrographic characteristics, the samples contain, apart from iron oxides, other coloring agents—namely, titanium, chromium, cobalt, phosphorus, and manganese oxides—in amounts of 0.03–0.05 wt%.

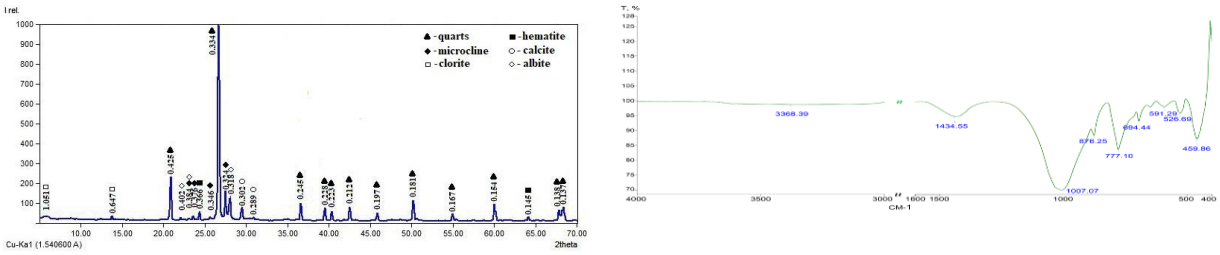

Figure 2 - X-ray Diffraction Pattern and IR Spectrum of the Feldspar-Quartz Sand Sample from the Khiva Deposit

Table 4 - Selected properties of accessory minerals in feldspar-bearing quartz sands of the Khiva deposit

Name of mineral	Density. g/cm³	Hardness (Mohs scale)	Refractive index	Magnetic behavior	Floatability
Muscovite	2.76-3.1	2.0-2.5	1.58-1.61	Non-magnetic	Floatable
Calcite	2.6-2.8	3.0-3.5	1.60-1.66	Non-magnetic	Not floatable
Chlorite	2.6-2.9	2.0-3.0	1.64-1.68	Non-magnetic	Floatable
Hematite	4.9-5.3	5.5-6.5	3.15-3.20	magnetic	Not floatable
Microcline	2.5-2.8	6.0-6.5	1.52-1.53	Non-magnetic	Not floatable

Table 5 - Changes in the content of major oxides during the beneficiation processes of samples taken from the Khiva deposit.

processes	Main oxide content change. wt.%			
	SiO_2	Al_2O_3	Fe_2O_3	others
Initial sample	86.32	4.56	1.05	8.33
gravity separation	88.86	3.12	1.02	7.00
classification	89.52	2.78	0.99	6.71
flotation	91.38	2.12	0.61	5.89

Based on the composition and the data provided above, it was determined that beneficiation of the sand samples using combinations of washing, gravity separation, classification, attrition scrubbing, separation in an electromagnetic field, and flotation methods is appropriate [23].

The beneficiation processes were mainly carried out using the following three methods:

Method 1 involved the following stages: washing, gravity separation, classification, and separation in an electromagnetic field. The sample obtained from this method (D-1) showed that the SiO_2 content increased by a factor of 1.04 compared to the initial raw material (D-0), while the contents of Al_2O_3 and Fe_2O_3 decreased by factors of 1.71 and 1.39, respectively. Method 2 differed from the first method by replacing gravity separation with flotation. The beneficiation stages followed this sequence: washing, flotation, classification, and electromagnetic separation. In the sample obtained by this method (D-2), the SiO_2 content increased by a factor of 1.05, while Al_2O_3 and Fe_2O_3 contents decreased by factors of 2.03 and 2.78, respectively.

Method 3, unlike the previous two, incorporated additional processes such as attrition scrubbing (mechanical rubbing). The stages were: washing, gravity separation, attrition scrubbing, classification, electromagnetic separation, and flotation. The resulting sample (D-3) showed an SiO_2 content increase by a factor of 1.13 compared to the initial sample (D-0), reaching 97.24 wt.%, which meets the requirements of GOST-22551-2019 for grade B-100-2. In comparison to the second method, Al_2O_3 content decreased by a factor of 1.69 to 1.32 wt.%, and Fe_2O_3 content decreased by a factor of 3.70 to 0.10 wt.%.

The quantities of major oxides identified during the analysis were evaluated based on the established normative documents and are presented in Table 6 below.

The photographic images of the samples separated after different stages are presented in Figure 3 below.

Table 6 - Chemical composition of quartz sands after beneficiation of samples taken from the Khiva deposit

Beneficiation method and sample	Main oxide content change. wt.%				Sand grade according to GOST 22551-2019
	SiO_2	Al_2O_3	Fe_2O_3	others	
Initial sample, D-0	86.32	4.56	1.05	8.33	Does not comply
First method, D-1	89.50	2.66	0.76	7.47	Does not comply
Second method, D-2	90.36	2.24	0.37	7.03	Does not comply
Third method, D-3	97.24	1.32	0.10	1.34	Complies with B-100-2

Figure 3 - Photographic images (magnified 100 times) of the initial and beneficiated samples of feldspar-containing quartz sand from the Khiva deposit: a) sample beneficiated by the first method; b) sample beneficiated by the second method; c) sample beneficiated by the third method.

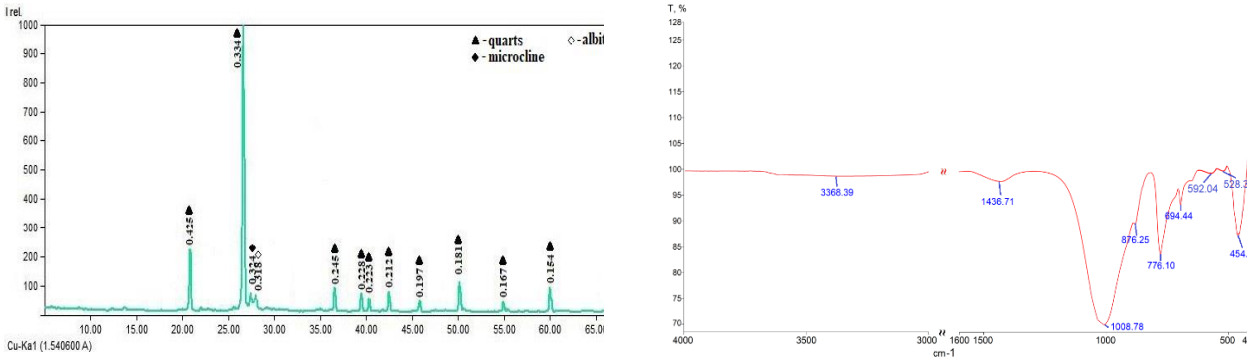

Figure 4 - X-ray diffractogram and IR spectrogram of the beneficiated feldspar-bearing quartz sand from the Khiva deposit

In this research, X-ray diffraction (XRD) and infrared (IR) spectroscopic analyses were conducted on the samples after the beneficiation of the quartz sands used as the object of study. The analysis results showed that, compared to the unprocessed samples (Figure 2), the intensity of the diffraction peaks of the minerals had decreased, and the peaks corresponding to iron-containing compounds such as hematite had completely disappeared (Figure 4).

Based on the results of numerous studies and the chemical-mineralogical composition of the Khiva feldspar-bearing quartz sand, a specific beneficiation technology with optimal technological parameters has been developed. According to the proposed technology, considering the easy washability of clayey materials in the composition, it was found that the additional use of a hydrocyclone unit is effective.

Conclusions

In this scientific study, the chemical, mineralogical, and granulometric composition as well as the beneficiation potential of feldspar-bearing quartz sands from the Khiva deposit were thoroughly investigated. Initial analyses revealed that the raw material primarily contains quartz, feldspar, calcite, chlorite, hematite, microcline, and other minerals, along with iron-bearing and clay-like impurities. These components limit the direct use of the sand in the glass industry.

During the study, the beneficiation processes were carried out using three main technological methods. The third method — which included washing, gravity separation, attrition scrubbing, classification, separation in an electromagnetic field, and flotation — was found to be the most effective. As a result of this method, the SiO_2 content in the beneficiated sample (D-3) increased to 97.24 wt.%, meeting the requirements of GOST 22551-2019 for the B-100-2 grade. Furthermore, the significant reduction in Al_2O_3 and Fe_2O_3 contents confirmed the improved suitability of the raw material for glass production.

Changes occurring during the beneficiation process were scientifically substantiated through X-ray diffraction and infrared spectroscopic analyses. A reduction — and in some cases, the complete removal — of hematite and other contaminant phases in the beneficiated sample was observed, further confirming the effectiveness of the beneficiation process.

Conflicts of interest. On behalf of all authors, the corresponding author states that there is no conflict of interest.

Acknowledgements. The author would like to express her deep gratitude to Sherzod Raimberganovich Kurambayev, Dean of the Faculty of Chemical Technologies at Urgench State University named after Abu Rayhon Beruni, for his practical assistance in conducting the experiments for this research. She also extends her sincere appreciation to Elyor Atashev Atashevich for his support in translation and language-related matters, and to my colleague Elyor Atashev Atashevich for his valuable contributions to the writing and editing of this article.

Formatting of funding sources. This research did not receive any specific grant from funding agencies in the public, commercial, or not-for-profit sectors.

Cite this article as: Buranova DB. Main characteristics of quartz-feldspar sands from the Khiva deposit, and the physico-chemical and technological fundamentals of obtaining an enriched concentrate. Kompleksnoe Ispolzovanie Mineralnogo Syra = Complex Use of Mineral Resources. 2027; 340(1):37-44. https://doi.org/10.31643/2027/6445.04

Хива кенорнының кварц-дала шпатты құмдарының негізгі сипаттамалары және байытылған концентрат алудың физикалық, химиялық және технологиялық негіздері

Буранова Д.Б.

Әбу Райхан Беруний атындағы Үргеніш мемлекеттік университеті, Үргеніш, Өзбекстан

Мақала келді: *21 шілде 2025*
Сараптамадан өтті: *8 тамыз 2025*
Қабылданды: *3 қыркүйек 2025*

ТҮЙІНДЕМЕ

Бұл зерттеу жұмысында Өзбекстан Республикасының Хорезм облысында орналасқан «Хива кені» кварц-дала шпатты құмдарын байытып, оларды силикат өнеркәсібінде қолдану бойынша зерттеулер баяндалған. Шикізат үлгілерінің құрамы заманауи рентгенографиялық және ИҚ-спектроскопиялық әдістермен зерттелді. Алынған нәтижелер негізінде BGMN/Profex Rietveld бағдарламалар жинағы арқылы үлгілердің минералогиялық сандық құрамы анықталды. Белгіленген мәліметтерге сәйкес, шикізаттың орташа құрамы массалық үлес түрінде келесідей болды: SiO_2 – 86,06%; Al_2O_3 – 2,64%; Fe_2O_3 – 1,37%; CaO – 1,37%; MgO – 0,22%; K_2O – 1,30%; Na_2O – 1,85%; TiO_2 – 0,04%; SO_3 – 0,4%, ал күйдірген кезде масса шығыны – 4,93% құрады. Шикізатты байыту процестері зерттелді. Құрамының ерекшеліктеріне сүйене отырып, келесі зерттеулерде байытудың – жуу, гравитациялық, классификация, үгіту арқылы жуу, электромагниттік өрісте сұрыптау, флотация әдістерінің комбинацияларын қолдану орынды деп танылды. Байытылған концентраттың құрамы бойынша SiO_2 мөлшері 86,06%-дан 97,07%-ға дейін артқаны, ал Al_2O_3 2,64%-дан 1,06%-ға, Fe_2O_3 1,37%-дан 0,05%-ға дейін азайғаны анықталды.

Түйін сөздер: кварц, мусковит, концентрат, электронды парамагниттік резонанс (ЭПР), байыту, флотация, магниттік сепарация, электрлік сепарация, рентгенографиялық талдау, ИҚ спектроскопиялық талдау.

Буранова Динара Бахтияровна

Авторлар туралы ақпарат:
Техника ғылымдарының философия докторы (PhD), Абу Райхан Беруни атындағы Үргеніш мемлекеттік университетінің Химиялық технология факультетінің доценті, Х. Олимжон көшесі, 14, 220100, Үргеніш, Өзбекстан. Email: dinara.b@urdu.uz; ORCID ID: https://orcid.org/0000-0001-5403-268X

Основные характеристики кварц-полевошпатовых песков Хивинского месторождения и физико-химические и технологические основы получения обогащённого концентрата

Буранова Д.Б.

Ургенчский государственный университет имени Абу Райхана Беруни, Ургенч, Узбекистан

Поступила: *21 июля 2025*
Рецензирование: *8 августа 2025*
Принята в печать: *3 сентября 2025*

В данном исследовании изложены результаты изучения возможности обогащения кварц-полевошпатовых песков месторождения «Хива», расположенного в Хорезмской области Республики Узбекистан, с целью их применения в силикатной промышленности. Состав образцов сырья был исследован с использованием современных рентгенографических и ИК-спектроскопических методов анализа. На основании полученных данных, с помощью программного комплекса BGMN/Profex Rietveld был определён количественный минералогический состав образцов. Согласно установленным данным, средний химический состав сырья в массовых процентах составил: SiO_2 – 86,06; Al_2O_3 – 2,64; Fe_2O_3 – 1,37; CaO – 1,37; MgO – 0,22; K_2O – 1,30; Na_2O – 1,85; TiO_2 – 0,04; SO_3 – 0,4; потеря при прокаливании – 4,93%. Были изучены процессы обогащения исходного сырья. С учётом особенностей его состава, в дальнейших исследованиях целесообразным признано применение комбинированных методов обогащения, включающих промывку, гравитацию, классификацию, истирающую промывку, сортировку в электромагнитном поле и флотацию. В результате обогащения содержание SiO_2 увеличилось с 86,06% до 97,07%, содержание Al_2O_3 снизилось с 2,64% до 1,06%, а Fe_2O_3 – с 1,37% до 0,05%.

Ключевые слова: кварц, мусковит, концентрат, электронный парамагнитный резонанс (ЭПР), обогащение, флотация, магнитная сепарация, электрическая сепарация, рентгенографический анализ, ИК-спектроскопический анализ *(инфракрасная спектроскопия).*

Буранова Динара Бахтияровна

Информация об авторах:
Доктор философии (PhD) в области технических наук, доцент факультета химической технологии Ургенчского государственного университета имени Абу Райхона Беруни, Ургенч, улица Х. Олимжона, 14, 220100, Узбекистан. Email dinara.b@urdu.uz; ORCID ID: https://orcid.org/0000-0001-5403-268X

References

[1] Akhmadjonov A, Kadyrova Z, & Usmanov Kh L. Quartz sands of the Tamdinskoe deposit: Promising raw material for glass production. Glass and Ceramics. 2022; 79(7-8):257-261. https://doi.org/10.1007/s10717-022-00496-z

[2] Anvarov AB, & Kadyrova Z R. Enrichment of Oinakum deposit quartz sands for synthesizing high-quality transparent glass. Glass and Ceramics. 2024; 80:435-439. https://doi.org/10.1007/s10717-023-00628-z

[3] Aripova MK, Mkrtchyan RV, & Erkinov FB. On the possibility of enriching quartz raw materials of Uzbekistan for the glass industry. Glass and Ceramics. 2021; 78:120-124. https://doi.org/10.1007/s10717-021-00359-z

[4] Niyazova Sh M, Kadyrova Z R, Usmanov Kh L, & Khomidov F G. Chemical and mineralogical studies of magmatic rocks of Uzbekistan for obtaining heat-insulating materials. Glass and Ceramics. 2019; 75(11-12):491-495. https://doi.org/10.1007/s10717-019-00119-0

[5] Eminov A A, Abdullaeva R I, & Kadyrova Z R. Dzherdanakskoe quartz rock for ceramic and refractory materials production. Glass and Ceramics. 2017; 74(1-2):64-66. https://doi.org/10.1007/s10717-017-9930-3

[6] Adinaev Kh A, & Kadyrova Z R. Physico-chemical analysis of quartz sand and technological waste used as a main raw material for glass production. Journal of Chemical Technology and Metallurgy. 2024; 59(3):599-604. https://doi.org/10.59957/jctm.v59.i3.2024.13

[7] Jumaniyazov M, Kurambayev Sh, Atashev E, Jumaniyozov A, & Buranova M. Determination of the composition of the Zinelbulak talc-magnesite deposit rock using modern physicochemical methods. E3S Web of Conferences. 2025; 633:06002. https://doi.org/10.1051/e3sconf/202563306002

[8] Tadjiev S, & Atashev E. Obtaining azosuperphosphate from low-grade phosphates of the Central Kyzyl-Kum. Journal of Critical Reviews. 2020; 7(5):472-477. https://doi.org/10.31838/jcr.07.05.101

[9] Khadzhiev A, Atabaev F. Influence of silica-containing additives on physical and mechanical properties of Portland Cement Co. Ltd Karakalpaksement. In: E3S Web of Conferences. 2023; 401:05051. https://doi.org/10.1051/e3sconf/202340105051

[10] Iskandarova MI, Atabaev FB, Khadzhiev AS. Utilization of natural silicate rocks to reduce the carbon footprint in the cement industry. Kompleksnoe Ispolzovanie Mineralnogo Syra = Complex Use of Mineral Resources. 2026; 338(3):40-50. https://doi.org/10.31643/2026/6445.27

[11] Tadjiev S, & Atashev E. Production of azosuperphosphate in the participation of Central Kyzylkum phospharites and ammonium sulphate. Journal of Critical Reviews. 2020; 7(7):358-362. https://doi.org/10.31838/jcr.07.07.59

[12] Buranova D B, Yunusov M Y, Babaev Z K, Kurambaev Sh R, & Atashev E A. The physico–chemical analysis of quartz sand of Khiva deposit. RA Journal of Applied Research. 2023; 9(10):506-509. https://doi.org/10.47191/rajar/v9i10.01

[13] Babaev Z K, Matchonov Sh K, Buranova D B, Iskandarov O D, Ibodullayev B O, & Pirnafasov AA. Condition and development of the Uzbekistan's glass industry. International Journal of Advanced Research in Science, Engineering and Technology. 2018; 5(11):7270–7273.

[14] GOST 22552.7-2019. Quartz sand, ground sandstone, quartzite and vein quartz for the glass industry. Method for determining the granulometric composition. Moscow: Standartinform. 2019. (in Russ.).

[15] GOST 13451-77. Syr'ye polevoshpatovoye i polevoshpatovo-kvartsevoye dlya stekol'noy promyshlennosti [Feldspar and feldspar-quartz raw materials for the glass industry]. Tekhnicheskiye usloviya (s izmeneniyami 1–4) [Technical specifications (with amendments 1–4)]. Moscow. 1977. (in Russ.).

[16] GOST 22552.2-2019. Pesok kvartsevyy, molotyy peschanik, kvartsit i zhil'nyy kvarts dlya stekol'noy promyshlennosti. Metody opredeleniya oksida zheleza [Quartz sand, ground sandstone, quartzite and vein quartz for the glass industry. Methods for determining iron oxide]. Moscow: Standartinform. 2019. (in Russ.).

[17] Downs RT, & Hall-Wallace M. The American Mineralogist crystal structure database. American Mineralogist. 2003; 88:247-250.

[18] Belkly A, Helderman M, Karen VL, & Ulkch R. New developments in the Inorganic Crystal Structure Database (ICSD): Accessibility in support of materials research and design. Acta Crystallographica Section B: Structural Science. 2002; 58(3):364-369.

[19] Agarwal BK. X-ray spectroscopy. Springer. 1991.

[20] Boekker Yu. Mir khimii. Spektroskopiya [World of chemistry. Spectroscopy]. Moscow: Tekhnosfera. 2017, 536. (in Russ.).

[21] Nyquist RA, & Kagel RO. Infrared spectra of inorganic compounds (3800–45 cm^{-1}). Academic Press. 1971.

[22] Monina LM. Rengenografiya. Kachestvenniy rentgenovazoviy analiz [X-ray diffraction. Qualitative X-ray phase analysis]. Moscow: Prospekt. 2017, 120. (in Russ.).

[23] Zschornack G. Handbook of X-ray data.- Berlin, Heidelberg: Springer- Verlag. 2007, 969.

[24] Stepanenko AI, & Stepanenko AA. Enrichment of glass sands. 2019. (in Russ.). Retrieved August 20, 2025, from https://gmexp.ru/netcat_files/userfiles/Broshyura_Peski_2019.pdf

Crossref
DOI: 10.31643/2027/6445.05
Engineering and Technology

Effect of multicomponent mineral additives on the microstructure and strength of composite cement

[1]Atabaev F.B., [2] Aripova M.Kh., [3*]Khadzhiev A.Sh., [1]Tursunova G.R., [4]Tursunov Z.R.

[1] Institute of General and Inorganic Chemistry of the Academy of Sciences of Uzbekistan, Tashkent
[2] Tashkent Institute of Chemical Technology, Tashkent, Uzbekistan
[3] Urgench State University named after Abu Rayhon Beruni, Urgench, Uzbekistan
[4] Navoi State University of Mining and Technology, Navoiy, Uzbekistan

** Corresponding author email: azamat.x@urdu.uz*

Received: *July 11, 2025*
Peer-reviewed: *August 29, 2025*
Accepted: *September 12, 2025*

ABSTRACT

In the face of growing environmental and energy challenges, the cement industry is shifting towards the use of composite Portland cements containing hybrid mineral additives to reduce clinker consumption and CO_2 emissions. This study investigates the pozzolanic activity and hydration behavior of thermally activated aluminosilicate additives (TAFM), quartz-feldspar sand, apobasalt-orthoshale (APO), and limestone. The chemical composition and calcium oxide binding capacity of each component were examined using the lime saturation method. Results showed that TAFM exhibits the highest pozzolanic reactivity, significantly binding free lime (CaO), followed by APO and limestone. Composite cement mixtures were formulated according to GOST 31108–2020 standards, incorporating 20% hybrid additives. Mechanical tests revealed that such compositions improve long-term compressive and flexural strength, early setting times, and structural density. In particular, the combination of TAFM, APO, and limestone showed synergistic effects in enhancing hydration kinetics and final performance. The findings support the feasibility of using local mineral resources as effective components in sustainable cement production and highlight the benefits of hybrid additives in reducing clinker demand while improving mechanical and durability characteristics of cementitious composites.

Keywords: Thermally activated additives, clinker reduction, sustainable construction materials, cement hydration, hybrid mineral additives, composite Portland cement.

Information about authors:

Atabaev Farrukh Bakhtiyarovich — *Doctor of Technical Sciences, Professor, Chief Scientific Researcher at the STROM Research Laboratory and Testing Center of the Institute of General and Inorganic Chemistry of the Academy of Sciences of Uzbekistan, 77 Mirzo Ulugbek Street, 100170, Tashkent. Email: atabaev_farruh@mail.ru; ORCID ID: https://orcid.org/0009-0004-4941-5060*

Aripova Mastura Khikimatovna — *Doctor of Technical Sciences, Professor, Head of the Department of "Technology of Silicate Materials and Rare Noble Metals", Tashkent Institute of Chemical Technology, 32 A. Navoi Street, Tashkent 100011, Republic of Uzbekistan. Email: aripova1957@yandex.com; ORCID ID: https://orcid.org/0000-0003-1365-7864*

Khadzhiev Azamat Shamuratovich — *Doctor of Philosophy in Technical Sciences, Associate Professor at the Faculty of Chemical Technology, Urgench State University named after Abu Rayhon Beruni, Urgench, H. Olimjon Street 14, 220100, Uzbekistan. Email: xadjiyev2019@mail.ru; ORCID ID: https://orcid.org/0000-0003-2131-8256*

Tursunova Gulsanam Ruzimuradovna — *DSC Student, Institute of General and Inorganic Chemistry, Academy of Sciences of the Republic of Uzbekistan, 77 Mirzo Ulugbek Street, Tashkent 100170, Uzbekistan. Email: gulsanamtursunova7@gmail.com; ORCID ID: https://orcid.org/0000-0002-5962-0322*

Tursunov Zarif Ruzimuradovich — *Doctor of Philosophy in Technical Sciences, Associate Professor, Navoi State University of Mining and Technology, 76v Galaba Avenue, Navoiy City, Navoiy Region, 210100, Republic of Uzbekistan Email: tzarif5658@gmail.com; ORCID ID: https://orcid.org/my-orcid?orcid=0009-0003-6432-4442*

Introduction

At present, the global construction materials industry faces the urgent challenge of developing and implementing new-generation materials. Key priorities in this domain include environmental protection, rational use of natural resources, reduction of production costs, and the adoption of energy-efficient technologies — all of which have become central components of modern scientific and technical policy. Among various industries, cement production is recognised as one of the leading contributors to carbon dioxide (CO_2) emissions, making the mitigation of its environmental impact a critical issue.

According to international research, the production of one ton of Portland cement releases on average 0.8 to 1 ton of CO_2 into the atmosphere,

which accounts for approximately 7–8% of total global greenhouse gas emissions. As a result, the production and use of composite Portland cements — aimed at reducing CO_2 emissions, minimizing raw material and fuel consumption, and improving energy efficiency — has significantly increased worldwide [[1], [2], [3], [4]].

Composite Portland cements are a new generation of binders that offer notable environmental and economic advantages over conventional Portland cement. These binders incorporate two or more types of active mineral additives, which partially replace clinker in the composition. This not only reduces thermal energy consumption during production but also enhances resource efficiency and ecological safety.

Consequently, the use of composite cements contributes not only to environmental sustainability but also to improving the quality, durability, and long-term performance of construction materials. For this reason, the industrial-scale application of such cements, the careful selection of their mineral additives, and the detailed study of their hydration behavior have become key areas of research in modern cement chemistry.

Composite Portland cements are regulated under GOST 31108–2003, which defines the permissible types and proportions of mineral additives, as well as performance indicators and technical requirements [5]. Based on this regulatory framework, cement compositions may include a variety of active natural or technogenic mineral additives, such as volcanic rocks, pozzolans, industrial by-products, limestone, and sand-stone mixtures.

Numerous scientific sources have noted that such mineral additives actively influence the cement hydration process by accelerating the onset of hydration, modifying the reaction depth, and determining the types of hydration products that are formed [[6], [7], [8], [9], [10]]. As a result, denser phases develop within the microstructure of the cement paste, thereby enhancing its compressive strength, impermeability, frost resistance, and durability under aggressive environmental conditions. In addition, these additives reduce the tendency of concrete mixtures to segregate, lower heat generation, minimize shrinkage-induced deformations, and contribute to the overall structural stability and mechanical strength of the hardened material.

Nevertheless, in practice, many large-scale cement manufacturers remain cautious about implementing such composite products at the industrial level. The primary reason for this hesitance lies in the insufficient understanding of the combined mechanisms of action when multiple active mineral additives are used together. Most scientific studies focus on the individual chemical reactivity or hydraulic behavior of single additives. However, when used in combination, these additives may interact synergistically, antagonistically, or neutrally — and there remains a lack of experimental data supporting these complex interrelations [11].

This scientific uncertainty introduces increased risks related to quality assurance, standardization, and technological consistency. Therefore, before introducing composite cement products into industrial-scale production, it is essential to conduct detailed experimental investigations into the mutual interactions between additives, phase transformations, and the mineralogical structure of the resulting hydration products.

Among the most widely used additives in practice are aluminosilicate-based mineral components, such as natural pozzolans, metakaolin, fly ash from thermal power plants (TPPC), thermally activated clays, and other silicate–aluminate-rich materials. These additives significantly influence the hydration kinetics of Portland cement. The reactive silicon dioxide (SiO_2) and aluminum oxide (Al_2O_3) in their composition engage in secondary pozzolanic reactions with the free calcium hydroxide ($Ca(OH)_2$) released during cement hydration, resulting in the formation of calcium silicate hydrates (CSH) and calcium aluminate silicate hydrates (CASH) [[12], [13], [14], [15], [16], [17]]. These secondary reactions contribute to the development of a dense and durable microstructure in the hardened cement paste, which plays a critical role in long-term performance and durability [18].

This process not only reduces the porosity of the cement stone but also improves its resistance to mechanical stress, water penetration, and freeze–thaw cycles. In addition, such mineral additives enhance the long-term durability of concrete by reducing microcracking and increasing resistance to sulfates and other chemically aggressive agents.

Moreover, recent studies have shown that carbonate-based additives — particularly finely ground and activated forms of limestone, dolomite, and other calcium carbonate materials — can significantly improve several key physical, mechanical, and technological properties of cement-based composites when incorporated into the cement matrix [[19], [20]]. These additives help mitigate segregation and bleeding in concrete

mixtures, leading to greater homogeneity and stability within the fresh mix.

Carbonate additives also improve the water-retaining capacity of concrete, thereby enhancing its workability and finishing properties. Furthermore, their inclusion contributes to a reduction in the heat of hydration, which is particularly important for massive concrete structures, where high internal temperatures can lead to thermal cracking. The use of such additives reduces internal temperature differentials and mitigates the risk of thermal stress-induced cracking [[21], [22]].

Another significant benefit is that carbonate-based additives substantially enhance the resistance of concrete to aggressive environments, including water, freezing conditions, acids, and chloride ions commonly found in marine water [[23], [24]]. This makes them especially suitable for the production of concrete used in marine infrastructure, transportation facilities, and chemical processing plants, where long-term chemical durability is critical.

Experimental part

This study focused on evaluating the effectiveness of hybrid mineral additives based on local raw materials in composite Portland cement production. The following components were used in the preparation of the hybrid additives: thermally activated aluminosilicate material (TAFM), quartz-feldspar sand, apobasalt-orthoshale (APO), and limestone. TAFM was obtained by calcining a mixture of 70% tuff and 30% shale at 800–850 °C. APO is a volcanic-origin rock rich in Al_2O_3 and Fe_2O_3, while limestone is a carbonate-based material with a high CaO content (50.28%).

The chemical composition of all additives was determined using standard chemical analysis methods. Their pozzolanic activity was assessed through the lime saturation method developed by Y.M. Butt and V.V. Timashev, which evaluates the capacity of the materials to bind free calcium oxide (CaO) in saturated lime solutions, thus reflecting their reactivity.

Two composite cement formulations were developed in accordance with GOST 31108:2020. The first composition contained 75% Portland cement clinker, 12% limestone, 3% TAFM, 5% APO, and 5% gyPCum. The second composition included 75% clinker, 12% limestone, 3% TAFM, and 5% gyPCum. As a control, a standard cement (PÇ-D0) consisting of 95% clinker and 5% gyPCum was prepared. All cement mixtures were ground in a laboratory ball mill until achieving a fineness of 90–94% passing through a 008 sieve.

Testing involved determining the normal consistency (water demand) and setting times in accordance with GOST 310.3. The flexural and compressive strength of the cement mortars, prepared at a cement-to-sand ratio of 1:3, was measured using prismatic samples of 4×4×16 cm after 3 and 28 days of curing, following GOST 310.4 procedures. Additionally, to assess pozzolanic activity, the cement pastes were stored in saturated lime solutions for 30 days, after which the concentration of CaO in the liquid phase was measured using titration techniques.

Results and Discussion

In this study, hybrid additives based on locally available mineral raw materials were selected with the aim of enhancing the composition of composite Portland cement and improving its physicomechanical, hydration, and microstructural characteristics. As a primary hybrid additive, a thermally activated aluminosilicate component was used, obtained by calcining a mixture of 70% natural tuffaceous rock (tuffite) and 30% shale at 800 °C. The thermal activation process significantly enhanced the reactivity of the material, increasing its pozzolanic activity. This combination exhibits hydraulic properties, reacting with free calcium hydroxide during hydration and forming secondary calcium silicate hydrates (CSH) and calcium aluminate silicate hydrates (CASH).

In addition, quartz-feldspar sand, consisting primarily of SiO_2 and alkali feldspars (K/Na–feldspar), was introduced into the composition. This component contributes to physicochemical balance in the cement mixture, improves particle size distribution, and functions as a microfiller by reducing void phases and enhancing the density of the hardened cement matrix.

The third component utilized was apobasalt–orthoshale rock, characterized by a basaltic structure rich in iron- and magnesium-bearing silicates. These provide high mechanical strength, chemical stability, and thermal resistance. The wide range of mineral phases present in this rock type contributes to stable hydration and the formation of strong structural compounds within the cement matrix.

The synergistic effect of these three components was investigated in detail. Special emphasis was placed on their influence on Portland

cement hydration behavior, including heat evolution, setting time, microstructural changes, and compressive strength. In addition, comparative measurements of compressive strength, water permeability, density, and porosity were performed on the hardened cement samples.

To evaluate the effectiveness of the hybrid additives, their chemical composition and the relative proportions of oxide components were studied. These parameters are critical in determining the hydraulic or pozzolanic activity of the additives when blended with cement, as well as their reactivity during hydration and their influence on the microstructure and mechanical properties of the final product.

Particular attention was paid to the quantitative ratios of key oxides such as SiO_2, Al_2O_3, Fe_2O_3, CaO, and MgO. These indicators allowed for the classification of each additive's geochemical group, its natural or artificial origin, and its expected reactivity within the cementitious system. The chemical composition of the components used in this study — including thermally activated aluminosilicate (TAFM), apobasalt–orthoshale (APO), quartz–feldspar sand, and limestone — is presented below (Table 1).

According to the analysis results, the quartz–feldspar sand sample (abbreviated as QFS) primarily consists of silicon dioxide (SiO_2), which accounts for 88.72% of its composition. This high SiO_2 content classifies the material as a quartz–feldspathic rock and highlights its suitability as a microfiller that contributes to the densification of the cementitious matrix. The low content of Al_2O_3, Fe_2O_3, and CaO indicates that the material is chemically inert and does not significantly participate in hydration reactions, confirming its role as a non-reactive mineral filler.

The apobasalt–orthoshale (APO) sample, in contrast, contains substantial amounts of SiO_2 (46.61%), Al_2O_3 (14.91%), and Fe_2O_3 (8.20%), which are characteristic of dense volcanic extrusive rocks belonging to the andesite–basalt group. The high content of these oxides indicates potential pozzolanic or latent hydraulic activity. Furthermore, the presence of CaO and MgO suggests partial reactivity, enabling the formation of secondary compounds during the hydration process, which can enhance the mechanical strength and durability of cement composites.

The thermally activated mineral additive (TAFM) is composed of a mixture of tuffite and shale calcined at 800–850 °C, and it contains SiO_2 (51.45%) and Al_2O_3 (8.62%). These values confirm its classification as an aluminosilicate pozzolanic additive. Additionally, the content of CaO (12.00%) and MgO (2.20%) indicates that the material exhibits both pozzolanic and hydraulic activity, enabling it to react with free calcium hydroxide to form calcium silicate hydrates (CSH) and calcium aluminate silicate hydrates (CASH), which contribute to improved microstructure and mechanical performance.

The limestone sample is distinguished by its very high CaO content (50.28%), which makes it an effective carbonate-based reactive component for incorporation into cement. The loss on ignition (LOI) value of 39.61% reflects the release of CO_2 during decomposition of carbonates. During cement hydration, limestone promotes the formation of calcium carbonate hydrates and calcium aluminate carbonate (C–A–C) compounds. These products enhance the density, impermeability, and resistance to aggressive environments of the hardened cement paste.

Table 1 - Results of chemical analysis of the additives

Type of Additive	LOI (%)	SiO_2 (%)	Al_2O_3 (%)	Fe_2O_3 (%)	CaO (%)	MgO (%)	SO_3 (%)	Others (%)
Quartz–feldspar sand	1.51	88.72	1.60	1.99	0.83	0.90	0.44	4.01
Apobasalt–orthoshale (APO)	9.47	46.61	14.91	8.20	8.76	3.79	0.30	5.80
TAFM (Thermally activated)	16.14	51.45	8.62	2.39	12.00	2.20	0.58	6.62
Limestone ($CaCO_3$)	39.61	4.99	1.33	0.47	50.28	2.72	0.20	0.40

Note: LOI – Loss on Ignition.

To determine the pozzolanic or hydraulic activity of the additives, special tests were conducted to evaluate their capacity to bind free calcium oxide (CaO) during the hydration process. The pozzolanic and hydraulic reactivity of the selected additives — TAFM, quartz–feldspar sand (QFS), apobasalt–orthoshale (APO), and limestone — was assessed based on their ability to fix CaO released during cement hydration. The testing methodology was based on the determination of the lime-binding capacity of mineral additives within the cement system, which serves as a criterion for assessing their potential reactivity.

The experimental procedure was carried out in the following stages:

- Representative samples of each additive (TAFM, QFS, APO, and limestone) were ground to a particle size of ≤1 cm and blended with Portland clinker and gyPCum in a laboratory ball mill.
- The cement mixture for each sample contained: 700 g of clinker, 300 g of additive, and 30 g of gyPCum.
- The resulting cement compositions were ground to a fineness corresponding to 90–94% passing through a No. 008 sieve, achieving standard cement particle size.

To evaluate pozzolanic activity, the saturation level of free CaO in the liquid phase was determined after hydration. This analysis was conducted according to the methodology developed by Yu.M. Butt and V.V. Timashev, in which cement pastes were hydrated for 30 days, followed by titrimetric analysis of the alkalinity (meq/L) and free CaO concentration (mmol/L) in the liquid phase.

The results showed that the TAFM-containing cement sample absorbed 287.14 mg of CaO from the saturated lime solution after 15 titration cycles, indicating a high level of pozzolanic activity. At the end of the test period, the TAFM cement sample exhibited the following values in the liquid phase:

- Free CaO concentration: 3.86 mmol/L
- Total alkalinity: 58.00 meq/L

These results confirm the high reactivity of TAFM, attributable to its rich content of reactive aluminosilicate components, and its active participation in pozzolanic reactions during hydration.

In contrast, the cement sample containing limestone exhibited a notable increase in the alkalinity of the liquid phase. While limestone is only weakly reactive, it affects the ionic balance of the solution, thereby exerting an indirect influence on the formation of hydration products (Table 2).

As shown in Table 2, the thermally activated mineral additive (TAFM) demonstrated the highest lime-binding capacity among the tested additives. The concentration of CaO in the liquid phase was measured at 3.86 mmol/L, while the total alkalinity reached 58.00 meq/L. These values confirm the high pozzolanic reactivity of TAFM, indicating its strong ability to actively react with free calcium hydroxide. This behavior reflects the material's high hydration reactivity and justifies its classification as a highly active pozzolanic additive.

On the other hand, the quartz–feldspar sand (QFS) sample exhibited the highest residual CaO concentration in the liquid phase (8.39 mmol/L) and the lowest amount of bound CaO (94.2 mg). These results indicate that QFS has very low pozzolanic or hydraulic reactivity and primarily behaves as an inert microfiller within the cement system. According to the standard GOST 24640–91 "Additives for Cement. Classification", such low-reactivity additives are typically used to economize clinker consumption without significantly contributing to hydration reactions.

Table 2 - Results of chemical analysis of the additives

Active Mineral Additive	Origin of Additive	CaO Content (mmol/L)	Total Alkalinity (meq/L)
TAFM (thermally activated)	Technogenic (artificial)	3.86	58.00
QFS (quartz–feldspar sand)	Natural (sedimentary)	8.39	56.80
APO (apobasalt–orthoshale)	Natural (volcanic)	6.80	57.20
Limestone	Natural (carbonate-based)	3.00	68.00

Note: The table presents the concentration of free calcium oxide (CaO) and total alkalinity (in meq/L) in the liquid phase in contact with cement pastes containing different additives.

The apobasalt–orthoshale (APO) additive showed intermediate reactivity, with a CaO concentration of 6.80 mmol/L and alkalinity of 57.20 meq/L, suggesting limited pozzolanic activity. Due to its content of reactive oxides (SiO_2, Al_2O_3, Fe_2O_3), APO can still positively influence the density and mechanical strength of cement composites and may be classified as a partially reactive or borderline pozzolanic additive.

Although the limestone sample showed the lowest CaO concentration in the liquid phase (3.00 mmol/L), this should not be interpreted as an indication of high pozzolanic activity. Instead, this result reflects the carbonate nature of limestone, which indirectly influences the alkalinity balance within the hydration environment. The high alkalinity value of 68.00 meq/L suggests that limestone contributes to ionic equilibrium, supporting the stable formation of hydration products. Rather than acting as a reactive catalyst, limestone typically functions as a stabilizing additive, improving final properties such as density and durability of the hardened cement paste.

Based on the results in Table 2, the concentration of CaO and total alkalinity for each cement sample containing different additives were analyzed. These data were used to construct comparative graphical plots, visually depicting the relative reactivity of each additive within the hydration environment. The plot allows for the assessment of the additives' alignment with pozzolanic or hydraulic activity criteria (Figure 1). The positions of points 1 (QFS), 2 (APO), 3 (TAFM), and 4 (Limestone) on the graph with respect to the lime solubility isotherm (curve A) were used to evaluate the qualitative performance of each additive. The concentration of free calcium oxide (CaO) in the liquid phase in direct contact with the cement paste serves as a key indicator of the additive's reactivity—i.e., its pozzolanic or hydraulic activity.

A point located below the isotherm indicates that the additive has a strong capacity to bind CaO from the liquid phase, which implies high reactivity. Conversely, a point on or above the isotherm reflects limited or negligible chemical interaction with CaO, indicating low reactivity.

The analysis of the plotted data reveals that all tested additives demonstrated some degree of CaO absorption during the hydration and hardening processes, but their levels of reactivity varied significantly:

- Point 1 (TAFM) is positioned well below the isotherm, indicating the highest pozzolanic and hydraulic activity among all additives. As a thermally activated artificial material, TAFM actively reacts with free lime in the hydration environment and forms strong secondary hydrates.

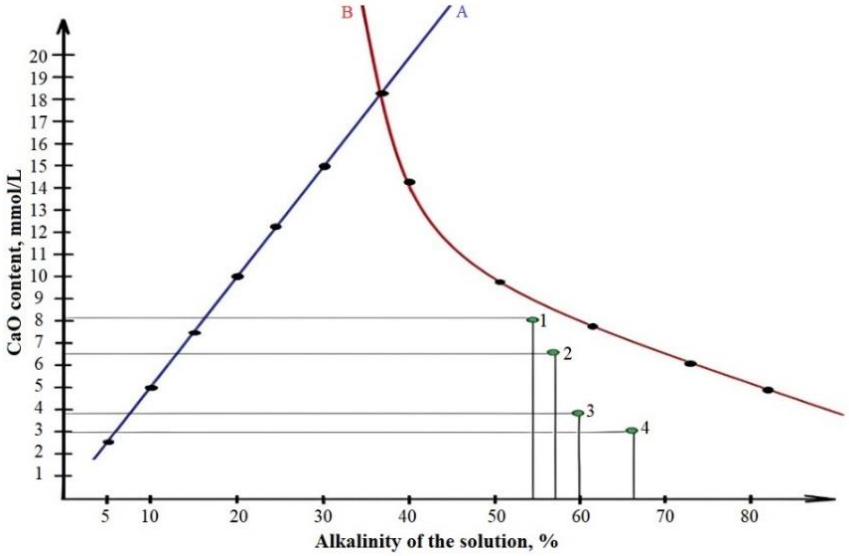

Figure 1 - Pozzolanic activity of mineral additives

A – Solubility isotherm of lime at 40 °C
B – Total alkalinity of the solution (excluding the contribution of CaO)
1 – Cement sample with QFS (quartz–feldspar sand)
2 – Cement sample with APO (apobasalt–orthoshale)
3 – Cement sample with TAFM (thermally activated mineral additive)
4 – Cement sample with limestone

- Point 2 (QFS) lies very close to the isotherm, suggesting that this additive exhibits very low pozzolanic reactivity. Quartz–feldspar sand behaves primarily as an inert filler, contributing little to CaO consumption.
- Point 3 (APO) is located between TAFM and QFS, signifying that it possesses moderate pozzolanic activity. APO may be classified as a semi-reactive or borderline pozzolanic material, due to its intermediate CaO-binding ability.
- Point 4 (Limestone) appears at a low CaO concentration but should not be interpreted as a sign of high pozzolanic activity. Instead, this is attributed to the carbonate nature of limestone, which influences the chemical balance of the hydration medium indirectly, rather than through direct lime binding.

Thus, the positioning of the data points relative to the solubility isotherm in Figure 1 provides a clear visual assessment of the pozzolanic or hydraulic activity of the studied additives. TAFM clearly stands out as the most effective and reactive component, whereas QFS (quartz–feldspar sand) demonstrates the lowest reactivity and can be classified as an inert mineral filler.

Based on the conducted research, the following conclusions were drawn:

- According to the Student's criterion for evaluating hydraulic activity, the tested raw materials do not meet the requirements specified in UzDSt 901:1998. Therefore, they cannot be used independently as active mineral additives for cement production.
- However, all studied mineral additives — TAFM, APO, limestone, and QFS — demonstrated a certain level of pozzolanic activity, which supports their potential application as reactive-filler components in the production of various types of Portland cement. These additives can bind free calcium oxide (CaO) released during cement hydration and setting.
- The highest lime-binding capacity was shown by TAFM, a thermally activated technogenic material. In contrast, QFS exhibited very low hydraulic activity, while the pozzolanic reactivity of APO fell between TAFM and QFS, indicating intermediate behavior.
- Based on the amount of CaO absorbed from the solution in which the cement samples were immersed, the additives may be ranked in the following descending order of pozzolanic activity:

TAFM → APO → QFS → Limestone

- To enhance the pozzolanic and hydraulic performance of these additives, it is recommended to formulate composite additives by combining them with various modifiers. This approach aims to improve their reactivity potential and contribute more significantly to the strength development of the cement matrix.

To produce composite Portland cements, raw material mixtures (clinker blends) were formulated in accordance with the requirements of GOST 31108:2020. The prepared mixtures were jointly ground in a laboratory ball mill to obtain cement samples for further testing.

Table 3 - Cement composition and its effect on setting time

No.	Type of Cement	Grinding Time, min	Residue on Sieve No. 008, %	Standard Water Demand (W/N), %	Initial Setting Time (h: min)	Final Setting Time (h: min)
1	PC-D0	30	10.0	25.7	3 h 20 min	5 h 00 min
2	PC-KD20	20	6.0	27.0	2 h 40 min	5 h 00 min

Notes:

- PC-D0 – pure Portland cement without additives (control sample).
- PC-KD20 – Portland cement with 20% composite additive (limestone + TAFM + APO or QFS).
- The reduction in grinding time for PC-KD20 is attributed to the softer structure and higher grindability of the ceramic components.
- Standard Water Demand (W/N) indicates the percentage of water required for normal consistency according to GOST methods.

The incorporation of ceramic-based additives into the cement composition has a significant impact on its physical-mechanical and technological properties. In particular, the PC-KD20 cement composition, which includes 20% composite additives (a mixture of limestone + TAFM + apobasalt–orthoshale or quartz–feldspar sand), exhibits a shorter grinding duration—only 20 minutes—compared to the reference pure Portland cement (PC-D0).

This behavior is attributed to the relatively softer texture and higher grindability of the ceramic additives, which facilitate faster milling to achieve the target fineness (Table 3).

In the PC-KD20 cement sample, the fineness is significantly higher, as evidenced by the fact that only 6.0% residue remains on sieve No. 008. This indicates a greater degree of particle dispersion and, consequently, higher reactivity of the cement. However, such fineness also leads to an increased water demand during the hydration process. As a result, the required standard water-to-cement ratio (W/N) for PC-KD20 is 27.0%, which is slightly higher than that of pure Portland cement (PC-D0), which stands at 25.7%.

Analysis of the setting times reveals that PC-KD20 cement initiates setting earlier (2 h 40 min) compared to the control PC-D0 (3 h 20 min). This is attributed to the increased surface area and higher number of reactive sites, which accelerate the hydration kinetics. However, the final setting time for both cement types remains the same at 5 hours (Figure 2). This suggests that the composite additives included in the cement matrix primarily enhance early-stage activity, without significantly altering the overall setting duration.

Thus, the incorporation of ceramic waste into the cement composition alters its physicochemical and rheological properties, which play an important role in optimizing construction material formulations.

The normal consistency (W/N) of the composite Portland cement (CPC) was slightly higher than that of the control (reference) cement. This increase is attributed to the enhanced water demand caused by the plasticizing effect of limestone and TAFM (thermally activated mineral additive). These components increase the mix's need for water due to their surface activity and specific particle structure.

The initial setting time of the experimental cement occurred significantly earlier compared to the control cement. This phenomenon is likely due to the rapid binding of free calcium hydroxide ($Ca(OH)_2$) released during hydration by the composite additives, which accelerates the formation of hydration products.

As a reference sample, plain Portland cement with 95% clinker and 5% gypsum was used, containing no mineral additives. The compressive strength of the composite Portland cement (CPC) samples was evaluated and compared with the reference sample (PC-D0) following the methodology outlined in GOST 310.4. Test specimens were prepared from a 1:3 cement-to-sand mixture, molded into 4×4×16 cm prisms, and cast using Volsk construction sand as the standard fine aggregate (Table 4).

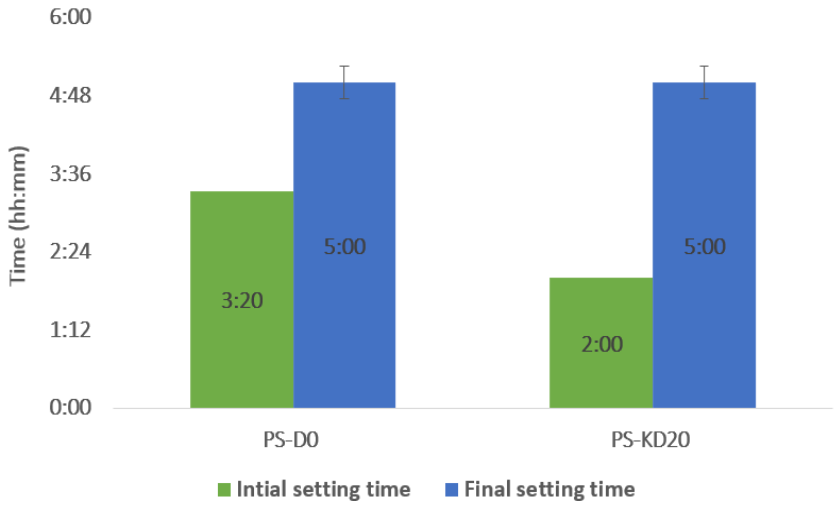

Figure 2 - Comparison of cement setting times

Table 4 - Effect of composite additives on flexural and compressive strength of portland cement (MPa)

№	Type of Cement	Flexural / Compressive Strength after 3 Days (MPa)	Flexural / Compressive Strength after 28 Days (MPa)
1	PC-D0	5.60 / 21.40	6.20 / 40.20
2	PC-KD20	4.65 / 21.40	7.25 / 41.00

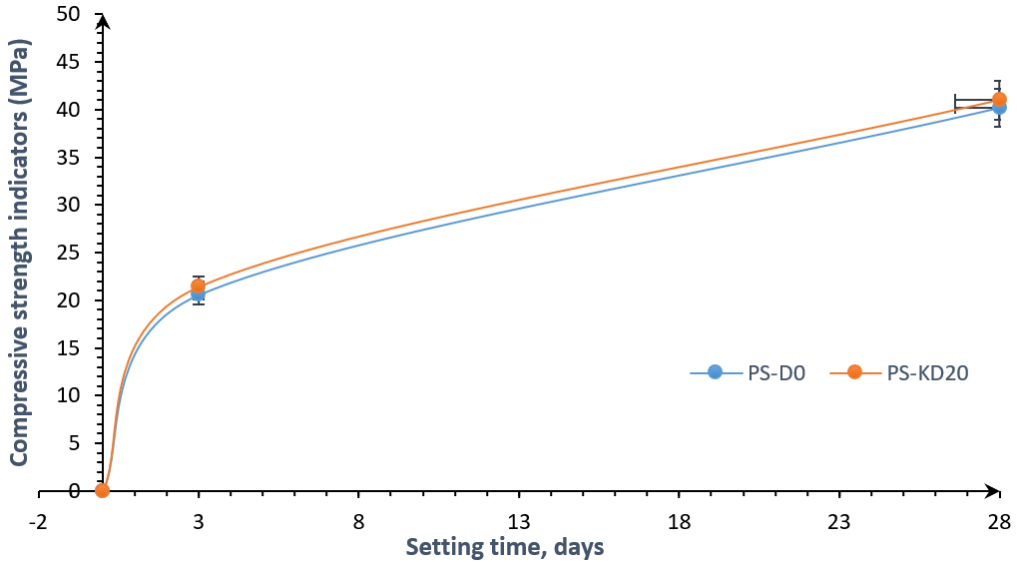

Figure 3 - Effect of KGCh-Based Composite Additive on Compressive Strength of Portland Cement (MPa)

The mechanical performance of Portland cement is significantly influenced by the type, quantity, and reactivity of mineral additives incorporated into its formulation. In the present study, a composite additive system comprising limestone, thermally activated mineral additive (TAFM), and either apobasalt-orthoshale (APO) or quartz–feldspathic sand (QFS) was introduced to partially replace clinker in Portland cement, aiming to improve sustainability without compromising performance.

The early-age flexural strength (3 days) of the composite cement (PC-KD20) was measured at 4.65 MPa, which is lower than that of the control cement (PC-D0) — 5.60 MPa. This reduction is attributable to the delayed reactivity of certain mineral phases within the composite additives. Specifically, materials like feldspathic sand and orthoshale may require a longer induction period to develop their pozzolanic or hydraulic potential. Moreover, the lower early-age strength may result from dilution of clinker content, which directly contributes to early hydration and strength gain.

In contrast, compressive strength at 3 days remained unchanged (21.4 MPa) across both cement types. This parity suggests that the filler effect and microstructural densification provided by the composite additives may partially compensate for the reduction in reactive clinker. These additives may act as nucleation sites, accelerating the formation of hydration products such as calcium silicate hydrate (C–S–H), thereby maintaining compressive performance.

By 28 days, the composite cement not only recovered but surpassed the control sample in flexural strength (7.25 MPa vs. 6.20 MPa) and slightly exceeded it in compressive strength (41.0 MPa vs. 40.2 MPa). This confirms the long-term pozzolanic contribution of TAFM and APO, which, over time, react with free calcium hydroxide to form additional C–S–H and calcium aluminosilicate hydrates (C–A–S–H). The synergy between limestone and active silicate/aluminate phases may also contribute to the refinement of pore structure and enhancement of interfacial transition zones (ITZs) within the cement matrix.

Furthermore, the observed strength development indicates that the composite additives do not negatively impact the long-term performance of cement but instead facilitate gradual densification and strength improvement, making them viable for sustainable cement design. These results align with previous studies demonstrating that carefully optimized hybrid mineral additives can simultaneously support the mechanical integrity and ecological performance of composite Portland cements.

The 28-day strength results clearly illustrate the long-term effectiveness of the composite additives. Specifically, the flexural strength of PC-KD20 cement reached 7.25 MPa, significantly higher than the 6.2 MPa observed for the control sample (PC-D0). This improvement is attributed to the progressive hydration activity of the mineral additives, which enhance the formation of strength-contributing hydrates, densify the cement matrix, and strengthen internal microstructural bonds over time.

In terms of compressive strength, PC-KD20 cement achieved 41.0 MPa, slightly exceeding the control sample's 40.2 MPa. This marginal gain further indicates that the composite additives contribute to refined microstructure, reduced microcracking, and improved compactness of the hardened cement paste.

Overall, the combination of limestone, TAFM, and either apobasalt-orthoshale or quartz–feldspathic sand demonstrates a substantial pozzolanic contribution, reacting with $Ca(OH)_2$ to form additional C–S–H and C–A–S–H gel phases that improve durability and mechanical performance. Particularly, TAFM and limestone play crucial roles due to their plasticizing effect and contribution to structural stability, respectively.

Therefore, these composite additives not only enhance cement quality but also contribute to environmental sustainability by incorporating industrial by-products. Their application in Portland cement production represents a technologically sound, mechanically efficient, and ecologically viable solution for the future of sustainable construction materials.

Conclusions

Based on the results of chemical analysis and pozzolanic activity evaluation, it was found that all tested mineral additives (TAFM, APO, and limestone) possess varying degrees of pozzolanic and hydraulic activity. Among them, the thermally activated aluminosilicate material (TAFM) demonstrated the highest reactivity by effectively binding free CaO in the hydrated cement matrix.

The experimental cement compositions prepared according to GOST 31108:2020, which included hybrid additives, showed improved physical and mechanical performance compared to the control cement. Notably, cement mixtures containing TAFM, APO, and limestone exhibited accelerated setting times, increased long-term strength, and better structural compactness.

The use of limestone as a partial clinker substitute is viable from an economic and ecological perspective, although its pozzolanic effect is limited. However, when combined with more active additives like TAFM, synergistic behavior was observed, enhancing the performance of the overall cementitious system.

The research confirms the potential of utilizing locally available mineral materials in hybrid form to develop environmentally sustainable and technically effective composite portland cements.

Conflicts of interest. On behalf of all authors, the corresponding author states that there is no conflict of interest.

CRediT author statement: **F. Atabaev**: Data curation, Writing draft preparation; **M. Aripova**: Conceptualization, Methodology, Software; **A. Khadzhiev**: Visualization, Investigation, Supervision; **G Tursunova**: Software, Validation; **Z. Tursunov:** Reviewing and Editing.

Acknowledgements. We express our deep gratitude to **Atabaev Farrukh Bakhtiyarovich**, Chief Scientific Researcher at the "STROM" Research Laboratory and Testing Center of the Institute of General and Inorganic Chemistry of the Academy of Sciences of Uzbekistan, for his practical assistance in conducting the experiments for this research. We also extend our sincere appreciation to **Jumaniyazov Arslon G'anibek o‘g‘li** for his translation support and language-related matters, as well as to the co-authors for their contributions to the writing and editing of the article.

Formatting of funding sources. This research did not receive any specific grant from funding agencies in the public, commercial, or not-for-profit sectors.

Cite this article as: Atabaev FB, Aripova MKh, Khadzhiev ASh, Tursunova GR, Tursunov ZR. Effect of multicomponent mineral additives on the microstructure and strength of composite cement. Kompleksnoe Ispolzovanie Mineralnogo Syra = Complex Use of Mineral Resources. 2027; 340(1):45-57. https://doi.org/10.31643/2027/6445.05

Көп компонентті минералды қоспалардың композициялық цементтің микрокұрылымы мен беріктігіне әсері

[1] Атабаев Ф.Б., [2] Арипова М.Х., [3]Хаджиев А.Ш., [1] Турсунова Г.Р., [4] Турсунов З.Р.

[1] Өзбекстан Республикасы Ғылым академиясының Жалпы және бейорганикалық химия институты, Ташкент, Өзбекстан
[2] Ташкент химия-технология институты, Ташкент, Өзбекстан
[3] Әбу Райхан Беруни атындағы Үргеніш мемлекеттік университеті, Үргеніш, Өзбекстан
[4] Навои мемлекеттік тау-кен және технологиялық университеті, Навои, Өзбекстан

Мақала келді: *11 шілде 2025*
Сараптамадан өтті: *29 тамыз 2025*
Қабылданды: *12 қыркүйек 2025*

ТҮЙІНДЕМЕ

Қоршаған орта мен энергияға қатысты артып келе жатқан қиындықтар жағдайында цемент өнеркәсібі клинкерді тұтынуды және CO_2 шығарындыларын азайту мақсатында гибридті минералдық қоспалар қосылған композициялық портланд цементтерін пайдалануға бет бұруда. Бұл зерттеуде термиялық белсендірілген алюмосиликатты қоспалар (ТБАҚ), кварц-далалық шпаттық құм, апобазальт-ортоалевролит (АПО) және әктас сияқты компоненттердің пуццоландық белсенділігі мен гидратациялық әрекеті зерттелді. Әр компоненттің химиялық құрамы мен кальций оксидімен байланыстыру қабілеті әкпен қанықтыру әдісімен анықталды. Нәтижелер ТБАҚ ең жоғары пуццоландық реакциялық белсенділікке ие және бос әктасты (CaO) айтарлықтай байланыстыратынын көрсетті, одан кейін АРО және әктас. Композициялық цемент қоспалары GOST 31108–2020 стандартына сәйкес, 20% гибридтік қоспаларды қосу арқылы дайындалды. Механикалық сынақтар мұндай қоспалар қысымға және иілуге беріктілікті арттыратынын, ерте қату уақытын қысқартатынын және құрылымдық тығыздықты жоғарылататынын көрсетті. Әсіресе ТБАҚ, АРО және әктас комбинациясы гидратация кинетикасын жеделдетуде және соңғы беріктік сипаттамаларын жақсартуда синергиялық әсер етеді. Бұл нәтижелер жергілікті минералдық ресурстарды орнықты цемент өндірісінде тиімді компонент ретінде қолданудың мүмкіндігін растайды және гибридтік қоспалардың клинкер тұтынуын азайта отырып, цементті композициялардың механикалық және ұзақ мерзімді қасиеттерін жақсартудағы артықшылықтарын айқындайды.

Түйін сөздер: Термиялық белсендірілген қоспалар, клинкер мөлшерін азайту, орнықты құрылыс материалдары, цементтің гидратациясы, гибридті минералдық қоспалар, композициялық портландцемент.

Авторлар туралы ақпарат:

Атабаев Фаррух Бахтияруллы — *Техника ғылымдарының докторы, профессор, Өзбекстан Республикасы Ғылым академиясының Жалпы және бейорганикалық химия институтының STROM ғылыми-зерттеу зертханасы мен сынақ орталығының жетекші ғылыми қызметкері, Мырза Ұлықбек көшесі, 77, 100170, Ташкент, Өзбекстан. Email: atabaev_farruh@mail.ru; ORCID ID: https://orcid.org/0009-0004-4941-5060*

Арипова Мастура Хикматовна — *Техника ғылымдарының докторы, профессор, Ташкент химия-технология институтының Силикатты материалдар және сирек бағалы металдар технологиясы кафедрасының меңгерушіс, А. Навои көшесі, 32, 100011, Ташкент, Өзбекстан Республикасы. Email: aripova1957@yandex.com; ORCID ID: https://orcid.org/0000-0003-1365-7864*

Хаджиев Азамат Шамуратұлы — *Техника ғылымдары бойынша философия докторы (PhD), Абу Райхан Беруни атындағы Үргеніш мемлекеттік университетінің Химиялық технология факультетінің доценті, Х. Олимжон көшесі, 14, 220100, Үргеніш, Өзбекстан. Email: xadjiyev2019@mail.ru; ORCID ID: https://orcid.org/0000-0003-2131-8256*

Турсунова Гулсанам Рузимуратқызы — *DSC докторанты, Өзбекстан Республикасы Ғылым академиясының Жалпы және бейорганикалық химия институты, Мырза Ұлықбек көшесі, 77, 100170, Ташкент қ., Өзбекстан. Email: gulsanamtursunova7@gmail.com; https://orcid.org/0000-0002-5962-0322*

Турсунов Зариф Рузимуратұлы — *Техника ғылымдары бойынша философия докторы (PhD), доцент, Навои мемлекеттік тау-кен және технологиялық университеті, Ғалаба даңғылы, 76в, Навои қ., Навои облысы, 210100, Өзбекстан. Email: tzarif5658@gmail.com; ORCID ID: https://orcid.org/0009-0003-6432-4442*

Влияние многокомпонентных минеральных добавок на микроструктуру и прочность композиционного цемента

[1] Атабаев Ф.Б., [2] Арипова М.Х., [3]Хаджиев А.Ш., [1] Турсунова Г.Р., [4] Турсунов З.Р.

[1] Институт общей и неорганической химии Академии наук Узбекистана, Ташкент, Узбекистан
[2] Ташкентский институт химической технологии, Ташкент, Узбекистан
[3] Ургенчский государственный университет имени Абу Райхана Беруни, Ургенч, Узбекистан
[4] Навоийский государственный горно-технический университет, Навои, Узбекистан

Поступила: *11 июля 2025*
Рецензирование: *29 августа 2025*
Принята в печать: *12 сентября 2025*

АННОТАЦИЯ

В условиях растущих экологических и энергетических вызовов цементная промышленность переходит к использованию композиционных портланд цементов, содержащих гибридные минеральные добавки, с целью сокращения потребления клинкера и выбросов CO_2. В данном исследовании изучена пуццолановая активность и гидратационное поведение термически активированных алюмосиликатных добавок (ТААД), кварц-полевошпатового песка, апобазальт-ортоалевролита (АПО) и известняка. Химический состав и способность связывать оксид кальция каждого компонента были определены методом известковой насыщенности. Результаты показали, что ТААД обладает наивысшей пуццолановой реакционной способностью и значительно связывает свободную известь (CaO), за ним следуют АПО и известняк. Композиционные цементные смеси были сформулированы в соответствии с требованиями стандарта ГОСТ 31108–2020 с добавлением 20% гибридных минеральных добавок. Механические испытания показали, что такие составы улучшают прочность на сжатие и изгиб в долгосрочной перспективе, сокращают ранние сроки схватывания и повышают структурную плотность. Особенно комбинация ТААД, АПО и известняка продемонстрировала синергетический эффект, способствуя интенсификации гидратации и улучшению конечных характеристик. Полученные данные подтверждают целесообразность использования местных минеральных ресурсов в качестве эффективных компонентов для устойчивого производства цемента и подчёркивают преимущества гибридных добавок в снижении потребления клинкера при одновременном улучшении механических и долговечных свойств цементных композитов.

Ключевые слова: Термически активированные добавки, снижение содержания клинкера, экологически устойчивые строительные материалы, гидратация цемента, гибридные минеральные добавки, композиционный портландцемент.

Информация об авторах:

Атабаев Фаррух Бахтияруллы *Доктор технических наук, профессор, главный научный сотрудник научно-исследовательской лаборатории и испытательного центра STROM Института общей и неорганической химии Академии наук Узбекистана, улица Мирзо Улугбека, 77, 100170, Ташкент. Email: atabaev_farruh@mail.ru; ORCID ID: https://orcid.org/0009-0004-4941-5060*

Арипова Мастура Хикиматовна *Доктор технических наук, профессор, заведующая кафедрой Технология силикатных материалов и редких благородных металлов Ташкентского института химической технологии, ул. А. Навои, 32, 100011, Ташкент, Узбекистан. Email: aripova1957@yandex.com; ORCID ID: https://orcid.org/0000-0003-1365-7864*

Хаджиев Азамат Шамуратович *Доктор философии в области технических наук, доцент факультета химической технологии Ургенчского государственного университета имени Абу Райхона Беруни, Ургенч, улица Х. Олимжона, 14, 220100, Узбекистан. Email: xadjiyev2019@mail.ru; ORCID ID: https://orcid.org/0000-0003-2131-8256*

Турсунова Гулсанам Рузимуратовна *Докторант DSC Института общей и неорганической химии Академии наук Республики Узбекистан, ул. Мирзо Улугбека, 77, 100170, Ташкент, Узбекистан. Email: gulsanamtursunova7@gmail.com; ORCID ID: https://orcid.org/0000-0002-5962-0322*

Турсунов Зариф Рузимуратович *Кандидат технических наук (PhD), доцент Навоийского государственного университета горного дела и технологий, проспект Галаба, 76в, Навои, Навоийская область, 210100, Республика Узбекистан. Email: tzarif5658@gmail.com; ORCID ID: https://orcid.org/0009-0003-6432-4442*

References

[1] Scrivener KL, John VM, & Gartner EM. Eco-efficient cements: Potential, economically viable solutions for a low-CO_2 cement-based materials industry. Cement and Concrete Research. 2018; 114:2-26. httpc://doi.org/10.1016/j.cemconres.2018.03.015

[2] Gartner E, & Hirao H. A review of alternative approaches to the reduction of CO_2 emissions associated with the manufacture of the binder phase in concrete. Cement and Concrete Research. 2015; 78:126-142. httpc://doi.org/10.1016/j.cemconres.2015.04.012

[3] Juenger MCG, Snellings R, & Bernal SA. Supplementary cementitious materials: New sources, characterization, and performance insights. Cement and Concrete Research. 2019; 122:257-273. httpc://doi.org/10.1016/j.cemconres.2019.05.015

[4] Habert G, d'Espinose de Lacaillerie JB, & Roussel N. An environmental evaluation of geopolymer based concrete production: Reviewing current research trends. Journal of Cleaner Production. 2011; 19(11):1229-1238. httpc://doi.org/10.1016/j.jclepro.2011.03.012

[5] GOST 31108–2003. Sementi obshestroitelnie. Texnicheskie usloviya. [Cement for general construction. Specifications. Moscow: Gosstandart of Russia. 2003. (in Russ.).

[6] Taylor HFW. Cement Chemistry (2nd ed.). London: Thomas Telford Publishing. 1997.

[7] Hewlett PC. (Ed.). Lea's Chemistry of Cement and Concrete (4th ed.). Oxford: Butterworth-Heinemann. 2004.

[8] Mehta PK, & Monteiro PJM. Concrete: Microstructure, Properties, and Materials (4th ed.). New York: McGraw-Hill Education. 2014.

[9] Juenger MCG, & Siddique R. Recent advances in understanding the role of supplementary cementitious materials in concrete. Cement and Concrete Research. 2015; 78:71-80. httPC://doi.org/10.1016/j.cemconres.2015.03.018

[10] Snellings R, Mertens G, & Elsen J. Supplementary cementitious materials. Reviews in Mineralogy and Geochemistry. 2012; 74(1):211-278. httPC://doi.org/10.2138/rmg.2012.74.6

[11] Mo L, Zhang F, Deng M, & Liu F. Effects of limestone powder on the hydration and microstructure development of cement-based materials. Construction and Building Materials. 2017; 152:471-478. httPC://doi.org/10.1016/j.conbuildmat.2017.07.054

[12] Antoni M, Rossen J, Martirena F, & Scrivener K. Cement substitution by a combination of metakaolin and limestone. Cement and Concrete Research. 2012; 42(12):1579-1589. httPC://doi.org/10.1016/j.cemconres.2012.09.006

[13] Shi C, Krivenko PV, & Roy DM. Alkali-activated cements and concretes. Boca Raton, FL: Taylor & Francis. 2006.

[14] Iskandarova MI, Atabaev FB, & Khadzhiev AS. Utilization of natural silicate rocks to reduce the carbon footprint in the cement industry. Kompleksnoe Ispolzovanie Mineralnogo Syra. 2026; 338(3):40-50. https://doi.org/10.31643/2026/6445.27

[15] Khadzhiev A, Atabaev F, & Tursunova G. Influence of sandstone on physical and chemical processes of interaction of components and genetic formation of cement composite. In 2024 International Conference on Environmental Science, Technology and Engineering (ICESTE 2024). E3S Web of Conferences. 2024, 563. Article 02027. https://doi.org/10.1051/e3sconf/202456302027

[16] Mindess S, Young JF, & Darwin D. Concrete (2nd ed.). Upper Saddle River, NJ: Prentice Hall. 2003.

[17] Wild S, Khatib JM, & Jones A. Relative strength, pozzolanic activity and cement hydration in superplasticised metakaolin concrete. Cement and Concrete Research. 1996; 26(10):1537-1544. httPC://doi.org/10.1016/0008-8846(96)00148-2

[18] Ben Haha M, Lothenbach B, Le Saout G, & Winnefeld F. Influence of slag chemistry on the hydration of alkali-activated blast-furnace slag—Part I: Effect of MgO. Cement and Concrete Research. 2011; 41(9):955-963. httPC://doi.org/10.1016/j.cemconres.2011.05.002

[19] Matschei T, Lothenbach B, & Glasser FP. The role of calcium carbonate in cement hydration. Cement and Concrete Research. 2007; 37(4):551-558. httPC://doi.org/10.1016/j.cemconres.2006.10.013

[20] Iskandarova M, Atabaev F, Tursunova G, Tursunov Z, Khadzhiev A, Atashev E, Berdimurodov E, Wan Nik W M N B, Rashidova K, & Demir M. Composite Portland cements: Innovations and future directions in cement technology. Innovative Infrastructure Solutions. 2025; 10(6). Article 249. https://doi.org/10.1007/s41062-025-02067-x

[21] Khadzhiev A, Atabaev F, Jumaniyozov A, & Yakubov Y. Study on pozzolanic activity of porphyrites of the Karatau deposit. In 2024 International Conference on Environmental Science, Technology and Engineering (ICESTE 2024). E3S Web of Conferences. 2024, 563. Article 02029. https://doi.org/10.1051/e3sconf/202456302029

[22] Kakali G, Tsivilis S, Aggeli E, & Bati M. Hydration products of C3A, C3S and Portland cement in the presence of $CaCO_3$. Cement and Concrete Research. 2000; 30(7):1073-1077. httPC://doi.org/10.1016/S0008-8846(00)00292-9

[23] Mo L, Deng M, & Tang M. Effects of calcite and calcined-clay on the hydration and strength development of Portland cement. Construction and Building Materials. 2010; 24(6):884-889. httPC://doi.org/10.1016/j.conbuildmat.2009.12.013

[24] Neville AM. Properties of concrete (5th ed.). Harlow: Pearson Education. 2011.

Crossref
DOI: 10.31643/2027/6445.06
Earth sciences

Experimental Study on Dry Magnetic Separation of Kharganat Iron Ore

[1] Khussan B., [1*] Yesendosova A.N., [1] Kenetaeva A.A., [1] Rabatuly M., [2] Matayev Zh.Sh., [3] Duissyen J., [4] Toshov J.B.

[1]Abylkas Saginov Karaganda Technical University, Karaganda, Kazakhstan
[2]Limited Liability Partnership Training Center Timerlan-2011, Karaganda, Kazakhstan
[3] National University of Mongolia, Ulaanbaatar, Mongolia
[4] Islam Karim Tashkent State Technical University, Tashkent, Uzbekistan

**Corresponding author email: a.yesendosova@ktu.edu.kz*

Received: *August 19, 2025*
Peer-reviewed: *August 25, 2025*
Accepted: *September 15, 2025*

ABSTRACT

A sample of iron ore from the Kharganat deposit was crushed to under 3 mm and subjected to dry magnetic separation, yielding a concentrate with 60.28% iron content and 98.92% metal recovery. When the sample was further crushed to under 1 mm and reprocessed, a concentrate with 66.7% iron content and 95.88% metal recovery was obtained. Through wet magnetic separation, a concentrate with 67.71% iron content and 96.9% metal recovery was produced. The tests confirmed that the most effective method was wet separation after crushing to under 1 mm and grinding for 40 minutes. In terms of beneficiation technology for the deposit, two process schemes—dry and wet magnetic separation—were developed. It was recommended that dry beneficiation be used in production instead of the water-intensive wet method. The sulfur and phosphorus content in the technological samples met standard requirements. Both previous studies and new exploration results were used in the resource estimation. It was confirmed that using a 10% cutoff grade for resource calculation is economically efficient. The minimum thickness of ore bodies was set at 2.0 meters, and the maximum thickness of waste rock at 4.0 meters. Resources were classified into Measured (B), Indicated (C), and Inferred (P1) categories. The geological structure of the deposit is simple, with a stable ore body distribution. The ore body thickness ranges from 5 to 40 meters, with an average of 23 meters. The deposit is suitable for open-pit mining, and no water drainage issues are expected in the initial years. It is planned to build an open-pit mine with an annual capacity of 500,000 tons of ore, with the cost of mining one ton of ore estimated at 4,312.8 MNT.

Keywords: Iron ore, Ore deposit, Mining hydrogeological conditions, Geological exploration.

Information about authors:

Khussan Bolatkhan — *Ph.D., Acting Associate Professor, Department of Development of Mineral Deposits of Abylkas Saginov Karaganda Technical University, 100027, The Republic of Kazakhstan, Karaganda, Ave. Nursultan Nazarbayev, 56. E-mail: h.bolathan@ktu.edu.kz; ORCID ID: https://orcid.org/ 0000-0003-0996-348X*

Yesendosova Ainel Nurtasovna — *Ph.D., Senior Lecturer, Department of Development of Mineral Deposits of Abylkas Saginov Karaganda Technical University, 100027, The Republic of Kazakhstan, Karaganda, Ave. Nursultan Nazarbayev, 56. E-mail: a.yesendosova@ktu.edu.kz; ORCID ID: https://orcid.org/0000-0001-7415-3630*

Kenetaeva Aigul Akanovna — *lecturer of Karaganda Technical University, Master of Engineering and Technology specialty Mining, Karaganda, Kazakhstan. E-mail: aigul_tate@bk.ru; ORCID ID: https:// orcid.org/0000-0001-7943-3279*

Rabatuly Mukhammedrakhym — *Ph.D., Acting Associate Professor, Department of Development of Mineral Deposits of Abylkas Saginov Karaganda Technical University, 100027, The Republic of Kazakhstan, Karaganda, Ave. Nursultan Nazarbayev, 56. E-mail: mukhammedrakhym@mail.ru; ORCID ID: https://orcid.org/0000-0002-7558-128X*

Mataev Zhanmurat Shagizatovich — *Director, Limited Liability Partnership Training Center Timerlan-2011, 100000, The Republic of Kazakhstan, Karaganda, 102/1 Ermekova Street. E-mail: too-timerlan-2011@bk.ru; ORCID ID: https://orcid.org/0009-0000-9839-7170*

Duissyen Janat — *PhD student, Department of Geology and Geophysics, School of Science, National University of Mongolia, 14201, Mongolia, Ulaanbaatar, University Street-1. E-mail: d_jagii@yahoo.com; ORCID ID: https://orcid.org/0000-0001-8757-5525*

Toshov Javokhir Buriewicz — *Doctor of Technical Sciences, Professor of Islam Karim Tashkent State Technical University, 100095 Republic of Uzbekistan, Tashkent, Almazar district, Universitetskaya street 2. E-mail: j.toshov@tdtu.uz; ORCID ID: https://orcid.org/0000-0003-4278-1557*

Introduction

In Mongolia, the mining and mineral resources sector has become one of the main driving forces of economic development, with iron ore extraction and beneficiation gaining particular importance. The Kharganat iron ore deposit is located in Naranbulag soum of Uvs province, and the quality and reserves of its ore occupy a key position in the region's development strategy [[1],[2]]. Efficient and economically optimized beneficiation and utilization of the deposit's ore is a primary goal, as it ensures effective use of the reserves and supplies the industrial sector with essential raw materials. Within this framework, testing the beneficiation technology using a dry magnetic separator is a critical step toward developing an efficient solution tailored to the characteristics of the ore. The dry beneficiation method offers distinct advantages in water-scarce regions and is also significant for minimizing environmental impact. Therefore, adapting the Kharganat iron ore to dry magnetic beneficiation technology constitutes a study of not only industrial but also environmental relevance. Research Objective [[2], [3]].

The main objective of this study is to experimentally determine the feasibility of beneficiating ore from the Kharganat iron deposit using dry magnetic separator technology at the laboratory level; to evaluate the ore's beneficiation potential; to optimize the beneficiation process parameters; and to develop the necessary technological foundation for future industrial implementation [4].

The experimental part

Iron ore is most commonly beneficiated using dry magnetic separation in industrial applications. The Kharganat iron ore sample was screened into fractions ranging from 3 mm to 0.125 mm, and each fraction was beneficiated using a dry magnetic separator set at a magnetic field strength of 2.5A. According to the test results, when the sample was crushed to under 3 mm and the 3–2 mm fraction was processed using a dry magnetic separator, a concentrate with 60.28% iron content and 98.92% metal recovery was obtained. To increase the concentrate grade, the sample was further crushed to under 1 mm and processed again using a dry magnetic separator, yielding a concentrate with 66.7% iron content and 95.88% metal recovery. From the test results, it was observed that when the ore was ground for 40 minutes and processed through wet magnetic separation, the concentrate yield was 92.05%, with an iron content of 67.71% and metal recovery of 96.9% [[5],[6]].

Therefore, under the conditions of wet magnetic separation, crushing the primary ore to under 1 mm and grinding for 40 minutes was selected as the most optimal parameter. To confirm the results, this test was repeated with a 10 kg sample, yielding a concentrate with 81.55% yield, 65.71% iron content, and 95.42% metal recovery.

Based on the results of the tests and research, two process flows for beneficiating the Kharganat iron ore using dry and wet magnetic separators were developed.

Both technological flows can be used in industrial applications. However, due to the high water consumption associated with wet magnetic separation, the use of the dry magnetic separation process is recommended.

In the technological sample, the contents of harmful impurities were low: sulfur was below 0.1%, and phosphorus was below 0.2%, which are not considered to affect the quality of the concentrate [[7], [8], [9]].

For the resource estimation at the Kharganat deposit, chemical analysis results from 374 core samples obtained from 49 boreholes, drilled by both the current and previous researchers within a 100 x 40-50-meter exploration grid, were used, along with the results from 253 trench samples collected from 27 surface channels.

To determine the key conditional parameters used in the resource calculation—such as cutoff grade, minimum industrial grade within a block, minimum thickness of ore intervals, and maximum thickness of barren intervals and waste rock—calculations were performed by comparing ore sections delineated at a 10% cutoff grade with those at 15% and 20% cutoff grades. As a result, the economically optimal cutoff grade, the minimum industrial grade within a block, and the corresponding thickness were determined.

After running calculations using all three scenarios, it was confirmed that each is economically viable, thereby justifying the use of a 10% cutoff grade. We concluded that this approach enables the full and efficient utilization of the ore from the deposit.

Therefore, based on the selected cut-off grade, the minimum ore grade required for production within the block was calculated using the cost of geological exploration incurred per ton of extracted, processed, and newly added ore reserve, using the following formula:

$$C_{\min prom} = \frac{(Z_{olb}Z_{bolov} + Z_{gha}) \cdot C_k(4312{,}2 + 10388{,}98 + 25{,}15) \cdot 67}{C_m \cdot K_m \cdot K_r} \quad 105400 \cdot 0{,}975 \cdot 0{,}9588 = 10\%$$

Where:

- Z_{olb} – Cost of extracting 1 ton of ore, 4,312.8₮
- Z_{bolov} – Cost of processing 1 ton of ore, 10,388.98₮
- Z_{gha} – Cost of geological exploration for increasing 1 ton of ore reserves, 25.55₮
- C_m – Metal price (price of 1 ton of concentrate based on the Ministry of Finance reference), 85 USD or 105,400₮

Based on the calculated result of the minimum grade within a block, it is fully feasible to adopt a cutoff grade of 10%.

Relying on the results of the above study, we determined that a minimum ore body thickness of 1.0 m is appropriate and used this value in the calculations. However, for the marginal boreholes, the minimum ore body thickness was taken as 2.0 m when outlining the boundaries. (This was based on the anticipated bucket size of the excavator to be used in the future.)

In cases where high-grade ore bodies in the cross-sections are relatively thin, setting a large thickness for barren rock layers or non-typical layers reduces the ore content in the cross-section. Therefore, we carefully selected a value of 4.0 m to minimise any excessive impact [[10], [11]].

Taking into account the above research and analysis results, the conditional indicators used in the resource calculation were as follows:

- Cutoff grades for delineating ore intervals – 10%, 15%, 20%
- Minimum industrial grade within a block – 15%
- Minimum ore body thickness – 2.0 m
- Thickness of barren rock and sub-economic layers – 4.0 m
- Bulk density of ore – 4.91%
- Minimum mineralization coefficient – 0.8

Using the key conditional indicators described above, the central part of the ore body was estimated as measured reserves (denoted by the letter B), while the marginal parts of the ore body were estimated as indicated reserves (denoted by the letter C). The remaining parts—namely, the northern, eastern, western, and southern sections of the ore body as defined by the magnetic anomalies identified during exploration, along with the deeper part of the deposit—were classified as inferred resources (denoted by P1).

The Kharganat deposit's ore body is geologically simple, with minimal variation in ore body thickness, uniform distribution of the main mineral components, and no fragmentation or significant internal alteration. Therefore, in accordance with the classification system of mineral deposits, it was categorized as Group II [[12], [13]].

After studying the rock samples and other materials collected during the Kharganat exploration, along with laboratory analysis results and ore distribution characteristics in the deposit area, it was concluded that the ore has no clearly defined distribution criteria or geological boundaries. Therefore, the boundaries of the ore body were defined solely based on drilling data and sample analysis results.

The boundary of the measured reserves (B) was delineated based on sample analysis results, conditional indicators, and constrained by exploration workings and boreholes. Since geological and geophysical indicators, along with some mine workings and boreholes, confirm that the ore body extends toward the margin, limited extrapolation methods were used on exploration lines X, V, I-1, and VIII. The indicated reserves (C) were also defined using the extrapolation method.

The ore body of the Kharganat iron ore deposit is a stable, massive body with consistent thickness, starting from the surface and extending to shallow depths. Fracturing across the deposit does not generally exceed 5–10 meters and significantly decreases with depth. Although the ore body is hard, slightly weathered and crumbled sections occur near the surface.

The Kharganat iron ore body extends from the southeast to the northwest, with a total length of approximately 1,100 meters. Its width is about 160-240 meters in the southeastern section, 80-170 meters in the northwestern section, and 160-200 meters in the central section, with an average width of 150.9 meters. The surface relief of the ore body gradually slopes downward from southeast to northwest, making the northwestern side especially suitable for mining operations.

In the blocks classified as measured reserves (denoted by B), the overburden thickness ranges from 0.0 to 17.5 meters, averaging 3.5 meters, while the ore body thickness ranges from 5 to 40 meters, with an average of 23 meters.

In the resource estimation, the average bulk density of the ore body was taken as 4.91 t/m³, as determined in 2010.

Iron ore can be mined using drilling and blasting methods, and it is fully feasible to selectively extract slightly weathered and fragmented sections near the surface. Within the deposit area, groundwater was encountered at a depth of 29.0 meters in the borehole drilled at the lowest point. Therefore, drainage measures will need to be implemented in the later years of operation. During the initial years of mining, the hydrogeological conditions are not problematic, as there is no groundwater or surface water, and the terrain is elevated, meaning that water accumulation in the open-pit is not expected [[14], [15]].

Considering the mining and technical conditions of the deposit, the structure and location of the ore body, and the volume of overburden removal, it was determined that open-pit mining would be appropriate. This report includes a preliminary technical and economic estimate for operating the deposit as an open-pit mine.

The boundaries of the open-pit were established based on the ratio of economically viable ore and waste in the measured reserves. The slope angle of the pit wall at a mining depth of 40-60 meters was determined to be 70 per mille ‰), taking into account the natural, climatic, hydrogeological conditions, and rock hardness characteristics during mining. Depending on the mining and technical conditions, during the first nine years, the slope angle in the upper 20-30 meters of depth may be close to 0°.

An open-pit mine with an annual capacity of 500,000 tons of ore is planned. The parameters for exploiting the Kharganat iron deposit via open-pit mining have been optimised, suitable mining machinery has been selected based on operational parameters, and the production cost has been calculated. The cost of mining 1 ton of ore (production cost) is estimated to be 4,312.8 MNT.

In the beneficiation cost estimate, the ore was first crushed to less than 30 mm and then processed by dry magnetic separation. The remaining low-grade portion was ground and also processed using a dry method. This selected technology was used to calculate the beneficiation cost. The cost of beneficiating 1 ton of ore (production cost) is 10,388.98 MNT [16].

The reserves of economically exploitable and geologically proven mineral resources are presented in the table below. The quantity of measured reserves selected for exploitation (denoted by B) amounts to 10.8 million tons of ore.

Table 1 - Reserves prepared for exploitation and identified through geological exploration [17]

No	Reserve Category	Average Thickness of Ore Body (m)	Volume (m³)	Bulk Density (t/m³)	Total Geological Reserves (million tons)
1	B	23	2.186.679.0	4.91	10.8
2	C	—	695.002	4.91	3.41
3	P1	—	72.000	4.91	11.74
	Total				25.94

When extracting mineral resources, it is not possible to recover the entire geological reserve identified through exploration, and to some extent, loss and dilution occur during mining. Factors such as geological-mining conditions, technical-technological limitations, and organizational factors contribute to the occurrence of loss and dilution of mineral resources.

During mining operations, the ore loss rate was estimated at 3%, and the dilution rate at 2.5%. Using these indicators, the production (exploitable) reserves were calculated as follows:

Table 2 - Ore Loss During Mining [18]

Reserve Category	Geological Reserves (million tons)	Loss (3%) (million tons)	Dilution (2.5%) (million tons)	Production Reserves (million tons)
B	10.8	0.324	0.27	10.7
C	3.41	0.102	—	3.3
Total	14.2	0.426	0.27	14.0

Discussion of the results

Within the area covered by Mining License No. 13766A, the Kharganat iron ore deposit was explored in 2010 by ELGT LLC using its own funds. The exploration work included core drilling, magnetic surveying, topographic and geodetic surveys, various types of sampling, and laboratory analyses.

The drilling was carried out by the drilling team of Naran Talst LLC, magnetic surveying by Geo Oron LLC, topographic and geodetic work by ATPP LLC, laboratory testing by the Central Geological Laboratory in Ulaanbaatar, external quality control by SGS Laboratory, geological studies by a team of geologists from ShShDB LLC, and the hydrogeological work was performed under contract by Dr. Professor M. Alei and others. It is important to note their contributions.

The results of trenches and boreholes excavated during previous exploration phases by researchers such as N.I. Modnova (1950) and O. Khongor (1990)—including channel and core sample chemical analyses—were reprocessed and integrated with the results from the complementary exploration conducted by ELGT LLC. This included magnetic surveys, geological traverses, borehole data, and laboratory test results. Based on these combined outcomes, this reserve report has been compiled.

The complementary exploration work carried out at the Kharganat deposit fully meets the requirements of the standard.

The Kharganat deposit is located at the margin of a 1,200 x 500 m xenolith body of the Tsagaanshiveet Formation, consisting of Lower to Middle Devonian volcanogenic-sedimentary rocks, which formed as a result of the intrusion of leucogranitic rocks from the Dulaanuushig intrusive complex of Late Devonian–Early Carboniferous age.

The ore body is hosted in a skarn formation that is intensely silicified and hornfelsed, containing actinolite-epidote minerals.

The ore body is concordantly hosted within skarn-altered volcanogenic-sedimentary rocks, trending northwest. Its strike length is 1,100 m. The width of the ore body varies: in the southeast it ranges from 160–240 m, in the central section from 110–160 m, and in the northwest from 90–120 m, with an average width of 151 m.

Morphologically, the iron ore body is continuous with no apophyses or significant disruptions, extending in a northwest direction both horizontally and vertically.

The total iron content in the ore ranges from 20.3-60.8% in exploration trenches, with an average of 44.26%, and from 10.28–62.0% in drill holes, with an average of 36.93%. Sampling has confirmed that the iron content is uniformly distributed along both the strike and vertical direction of the ore body.

The mineral composition of the Kharganat iron ore consists mainly of magnetite, with smaller amounts of martite, hydrogoethite, pyrite, malachite, millerite, hematite, chalcopyrite, and other minerals. Magnetite accounts for 80–85% of the iron ore, martite 5–10%, and the rest are minor minerals. The ore is classified as skarn-type magnetite.

For technological testing and the development of a beneficiation process flow, a 180 kg technological sample was processed at the Central Geological Laboratory using both dry and wet magnetic separation. The dry magnetic separation yielded a concentrate with 66.7% iron content and 95.88% metal recovery, while wet magnetic separation resulted in 65.71% iron content and 95.42% metal recovery.

The iron content in the tailings was about 14%, which chemical analysis confirmed to be low-magnetic martite.

Based on these results, two beneficiation flowsheets using dry and wet magnetic separation were developed, and due to the high-water consumption of the wet process, the dry magnetic separation process was recommended for industrial application [19].

The hydrogeological conditions of the deposit are very simple.

The southeastern part of the ore body will remain dry during operation, while groundwater will begin to seep only in the northwestern part of the mine at depths below 25 m (elevation 1,498 m). The water inflow is estimated at 676 m^3 per day, or 28.2 m^3 per hour, which will not pose any difficulties for mining operations.

The mining and technical conditions of the Kharganat deposit are simple.

Most of the ore body is exposed at the surface, with the deepest part located at 17.5 m depth. The stripping ratio is 0.05 m^3/ton.

As a result of the complementary exploration work conducted at the Kharganat deposit in 2024, the classification of the iron ore production reserves was upgraded, and the quantity of ore contained within the ore body was redefined. The figures are shown in the table below:

Table 3 - Reserves prepared for exploitation and identified through geological exploration [20]

No	Indicators	Unit	Ore Reserves and Cutoff Grade		
			10%	15%	20%
1	Measured reserves (Category B) Total iron average grade	Million.t %	10.82 41.9	9.87 44.96	9.33 46.08
2	Measured reserves (Category C) Total iron average grade	Million.t %	3.41 27.82	2.15 39.41	1.33 42.35
3	Inferred resources (Category P1)	Million.t	11.74	12.61	13.52
4	Total ore reserves, B+C Total resources B+C+P1	Million.t Million.t	14.2 26.8	12.02 24.63	10.67 24.19

It is planned to develop the deposit through open-pit mining and to construct a beneficiation plant capable of processing 500,000 tons of ore per year. A preliminary economic assessment has shown that the exploitation of the Kharganat iron ore deposit would be economically viable. Bringing this deposit into economic circulation would not only contribute to the development of the local economy but also help to reduce unemployment to some extent.

Conclusion

Beneficiation tests conducted on samples from the Kharganat iron ore deposit confirmed that both dry and wet magnetic separation technologies are effective. Dry beneficiation produced concentrates with iron content ranging from 60.28% to 66.7%, while wet beneficiation yielded a concentrate with 67.71% iron content, demonstrating high technological efficiency. Since wet beneficiation requires significant water consumption, it is recommended to apply dry beneficiation technology in production.

The geological structure of the ore body is simple, and the ore distribution is consistent. The deposit is suitable for open-pit mining, with a planned annual production capacity of 500,000 tons of ore. From an economic perspective, calculating reserves at a 10% cutoff grade is considered appropriate, and the cost of mining is within a feasible range.

Thus, based on technical-economic indicators and beneficiation results, the Kharganat iron ore deposit has been confirmed to be suitable for industrial exploitation.

Conflict of interest. On behalf of all the authors, the corresponding author declares that there is no conflict of interest.

***CRediT author statement*: B.Khussan, M.Rabatuly:** Conceptualization, Methodology, Software; **J.Duissyen, Zh.Matayev**: Data curation, Writing-Original draft preparation; **A.Yesendosova, A.Kenetayeva:** Visualization, Investigation; **B.Khussan, J.Toshov:** Software, Validation.

Cite this article as: Khussan B, Yesendosova AN, Kenetaeva AA, Rabatuly M, Matayev ZhSh, Duissyen J, Toshov JB. Experimental Study on Dry Magnetic Separation of Kharganat Iron Ore. Kompleksnoe Ispolzovanie Mineralnogo Syra = Complex Use of Mineral Resources. 2027; 340(1):58-66. https://doi.org/10.31643/2027/6445.06

Харганат темір кенін құрғақ магниттік бөлу арқылы эксперименттік зерттеу

[1] Хусан Б., [1] Есендосова А.Н., [1] Кенетаева А. А., [1] Рабатұлы М., [2] Матаев Ж.Ш., [3] Дуйсен Ж., [4] Тошов Ж.Б.

[1] Ә. Сағынов атындағы Қарағанды техникалық университеті, Қарағанды, Қазақстан
[2] Тимерлан-2011 ЖШС оқу орталығы, Қарағанды, Қазақстан
[3] Моңғолия ұлттық Университеті, Ұлан-Батор, Моңғолия
[4] Ислам Кәрім атындағы Ташкент Мемлекеттік Техникалық Университеті, Ташкент, Өзбекстан

Мақала келді: *19 тамыз 2025*
Сараптамадан өтті: *25 тамыз 2025*
Қабылданды: *15 қыркүйек 2025*

ТҮЙІНДЕМЕ

Харганат кен орнынан алынған темір кенінің сынамасы 3 мм-ге дейін ұсақталып, құрғақ магниттік бөлінуге ұшырап, құрамында 60,28% темір бар концентрат және 98,92% металл алынды. Үлгіні одан әрі 1 мм-ге дейін ұсақтап, қайта өңдеген кезде құрамында 66,7% темір және 95,88% метал болатын концентрат алынды. Ылғалды магниттік сепарацияны қолдана отырып, құрамында темір мөлшері 67,71% және металл экстракциясы 96,9% болатын концентрат алынды. Сынақтар ең тиімді әдіс 1 мм-ден төмен ұсақталғаннан кейін және 40 минут бойы ұнтақталғаннан кейін ылғалды бөлу екенін растады. Кен орнын байыту технологиясына келетін болсақ, екі технологиялық схема әзірленді—құрғақ және дымқыл магнитті бөлу. Өндірісте суды көп қажет ететін дымқыл әдістің орнына құрғақ байытуды қолдану ұсынылды. Технологиялық үлгілердегі күкірт пен фосфордың мөлшері стандартты талаптарға сай болды. Ресурстарды бағалау кезінде алдыңғы зерттеулер де, геологиялық барлаудың жаңа нәтижелері де пайдаланылды. Ресурстарды есептеу үшін шекті бағаны 10% пайдалану экономикалық тұрғыдан тиімді екендігі расталды. Кен денелерінің минималды қалыңдығы 2,0 метр, ал қалдық жыныстардың максималды қалыңдығы 4,0 метр болып белгіленді. Ресурстар Өлшенген (В), Көрсетілген (С) және Болжамды (Р1) санаттарға жіктелді. Кен орнының геологиялық құрылымы қарапайым, кен денелері тұрақты таралған. Кен денесінің қалыңдығы 5-тен 40 метрге дейін, орташа есеппен 23 метрді құрайды. Кен орны ашық әдіспен өндіруге жарамды және алғашқы жылдары суды ағызуда қиындықтар күтілмейді. Қуаттылығы жылына 500 000 тонна кенді құрайтын ашық кеніш салу жоспарлануда, бұл ретте бір тонна кенді өндіру құны 4 312,8 млн тугрикке бағаланады.

Түйін сөздер: темір кені, кен орны, тау-кен гидрогеологиялық жағдайы, геологиялық барлау.

Авторлар туралы ақпарат:

Хусан Болатхан
PhD докторы, Әбілқас Сағынов атындағы Қарағанды техникалық университетінің Пайдалы қазбалар кенорындарын өндіру кафедрасының доцент м.а., 100027, Нұрсұлтан Назарбаев даңғ. 56, Қарағанды, Қазақстан. E-mail: h.bolathan@ktu.edu.kz; ORCID ID: https://orcid.org/ 0000-0003-0996-348X

Есендосова Айнель Нуртасовна
PhD докторы, Әбілқас Сағынов атындағы Қарағанды техникалық университетінің Пайдалы қазбалар кенорындарын өндіру кафедрасының аға оқытушысы, 100027, Нұрсұлтан Назарбаев даңғ. 56, Қарағанды, Қазақстан. E-mail: a.yesendosova@ktu.edu.kz; ORCID ID: https://orcid.org/0000-0001-7415-3630

Кенетаева Айгуль Акановна
Техника ғылымдарының магистрі, Әбілқас Сағынов атындағы Қарағанды техникалық университетінің Геология және пайдалы қазбалар кен орындарын барлау кафедрасының оқытушысы, 100027, Нұрсұлтан Назарбаев 56, Қарағанды, Қазақстан. E-mail: aigul_tate@bk.ru; ORCID ID: https://orcid.org/0000-0001-7943-3279

Рабатұлы Мұхаммедрахым
PhD докторы, Әбілқас Сағынов атындағы Қарағанды техникалық университетінің Пайдалы қазбалар кенорындарын өндіру кафедрасының доцент м.а., 100027, Нұрсұлтан Назарбаев даңғ. 56, Қарағанды, Қазақстан. E-mail: mukhammedrakhym@mail.ru; ORCID ID: https://orcid.org/0000-0002-7558-128X

Матаев Жанмурат Шагизатович
Тимерлан-2011 Жауапкершілігі шектеулі серіктестігі оқу орталығының директоры, 100000, Ермеков к-сі, 102/1, Қарағанды, Қазақстан. E-mail: too-timerlan-2011@bk.ru; ORCID ID: https://orcid.org/0009-0000-9839-7170

Дуйсен Жанат
PhD докторанты, Геология және геофизика факультеті, Жаратылыстану ғылымдары мектебі, Моңғолия Ұлттық университеті, 14201, Моңғолия, Ұлан-Батор, Университет көшесі-1. E-mail: d_jagii@yahoo.com; ORCID ID: https://orcid.org/0000-0001-8757-5525

Тошов Жавохир Буриевич
Техника ғылымдарының докторы, Ислам Карим атындағы Ташкент мемлекеттік техникалық университетінің профессоры, 100095, Алмазар ауданы Университетская көшесі 2, Ташкент, Өзбекстан. E-mail: j.toshov@tdtu.uz; ORCID ID: https://orcid.org/0000-0003-4278-1557

Экспериментальное исследование по сухой магнитной сепарации Харганатской железной руды

[1] Хусан Б., [1] Есендосова А.Н., [1] Кенетаева А. А., [1] Рабатұлы М., [2] Матаев Ж.Ш., [3] Дуйсен Ж., [4] Тошов Ж.Б.

[1] Карагандинский технический университет имени А. Сагинова, Караганда, Казахстан
[2] ТОО Учебный центр Тимерлан-2011, Караганда, Казахстан
[3] Национальный университет Монголии, Улан-Батор, Монголия
[4] Ташкентский государственный технический университет имени Ислама Карима, Ташкент, Узбекистан

Поступила: *19 августа 2025*
Рецензирование: *25 августа 2025*
Принята в печать: *15 сентября 2025*

АННОТАЦИЯ

Образец железной руды с месторождения Харганат был измельчен до размера менее 3 мм и подвергнут сухой магнитной сепарации, в результате чего был получен концентрат с содержанием железа 60,28% и извлечением металла 98,92%. Когда образец был дополнительно измельчен до размера менее 1 мм и подвергнут повторной обработке, был получен концентрат с содержанием железа 66,7% и извлечением металла 95,88%. С помощью мокрой магнитной сепарации был получен концентрат с содержанием железа 67,71% и извлечением металла 96,9%. Испытания подтвердили, что наиболее эффективным методом является мокрая сепарация после дробления до размера менее 1 мм и измельчения в течение 40 минут. Что касается технологии обогащения для месторождения, то были разработаны две технологические схемы — сухая и мокрая магнитная сепарация. Было рекомендовано использовать сухое обогащение в производстве вместо водоемкого мокрого метода. Содержание серы и фосфора в технологических образцах соответствовало стандартным требованиям. При оценке ресурсов были использованы как предыдущие исследования, так и новые результаты геологоразведочных работ. Было подтверждено, что использование 10%-ной нормы отсечения для расчета ресурсов является экономически эффективным. Минимальная толщина рудных тел была установлена на уровне 2,0 метров, а максимальная толщина пустой породы - 4,0 метра. Ресурсы были классифицированы на категории "Измеренные" (B), "Указанные" (C) и "предполагаемые" (P1). Геологическое строение месторождения простое, со стабильным распределением рудных тел. Мощность рудного тела колеблется от 5 до 40 метров, в среднем 23 метра. Месторождение подходит для разработки открытым способом, и в первые годы не ожидается проблем с отводом воды. Планируется строительство открытого месторождения мощностью 500 000 тонн руды в год, при этом стоимость добычи одной тонны руды оценивается в 4 312,8 млн тугриков.

Ключевые слова: железная руда, рудное месторождение, горно-гидрогеологические условия, геологоразведка.

Хусан Болатхан — *Доктор PhD, и.о. доцента кафедры Разработки месторождений полезных ископаемых Карагандинского технического университета имени Абылкаса Сагинова, 100027, пр. Нурсултана Назарбаева, 56, Караганда, Казахстан. E-mail: h.bolathan@ktu.edu.kz; ORCID ID: https://orcid.org/ 0000-0003-0996-348X*

Есендосова Айнель Нуртасовна — *Доктор PhD, старший преподаватель кафедры Разработки месторождений полезных ископаемых Карагандинского технического университета имени Абылкаса Сагинова, 100027, пр. Нурсултана Назарбаева, 56, Караганда, Казахстан. E-mail: a.yesendosova@ktu.edu.kz; ORCID ID: https://orcid.org/0000-0001-7415-3630*

Кенетаева Айгуль Акановна — *Магистр технических наук кафедры Геология и разведка месторождений полезных ископаемых Карагандинского технического университета имени Абылкаса Сагинова, 100027, пр. Нурсултана Назарбаева, 56, Караганда, Казахстан. E-mail: aigul_tate@bk.ru; ORCID ID: https://orcid.org/0000-0001-7943-3279*

Рабатулы Мухаммедрахым — *Доктор PhD, и.о. доцента кафедры Разработки месторождений полезных ископаемых Карагандинского технического университета имени Абылкаса Сагинова, 100027, пр. Нурсултана Назарбаева, 56, Караганда, Казахстан. E-mail: mukhammedrakhym@mail.ru; ORCID ID: https://orcid.org/0000-0002-7558-128X*

Матаев Жанмурат Шагизатович — *Директор Учебного центра Товарищество с ограниченной ответственностью Тимерлан-2011, 100000, ул. Ермекова, 102/1. Караганда, Казахстан. E-mail: too-timerlan-2011@bk.ru; ORCID ID: https://orcid.org/0009-0000-9839-7170*

Дуйсен Жанат — *PhD докторант, Факультет геологии и геофизики, Школа естественных наук, Национальный университет Монголии, 14201, улица Университетская 1. Улан-Батор, Монголия. E-mail: d_jagii@yahoo.com; ORCID ID: https://orcid.org/0000-0001-8757-5525*

Тошов Жавохир Буриевич — *Доктор технических наук, профессор Ташкентского государственного технического университета имени Ислама Карима, 100095, Алмазарский район, улица Университетская 2, Ташкент, Узбекистан. E-mail: j.toshov@tdtu.uz; ORCID ID: https://orcid.org/0000-0003-4278-1557*

References

[1] Dorj B. Study of Iron Ore Deposits in Mongolia. Publishing House of MUST. 2018.

[2] Tumenjargal S, & Ochirbat G. Mineral Beneficiation Technology. National University of Mongolia Press. 2015.

[3] Gombosuren D. Study of Water Resources in Mongolia and Mine Water Use. UB Press. 2019.

[4] Tang S, Li Y. Experimental study on mineral processing of iron bearing rocks in Bayan Obo West Mine. China Mining Magazine. 2024; 33(1):226-234. https://doi.org/10.12075/j.issn.1004-4051.20230279

[5] Luo Y, Xiao J, Shi Y, Xie B. Experimental study on beneficiation of a low-grade refractory iron ore in Qinghai province. Iron Steel Vanadium Titanium. 2023; 44(5):28-35. https://doi.org/10.7513/j.issn.1004-7638.2023.05.005

[6] Chen H, Du X, Wang Y. Application of Fine Screen in Reconstruction and Expansion process of Iron Mine in Sichuan Province. Multipurpose Utilization of Mineral Resources. 2023; 44(1):168-171. https://doi.org/10.3969/j.issn.1000-6532.2023.01.023

[7] Fu J, Hu S. Experimental Study on a Refractory Low-grade Ferromanganese Ore. Multipurpose Utilization of Mineral Resources. 2021; 42(3):158-164. https://doi.org/10.3969/j.issn.1000-6532.2021.03.025

[8] Champan K, Shauet Kh. Brief Geological Exploration Report of Burd Lake Prospecting Area (4123X), Near the Kharganat Deposit. 2009.

[9] Nunna V, Suthers SP, Pownceby MI, Sparrow GJ. Beneficiation strategies for removal of silica and alumina from low-grade hematite-goethite iron ores. Miner Process Extr Metall Rev. 2021; 43(8):1049-1067.

[10] Nameni A, Nazari M, Shahmardan MM, Nazari M, Mashayekhi V. Separation and trapping of magnetic particles by insertion of ferromagnetic wires inside a microchip: Proposing a novel geometry in magnetophoresis. Journal of Magnetism and Magnetic Materials. 2022; 560:169424. https://doi.org/10.1016/j.jmmm.2022.169424

[11] Golik VI, Dmitrak YuV, Razorenov YuI, Maslennikov SA, Lyashenko VI. Mekhanokhimicheskaya tekhnologiya izvlecheniya zheleza iz khvostov obogashcheniya [Mechanochemical technology of iron extraction from enrichment tailings]. Izvestiya. Ferrous Metallurgy. 2021; 64(4):282-291. (In Russ.). https://doi.org/10.17073/0368-0797-2021-4-282-291

[12] Tang D, Yan Y, Tian X, Wu L, Wang F. Separation mechanism of a pneumatic dry low-intensity drum magnetic separator and optimization of magnetic fields. Minerals Engineering. 2025, 231. https://doi.org/109451 2025 10.1016/j.mineng.2025.109451

[13] Fariss AHB, Ibrahim AII, Ozdemir AC, Kursunoglu S, Altiner M. Beneficiation of Low-Grade Iron Ore Using a Dry-Roll Magnetic Separator and its Modeling via Artificial Neural Network. Journal of Sustainable Metallurgy. 2025; 11(2):1133-1149. https://doi.org/10.1007/s40831-025-01030-5

[14] Alikulov Sh, Toshov J, Mussin R, Rabatuly M, Tolovkhan B, Bogzhanova Zh, Gabitova A. Study of rational solution parameters during in-situ uranium leaching. Mining of Mineral Deposits. 2025; 19(1):37-46. https://doi.org/10.33271/mining19.01.037

[15] Toshov JB, Rabatuly M, Bogzhanova ZhK, Zheldikbayeva AT, Malikov ShR, Toshov BR, Ergashev OS. Influence of Radiation and Magnetic Pulse Treatment on The Wear Resistance of Carbide Tools. Kompleksnoe Ispolzovanie Mineralnogo Syra = Complex use of mineral resources. 2026; 337(2):47-54. https://doi.org/10.31643/2026/6445.16

[16] Chaib A, Bouabdallah S, Ferfar M, Dovbash N, Bellucci S. Investigation of Physicochemical Characterization and Magnetic Enrichment Of Iron Ore From Sidi Maarouf Deposit. Technology Audit and Production Reserves. 2024; 1(3(75):37-42. https://doi.org/10.15587/2706-5448.2024.297846

[17] Ministry of Mining and Heavy Industry of Mongolia. Iron Ore Mining and Export Report. Ulaanbaatar: MMHI. 2020.

[18] Khongor O. Report on the Results of Prospecting and Exploration for Cement Raw Materials in Khovd and Uvs Provinces. GAF No. 4820.

[19] Sukhbat Ch, Vanchindorj B. Results Report of 1:50,000 Scale Geological Mapping and General Prospecting Work Conducted in Ulaangom Area, 1998–2000 (M-46-77-VG, 78V, 89-ABVT, 90-AB). 2000. GAF No. 5320.

[20] Jamyandorj Ö, Bespechinsky VS. Report of 1:200,000 Scale Geological Mapping Work Conducted in the Great Lakes Depression, 1974–1975. UB, 1975. GAF No. 2740

Crossref

DOI: 10.31643/2027/6445.07
Earth sciences

A study of the geochemical features of the Nurkazgan copper-porphyry deposit

[1] Kopobayeva A.N., [1] Zharylgapov Ye.Ye., [2]Ulgibayeva B.S., [1*]Amangeldikyzy A., [1*]Askarova N.S., [1*]Kabyken A.B.

[1]Abylkas Saginov Karaganda Technical University, Karaganda, Kazakhstan
[2]LLP Geotek, Karaganda, Kazakhstan

**Corresponding author's email: a.amangeldykyzy@ktu.edu.kz*

Received: *July 12, 2025*
Peer-reviewed: *July 21, 2025*
Accepted: *September 22, 2025*

ABSTRACT

Porphyry copper deposits are the source of most of the world's copper, molybdenum and significant amounts of gold. This makes them a major focus of scientific research due to their economic significance. The article is devoted to the study of the geochemistry of host rocks and copper-porphyry ores at the Nurkazgan deposit. It identifies geochemical criteria for the distribution of gold in copper-porphyry systems, as well as refines ore formation mechanisms in order to improve predictive criteria. The results were obtained by interpreting analytical data obtained using the ICP-OES (ICP-AES) method and the geostatistical method. Based on this research, key factors have been identified that determine the distribution of element content. As a result of studying the distribution of REEs in the host rocks, conditions for ore formation were established: the deposit has an igneous origin with signs of prolonged fractionation of the magma; a negative Eu anomaly confirms the involvement of plagioclase fractionation typical of medium and acidic magmas; LREE enrichment indicates an evolved magma involving the continental crust, while moderate depletion of HREE indicates a deep source of magmatism with residual garnet involvement. The established strong positive correlation between REES indicates a single geochemical process and reflects the primary magmatic identity. A porphyry system with a deep magmatic source has been revealed, where ore fluids are separated from the residual melt, which is already depleted in Eu but enriched in LREEs and metals.

Keywords: geochemistry, geological processes, mineralization zones, distribution of elements, localization of minerals, ore-forming processes, copper mineralization, ore deposits.

Information about authors:

Kopobayeva Aiman Nygmetovna — *PhD, associate professor of the Geology and Exploration MD Department of Abylkas Saginov Karaganda Technical University, 100000, Karaganda, Kazakhstan. E-mail: kopobayeva@inbox.ru; ORCID ID: https://orcid.org/0000-0002-0601-9365*

Zharylgapov Yerassyl Yerboluly — *Master's student of the Geology and Exploration MD Department of Abylkas Saginov Karaganda Technical University, 100000, Karaganda, Kazakhstan. E-mail: erasyl.zharylgapov@mail.ru; ORCID ID: https://orcid.org/0009-0001-8389-4710*

Ulgibayeva Begim Sarkytbaykyzy — *Geologist, LLP Geotek, 100027, Karaganda, Republic of Kazakhstan. E-mail: begimay.97@mail.ru; ORCID ID: https://orcid.org/0009-0003-1644-4183*

Amangeldikyzy Altynay — *PhD, acting associate professor of the Geology and Exploration MD Department of Abylkas Saginov Karaganda Technical University, 100000, Karaganda, Kazakhstan. E-mail: a.amangeldykyzy@ktu.edu.kz; ORCID ID: https://orcid.org/0000-0002-6665-8804*

Askarova Nazym Srazhadinkyzy — *PhD, senior lecturer of the Department of Geology and Exploration of Mineral Resources, Abylkas Saginov Karaganda Technical University, 100027, Karaganda, Kazakhstan. E-mail: n.askarova@ktu.edu.kz; ORCID ID: https://orcid.org/0000-0002-2103-6198*

Kabyken Aidyn Bakytzhanuly — *Doctoral student of the Geology and Exploration MD Department of Abylkas Saginov Karaganda Technical University, 100000, Karaganda, Kazakhstan. E-mail: aidynkabyken@yandex.ru; ORCID ID: https://orcid.org/0009-0008-2020-6141*

Introduction

Copper is a critical and vital component in various modern green technologies [[1], [2]]. In this regard, molybdenum-copper deposits in veined ores or the so-called porphyry copper deposits are becoming increasingly important. Copper porphyry deposits are key sources of non-ferrous metals and precious metals, and play an important role in mining, stimulating research and exploration [[3],[4],[5],[6],[7],[8]]. Significant are ore zones containing significant concentrations of gold and silver, which act as both associated components and valuable target products [8]. These deposits, which are often characterized by poorer ores compared to pyrites, skarns, and veins, should have sufficiently large reserves of copper ore and be mined using open-pit methods to be profitable for development. The appeal of this type of deposit is also determined by the possibility not only to organise open-cast

mining, but also to extract complex ores containing valuable impurities such as gold, silver, rhenium, selenium, tellurium, bismuth, and others.

The low cost of open-pit copper mining and the complex nature of ores justify the industry's focus on this type of deposit as a main source of copper production, not only in the past and present, but also in the future. This is why many geologists around the world are interested in open-pit mining. For example, Ferraq et al. (2024) conducted a comprehensive geochemical and geochronological study of the Imourkhsen porphyry deposit in Morocco, showing the relationship between empirical data and the stages of large-scale magmatism [9]. Studies on the analysis of Côte Gold-type deposits in Canada [10] have revealed typical alteration zones and their geochemical markers, which are important for predicting ore formation. Chinese scientists [11] have provided new data on U-Pb and Hf isotopes, indicating magmatic intrusions in a post-collision context at the Wubaduolai deposit. Zhangetal. (2024) [12], through the Sr-Nd isotope analysis of Sinondo granitoids in Tibet, confirmed the genetic link between magmatism and Ag-Pb-Zn enrichment. All this indicates that the integration of the latest isotopic, geochemical, and geochronological data is crucial for understanding porphyry ore formation processes and can be applied to systems such as the Nurkazgan deposit.

In Kazakhstan, copper-porphyry deposits such as Aktogay, Aidarly, Bozshakol, and Koksai are of significant importance for the extraction of copper and other precious metals. These deposits contain low levels of copper, but have substantial reserves. Moreover, spatial analysis of precious metal distribution contributes to the development of three-dimensional ore body models, enabling more accurate prediction of metal content at different levels within a deposit. This is crucial for the economic evaluation of a deposit, planning of mining operations, and selection of optimal mining methods [13].

It is also important to take into account that the localization of gold and silver can be caused not only by primary ore formation processes but also by secondary hydrothermal processes that redistribute metals within ore bodies. Understanding these processes helps to make a more accurate interpretation of geological data and increase efficiency.

The Nurkazgan deposit is of particular interest due to its unique geological and structural characteristics. The development of this deposit is associated with several tasks, including the high variability of the precious metal content, challenging extraction conditions, and the need for environmentally sound technologies for ore processing. Geochemical analysis of the composition of ores and their structural features makes it possible not only to understand the processes of ore formation, but also to significantly increase the efficiency of prospecting operations. One of the directions of its solution is to improve the geological and genetic foundations of forecasting, taking into account which forecasting and prospecting models of ore regions and fields are built, to modernize methods and technologies of forecasting, prospecting and evaluation of deposits and, above all, hidden ones, that is, those that do not go out to the daytime surface.

The purpose of the study is to identify geochemical features and to study the distribution of gold and silver in copper-porphyry ores at the Nurkazgan deposit, in order to determine the factors that influence ore formation and conditions for deposit formation, with a view to increasing the efficiency of exploration operations. Scientific knowledge of ore-forming processes is of direct practical significance for improving the effectiveness of mining operations in Kazakhstan. This work is based on materials published and collected by the authors.

Experimental part

Methodology. Analytical and published data were used to study the geochemical characteristics of the deposit. When studying the distribution of gold, silver, and other elements in the ore of the Nurkazgan deposit, complex geochemical studies were conducted using the interpretation of data with geostatistical methods. Analytical work was performed in the laboratory of EcoNus LLP in Karaganda, utilizing ICP-OES (Inductively Coupled Plasma-Optical Emission Spectrometry) for eight elements (Ag, As, Au, Cu, Mo, Pb, S, and Zn), atomic absorption analysis for gold assays, and published data on the chemical makeup of host rocks, which were subsequently interpreted by the authors.

Samples of ore and host rock from various zones of the studied deposit were collected. These samples were subjected to a detailed geochemical analysis to determine the concentrations of major and trace elements and their spatial distribution. The analysis was conducted in the laboratory of EkoNus LLP in Karaganda. The depth distribution of elements was analyzed based on drilled wells, which

made it possible to identify the enrichment zones of copper, gold, and silver. Standard classification diagrams and ratios such as Sr/Y and Eu/Eu* were used to interpret the geochemical data and analyze the magma source and ore-forming processes.

Geological characteristics of the deposit. The Nurkazgan deposit is located in the Bukhar-Zhyrau district of the Karaganda region, 30 km north of Karaganda and 10 km northeast of Temirtau. It is also 2.5 km away from the northern shore of the Samarqand reservoir. The closest railway station is Murza (Aktau), which is 8 km away. The nearest highway is 3-4 km to the north-west and the Astana-Almaty highway is about 7 km west (Fig. 1).

Figure 1 – Overview map of the Nurkazgan deposit area

The Nurkazgan deposit has a complex geological structure, owing to its location within the Karaganda tectonic block, which is part of the Hercynian fold belt. The geological composition of the deposit includes sedimentary, volcanic, and intrusive rock formations from the Paleozoic era. Sedimentary deposits comprise mudstones, silts, sandstones, and conglomerates. Volcanic rocks include andesite, basalt, and their associated tuff formations. Intrusive rocks include granite, diorite, and gabbro. The deposit is classified as a porphyry copper deposit and contains significant reserves of copper, gold, and lead. The primary ore minerals of the deposit are chalcopyrite, bornite, pyrite, and magnetite. Associated minerals include quartz and calcite. The deposits have a predominantly lenticular or laminated shape and occur at depths ranging from 500 to 600 m. They are associated with fault zones and fractures. On the surface, there is an oxidation zone enriched in secondary copper minerals that makes it potentially suitable for the extraction of oxidised ores [14].

The Nurkazgan deposit consists of several sites, each with its own geological characteristics and level of industrial development. The ore-bearing rocks in the areas of active mining include granodiorite-porphyry, quartz-dioritic porphyry, quartz diorite and diorite (Fig. 2).

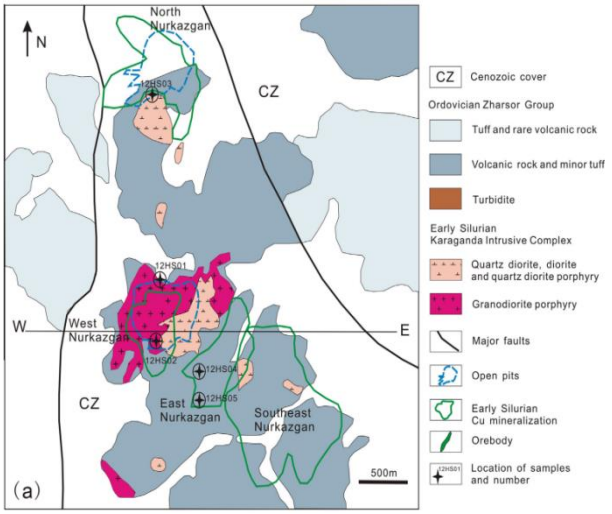

Figure 2 – Geological map of the Nurkazgan deposit (based on Yakubchuk et al. (2012), with modifications) [15]

The main feature of the deposit is the central ore-bearing area, which contains the main reserves of copper and related elements such as gold, silver, and molybdenum. The most significant occurrences of porphyry-type copper mineralization are observed here, primarily in the form of disseminated and vein-disseminated deposits. The central location is being actively explored and forms the core of all operational activities within the field. The western section of the area is adjacent to the main area and is characterized by dispersed mineralization. This area has a lower concentration of useful components compared to other parts of the site, but it has been identified as promising for further exploration and potential expansion of ore reserves. The eastern section contains ore bodies with predominant copper-pyrite mineralization, with some areas showing increased gold content. This makes this part of the site interesting for the complex processing of raw materials. The southern area has a high copper content, reaching up to 4% in certain locations. In this region, ore bodies often have a complicated structure formed through the influence of tectonic processes. Both open-pit and underground mining operations are taking place in the southern area. The northern section is poorly studied, but geophysical and geochemical data indicate the presence of potentially promising

structures that could contain ore bodies at greater depths. It is considered a potential target for future exploration efforts. In addition to the primary ore zones, the deposit has overburden areas and spent quarries that have been used to store overburden rock and man-made structures.

Thus, the Nurkazgan field is a complex, multi-stage structure that combines both currently developed areas and promising areas for future exploration and development.

Results and Discussion

For a detailed geochemical analysis, published chemical composition data on 14 samples of intrusive rocks from the Nurkazgan deposit were used [16]. Based on the results obtained, a TAC diagram (Fig. 3) was constructed to determine the types of intrusive rocks. The studied igneous rocks demonstrate a wide range of SiO_2 content (52.78-68.92%) and varying potassium content (1.08-8.62%). Intrusive rocks associated with porphyritic copper mineralization are characterized by a high content of SiO_2 (65.45-68.92%) and potassium (6.16-8.62%), and all samples are classified as granitoids and located in the granite field (Fig. 3). In comparison, the intrusive rocks associated with copper-gold mineralization have a lower content of SiO_2 (52.78-65.15%) and K_2O (1.08-6.25%). They form a wide field on the diagram covering the range from diorites to monzonites (Fig. 3).

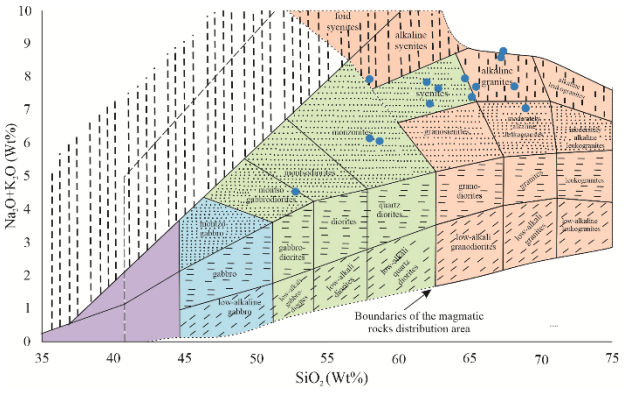

Figure 3 – TAC diagram, definition of rock types

To determine the sources of ore formation, graphs of the distribution of rare earth elements are constructed (Fig. 4). Rare earth elements are indicated on the X-axis, and their contents in rocks are normalized to the UCC on the Y-axis. (Taylor and McLennan, 1985). The characteristic geochemical features of igneous rocks are established. In most cases, there is a predominance of light rare earth elements over heavy ones, which may indicate processes of plagioclase crystallization or post-magmatic differentiation. Samples from $12HSO_4^{-4}$* to $12HSO_5^{-4}$ (Fig. 4, c), $12HSO_1^{-2}$** (Fig. 4, b) clearly show a positive Eu anomaly. The content is significantly higher than in neighboring Sm and Gd. This may be the result of reduced conditions, the crystallization of ores in plagioclase-containing rocks, and fluid action [[16],[17]], as well as $12HSO_3^{-1}$* shows a slight increase in Eu, which may indicate the absence of a pronounced anomaly.

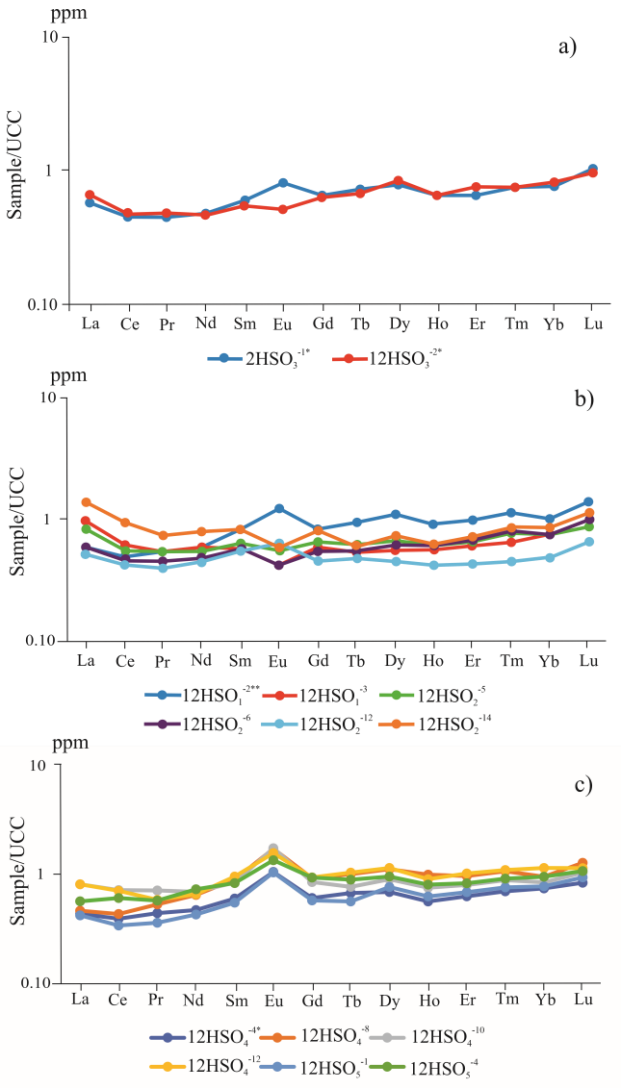

Figure 4 – Distribution of rare earth elements in the Nurkazgan deposit

The europium anomaly manifests itself as a deviation of the europium concentration from the general trend of the REE distribution. The diagrams show that the europium content is noticeably lower in sample $12HSO_3^{-2}$* sample (Fig. 4, a), as well as samples from $12HSO_1^{-3}$ to $12HSO_2^{-14}$ (Fig. 4, b), than in the neighbouring elements, samarium or

gadolinium. This indicates a negative europium anomaly.

Such anomalies are typical of igneous rocks that have undergone differentiation, especially granitoids. In addition, a negative europium anomaly may be associated with a high degree of partial melting of crustal material, resulting in europium remaining in the residual rock rather than enriching the magma [[16], [17]]. The influence of hydrothermal processes may also contribute to additional europium leaching. As a result of studying the REE distribution at the Nurkazgan deposit, it was found that light REEs (L-REE) enrichment occurs, with La, Ce, Pr and Nd being noticeably enriched relative to VCC. This indicates the fractionated nature of the source, and possibly the participation of crustal material or prolonged magma differentiation. There is a smooth decline in Sm to Lu (HREEs), heavy REE (Gd-Lu) are gradually decreasing, indicating a moderate depletion in HREE, which may indicate the residual presence of garnet in the source. A clearly pronounced negative Eu anomaly is visible on graphs, with Eu/Eu<1 indicating the fractionation of plagioclase, which selectively accumulates Eu^{2+}. This suggests that the rocks formed after plagioclasic crystallization or from a depleted melt in europium [[18], [19], [20]].

For the effective development of a field, it is essential not only to consider the identified patterns but also to identify additional parameters that influence the distribution of valuable elements. This approach will provide a more accurate understanding of ore formation processes [[21], [22]].

An analysis of the relationships between rare earth elements shows (Fig. 5) that most of them exhibit a high degree of correlation (R≤0,7) within their groups: Ce-La, Pr-Ce, Nd-Pr, Sm-Nd, Lu-Yb, Tm-Er, Yb-Tm. This indicates similar mechanisms of their fractionation and deposition in geochemical processes [[23], [24]]. The most pronounced relationships are observed between elements of the light group, such as La, Ce, Pr, and Nd. These elements indicate their joint migration and accumulation in geological systems. Medium rare earth elements, including Sm, Gd and Tb, exhibit less pronounced correlations. This may be due to their more complex behavior during crystallization processes. Eu has a low correlation with most other elements. This is probably due to its ability to redox changes affecting the degree of its accumulation. Heavy rare earth elements, such as Dy, Ho, Er and Tm, show less pronounced dependencies, and their relationship to lighter elements varies. Some of these elements show weak or negative correlations, which may be a reflection of the processes of selective separation during hydrothermal alteration of rocks.

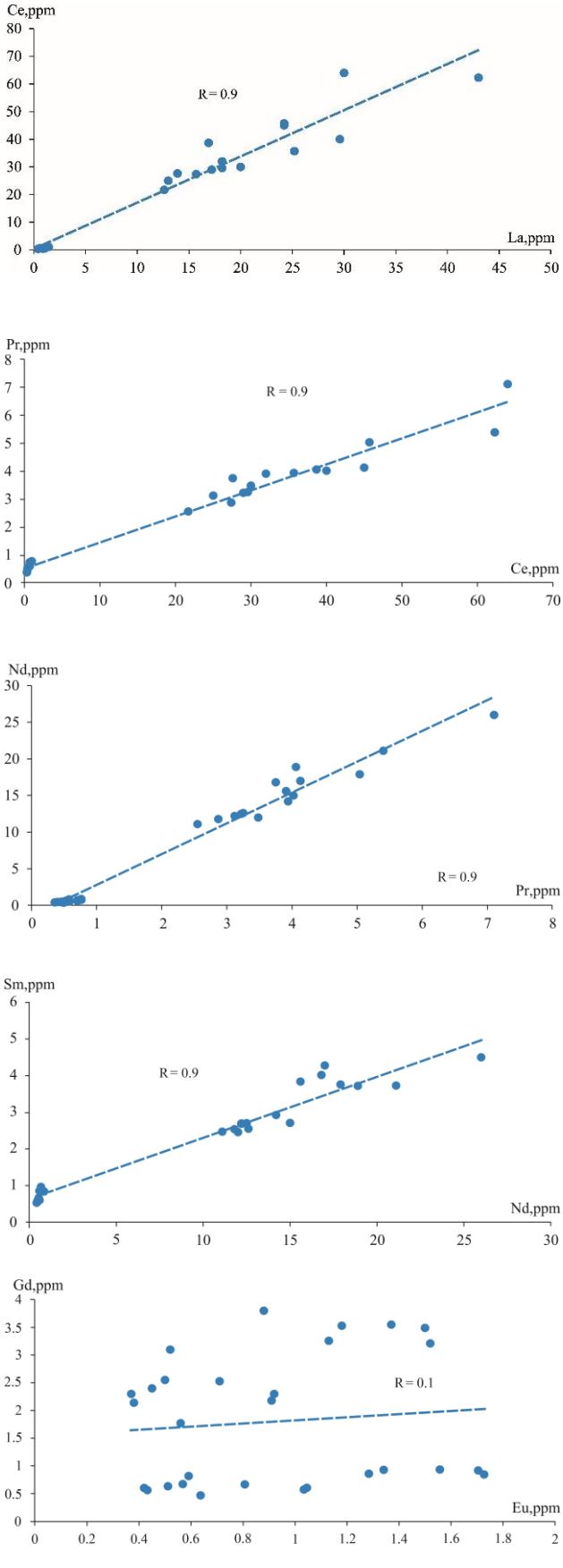

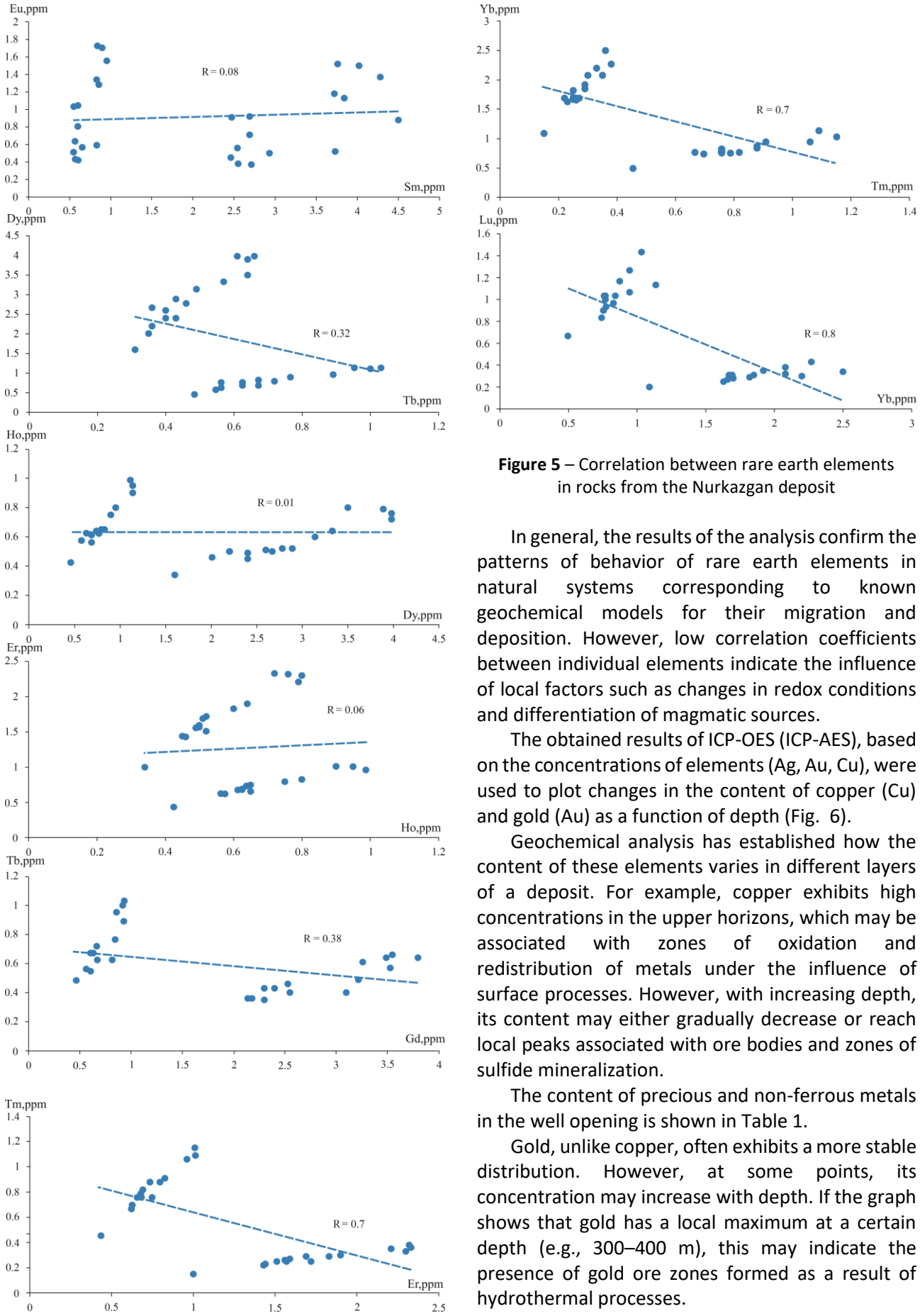

Figure 5 – Correlation between rare earth elements in rocks from the Nurkazgan deposit

In general, the results of the analysis confirm the patterns of behavior of rare earth elements in natural systems corresponding to known geochemical models for their migration and deposition. However, low correlation coefficients between individual elements indicate the influence of local factors such as changes in redox conditions and differentiation of magmatic sources.

The obtained results of ICP-OES (ICP-AES), based on the concentrations of elements (Ag, Au, Cu), were used to plot changes in the content of copper (Cu) and gold (Au) as a function of depth (Fig. 6).

Geochemical analysis has established how the content of these elements varies in different layers of a deposit. For example, copper exhibits high concentrations in the upper horizons, which may be associated with zones of oxidation and redistribution of metals under the influence of surface processes. However, with increasing depth, its content may either gradually decrease or reach local peaks associated with ore bodies and zones of sulfide mineralization.

The content of precious and non-ferrous metals in the well opening is shown in Table 1.

Gold, unlike copper, often exhibits a more stable distribution. However, at some points, its concentration may increase with depth. If the graph shows that gold has a local maximum at a certain depth (e.g., 300–400 m), this may indicate the presence of gold ore zones formed as a result of hydrothermal processes.

Table 1 – ICP-OES (ICP-AES) analysis results for (Ag, Au, Cu)

No.	Sample number	Interval		Elements		
		from	to	Ag, g/t	Cu, g/t	Au, g/t
1	1	0	1	2.324	8.62	0.846
2	2	1	2	0.78	3.49	1.024
3	3	2	3	1.452	6.34	0.674
4	4	3	4	6.035	15.48	0.558
5	5	4	5	1.314	2.51	0.116
6	6	5	6	1.356	2.26	0.095
7	7	6	7	1.686	5.53	0.533
8	8	7	8	1.731	5.72	0.253
9	9	8	9	0.99	2.14	0.163
10	10	9	10	0.228	0.67	0.055

In addition, the ratio of Cu and Au at different depths may indicate their genetic relationship. If, for example, concentrations of copper and gold grow simultaneously at certain levels, this indicates that the metals could have been deposited together during ore formation. However, if their distribution is different, gold may be associated with other minerals, such as quartz or pyrite.

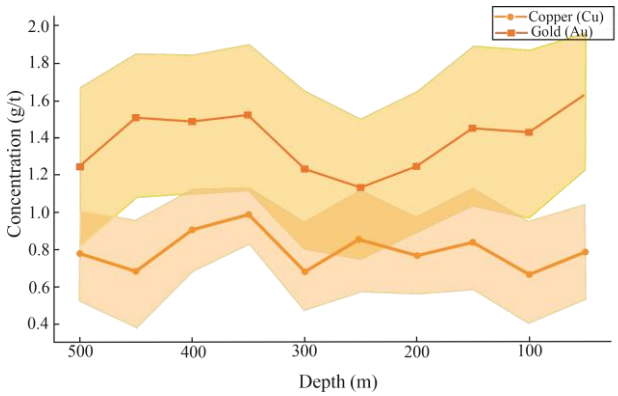

Figure 6 – Changes in the concentrations of copper (Cu) and gold (Au) with depth

The analysis of this distribution is important for assessing the depth of the deposit. It allows us to identify the most promising areas for future development and refine the mining strategy.

Conclusions

The geochemical analysis made it possible to identify patterns in the distribution of rare earth elements within the intrusive rocks at the deposit, which made it possible to determine the sources of ore formation and the conditions under which they formed. The deposit is of igneous origin with signs of long-term melt fractionation. The negative Eu anomaly confirms involvement of plagioclase fractionation typical of intermediate and acid magmas. LREE enrichment indicates evolved magma with participation of continental crust, while moderate depletion of HREE indicates a deep origin or influence of garnet from the source.

From the correlation analysis of the REE distribution, it has been established that REE behavior is consistent during rock formation and the uniformity of geochemical conditions for rock formation. REEs were jointly fractionated during crystallization and did not undergo significant secondary redistribution, such as hydrothermal leaching, but retained their original magmatic characteristics and identity. A positive linear relationship (R~0.9) suggests a single source for REEs; the same REE behavior during magma differentiation, with no strong fractionation of individual REEs relative to others, except possibly Europium.

The geochemical analysis of the copper-porphyry ores of the Nurkazgan deposit revealed that copper and silver demonstrate a high degree of correlation, indicating their joint mineralogical association in the composition of sulfide phases, mainly chalcopyrite and bornite. Gold is characterized by a moderate bond with copper, which is typical for gold-copper porphyry systems, but its distribution is largely determined by secondary hydrothermal processes.

Deep profiles have shown that copper is more concentrated in near-surface zones, where oxidation and leaching processes dominate. At the same time, gold exhibits a relatively stable distribution with local peaks at certain depths, which may indicate the presence of hidden gold ore bodies. This is important for planning mining operations and further exploration.

The established patterns of metal distribution in ores allowed us to reconstruct the processes of ore formation, which is important for predicting copper porphyry deposits.

Conflict of interest. On behalf of all authors, the corresponding author declares that there is no conflict of interest.

CRediT author statement: **A. Kopobayeva**: Writing - Original Draft, Conceptualization, Methodology, Supervision; **Ye. Zharylgapov**: Data curation, Investigation, Writing draft preparation; **B. Ulgibayeva**: Visualization, Investigation, Resources; **A. Amangeldikyzy**: Writing - Review & Editing, Visualization; **A. Askarova:** Visualization, Software, Validation, Software; **A. Kabyken:** Software, Formal analysis.

Cite this article as: Kopobayeva AN, Zharylgapov YeYe, Ulgibayeva BS, Amangeldikyzy A, Askarova NS, Kabyken AB. A study of the geochemical features of the Nurkazgan copper-porphyry deposit. Kompleksnoe Ispolzovanie Mineralnogo Syra = Complex Use of Mineral Resources. 2027; 340(1):67-76. https://doi.org/10.31643/2027/6445.07

Нұрқазған мыс-порфирлі кен орнының геохимиялық ерекшеліктерін зерттеу

[1] Копобаева А. Н., [1] Жарылғапов Е.Е, [2] Үлгібаева Б. С., [1]Амангелдіқызы А., [1]Асқарова Н. С., [1]Қабыкен А.Б.

[1]Әбілқас Сағынов Атындағы Қарағанды Техникалық Университеті, Қарағанды, Қазақстан
[2] Геотек ЖШС, Қарағанды, Қазақстан

Мақала келді: *12 шілде 2025*
Сараптамадан өтті: *21 шілде 2025*
Қабылданды: *22 қыркүйек 2025*

ТҮЙІНДЕМЕ

Порфирлі мыс кен орындары дүние жүзіндегі мыстың, молибденнің және алтынның едәуір бөлігінің негізгі көзі болып табылады. Бұл олардың экономикалық маңыздылығына байланысты ғылыми зерттеудің негізгі объектісіне айналдырады. Мақала Нұрқазған кен орнының негізгі жыныстары мен порфирлі мыс кендерінің геохимиясын зерттеуге арналған. Онда порфирлі мыс жүйелерінде алтынның таралуының геохимиялық критерийлері анықталады, болжау критерийлерін жетілдіру мақсатында кен түзілу механизмдері нақтыланады. Нәтижелер ICP-OES (ICP-AES) және геостатистикалық әдістерді қолдану арқылы алынған аналитикалық деректерді интерпретациялау арқылы алынды. Осы зерттеу негізінде элементтердің мөлшері бойынша таралуын анықтайтын негізгі факторлар анықталды. Негізгі жыныстардағы СЖЭ таралуын зерттеу нәтижесінде кен түзілу жағдайлары анықталды: кен орны магманың ұзақ мерзімді фракциялану белгілері бар магмалық текті; теріс Eu аномалиясы аралық және қышқыл магмаларға тән плагиоклазды фракциялануды қатысатынын дәлелдейді; СЖЭ-ның байытылуы континенттік жер қыртысындағы магманың эволюциясын көрсетеді, ал СЖЭ-ның қалыпты азаюы қалдық гранатпен магматизмнің терең көзін көрсетеді. СЖЭ арасындағы күшті оң корреляция бір геохимиялық процесті көрсетеді және бастапқы магмалық сәйкестікті көрсетеді. Терең магмалық көзі бар порфир жүйесі ашылды, онда кен сұйықтары Ес-да таусылған, бірақ сирек жер элементтері мен металдарға байытылған қалдық балқымадан бөлінеді.

Түйін сөздер: геохимия, геологиялық процестер, минералдану аймақтары, элементтердің таралуы, пайдалы қазбалардың локализациясы, кен түзу процестері, мыстың минералдануы, кен орындары.

Авторлар туралы ақпарат:

Копобаева Айман Ныгметовна — *PhD, Геология және пайдалы қазбалар кен орындарын барлау кафедрасының қауымдастырылған профессоры, Әбілқас Сағынов атындағы Қарағанды техникалық университеті, 100000, Қарағанды, Қазақстан. E-mail: kopobayeva@inbox.ru; ORCID ID: https://orcid.org/0000-0002-0601-9365*

Жарылғапов Ерасыл Ерболұлы — *Геология және пайдалы қазбалар кен орындарын барлау кафедрасының магистранты, Әбілқас Сағынов атындағы Қарағанды техникалық университеті, 100000, Қарағанды, Қазақстан. E-mail: erasyl.zharylgapov@mail.ru; ORCID ID: https://orcid.org/0009-0001-8389-4710*

Үлгібаева Бегім Сарқытбайқызы — *Геолог, ЖШС Geotek, 100027, Қарағанды, Қазақстан. E-mail: begimay.97@mail.ru; ORCID ID: https://orcid.org/0009-0003-1644-4183*

Амангелдіқызы Алтынай — *PhD, Геология және пайдалы қазбалар кен орындарын барлау кафедрасы доцентінің міндетін атқарушы, Әбілқас Сағынов атындағы Қарағанды техникалық университеті КеАҚ, 100000, Қарағанды, Қазақстан. E-mail: a.amangeldykyzy@ktu.edu.kz; ORCID ID: https://orcid.org/0000-0002-6665-8804*

Асқарова Назым Сражадинқызы — *PhD, Геология және пайдалы қазба кен орындарын барлау» кафедрасының аға оқытушысы, Әбілқас Сағынов атындағы Қарағанды техникалық университеті, 100000, Қарағанды. Қазақстан. E-mail: n.askarova@ktu.edu.kz; ORCID ID: https://orcid.org/0000-0002-2103-6198*

Қабыкен Айдын Бақытжанұлы — *Геология және пайдалы қазбалар кен орындарын барлау кафедрасының докторанты, Әбілқас Сағынов атындағы Қарағанды техникалық университет, 100000, Қарағанды, Қазақстан. E-mail: aidynkabyken@yandex.ru; ORCID ID: https://orcid.org/0009-0008-2020-6141*

Изучение геохимических особенностей Нурказганского медно-порфирового месторождения

[1] Копобаева А. Н., [1] Жарылгапов Е. Е., [2] Ульгибаева Б. С., [1] Амангелдіқызы А., [1] Асқарова Н. С., [1]Кабыкен А. Б.

[1] Карагандинский технический университет имени Абылкаса Сагинова, Караганда, Казахстан
[2] ТОО Геотек, Караганда, Казахстан

Поступила: *12 июля 2025*
Рецензирование: *21 июля 2025*
Принята в печать: *22 сентября 2025*

АННОТАЦИЯ
Медно-порфировые месторождения являются источником большей части мировых запасов меди, молибдена и значительного количества золота. Это делает их основным объектом научных исследований из-за их экономической значимости. Статья посвящена изучению геохимии вмещающих пород и медно-порфировых руд месторождения Нурказган. В нем определены геохимические критерии распределения золота в медно-порфировых системах, а также уточнены механизмы рудообразования с целью улучшения прогнозных критериев. Результаты были получены путем интерпретации аналитических данных, полученных с использованием метода ICP-OES (ICP-AES) и геостатистического метода. На основе этого исследования были определены ключевые факторы, определяющие распределение содержания элементов. В результате изучения распределения РЗЭ во вмещающих породах были установлены условия для рудообразования: месторождение имеет магматическое происхождение с признаками длительного фракционирования магмы; отрицательная аномалия Eu подтверждает участие плагиоклазового фракционирования, характерного для средне- и кислых магм; Обогащение РЗЭ указывает на эволюцию магмы в континентальной коре, в то время как умеренное истощение РЗЭ указывает на глубинный источник магматизма с остаточным участием граната. Установленная сильная положительная корреляция между РЗЭ указывает на единый геохимический процесс и отражает первичную магматическую идентичность. Была обнаружена порфировая система с глубинным магматическим источником, где рудные флюиды отделяются от остаточного расплава, который уже истощен в Ec, но обогащен редкоземельными элементами и металлами.

Ключевые слова: геохимия, геологические процессы, зоны минерализации, распределение элементов, локализация минералов, процессы рудообразования, медная минерализация, месторождения.

Информация об авторах:

Копобаева Айман Ныгметовна
PhD, ассоциированный профессор кафедры Геология и разведка МПИ, Карагандинский технический университет имени Абылкаса Сагинова, 100000, Караганда, Казахстан. E-mail: kopobayeva@inbox.ru; ORCID ID: https://orcid.org/0000-0002-0601-9365

Жарылгапов Ерасыл Ерболулы
Магистрант кафедры Геология и разведка МПИ, Карагандинский технический университет имени Абылкаса Сагинова, 100000, Караганда, Казахстан. E-mail: erasyl.zharylgapov@mail.ru; ORCID ID: https://orcid.org/0009-0001-8389-4710

Ульгибаева Бегим Саркытбайкызы
Геолог, ТОО Геотек, 100027, Караганда, Казахстан. E-mail: begimay.97@mail.ru; ORCID ID: https://orcid.org/0009-0003-1644-4183

Амангелдiқызы Алтынай
PhD, и.о. доцента кафедры Геология и разведка МПИ, Карагандинский технический университет имени Абылкаса Сагинова, 100000, Караганда, Казахстан. E-mail: a.amangeldykyzy@ktu.edu.kz; ORCID ID: https://orcid.org/0000-0002-6665-8804

Аскарова Назым Сраждадиновна
PhD, старший преподаватель кафедры Геология и разведка МПИ, Карагандинский государственный технический университет имени Абилкаса Сагинова, 100000, Караганда, Казахстан. E-mail: n.askarova@ktu.edu.kz; ORCID ID: https://orcid.org/0000-0002-2103-6198

Кабыкен Айдын Бакытжанулы
Докторант кафедры Геология и разведка МПИ, Карагандинский технический университет имени Абылкаса Сагинова, 100000, Караганда, Казахстан. E-mail: aidynkabyken@yandex.ru; ORCID ID: https://orcid.org/0009-0008-2020-6141

References

[1]Sillitoe RH. Porphyry Copper Systems. Economic Geology. 2010; 105:3-41. https://doi.org/10.2113/gsecongeo.105.1.3

[2]Sun W, Huang RF, Li H, Hu YB, Zhang CC, Sun SJ, Zhang LP, Ding X, Li CY, Zartman RE, and etc. Porphyry deposits and oxidized magmas. Ore Geology Reviews. 2015; 65:97-131. https://doi.org/10.1016/j.oregeorev.2014.09.004

[3]Serykh VI, Kopobayeva AN. Patterns of distribution of rare metal deposits in Central Kazakhstan. News of the National Academy of Sciences of the Republic of Kazakhstan, Series of Geology and Technical Sciences. 2019, 143-150. https://doi.org/10.32014/2019.2518-170X.18

[4]Windley BF, Xiao W. Ridge subduction and slab windows in the Central Asian Orogenic Belt: Tectonic implications for the evolution of an accretionary orogen. Gondwana Res. 2018; 61:73-87. https://doi.org/10.1016/j.gr.2018.05.003

[5]Xu XW, Li H, Peters SG, Qin KZ, Mao Q, Wu Q, Hong T, Wu C, Liang GL, Zhang ZF, and et al. Cu-rich porphyry magmas produced by fractional crystallization of oxidized fertile basaltic magmas (Sangnan, East Junggar, PR China). Ore Geology Reviews. 2017; 91:296-315. https://doi.org/10.1016/j.oregeorev.2017.09.020

[6]Fu Y, Cheng Q, Jing L, Ye B, Fu H. Mineral Prospectivity Mapping of Porphyry Copper Deposits Based on Remote Sensing Imagery and Geochemical Data in the Duolong Ore District, Tibet. Remote Sens. 2023; 15:439. https://doi.org/10.3390/rs15020439

[7]Liu C, Qiu C, Wang L, Feng J, Wu S, WangY. Application of ASTER Remote Sensing Data to Porphyry Copper Exploration in the Gondwana Region. Minerals 2023; 13:501. https://doi.org/10.3390/min13040501

[8]Orynbassarova E, Ahmadi H, Adebiyet B, Bekbotayeva A, Abdullayeva T, Beiranv andPour A, Ilyassova A, Serikbayeva E, Talgarbayeva D, Bermukhanova A. Mapping Alteration Minerals Associated with Aktogay Porphyry Copper Mineralizationin Eastern Kazakhstan Using Landsat-8 and ASTER Satellite Sensors. Minerals. 2025; 15:277. https://doi.org/10.3390/min15030277

[9]Ferraq M, Belkacim S, Cheng LZ, Davies JHFL, Perrot MG, Ben-Tami A, Bouabdellah M. New Geochemical and Geochronological Constraints on the Genesis of the Imourkhssen Cu±Mo±Au±Ag porphyry deposit (Anti-Atlas, Morocco): geodynamic and metallogenic implications. Minerals. 2024; 14(8):832. https://doi.org/10.3390/min14080832

[10] Kontak DJ, and et al. Alteration lithogeochemistry of the Archean porphyry-type Côté Gold Au(-Cu) deposit, Ontario, Canada: implications for exploration. Minerals. 2023; 15(3):256. https://doi.org/10.3390/min15030256

[11] Gao K, Zhang Z, Zhang L, Xu P, Yang Y, Wu J, Li Y, Sun M, Su W. Significance of Adakitic Plutons for Mineralization in Wubaduolai Copper Deposit, Xizang: Evidence from Zircon U-Pb Age, Hf Isotope, and Geochemistry. Minerals. 2025; 15(5):500. https://doi.org/10.3390/min15050500

[12] Zhang P, Li Z, Zhao F, Liu X. Petrogenesis and Tectonic Implications of the Granite Porphyry in the Sinongduo Ag-Pb-Zn deposit, Central Tibet: constraints from geochronology, geochemistry, and Sr-Nd isotopes. Minerals. 2024; 14(7):710. https://doi.org/10.3390/min14070710

[13] Cooke DR, Hollings P, Wilkinson JJ, Tosdal R. Geochemistry of porphyry deposits. Treatise on Geochemistry (Second Edition).2014; 13;357-381. https://doi.org/10.1016/B978-0-08-095975-7.01116-5

[14] Otchet s podschetom zapasov zoloto-mednyh rud Vostochnogo uchastka mestorozhdeniya Nurkazgan po sostoyaniyu na 01.01.2019 g. [Report on thecalculationofgold and copperore reserves in the Eastern section of the Nurkazgan depositas of 01.01.2019]. Nur-Sultan. (in Russ.).

[15] Yakubchuk A, Degtyarev K, Maslennikov V, Wurst A, Stekhin A, Lobanov K. Tectonomagmatic Settings, Architecture, and Metallogeny of the Central Asian Copper Province. Society of Economic Geologists. Inc. Special Publication. 2012; 16:403-432. https://doi.org/10.5382/SP.16.16

[16] Feng H, Seltmann R, Shen P, Chu X, Suo Q, Seitmuratova E, Shatov V. Hydrothermal rutile chemistry and U-Pb age fingerprinting of the formation of the giant Nurkazgan porphyry Cu-Au deposit, Central Kazakhstan. Ore Geology Reviews. 2024, 174. https://doi.org/10.1016/j.oregeorev.2024.106293

[17] Shen P, Pan H, Seitmuratova E, Jakupova S. U-Pb zircon, geochemical and Sr-Nd-Hf-O isotopic constraints on age and origin of the ore-bearing intrusions from the Nurkazgan porphyry Cu-Au deposit in Kazakhstan. Journal of Asian Earth Sciences. 2016, 116. https://doi.org/10.1016/j.jseaes.2015.11.018

[18] Bouzari F, Hart CJR., Bissig T, Barker S. Hydrothermal alteration revealed by apatite luminescence and chemistry: a potential indicator mineral for exploring covered porphyry copper deposits. Economic Geology. 2016; 111:1397-1410. https://doi.org/0361-0128/16/4423/1397-14

[19] Mishin LF. Eu Geochemistry in Magmatic Rocks of Continental Marginal Volcanic Belts. Geochemistry International. 2010; 48(6):580-592. https://doi.org/10.1134/S0016702910060054

[20] Tatnell L, Anenburg M, Loucks R. Porphyry Copper Deposit Formation: Identifying Garnet and Amphibole Fractionation With REE Pattern Curvature Modeling. Geophysical Research Letters. 2023; 50(14):1-10. https://doi.org/10.1029/2023GL103525

[21] Tosdal RM, DillesJH, Cooke DR. From source to sinks in auriferous magmatic-hydrothermal porphyry and epithermal deposits. Elements. 2009; 5:289-295. https://doi.org/10.2113/gselements.5.5.289

[22] Seedorf E, Dilles JH, Proffett JM, Einaudi MT, Zurcher L, Stavast WJA, Johnson DA, Barton MD. Porphyry Deposits: Characteristics and Origin of Hypogene Features. Economic Geology 100th Anniversary. 2005; 1905-2005:251-298. https://doi.org/10.5382/AV100.10

[23] Vodyanitskii YN. Geochemical Fractionation of Lanthanides in Soils and Rocks: A Review of Publications. EurasianSoil Science. 2012; 45(1):56-67. https://doi.org/10.1134/S1064229312010164

[24] Wu C, Wang C, Hong T, Xu X, Zheng X, Liang W, Sun K, Zhang H, Dong L, Wang B. Constraints on the Formation of the Shiwu Porphyry Cu–Au Deposit in West Junggar, NW China: Insights from Tourmaline-Rich Igneous Rocks. Minerals. 2023; 13:612. https://doi.org/10.3390/min13050612

Crossref

DOI: 10.31643/2027/6445.08

Metallurgy

To the question of pyrometallurgical technology for processing antimony-gold-bearing ores and concentrates

[1]Akilbekova Sh.K., [2*]Moldabayeva G.Zh., [1]Myrzalieva S.K., [1]Seidakhmetova N.M.

[1]RSE National Center on complex processing of mineral raw materials of the Republic of Kazakhstan, Almaty, Kazakhstan
[2]Satbayev University, Almaty, Kazakhstan

**Corresponding author email: gulnara.moldabayeva@satbayev.university*

Received: *May 13, 2025*
Peer-reviewed: *July 15, 2025*
Accepted: *September 23, 2025*

ABSTRACT

The increasing demand for non-ferrous, precious, and rare metals necessitates more comprehensive and efficient use of mineral raw materials, such as gold-antimony ores and concentrates. A promising approach is the use of pyrometallurgical processing in a fluidized bed, which offers more efficient heat and mass transfer than conventional technologies. This study aims to investigate the evaporation kinetics of antimony sulfide (Sb_2S_3) from gold-antimony ores and concentrates in a fluidized bed under various conditions. The experiments involved varying temperature (923-1223 K), particle size (0.09-2.0 mm), and layer thickness (5-15 mm) to determine the evaporation rate of Sb_2S_3. The experimental setup consisted of a laboratory-scale fluidized bed reactor equipped with a controlled gas flow of nitrogen mixed with sulfur vapor. The evaporation rates were measured using a gravimetric method and confirmed by X-ray diffraction and microscopic analysis of samples. The results show that the evaporation rate of Sb_2S_3 in a fluidized bed is 7-9 times higher than in a fixed bed. This is due to significantly improved heat and mass transfer in the fluidized system. At 1023 K, the overall evaporation rate increased with decreasing grain size. This is associated with an increase in the total surface area of the material, but the specific evaporation rate normalized to unit surface area was independent of particle size. The process was not significantly affected by bed height in the range of 5-15 mm. Antimony recovery into sublimates improved by 2-3% compared to conventional technology. It reached 98-99% due to suppression of Sb_2O_5 formation. These findings confirm the efficiency of supplying an inert gas with sulfur vapors into the fluidized bed. This reduces harmful gas emissions and minimizes dust entrainment. It also allows for effective distillation of volatile components at lower temperatures.

Keywords: Sulphiding roasting, oxidising roasting, neutral gas, condensation.

Information about authors:

Akilbekova Sholpan Kalykulovna — *Candidate of Technical Sciences, RSE National center for complex processing of mineral raw materials of the Republic of Kazakhstan, Leading researcher at the Laboratory of Hydroelectrometallurgy, 050036, Almaty, Kazakhstan. E-mail: cadikova74@mail.ru, ORCID ID: https://orcid.org/0000-0002-3696-1028*

Moldabayeva Gulnara Zhaksylykovna — *Candidate of Technical Sciences, Associate Professor of the Department of Metallurgy and Mineral Processing, Satbayev University, 050013, Almaty, Kazakhstan. E-mail: gulnara.moldabayeva@satbayev.university; ORCID ID: https://orcid.org/0000-0002-3716-213X*

Myrzalieva Saule Kerchaizovna — *Doctor of Chemical Sciences, Head of the Department for training of scientific personnel, National Centre for Complex Processing of Mineral Raw Materials of the Republic of Kazakhstan, 050036, Almaty, Kazakhstan. Email: saulekerchaiz@mail.ru; ORCID ID: https://orcid.org/0000-0003-2997-0716*

Seidakhmetova Nazira Makhmutovna — *PhD, RSE National center for complex processing of mineral raw materials of the Republic of Kazakhstan, Head of the hydroelectrometallurgy laboratory, 050036, Almaty, Kazakhstan. E-mail: erkej@mail.ru, ORCID ID: https://orcid.org/0000-0002-6487-1900*

Introduction

Antimony concentrates are supplied to the metallurgical processing stage from beneficiation plants already in a finely ground form, and, if necessary, are subjected to only drying. Antimony ores are supplied to plants, as a rule, in a wet lump form, so it is necessary to subject them to the processes of drying, crushing and grinding. Drying is carried out in tubular rotary kilns with gases from the combustion of fuel oil. After drying, the raw material is crushed in jaw and roller crushers and ground in ball mills. Antimony is present in gold-antimony ores and concentrates in the form of the mineral antimonite, Sb_2S_3 and in small quantities in the form of the following minerals: tetrahedrite

Cu_3SbS_3, valentinite Sb_2O_3, and servantite Sb_2O_4 (over 93%). According to the classical technology of processing gold-antimony polymetallic raw materials in fluidized bed furnaces [[1], [2]], the liquefaction of the charge is carried out with ordinary air, which leads to the formation of volatile antimony compounds and partially non-volatile antimony pentoxide Sb_2O_5, which remains in the cinder.

The authors of this work propose a technology for liquefying the charge with a mixture of neutral gas (N_2) with elemental sulfur vapor, which allows increasing the extraction of antimony into marketable sublimates by 2-3%, due to the exclusion of the formation of non-volatile Sb_2O_5, while the degree of antimony extraction was 98-99%, whereas using standard technology it did not exceed 95-96%.

Research was conducted at various rates and concentrations of the gas mixture supplied to the layer of the processed material to determine the optimal flow rate of the mixture of neutral gas with elemental sulfur vapor.

The materials of the following composition were studied in the work, %: gold - antimony concentrate containing: Sb-58.8; S-21.6; SiO_2-18.1; As-0.27; Pb-0; Fe-0.12; Al_2O_3 -0; MgO-0; C-0; Au-38.0 g/t Ag-0.0 g/t and gold – antimony ore containing: Sb-22.4; S-8.3; SiO_2-53.0; As-0.6; Pb-0.05; Fe-2.2; Al_2O_3 -5.3; MgO-0.3; C-4.5; Au-21.0 g/t Ag-0.001 g/t.

Experimental part

Laboratory installation: design and operating principle

Studies on the processing of polymetallic raw materials in a fluidized bed were carried out using a laboratory installation schematically shown in Figure 1. To avoid disproportionate consumption of elemental sulfur, the system was equipped with an evaporator, which supplied sulfur vapors into a separate reaction vessel containing the charge throughout the experiment. This solution enabled precise control of sulfur consumption and ensured a uniform supply of sulfur vapors mixed with nitrogen into the bed, providing stable fluidization and effective sulfidation of the material.

The experiment started when the charge reached the specified temperature. At the end of the run, the retort was removed from the furnace, cooled, and the obtained products were weighed and analyzed.

The procedure was as follows. The feed material was loaded from hopper (1) into the reaction vessel (2). The system was sealed and heated to the target temperature. Sulfur powder was charged into the evaporator (4) through hoppers (3). After the furnaces (5) were heated, the gas flow was adjusted with a rotameter to achieve stable fluidization in the vessel. The electric furnace (5) was then lowered so that the material bed was positioned within the isothermal zone.

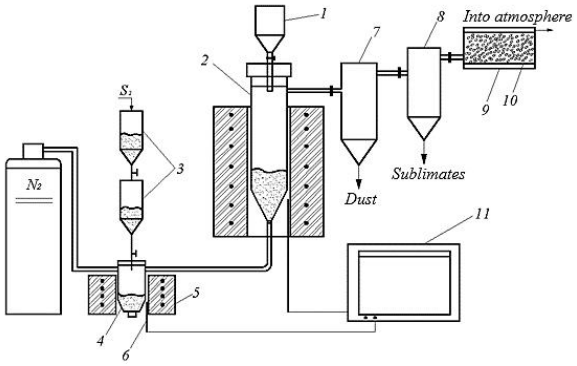

1 – feed hopper; 2 – evaporative reaction vessel; 3 – sulfur powder feed hoppers; 4 – sulfur evaporator; 5 – electric furnaces for the initial charge and sulfur evaporators; 6 – thermocouples; 7 – cyclone; 8 – condenser; 9 – filter; 10 – filter packing; 11 – electric potentiometer

Figure 1 - Schematic diagram of the laboratory fluidized-bed installation

The temperatures in both the sulfur evaporator and the charge were measured with platinum–platinum-rhodium thermocouples and recorded using a potentiometer. Dust and sublimates generated during the process were collected in a cyclone (7) and a condenser (8), with the remaining volatiles captured in a filter (9).

The moment when the charge reached the target temperature was defined as the start of the experiment. After completion, the furnace was raised, the charge cooled, and the system disassembled.

Research methods

Features of the transition of a layer of granular material into a fluidized state. In order to create a stable boiling bed regime when blowing gas through a granular material layer placed in a vessel with a porous bottom, the layer can be in two qualitatively different stationary states.

At flow rates W below a certain critical value W_0, solid particles are motionless, the "penetrating" of the layer ε (the volume fraction of free space between particles) remains unchanged, and its hydraulic resistance P_{re} increases with the speed W. Upon reaching the speed W_0, the hydraulic

resistance of the layer becomes equal to its mass, the layer is suspended, gas bubbles are observed jumping through it, and waves and splashes are observed on its free surface. In this state, the layer resembles a boiling liquid, due to which it is called pseudo-liquefied or boiling. The gas speed at which these phenomena begin is called the critical liquefaction speed - W_0 [[3], [4], [5], [6]].

There are a large number of theoretical and empirical formulas that describe with varying degrees of accuracy the moment of transition of a layer to a pseudo-fluidized state [[7], [8], [9], [10], [11], [12], [13], [14], [15]]. In this case, there are two different approaches to determining the rate of onset of liquefaction. One of them is based on the calculation of the hydrodynamic resistance of the pores and channels of a stationary layer; the second is based on the calculation of the speed of movement of individual particles of the layer with subsequent transition through certain pseudo-fluidized states.

The geometry of a layer consisting of spherical particles of the same size is determined by their diameter d and packing density. In practice, however, one often has to work with mixtures composed of particles of different sizes and shapes.

In this case, the conventional particle size d_0 is calculated using the formula:

$$d_0 = 1/ \Sigma (\Delta_i/d_i) \quad (1)$$

where Δ_i – mass fraction of particles with diameter d_i (geometric mean of the cell sizes of adjacent sieves).

The surface area of a non-spherical particle S_P always exceeds that of a sphere S_S having the same volume. To take this difference into account, the concept of the shape factor is introduced:

$$F_S = \sqrt{\frac{S_s}{S_p}} < 1 \quad (2)$$

The numerical values of F_S are determined experimentally.

The concentration of solid material in the fluidized bed γ_{fl} can be calculated from the specific mass of solid particles γ_s and the porosity of the bed ε:

$$\gamma_{fl} = \gamma_s (1 – \varepsilon) \quad (3)$$

Then the bulk density of the stationary layer γ_0 with porosity ε_0 will be:

$$\gamma_0 = \gamma_s (1 – \varepsilon_0) \quad (4)$$

The transition of a stationary layer to a fluidized state occurs under the condition that the force of hydrodynamic resistance of the layer and the effective mass of suspended solid particles G_e are equal:

$$P_{fl} f_s = G_e, \quad (5)$$

where f_s – cross-sectional area of the layer.

Taking into account the layer penetrability ε and the buoyancy (Archimedes) force proportional to the difference in the specific masses of particles γ_s and the fluidizing agent γ, we obtain:

$$G_e = (\gamma_s – \gamma) (1 – \varepsilon) \cdot f_c \cdot H \quad (6)$$

where H – fluidized bed height.

Then

$$P_{fl} = (\gamma_s – \gamma) (1 – \varepsilon) \cdot H \quad (7)$$

Obviously, if the fluidizing agents are gases at low pressures, then $\gamma_s – \gamma \rightarrow \gamma_s$, and

$$P_{fl} = \gamma_т (1 – \varepsilon) H \quad (8)$$

To calculate the liquefaction rate at which the required pressure drop in the layer is ensured, the Todes formula [16] is widely used, with $\varepsilon_0 = 0.4$ having the form,

$$Re_0 = -\frac{Ar}{1400+5{,}22\sqrt{Ar}}, \quad (9)$$

where $Re_0 = W_0 d/\mu$ – Reynolds criterion (μ – viscosity of the fluidizing agent);

$Ar = \frac{gd^3}{\mu^2} \cdot \frac{\gamma_T – \gamma}{\gamma}$ Archimedes criterion (g – acceleration of gravity).

Formula (9) has been tested in many studies over a wide range of variable changes and the results have shown good agreement with experimental data.

Effect of fluidization on gas flow rate and fluidized bed height. The intensity of the mutual movement of solid particles in a fluidized bed increases with the increase of the fluidization number. The speed of the pulsating movement of particles is usually at the level of tens of centimeters per second, and the free path of a particle between two collisions is measured in millimeters or centimeters. In this case, the movement of particles in the vertical direction is more intense than in the horizontal direction.

When gas bubbles appear in the layer, a significant role is played by the movements of not individual particles, but their aggregates. The chaotic movement of particles and aggregates leads to the equalization of temperature and other properties in the volume of the fluidized bed. Along with the chaotic (pulsating) movement of solid particles, depending on the configuration and geometric dimensions of the layer, a directed circulation of granular material may also occur in it, largely due to the bubbling of bubbles. Thus, with a ratio of the layer height to its diameter close to one, in devices of small diameters, predominantly an ascending movement of solid particles and a descending movement along the periphery of the layer is observed. In a layer of significant height, several such zones are formed along the height, which is quite clearly seen in Figure 2, which shows a typical scheme of circulation flows of solid material (dotted lines) and gas (solid lines) during fluidization in a small diameter device.

The intensity of mixing of solid particles determines the nature of mixing of the fluidizing agent in the fluidized bed, which also depends significantly on the properties of the fluidizing agent and the solid material.

The first of them is characterized by complete equalization of the properties of the working bodies, and the residence time of different portions of gas (or different solid particles in a layer with continuous input and output of the solid phase) is not the same.

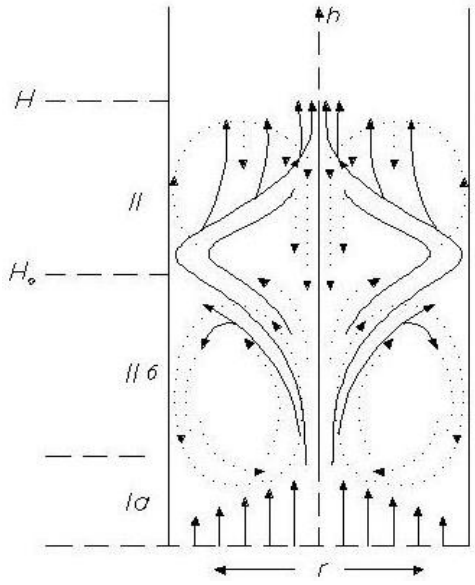

Figure 2 - Typical diagram of the circulation flows of solid material (dashed lines) and gas (solid lines) during fluidization in a small diameter apparatus

In contrast, ideal displacement systems are characterized by a flat front of movement of particles of the solid phase and the fluidizing agent (without longitudinal mixing) and, consequently, the same residence time, z_0, in the working volume. The value of z_0 is determined by the flow of each phase and the working volume of the apparatus. For example, for a solid material it will be:

$$z_0 = G_w / G_c, \quad (10)$$

where G_w – weight of material in a layer;
G_c – weight consumption of material.

A complete mixing system is characterized by the probability of the time an object stays in the system x. For example, for solid particles:

$$x = e^{-\tau / z_o} \quad (11)$$

or

$$1 - x = 1 - e^{-\tau / z_o}, \quad (12)$$

where x – is the weight fraction of particles whose residence time τ exceeds (or the probability that athe rticle will remain in the layer for a period of time τor longer);

(1-x) – is the probability that the particle's stay time, τ will not exceed.

The uniformity of the residence time of particles in the system can be greatly increased by dividing the fluidized bed into several sections. In this case, complete mixing of particles occurs in each section, but their transfer from section to section is possible only in one direction (from the previous section to the next) and in quantities equal to the flow rate.

The residence time of particles in the N-section apparatus is determined by the formula:

$$1\text{-}x=1\text{-}e-\frac{\tau}{zo\backslash N}\left[1+\frac{\tau}{zo\backslash N}\right]+ +\frac{1}{21}\left(\frac{\tau}{zo\backslash N}\right)^{2+\ldots..+}\frac{1}{(N-1)}\left(\frac{\tau}{zo\backslash N}\right)^{N-} \quad (13)$$

Studies have shown that in a single-section apparatus, pseudo-fluidized systems are close to systems with complete mixing of particles. The exception is high layers, pseudo-fluidized in small-diameter apparatuses, where the process occurs in a piston mode. When using apparatuses with 8-10 sections, the movement of particles in the pseudo-fluidized layer approaches ideal displacement by its nature. Note also that the placement of nets, partitions, packing, etc., in the apparatus also brings the pseudo-fluidized layer closer to an ideal displacement system [[17], [18]].

In a fixed granular bed, the nature of the gas movement is close to ideal displacement, and in a fluidized bed, it occupies an intermediate position between ideal displacement and complete mixing. Mixing of the fluidizing agent is also prevented by the sectioning of the apparatus. Often, 4-6 sections (and sometimes fewer) are sufficient to bring the nature of the fluidizing agent movement closer to ideal displacement. Figure 3 shows a cross-section of a fluidized bed of solid particles at different fluidization numbers.

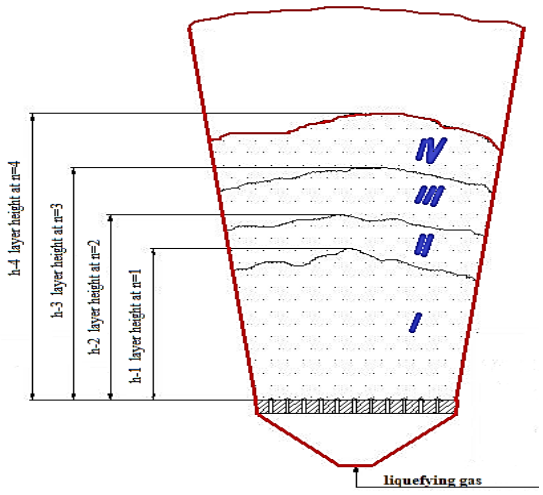

where: N = n * Pi, where N is the gas consumption for liquefaction; n is the fluidization number (0.5; 1; 2, etc.); P is the gas consumption at a fluidization number equal to 1

Figure 3 - Cross-section of a fluidized bed of solid particles at different fluidization numbers

A fluidization number equal to 1 corresponds to a gas flow rate at which solid particles pass into a state of fluidization over the entire surface of the fluidized bed mirror, i.e., there are no stagnant zones on the entire surface of the fluidized bed. When the fluidization number increases to 2, 3, etc., the gas flow rate for fluidization increases accordingly, as does the height of the fluidized bed of the material.

Results and Discussion

The main criterion for assessing the behavior of a component when heated in a fluidized bed can be the saturated vapor pressure of metal sulfides.

Figure 4 shows the dependence of the vapor pressure not only of the sulfides considered, but also of other substances that may be present in ores and concentrates.

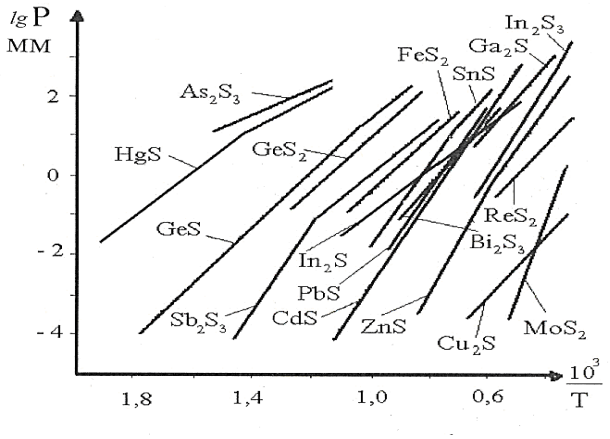

Figure 4 - Dependence of vapor pressure of non-ferrous metal sulfides on temperature

From the data on the dependence of the vapor pressure of non-ferrous metal sulfides on temperature, it follows that one of the promising methods for processing or enriching complex polymetallic raw materials, mainly sulfide, is pyroselection in a fluidized bed with the supply of a mixture of neutral gas with vapors of elemental sulfur into the layer of the material being processed, based on the difference in vapor pressure, dissociation of sulfides and their decomposition products.

In comparison with the processing of materials in conventional fluidized bed furnaces, where the liquefaction of the material is carried out by ordinary air, according to the proposed technology, the supply of a mixture of neutral gas with elemental sulfur into the bed is characterized by the formation of a much smaller amount of reaction gases, and therefore a sharp reduction in the emitted gases and better conditions for the condensation of vapors, reduced dust entrainment and the possibility of distilling off volatile components at lower temperatures [[19], [20]].

Microscopic examination of the residues revealed that the size of the particles located deep in the layer remained unchanged.

The influence of the layer height, duration and temperature of the initial sample processing on the evaporation rate of Sb_2S_3 was investigated. The experiments were conducted with antimony sulfide of a size of - 0.5 + 0.1 mm at a temperature of 923 – 1023 K, respectively. The layer height varied from 5 to 15 mm. The experimental data are presented in Table 1.

Table 1 - Effect of grain size on the evaporation rate of Sb_2S_3

Experience number	T, K	Grain size, mm	Evaporation rate of Sb_2S_3, $g/cm^2 \cdot sec$
1	923	- 2.0 + 1,0	$0.070 \cdot 10^{-5}$
2	923	- 0.5 + 0.25	$0.072 \cdot 10^{-5}$
3	923	- 0.1 + 0.09	$0.072 \cdot 10^{-5}$
4	923	- 0.1 + 0.09	$0.072 \cdot 10^{-5}$
5	1023	- 2.0 + 1.0	$5.45 \cdot 10^{-5}$
6	1023	- 0.5 + 0.25	$5.62 \cdot 10^{-5}$
7	1023	- 0.25+ 0.1	$5.66 \cdot 10^{-5}$
8	1023	- 0.1 + 0.09	$5.70 \cdot 10^{-5}$

For comparison, the results of the study of the kinetics of antimony sulfide Sb_2S_3 evaporation from a fixed bed, we conducted experiments on the evaporation of antimony sulfide from a fluidized bed. The results of the experiments on the kinetics of antimony sulfide evaporation from fixed and fluidized beds are given in Table 2.

As can be seen from the data provided, X-ray structural analysis established that in both cases (for freshly ground and calcined), the preparation consisted of Sb_2S_3 with a rhombic structure.

Microscopic examination revealed that the sample was crystals of perfect shape with smooth edges. Apparently, the decrease in the evaporation rate when the sample was kept in its vapor occurred due to a decrease in crystal defects, a noticeable elimination of microscopic irregularities and surface roughness.

When studying the effect of foreign impurities on the kinetics of Sb_2S_3 evaporation, it was found that the rate of evaporation of a volatile component from its mixture with an inert substance can be affected by the physical properties of the surface of the non-volatile, its adsorption capacity, gas permeability and the nature of the bonds. The hydrodynamic resistance of the layer of non-volatile granular material formed in the process of incongruent evaporation of the mixture with the non-volatile component should have a great influence on the rate of evaporation from the mixture. Thus, it was established that the rate of antimonite evaporation does not depend on the height of the layer and the size of the grains, but depends on the preliminary treatment of the preparation.

Figure 5 shows the kinetic dependences of the Sb_2S_3 evaporation rate on the duration and temperature of the treatment.

Table 2 - Effect of sample layer height and experimental temperature on the evaporation rate of Sb_2S_3

Experience number	Temperature, K	Layer height, mm	Sb_2S_3 evaporation rate $g/cm^2 \cdot sec$	Lg K $g/cm^2 \cdot sec$ Sb_2S_3	evaporation rate $g/cm^2 \cdot sec$	Lg K $g/cm^2 \cdot sec$
			Fixed layer		Fluidized bed	
1	923	5	$0.070 \cdot 10^{-5}$	- 5.154	$0.56 \cdot 10^{-5}$	- 4.251
2	923	15	$0.066 \cdot 10^{-5}$	- 5.180	$0.50 \cdot 10^{-5}$	- 4.301
3	1023	5	$5.450 \cdot 10^{-5}$	- 3.263	$3.28 \cdot 10^{-4}$	- 3.484
4	1023	15	$5.420 \cdot 10^{-5}$	- 3.266	$3.19 \cdot 10^{-4}$	-3.496
5	1073	5	$0.9 \cdot 10^{-4}$	- 4.045	$7.80 \cdot 10^{-4}$	- 3.107
6	1073	15	$0.84 \cdot 10^{-4}$	- 4.075	$7.56 \cdot 10^{-4}$	- 3.121
7	1123	5	$2.4 \cdot 10^{-4}$	- 3.619	$1.2 \cdot 10^{-3}$	- 3.920
8	1123	15	$2.32 \cdot 10^{-4}$	- 3.634	$1.16 \cdot 10^{-3}$	- 3.935
9	1173	5	$4.2 \cdot 10^{-4}$	- 3.376	$2.8 \cdot 10^{-3}$	- 3.552
10	1173	15	$4.15 \cdot 10^{-4}$	- 3.381	$2.74 \cdot 10^{-3}$	- 3.562
11	1223	5	$8.7 \cdot 10^{-4}$	- 3.060	$4.75 \cdot 10^{-3}$	- 2.323
12	1223	15	$8.6 \cdot 10^{-4}$	- 3.065	$4.6 \cdot 10^{-3}$	- 2.337

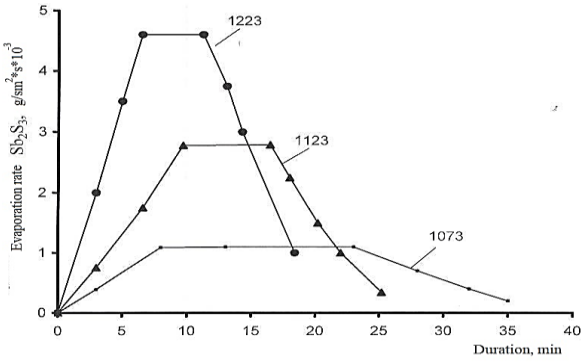

Figure 5 - Kinetic dependences of the evaporation rate of Sb_2S_3 on the duration of the experiment at temperatures of 1073, 1123 and 1223 °K

The data obtained show that the evaporation rate of pure antimony sulfide reaches its maximum value in fairly short periods of treatment time, this is especially noticeable for high temperatures. Thus, if at a temperature of 1073 K the evaporation rate during a treatment time of 7 minutes was 0.98 $g/cm^2 \cdot sec \cdot 10^{-3}$, then at a temperature of 1223 K it reached 4.7 $g/cm^2 \cdot sec \cdot 10^{-3}$, i.e. it exceeded the evaporation rate of Sb_2S_3 for the same treatment time by almost 5 times.

Conclusions

Hydrodynamic and heat transfer processes in a fluidized bed were investigated, and the feasibility of forming a stable fluidized bed through throttling of an inert gas or a mixture of inert gas and sulfur vapor was experimentally confirmed.

The optimal process parameters were determined as follows: particle size between 0.25 and 0.5 mm, bed height between 5 and 15 mm (minimal influence was observed), and operating temperature between 1023 and 1073 K with a gas mixture consisting of nitrogen and sulfur vapor.

It was established that the specific evaporation rate of Sb_2S_3, calculated per unit surface area, is nearly identical for particles of different sizes. At the same time, a decrease in particle size increases the total surface area, which leads to a higher overall evaporation rate of the sample. This effect was experimentally confirmed (Table 1, temperature 1023 K).

Evaporation rates of Sb_2S_3 in a fluidized bed are 7-9 times higher than those in a fixed bed due to enhanced heat and mass transfer. Vapor removal rates from the fluidized bed significantly exceed those from a fixed bed, improving process efficiency.

The evaporation rate does not depend on the bed height within the range of 5-15 mm and occurs mainly from the surface of the particles.

Antimony recovery in sublimates has increased by 2-3% compared to conventional technology, reaching 98-99%, due to the suppression of Sb_2O_5 formation.

The proposed technology of introducing an inert gas with sulfur vapor into the fluidized bed offers ecological and technological benefits: reduced formation of secondary reaction gases, lower dust entrainment, improved vapor condensation, and efficient distillation of volatile components at lower temperatures.

Conflicts of interest. On behalf of all authors, the corresponding author states that there is no conflict of interest.

CRediT author statement: **Sh.Akilbekova**: Conceptualization, Methodology, Supervision; **G.Moldabayeva**: Data curation, Writing-Original draft preparation; **S.Myrzalieva**: Visualization, Investigation; **N.Seidakhmetova**: Software, Validation

Formatting of funding sources. This research is funded by the Committee of Industry of the Ministry of Industry and Construction of the Republic of Kazakhstan (grant BR23991563).

Cite this article as: Akilbekova ShK, Moldabayeva GZh, Myrzalieva SK, Seidakhmetova NM. To the question of pyrometallurgical technology for processing antimony-gold-bearing ores and concentrates. Kompleksnoe Ispolzovanie Mineralnogo Syra = Complex Use of Mineral Resources. 2027; 340(1):77-86. https://doi.org/10.31643/2027/6445.08

Құрамында алтыны бар сурьма кендері мен концентраттарын өңдеудің пирометаллургиялық технологиясы мәселесі бойынша

[1]Акильбекова Ш.К., [2]Молдабаева Г.Ж., [1]Мырзалиева С.К., [1]Сейдахметова Н.М.

[1] Қазақстан Республикасының минералдық шикізатты кешенді қайта өңдеу ұлттық орталығы РМК, Алматы, Қазақстан
[2] Сәтбаев университеті, Алматы, Қазақстан

Мақала келді: *13 мамыр 2025*
Сараптамадан өтті: *15 шілде 2025*
Қабылданды: *23 қыркүйек 2025*

ТҮЙІНДЕМЕ

Түсті, асыл және сирек металдарға сұраныстың артуы минералдық шикізатты, соның ішінде алтын-сурьма кендері мен концентраттарын барынша кешенді әрі тиімді пайдалануды қажет етеді. Перспективалы бағыттардың бірі – дәстүрлі технологиялармен салыстырғанда жылу- және масса алмасу үдерістерін анағұрлым қарқынды жүргізетін жалған сұйықтанған қабаттағы пирометаллургиялық қайта өңдеу болып табылады. Осы зерттеудің мақсаты – алтын-сурьма кендері мен концентраттарынан сурьма сульфидінің (Sb_2S_3) булану кинетикасын жалған сұйықтанған қабат жағдайында зерттеу. Эксперименттер температураны (923–1223 К), бөлшектер өлшемін (0,09–2,0 мм) және қабат қалыңдығын (5–15 мм) өзгерту арқылы жүргізілді. Зертханалық қондырғы құрамында азот пен күкірт буларынан тұратын газ қоспасының реттелетін ағынымен жабдықталған жалған сұйықтанған қабатты реактор болды. Булану жылдамдықтары гравиметриялық әдіспен анықталып, рентгенқұрылымдық және микроскопиялық талдаулармен расталды. Зерттеу нәтижесінде Sb_2S_3 булану жылдамдығы жалған сұйықтанған қабатта қозғалмайтын қабатқа қарағанда 7–9 есе жоғары екендігі анықталды, бұл жылу- және масса алмасу үдерістерінің қарқындануымен түсіндіріледі. 1023 К температурасында бөлшектер өлшемі кішірейген сайын олардың меншікті бетінің ұлғаюына байланысты жалпы булану жылдамдығы артты, ал ауданның бірлігіне шаққандағы жылдамдық өзгеріссіз қалды. 5-15 мм шегінде қабат биіктігі айтарлықтай әсер етпейді. Сурьманы ұшырындыларға шығару дәрежесі 98–99% жетіп, дәстүрлі технологиямен салыстырғанда 2–3% жоғары болды, бұл Sb_2O_5 түзілуін болдырмау есебінен мүмкін болды. Алынған нәтижелер инертті газ бен күкірт буларын жалған сұйықтанған қабатқа беру тиімділігін дәлелдейді, бұл зиянды газдардың бөлінуін азайтуға, шаңның таралуын төмендетуге және ұшқыш компоненттерді төменірек температурада тиімді айдауға мүмкіндік береді.

Түйін сөздер: Күкірттендіре күйдіру, тотықтырып күйдіру, бейтарап газ, конденсация.

Авторлар туралы ақпарат:

Акильбекова Шолпан Қалыкуловна
Т.ғ.к., Қазақстан Республикасының минералдық шикізатты кешенді қайта өңдеу ұлттық орталығы РМК гидроэлектрометаллургия зертханасының жетекші ғылыми қызметкері, 050036, Алматы, Қазақстан. E-mail: cadikova74@mail.ru; ORCID ID: https://orcid.org/0000-0002-3696-1028

Молдабаева Гульнара Жаксылыковна
Т.ғ.к., Металлургия және пайдалы қазбаларды байыту кафедрасының қауымдастырылған профессоры, Сәтбаев университеті, 050013, Алматы, Қазақстан. E-mail: gulnara.moldabayeva@satbayev.university; ORCID ID: https://orcid.org/0000-0002-3716-213X

Мырзалиева Сауле Керчаизовна
Х.ғ.д., профессор, Қазақстан Республикасының минералдық шикізатты кешенді қайта өңдеу ұлттық орталығы РМК ғылыми кадрларды даярлау бөлімінің меңгерушісі, 050036, Алматы, Қазақстан. E-mail: saulekerchaiz@mail.ru; ORCID ID: https://orcid.org/0000-0003-2997-0716

Сейдахметова Назира Махмутовна
PhD, Қазақстан Республикасының минералдық шикізатты кешенді қайта өңдеу ұлттық орталығы РМК, Гидроэлектрометаллургия зертханасының меңгерушісі, 050036, Алматы, Қазақстан. E-mail: erkej@mail.ru; ORCID ID: https://orcid.org/0000-0002-6487-1900

К вопросу о пирометаллургической технологии переработки сурьмяно-золотосодержащих руд и концентратов

[1]Акильбекова Ш.К., [2]Молдабаева Г.Ж., [1]Мырзалиева С.К., [1]Сейдахметова Н.М.

[1]РГП Национальный центр по комплексной переработке минерального сырья Республики Казахстан, Алматы, Казахстан
[2] Satbayev University, Алматы, Казахстан

Поступила: *13 мая 2025*
Рецензирование: *15 июля 2025*
Принята в печать: *23 сентября 2025*

АННОТАЦИЯ

Растущий спрос на цветные, благородные и редкие металлы обусловливает необходимость более комплексного и эффективного использования минерального сырья, в том числе золото-сурьмяных руд и концентратов. Перспективным направлением является пирометаллургическая переработка в псевдоожиженном слое, обеспечивающая более интенсивный тепло- и массообмен по сравнению с традиционными технологиями. Целью данного исследования являлось изучение кинетики испарения сульфида сурьмы (Sb_2S_3) из золото-сурьмяных руд и концентратов в условиях псевдоожиженного слоя. Эксперименты проводились при изменении температуры (923–1223 К), размера частиц (0,09–2,0 мм) и толщины слоя (5–15 мм). Лабораторная установка включала реактор с псевдоожиженным слоем, снабжённый регулируемым потоком газовой смеси на основе азота и паров серы. Скорости испарения определялись гравиметрическим методом и подтверждались рентгеноструктурным и микроскопическим анализом образцов. Установлено, что скорость

	испарения Sb_2S_3 в псевдоожиженном слое в 7–9 раз выше, чем в неподвижном, что связано с интенсификацией процессов тепло- и массообмена. При температуре 1023 К общая скорость испарения возрастает с уменьшением размера частиц вследствие увеличения их удельной поверхности, тогда как скорость, отнесённая к единице площади, остаётся постоянной. Высота слоя в пределах 5–15 мм существенного влияния не оказывает. Степень извлечения сурьмы в возгоны достигала 98–99%, что на 2–3% выше по сравнению с традиционной технологией, благодаря подавлению образования Sb_2O_5. Полученные результаты подтверждают эффективность подачи инертного газа с парами серы в псевдоожиженный слой, что обеспечивает снижение газовых выбросов, уменьшение пылеуноса и эффективную дистилляцию летучих компонентов при более низких температурах.
	Ключевые слова: Сульфидирующий обжиг, окислительный обжиг, нейтральный газ, конденсация.
Акильбекова Шолпан Қалыкуловна	***Информация об авторах:*** *К.т.н., ведущий научный сотрудник лаборатории гидроэлектрометаллургии РГП Национальный центр по комплексной переработке минерального сырья Республики Казахстан, 050036, Алматы, Казахстан. E-mail: cadikova74@mail.ru; ORCID ID: https://orcid.org/0000-0002-3696-1028*
Молдабаева Гульнара Жаксылыковна	*К.т.н., ассоцированный профессор кафедры Металлургия и обогащение полезных ископаемых, Satbayev University, 050013, Алматы, Казахстан. E-mail: gulnara.moldabayeva@satbayev.university; ORCID ID: https://orcid.org/0000-0002-3716-213X*
Мырзалиева Сауле Керчаизовна	*Д.х.н., профессор, заведующая отделом подготовки научных кадров РГП Национальный центр по комплексной переработке минерального сырья Республики Казахстан, 050036, Алматы, Казахстан. E-mail: saulekerchaiz@mail.ru; ORCID ID: https://orcid.org/0000-0003-2997-0716*
Сейдахметова Назира Махмутовна	*PhD, заведующая лабораторией гидроэлектрометаллургии РГП Национальный центр по комплексной переработке минерального сырья Республики Казахстан, 050036, Алматы, Казахстан. E-mail: erkej@mail.ru; ORCID ID: https://orcid.org/0000-0002-6487-1900*

References

[1] Optimization of sulfuric acid leaching of roasted chalcopyrite concentrate using KCl salt roasting. SN Applied Sciences. 2020; 2. http://dx.doi.org/10.1007/s42452-020-03341-6

[2] Rogozhnikov DA, Mamyachenkov SV, Anisimova OS. Nitric acid leaching of copper-zinc sulfide middlings. Metallurgist. 2016; 60:229-233. http://dx.doi.org/10.1007/s11015-016-0278-7

[3] Nie W, Dong L, Hao Z, Cheng Z. Influence of pressure on fundamental characteristics in gas fluidized beds of coarse particle. International Journal of Chemical Reactor Engineering. 2018; 17(2). https://doi.org/10.1515/ijcre-2017-0217

[4] Barros WR. Gas flow patterns in a granular fluidized bed. Granular Matter. 2024; 26:44. http://dx.doi.org/10.1007/s10035-024-01415-5

[5] Chen J, Zhang Y, Liu C, Wang X. Recent advances in fluidized bed hydrodynamics and transport phenomena – Progress and understanding. Processes. 2021; 9(4):639. http://dx.doi.org/10.3390/pr9040639

[6] Balag J, Franco DAT, Miral VG, Reyes V, Tongco LJ, Lopez ECR. Recent Advances in Particle Fluidization. Engineering Proceedings. 2023; 56(1):62. http://dx.doi.org/10.3390/ASEC2023-15321

[7] Popsuev MV, Skorik LF. Osobennosti pererabotki zolotosur'myanykh rud [Features of gold-antimony ores processing]. The Way of Science – International Scientific Journal. 2016; 4(26):47-50. (in Russ.).

[8] Rakhimov KhSh. Mechanical activation of antimony sulfide concentrates combined with pyrometallurgical chlorination. Journal of Mineral and Material Science. 2023; 4(5). https://doi.org/10.54026/JMMS/1071

[9] Pat. TJ 2301804. Method for processing sulfide gold-bearing antimony concentrates: minor patent. Rakhimov KhSh, Eskhov BB, Kodirov AA, Badalov A. 2023, 8.

[10] Shpotyuk O, Kozdras A, Baláž P, Bujňáková Z, Shpotyuk Y. Thermal alteration interphase transformations in natural and synthetic arsenic sulfide polymorphs. Journal of Chemical Thermodynamics. 2019; 128:110-118. https://doi.org/10.1016/j.jct.2018.08.019

[11] Öztürk İ, Ozkaya Kaplan M. Thermodynamic evaluation and optimization of the Ag–As–S system. Journal of Phase Equilibria and Diffusion. 2023; 44(3):269-299. https://doi.org/10.1007/s11669-023-01040-4

[12] Liu H, Pan W-P, Wang C, Zhang Y. Volatilization of arsenic during coal combustion based on isothermal thermogravimetric analysis at 600–1500 °C. Energy & Fuels. 2016; 30(8):6790-6798. https://doi.org/10.1021/acs.energyfuels.6b00816

[13] Li Z, Li X, Tang Z, Xu W, Song Q. Optimization of thermogravimetric method for measuring very low saturation vapor pressure. Qingdao Journal of Hydrodynamics. 2023; 26:30-38. https://www.sciopen.com/article/10.16511/j.cnki.qhdxxb.2023.26.030

[14] Novoselova AV, Pashinkin AS. Davleniye para letuchikh khal'kogenidov metallov [Vapor pressure of volatile metal chalcogenides]. Moscow: Nauka. 1978, 112. (in Russ.). https://n.eruditor.one/file/1851012/

[15] Brunetti B, Piacente V, Scardala P. Torsion vapor pressures and sublimation enthalpies of arsenic triselenide and tritelluride. Journal of Chemical & Engineering Data. 2007; 52(1):24-29. https://doi.org/10.1021/je060083k

[16] Baláž P. Extraction of antimony and arsenic from sulphidic concentrates. Acta Montanistica Slovaca. 2000; 5(3):265-268. https://www.researchgate.net/publication/26403147_Extraction_of_antimony_and_arsenic_from_sulphidic_concentrates

[17] Mohanty CR, Meikap BC. Studies on solid mean residence time in a three-stage gas-solid fluidized bed with downcomer. Korean Journal of Chemical Engineering. 2011; 28:969-973. https://doi.org/10.1007/s11814-010-0455-5

[18] Zou Z, Zhao Y, et al. CFD simulation of solids residence time distribution in a multi-compartment fluidized bed. Chinese Journal of Chemical Engineering. 2017; 25(12):1706-1713. https://doi.org/10.1016/j.cjche.2017.02.010

[19] Deng Y, Ansart R, Baeyens J, Zhang H. Flue gas desulphurization in circulating fluidized beds. Energies. 2019; 12(20):3908. https://doi.org/10.3390/en12203908

[20] Akilbekova Sh, Myrzalieva S, Moldabayeva G, Mamyrbayeva K, Turkmenbayeva M. Investigation of the process of sulfide-firing of gold-antimony concentrate. Journal of Chemical Technology and Metallurgy. 2021; 56(5):1051-1057. https://www.scopus.com/record/display.uri?eid=2-s2.0-85111758467&origin=resultslist&sort=plf-f

Crossref
DOI: 10.31643/2027/6445.09
Metallurgy

Sorption Concentration of Uranium and Vanadium from Productive Solutions of Black Shale Ores

Bulenbayev M., *Altaibayev B., Magomedov D., Bakrayeva A., Bekpeisov Zh.

Institute of Metallurgy and Ore Beneficiation JSC, Satbayev University, Almaty, Kazakhstan

**Corresponding author email: bagdataltai9@gmail.com*

Received: *September 2, 2025*
Peer-reviewed: *September 5, 2025*
Accepted: *September 25, 2025*

ABSTRACT

This study examines the sorption and desorption processes of uranium and vanadium from acidic solutions produced during the processing of black shale ores in Southern Kazakhstan. Such ores are considered unconventional sources of strategic metals and are of particular interest under the conditions of limited traditional mineral resources. To evaluate efficiency, several anion-exchange resins (AMP, AV-17, A-140, and Amberlite) were tested, allowing a comparative analysis of their sorption capacity and selectivity. The AMP resin demonstrated the most favorable performance, providing high uranium uptake and satisfactory vanadium recovery in sulfuric acid media. Desorption experiments confirmed the possibility of efficient uranium transfer into the eluate, which is of great importance for subsequent concentration and purification stages. Vanadium recovery was limited due to the coexistence of different ionic forms of the element. The obtained results confirm the potential of sorption technology as a reliable stage for uranium concentration and indicate the need to apply additional methods, such as solvent extraction or selective precipitation, to enhance the completeness of separation and recovery of the target components.

Keywords: uranium, vanadium, sorption, desorption, anion-exchange resin.

Information about authors:

Bulenbayev Maxat Zhumabaevich — *PhD, Researcher, Institute of Metallurgy and Ore Beneficiation JSC, Satbayev University, Shevchenko str., 29/133, 050010, Almaty, Kazakhstan. Email: mbulenbaev@mail.ru; ORCID ID: https://orcid.org/0000-0002-5437-5436*

Altaybayev Bagdat Tolbasuly — *PhD, Researcher, Institute of Metallurgy and Ore Beneficiation JSC, Satbayev University, Shevchenko str., 29/133, 050010, Almaty, Kazakhstan. Email: bagdataltai9@gmail.com; ORCID ID: https://orcid.org/0000-0002-7405-6854*

Magomedov David Rasimovich — *Researcher, Institute of Metallurgy and Ore Beneficiation JSC, Satbayev University, Shevchenko str., 29/133, 050010, Almaty, Kazakhstan. E-mail: davidmag16@mail.ru; ORCID ID: https://orcid.org/0000-0001-7216-2349*

Bakraeva Akbota Nurdildakyzy — *Junior Research Fellow, Institute of Metallurgy and Ore Beneficiation JSC, Satbayev University, Shevchenko str., 29/133, 050010, Almaty, Kazakhstan. E-mail: bakraeva.akbota@mail.ru; ORCID ID: https://orcid.org/0000-0002-2062-9573*

Bekpeisov Zhasulan Koilybaevich — *Engineer, Institute of Metallurgy and Ore Beneficiation JSC, Satbayev University, Shevchenko str., 29/133, 050010, Almaty, Kazakhstan. Email: zhasulan222@mail.ru*

Introduction

The modern development of science and industry highlights the urgent need for sustainable access to strategic mineral resources, primarily uranium, vanadium, and rare-earth elements. These elements are key components in nuclear energy, high-temperature alloys, catalysts, rechargeable batteries, and other advanced technologies [[1], [2]]. In light of limited traditional deposits and increasing geopolitical risks, growing attention has been directed toward unconventional sources of raw materials, among which black shales occupy a special place.

Black shale formations are fine-layered sedimentary rocks enriched in carbon, organic matter, and finely dispersed mineral phases. Their characteristic features include high sorption capacity and the presence of complex element associations such as V, Mo, U, Ni, Zn, and REEs [[3], [4], [5]]. However, the complex matrix structure, the occurrence of uranium in sparingly soluble forms, and the incorporation of vanadium into phyllosilicates significantly complicate their processing [6]. Consequently, the treatment of black shales requires combined technological schemes that include beneficiation, activation, and subsequent hydrometallurgical extraction stages.

One of the most promising approaches involves the use of sorption technologies, which allow effective concentration of uranium and associated elements from productive solutions. A number of international

studies have demonstrated that uranium in sulfuric acid media forms stable anionic complexes, which can be effectively recovered by anion-exchange resins with high selectivity [7]. The sorption capacity of modern resins may reach tens of milligrams per gram of material [[8], [9]], while desorption efficiency can exceed 90% [10].

Recent research emphasizes the application of sorption for uranium recovery from complex solutions, including those derived from black shales, through the use of various types of anion exchangers and optimization of process parameters [11]. To ensure the reliability of results, sorption has been studied under both static and dynamic conditions, including column experiments and mass-transfer modeling [12]. Theoretical approaches, such as modeling the selectivity of U and V, have also been applied to justify sorbent selection and to predict performance [[13], [14]].

Thus, a review of the literature confirms that sorption methods represent an efficient tool for concentrating uranium and separating it from other elements, including vanadium. In combination with acid leaching, sorption forms the basis of promising technologies for processing unconventional mineral resources.

In our previous studies [15], it was established that the combination of reverse coal flotation and sulfuric acid leaching with the use of trichloroisocyanuric acid ensured high uranium recovery (up to 94–95%) and resulted in productive solutions containing uranium and vanadium. These findings highlighted the importance of preliminary carbon removal and oxidation of uranium-bearing phases to enhance metal accessibility and improve subsequent hydrometallurgical operations. The present study focuses on further investigation of these productive solutions, specifically the sorption recovery of uranium and vanadium, in order to evaluate the effectiveness of different anion-exchange resins and to determine the optimal process parameters for maximizing metal recovery. The scientific novelty of the study lies in the mass balance analysis of sorption and desorption processes for both uranium and vanadium, as well as in identifying the limitations of vanadium recovery caused by its mixed ionic forms. The obtained results broaden the understanding of sorption behavior in complex acidic systems and provide a basis for improving technological flowsheets aimed at processing black shale ores and unconventional mineral raw materials.

Materials and methods

Materials

The object of the study was productive solutions obtained after sulfuric acid leaching of uranium-bearing black shale ore that had been preliminarily beneficiated by reverse coal flotation. The ore was mined in Southern Kazakhstan. The uranium concentration in the productive solutions ranged from 45 to 48 mg/L, while vanadium concentrations were 155 to 168 mg/L.

As sorbents, the following anion-exchange resins were used: AMP, AV-17, A-140, and Amberlite. For desorption of the saturated anion exchangers, a 1 M ammonium carbonate solution $(NH_4)_2CO_3$ was applied. Laboratory glassware, beakers, a sorption column, and vessels of various volumes were employed in the experimental work.

Methods

Sorption and desorption experiments were carried out in batch-operated columns. Productive solutions were passed through a layer of anion-exchange resin until equilibrium was achieved, after which the saturated resin was subjected to desorption using ammonium carbonate solution. The process was performed under controlled hydrodynamic and temperature conditions, ensuring reproducibility of results.

The efficiency of sorption and desorption of uranium and vanadium was calculated according to the following relationships:

Mass of element in solution (m, mg):

$$m=C\times V_m \quad (1)$$

Sorption capacity of the resin (q, g/kg):

$$q=m/m_{resin} \quad (2)$$

Recovery degree (E, %):

$$E=m_{sorb}m_{init}\times 100 \quad (3)$$

where C is the concentration of the element (mg/L); V is the volume of solution (L); m_{resin} is the mass of the sorbent (kg); m_{sorb} is the mass of the element fixed on the resin or transferred to the eluate (mg); and m_{init} is the mass of the element in the initial productive solution (mg).

Analytical Methods and Equipment

The elemental composition of the initial and treated samples was determined using inductively coupled plasma optical emission spectrometry (ICP-OES) and X-ray fluorescence (XRF) analysis. Sorption–desorption experiments were carried out under controlled

hydrodynamic and temperature conditions with the use of a BT20-21 liquid thermostat (Russia) and an LS-301 peristaltic pump (China).

Results and discussion

The productive sulfuric acid solutions obtained as a result of leaching were used in experiments on the sorption recovery of target components-uranium and vanadium. Uranium sorption on anion exchangers occurs mainly due to ion exchange and complexation with uranyl sulfate anions. The process can be represented by the following reaction [11]:

$$(RN)_2SO_4 + [UO_2(SO_4)_2]^{2-} = (RN)_2(UO_2(SO_4)_2) + (SO_4)^{2-} \quad (4)$$

where RN is the matrix of the anion exchanger.

The kinetics of uranium sorption is governed by mass transfer across the diffusion layer surrounding the resin grains and strongly depends on the acidity of the medium. As the pH increases, the sorption rate decreases, thus prolonging the time required to reach equilibrium. Under industrial conditions, effective uranium recovery requires extended contact of the sorbent with the solution [16].

Unlike uranium, vanadium exists in solutions in various ionic forms: both as cations (in oxidation state IV) and as anionic complexes (in oxidation state V) [17]. Consequently, two mechanisms-cation exchange and anion exchange-are simultaneously involved in its recovery. This particularity complicates the selective extraction of vanadium and reduces efficiency compared with uranium, which predominantly exists in a single form.

The efficiency of uranium and vanadium sorption depends on the concentration of metals, the type of ion-exchange resin, the acidity of the medium, and the presence of interfering ions such as SO_4^{2-}, NO_3^-, Cl^-, and Fe^{3+}. At low uranium concentrations (1–25 mg/L), distribution coefficients are considerably higher than at elevated concentrations (100–1000 mg/L), regardless of the type of anion exchanger. Increased acidity, especially when using strongly basic resins, significantly reduces sorption capacity. Depressor anions also diminish recovery, with their effect intensifying as their affinity for the functional groups of the resin increases (Figure 1) [18].

Figure 1 – Sequence of increasing depressive effects of anions

At the stage of uranium and vanadium sorption studies, four types of anion exchangers were tested: AMP, AV-17, A-140, and Amberlite. The dependence of recovery efficiency on temperature (25, 35, and 45 °C) was also examined. The initial concentrations of uranium and vanadium in the solution were 48 mg/L and 168 mg/L, respectively. Each sorbent was loaded in a single-stage mode, and the residual metal concentrations in the raffinate were determined to calculate recovery degrees. The efficiency of uranium and vanadium recovery by different sorbents at various temperatures is shown in Figures 2 and 3.

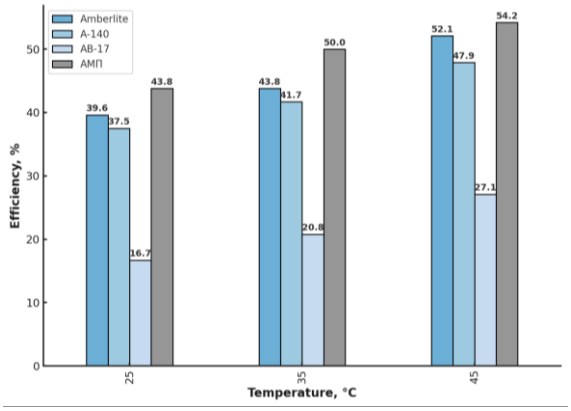

Figure 2 – Uranium recovery as a function of temperature

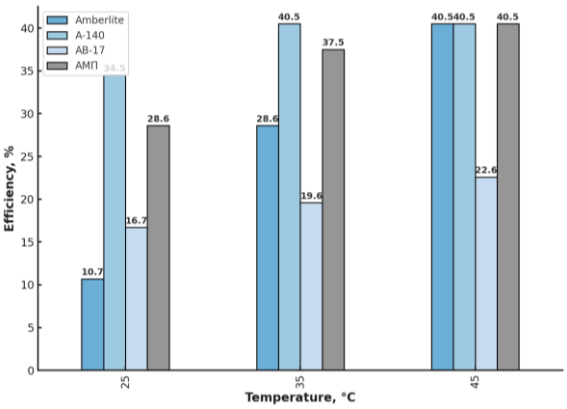

Figure 3 – Vanadium recovery as a function of temperature

For laboratory experiments, AMP resin was selected as the sorbent due to its high sorption capacity in acidic media (up to 80.0 g/kg at pH ≥ 2.0). The initial productive solution volume of 50.0 L contained uranium and vanadium at concentrations of 45.0 and 155.0 mg/L, respectively, corresponding to total masses of 2250.0 mg U and 7750.0 mg V. A total of 100 g of AMP resin was loaded into the column, which under the given conditions excluded reaching the maximum sorption capacity. Solution delivery was provided by a peristaltic pump at a flow rate of 0.5 L/h, while heating to 45 °C was maintained in a thermostatic water bath (Figure 4).

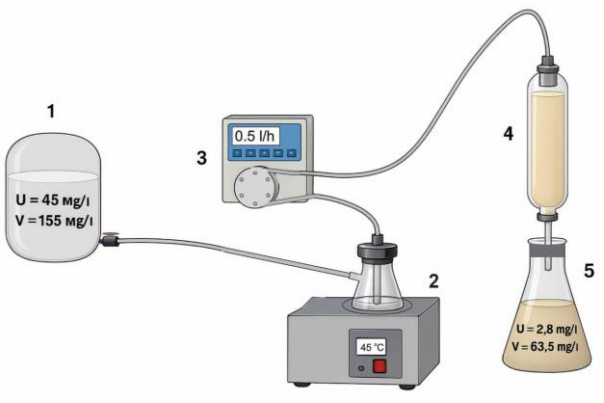

Figure 4 – Laboratory setup scheme for sorption experiments: 1 – tank with productive solution; 2 – flask with solution in thermostatic bath; 3 – peristaltic pump; 4 – column filled with resin; 5 – raffinate container

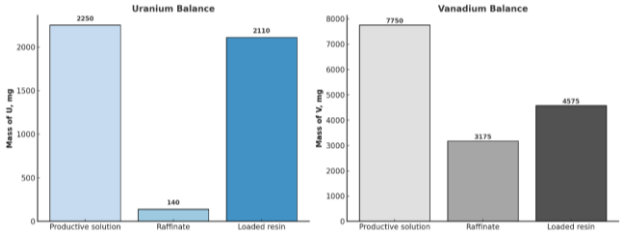

Figure 5 – Mass balance of uranium and vanadium during sorption

Figure 6 – Visual changes in AMP resin appearance

Sorption loading of the resin was conducted over three consecutive days, 10 hours each day. As the process progressed, a systematic decrease in the concentrations of target elements in the solution was observed: in the final raffinate, the residual uranium concentration was 2.8 mg/L, and vanadium was 63.5 mg/L. Mass balance calculations showed that 2110.0 mg U (21.1 g/kg) and 4575.0 mg V (45.75 g/kg) were sorbed onto 100 g of resin, corresponding to recovery efficiencies of 93.78% and 59.0%, respectively. The total resin loading with target components reached 66.85 g/kg. The distribution of uranium and vanadium masses between raffinate and resin is presented in Figure 5.

In addition to recovery of the target components, partial uptake of impurity elements, mainly iron and copper, was observed. After completion of the process, changes in the physical characteristics of the resin were noted: its mass increased by 15 g, granules swelled, and their color darkened, reflecting intensive loading of active sites with uranium and vanadium ions (Figure 6).

Comparative X-ray fluorescence analysis of the original and saturated AMP resin samples revealed pronounced structural and chemical modifications. In the saturated resin, oxygen content increased from 11.49% to 15.88% and sulfur from 4.09% to 10.41%, reflecting the accumulation of sulfate ions from the sulfuric acid solution and a higher oxidation degree of the organic matrix. Target elements—vanadium (4.5%) and uranium (2.1%)—were detected in the resin, with amounts consistent with the calculated sorption balance.

The chlorine content decreased nearly threefold (from 20.7% to 7.18%), indicating chloride substitution as a result of ion exchange, characteristic of chloride-type resins. The organic backbone, represented by C_nH_{2n} spectra below oxygen, decreased by 2.7%, indicating partial involvement of functional groups in sorption. At the same time, the experiments demonstrated that the chlorine-active components of TCCA, used for preliminary oxidation of black shale ores, do not exert a depressive effect on the sorption capacity of the resin.

At the next stage of the technological process, desorption of uranium and vanadium from the saturated AMP resin was carried out. A 1 M ammonium carbonate solution heated to 60 °C was used in the experiments. The column was loaded with 100 g of resin previously washed of acid residues. The eluate volume was 0.2 L, and the process duration was 8 hours; the apparatus remained identical to the sorption stage.

According to mass balance analysis (Figure 7), out of the 2110 mg of uranium accumulated in the resin (21.1 g/kg), 1996 mg was transferred to the eluate, while the residual mass was only 120 mg (1.2 g/kg). Thus, desorption efficiency reached 94–95%, and the overall uranium recovery into the eluate amounted to 88–89%. The uranium concentration in the final eluate was 9.98 g/L, confirming a high degree of enrichment.

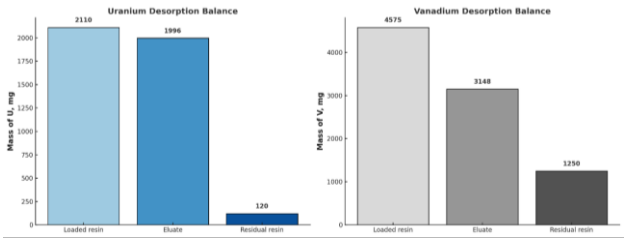

Figure 7 – Mass balance of uranium and vanadium during desorption

The behavior of vanadium differed substantially. With an initial loading of 4575 mg (45.8 g/kg) in the resin, only 3148 mg transferred to the eluate, while about 1250 mg remained in the sorbent. Desorption efficiency was approximately 69%, while the overall recovery of vanadium did not exceed 41–43%. Nevertheless, the concentration of vanadium in the eluate was relatively high, 15.74 g/L, g/L-confirming the feasibility of its further processing.

The difference in recoverability between uranium and vanadium is determined by their chemical nature. Uranium in sulfuric acid solutions forms stable anionic uranyl sulfate complexes, which are effectively desorbed by carbonate solutions. Vanadium, in contrast, occurs in mixed forms – both anionic and cationic – limiting its transfer into the carbonate eluate and lowering desorption efficiency. These observations are consistent with the literature, which emphasizes the need for additional steps, including pH-controlled precipitation, to enhance extraction completeness [[19], [20]]. The presence of vanadium in productive solutions also exerts a competitive influence on uranium sorption and desorption, reducing their selectivity and efficiency, which makes the problem of separation particularly relevant [21].

The obtained results convincingly confirm the high efficiency of uranium sorption on AMP resin: high recovery rates were achieved while forming a saturated sorbent with predictable loading parameters. This allows sorption to be considered a reliable stage of preliminary concentration. To achieve residual uranium and vanadium concentrations of less than 1–2 mg/L in solutions, it is advisable to use multi-stage sorption. In industrial practice, this approach is implemented through cascade passage of solution through multiple columns, ensuring complete resin saturation at the point of “breakthrough” of target ions past the last column. Optimal parameters, including the sorption layer length and the number of columns, are determined by solution acidity and salt composition.

At the same time, the limitations observed in vanadium recovery highlight the need to improve the technological scheme. To increase selectivity and ensure comprehensive separation of target components, supplementing the sorption stage with extraction methods is recommended, which can serve as an effective tool for the subsequent processing of productive solutions.

Conclusions

The conducted research confirmed the high efficiency of the sorption method for concentrating uranium from productive solutions of black shale ores. Several types of anion-exchange resins (AMP, AV-17, A-140, and Amberlite) were tested, enabling a comparative evaluation of their performance. Among them, the AMP resin demonstrated the best results, achieving the highest sorption efficiency (93.8%) and stable desorption parameters (94–95%), which ensured an overall uranium recovery into the eluate of 88–89%.

For vanadium, sorption efficiency was 59.0%, while desorption efficiency was approximately 41–43%. This is attributed to the complex chemical nature of the element and the coexistence of both anionic and cationic forms. Thus, AMP resin can be considered the most promising sorbent for uranium recovery, providing selective separation and enrichment compared with the other tested resins.

At the same time, the limited recoverability of vanadium and its relatively low desorption efficiency indicate the need for further improvement of processing schemes. To enhance separation efficiency and selectivity, it is recommended to supplement the sorption stage with extraction methods, which would enable more complete recovery and separation of uranium and vanadium within complex technological flowsheets. Black shale ores of Southern Kazakhstan are large-tonnage, unconventional sources of strategic metals; therefore, the proposed approaches may be applied in industrial processing of this type of raw material, contributing to a more comprehensive and efficient use of the mineral resource base.

Conflicts of interest. On behalf of all authors, the corresponding author states that there is no conflict of interest.

CRediT author statement: **M. Bulenbayev**: Conceptualization, Methodology, Supervision; **B. Itaybayev**: Data curation, Writing-Original draft preparation; **D. Magomedov**, **A. Bakrayeva**: Visualization, Investigation; **A. Bakrayeva**: Software; **Zh. Bekpeisov** and **D. Magomedov**: Validation.

Acknowledgements. This research was funded by the Committee of Science of the Ministry of Science and Higher Education of the Republic of Kazakhstan (Grant No. AP19576384).

Cite this article as: Bulenbayev M, Altaibayev B, Magomedov D, Bakrayeva A, Bekpeisov Zh. Sorption Concentration of Uranium and Vanadium from Productive Solutions of Black Shale Ores. Kompleksnoe Ispolzovanie Mineralnogo Syra = Complex Use of Mineral Resources. 2027; 340(1):87-94. https://doi.org/10.31643/2027/6445.09

Қара тақтатас кендерінің өнімді ерітінділерінен уран мен ванадийді сорбциялық концентрациялау

Буленбаев М.Ж., Алтайбаев Б.Т., Магомедов Д.Р., Бакраева А.Н., Бекпеисов Ж.К.

Металлургия және кен байыту институты АҚ, Сәтбаев университеті, Алматы, Қазақстан

Мақала келді: *2 қыркүйек 2025*
Сараптамадан өтті: *5 қыркүйек 2025*
Қабылданды: *25 қыркүйек 2025*

ТҮЙІНДЕМЕ

Бұл жұмыста Оңтүстік Қазақстанның қара тақтатас кендерін өңдеу кезінде алынған өнімді қышқыл ерітінділерінен уран мен ванадийді сорбциялау және десорбциялау процестері зерттелді. Мұндай кендер стратегиялық металдардың дәстүрлі емес көздері болып табылады және дәстүрлі минералды-шикізат базасының шектеулі жағдайында ерекше қызығушылық тудырады. Тиімділікті бағалау үшін аниониттердің бірнеше түрі (АМР, AV-17, А-140 және Amberlite) сыналған, бұл олардың сорбциялық қабілеті мен селективтілігін салыстырмалы талдауға мүмкіндік берді. Ең жақсы нәтижелерді АМР шайыры көрсетті, ол күкірт қышқылды ортада ураны жоғары дәрежеде сіңіруді және ванадий бойынша қанағаттанарлық көрсеткіштерді қамтамасыз етті. Десорбциялық тәжірибелер ураны элюатқа тиімді көшіру мүмкіндігін растады, бұл концентрация мен тазартудың кейінгі кезеңдері үшін үлкен маңызға ие. Ванадийді бөліп алу элементтің әртүрлі иондық формаларда болуына байланысты шектеулі болды. Алынған нәтижелер ураны концентрациялаудың сенімді сатысы ретінде сорбциялық технологияның болашағын растайды және мақсатты компоненттерді бөлу мен қалпына келтірудің толықтығын жақсарту үшін экстракция немесе селективті тұндыру сияқты қосымша әдістерді қолдану қажеттілігін көрсетеді.

Түйін сөздер: уран, ванадий, сорбция, десорбция, анионит.

Авторлар туралы ақпарат:

Буленбаев Максат Жумабаевич — *PhD, Ғылыми қызметкер, Металлургия және кен байыту институты АҚ, Сәтбаев Университеті, 050010, Шевченко к-сі, 29, Алматы, Қазақстан. Email: mbulenbaev@mail.ru; ORCID ID: https://orcid.org/0000-0002-5437-5436*

Алтайбаев Багдат Төлбасұлы — *PhD, Ғылыми қызметкер, Металлургия және кен байыту институты АҚ, Сәтбаев Университеті, 050010, Шевченко к-сі, 29, Алматы, Қазақстан. Email: bagdataltai9@gmail.com; ORCID ID: https://orcid.org/0000-0002-7405-6854*

Магомедов Давид Расимович — *Ғылыми қызметкер, Металлургия және кен байыту институты АҚ, Сәтбаев Университеті, 050010, Шевченко к-сі, 29, Алматы, Қазақстан. E-mail: davidmag16@mail.ru; ORCID ID: https://orcid.org/0000-0001-7216-2349*

Бакраева Ақбота Нұрділдақызы — *Кіші ғылыми қызметкер, Металлургия және кен байыту институты АҚ, Сәтбаев Университеті, 050010, Шевченко к-сі, 29, Алматы, Қазақстан. Email: bakraeva.akbota@mail.ru; ORCID ID: https://orcid.org/0000-0002-2062-9573*

Бекпеисов Жасулан Койлыбаевич — *Инженер, Металлургия және кен байыту институты АҚ, Сәтбаев Университеті, 050010, Шевченко к-сі, 29, Алматы, Қазақстан. Email: zhasulan222@mail.ru*

Сорбционное концентрирование урана и ванадия из продуктивных растворов черносланцевых руд

Буленбаев М.Ж., Алтайбаев Б.Т., Магомедов Д.Р., Бакраева А.Н., Бекпеисов Ж.К.

АО Институт металлургии и обогащения, Satbayev University, Алматы, Казахстан

Поступила: *2 сентября 2025*
Рецензирование: *5 сентября 2025*
Принята в печать: *25 сентября 2025*

АННОТАЦИЯ

В данной работе исследованы процессы сорбции и десорбции урана и ванадия из продуктивных кислотных растворов, полученных при переработке черносланцевых руд Южного Казахстана. Такие руды относятся к нетрадиционным источникам стратегических металлов и представляют особый интерес в условиях ограниченности традиционной минерально-сырьевой базы. Для оценки эффективности были испытаны несколько типов анионитов (АМП, АВ-17, А-140 и Amberlite), что позволило провести сравнительный анализ их сорбционной ёмкости и селективности. Наилучшие результаты показала смола АМП, обеспечившая высокую степень извлечения урана и удовлетворительные показатели по ванадию в сернокислой среде. Десорбционные эксперименты подтвердили возможность

	эффективного переноса урана в элюат, что имеет важное значение для последующих стадий концентрирования и очистки. Извлечение ванадия оказалось ограниченным вследствие существования элемента в различных ионных формах. Полученные результаты подтверждают перспективность сорбционной технологии как надёжного этапа концентрирования урана и указывают на необходимость применения дополнительных методов – таких как экстракция или селективное осаждение – для повышения полноты разделения и извлечения целевых компонентов.
	Ключевые слова: уран, ванадий, сорбция; десорбция; анионит.
Буленбаев Максат Жумабаевич	***Информация об авторах:*** *PhD, Научный сотрудник, АО Институт металлургии и обогащения, Satbayev University, ул. Шевченко, 29/133, Алматы, Казахстан. Email: mbulenbaev@mail.ru; ORCID ID: https://orcid.org/0000-0002-5437-5436*
Алтайбаев Багдат Толбасулы	*PhD, Научный сотрудник, АО Институт металлургии и обогащения, Satbayev University, ул. Шевченко, 29/133, Алматы, Казахстан. Email: bagdataltai9@gmail.com; ORCID ID: https://orcid.org/0000-0002-7405-6854*
Магомедов Давид Расимович	*Научный сотрудник, АО Институт металлургии и обогащения, Satbayev University, ул. Шевченко, 29/133, Алматы, Казахстан. E-mail: davidmag16@mail.ru; ORCID ID: https://orcid.org/0000-0001-7216-2349*
Бакраева Ақбота Нұрділдақызы	*Младший научный сотрудник, АО Институт металлургии и обогащения, Satbayev University, ул. Шевченко, 29/133, Алматы, Казахстан. E-mail: bakraeva.akbota@mail.ru; ORCID ID: https://orcid.org/0000-0002-2062-9573*
Бекпеисов Жасулан Койлыбаевич	*Инженер, АО Институт металлургии и обогащения, Satbayev University, ул. Шевченко, 29/133, Алматы, Казахстан. E-mail: zhasulan222@mail.ru*

References

[1] International Atomic Energy Agency. Uranium extraction technology. Technical Reports Series. Vienna: IAEA; 1993; 359. https://www-pub.iaea.org/MTCD/Publications/PDF/trs359_web.pdf

[2] International Energy Agency. Global critical minerals outlook. Paris: IEA. 2025. https://www.iea.org/reports/global-critical-minerals-outlook-2025

[3] Parviainen A, Loukola-Ruskeeniemi K. Environmental impact of mineralised black shales. Earth-Science Reviews 2019; 192:65-90. https://doi.org/10.1016/j.earscirev.2019.01.017

[4] Wu T, Yang R, Gao L, Li J, Gao J. Origin and enrichment of vanadium in the Lower Cambrian black shales, South China. ACS Omega. 2021; 6(39):26870-26879. https://doi.org/10.1021/acsomega.1c02318

[5] Vind J, Tamm K. Review of the extraction of key metallic values from black shales in relation to their geological and mineralogical properties. Minerals Engineering. 2021; 174:107271. https://doi.org/10.1016/j.mineng.2021.107271

[6] Kenzhaliev BK, Kul'deev EI, Luganov VA, et al. Production of Very Fine, Spherical, Particles of Ferriferous Pigments from the Diatomaceous Raw Material of Kazakhstan. Glass Ceram. 2019; 76:194-198. https://doi.org/10.1007/s10717-019-00163-w

[7] Abdel Aal MM. Uranium extraction from sulphuric acid solution using anion-exchange resin. Chemical Technology and Applications Industrial Journal. 2019; 14(2):1-7.

[8] Mattigod SV, Golovich EC, Wellman DM, Cordova EA, Smith RM. Uranium adsorption on ion-exchange resins: Batch testing. Report. Richland (WA): Pacific Northwest National Laboratory; 2010; 20135. https://doi.org/10.2172/1009765

[9] Abd El-Magied MO. Sorption of uranium ions from their aqueous solution by resins containing nanomagnetite particles. International Journal of Polymer Science. 2016; 2016:1029637. https://doi.org/10.1155/2016/1029637

[10] Zhang P, Wang H, Chen L, Li W, Fujita T, Ning S, Wei Y. Efficient uranium removal from aqueous solutions using silica-based adsorbents functionalized with various polyamines. Toxics. 2024; 12(10):704. https://doi.org/10.3390/toxics12100704

[11] Baigenzhenov O, Khabiyev A, Mishra B, Turan MD, Akbarov M, Chepushtanova T. Uranium (VI) recovery from black shale leaching solutions using ion exchange: Kinetics and equilibrium studies. Minerals. 2020; 10(8):689. https://doi.org/10.3390/min10080689

[12] Baqer Y, Thornton S, Stewart DI, Norris S, Chen X. Analysis of uranium sorption in a laboratory column experiment using a reactive transport and surface complexation model. Transport in Porous Media. 2023; 149(2):423-452. https://doi.org/10.1007/s11242-023-01956-y

[13] Ivanov AS, Das S, Bryantsev VS, Tsouris C, Ladshaw AP, Yiacoumi S. Predicting selectivity of uranium vs. vanadium from first principles: Complete molecular design and adsorption modeling. Report No. FCRD-2016-M2FT-16OR030201032. Oak Ridge (TN): Oak Ridge National Laboratory. 2016.

[14] Kenzhaliyev BK, Surkova TYu, Azlan MN, Yulusov SB, Sukurov BM, Yessimova DM. Black shale ore of Big Karatau is a raw material source of rare and rare earth elements. Hydrometallurgy. 2021; 205:105733. https://doi.org/10.1016/j.hydromet.2021.105733

[15] Bulenbayev M, Altaibayev B, Magomedov D, Omirgali A, Bakrayeva A, Koizhanova A. Study of an effective method for extracting uranium from black shale rock using a factor of oxidation and reverse coal flotation. Acta Metallurgica Slovaca. 2025; 31(1):5-10. https://doi.org/10.36547/ams.31.1.2084

[16] Riegel M, Tokmachev M, Hoell WH. Kinetics of uranium sorption onto weakly basic anion exchangers. Reactive and Functional Polymers. 2008; 68(6):1072-1080. https://doi.org/10.1016/j.reactfunctpolym.2008.02.009

[17] Wang L, Zhang Y, Liu T, Huang J, Wang Y. Comparison of ion exchange and solvent extraction in recovering vanadium from sulfuric acid leach solutions of stone coal. Hydrometallurgy. 2013; 131-132:1-7. https://doi.org/10.1016/j.hydromet.2012.09.009

[18] International Atomic Energy Agency. Ion exchange technology in the nuclear fuel cycle. IAEA-TECDOC-365. Vienna: IAEA. 1986.

[19] Osin OA, Lin S, Gelfand BS, Lee SLJ, Shimizu GKH. A molecular extraction process for vanadium based on tandem selective complexation and precipitation. Nature Communications. 2024; 15(1):2614. https://doi.org/10.1038/s41467-024-46958-6

[20] Abbas Z, Jung SM. Green and selective recovery process of Mo, V, and Ni from spent hydrodesulfurization catalysts via novel ionic liquids and deep eutectic solvents technology. Separation and Purification Technology. 2024;3 46:127450. https://doi.org/10.1016/j.seppur.2024.127450

[21] Xu L, Chen Y, Zhang Y, Wang M, Wei S, Zhao X. Antibacterial MXene composite with excellent U/V selectivity for uranium extraction. Desalination. 2024; 583:117718. https://doi.org/10.1016/j.desal.2024.117718

Crossref
DOI: 10.31643/2027/6445.10
Metallurgy

Innovative approaches to the processing of vanadium- and molybdenum-containing technogenic waste

[1]Yulusov S.B., [1]Sarsembayeva M.R., Khabiyev A.T.[1], [2]Retnawati H., [1*]Merkibayev Y.S., [1]Akbarov M.S., [1]Baltabay T.Y.

[1]Satbayev University, Almaty, Kazakhstan
[2]Yogyakarta State University, Indonesia

** Corresponding author email: y.merkibayev@satbayev.university*

Received: *July 17, 2025*
Peer-reviewed: *August 15, 2025*
Accepted: *September 26, 2025*

ABSTRACT

This article explores the consumption trends of vanadium and molybdenum across various industrial sectors, highlighting their strategic importance and the growing demand for a sustainable supply of raw materials. It analyses the sources of these elements of both natural and technogenic origin, including metallurgical slags, ashes, spent catalysts, and other industrial waste products. Particular attention is given to the environmental risks associated with the accumulation of vanadium and molybdenum compounds, which can have toxic effects on the environment. The study emphasises the need to incorporate secondary resources into industrial circulation to ensure the rational use of the mineral resource base and improve the efficiency of metal extraction from primary raw materials. A review is provided of existing chemical and hydrometallurgical methods for extracting vanadium and molybdenum, taking into account the composition of the processed material, technological conditions, and the limitations of specific approaches. The article underscores the potential of integrated waste processing, which enables the recovery of multiple valuable components and supports the transition to a circular economy.

Keywords: vanadium, molybdenum, ash and slag wastes, metallurgical slags, filtrate, hydrometallurgical methods, pyrometallurgical methods, bacterial leaching.

Information about authors:

Yulusov Sultan Baltabayevich — *Associate Professor of the Department of Metallurgy and Mineral Processing, O.A. Baikonurov Mining and Metallurgical Institute, Satbayev University, Almaty, Kazakhstan. Email: s.yulussov@satbayev.university; ORCID ID: https://0000-0001-8044-4186*

Sarsembayeva Marzhan Rahatovna — *PhD student of the Department of Metallurgy and Mineral Processing, O.A. Baikonurov Mining and Metallurgical Institute, Satbayev University, Almaty, Kazakhstan. Email: m.sarsembayeva@satbayev.university; ORCID ID: https://orcid.org/0009-0007-2315-3009*

Khabiyev Alibek Talgatbekuly — *Doctor Ph.D., Assoc. Professor, U. Joldasbekov Institute of Mechanics and Engineering, Almaty, Kazakhstan. E-mail: alibek1324@mail.ru; ORCID ID: https://orcid.org/0000-0001-9397-2367*

Heri Retnawati — *Professor, Yogyakarta State University, Indonesia. Email: heri_retnawati@uny.ac.id; ORCID ID: https://orcid.org/0000-0002-1792-5873*

Merkibayev Yerik Serikovich — *Ph.D., senior Lecturer of the Satbayev University, O.A. Baikonurov Mining and Metallurgical Institute, Almaty, Kazakhstan. Email: y.merkibayev@satbayev.university; ORCID ID: https://orcid.org/0000-0003-3869-6835*

Abarov Merey Sabituly — *Master of Engineering Sciences, Engineer of the Department of Metallurgy and Mineral Processing, O.A. Baikonurov Mining and Metallurgical Institute, Satbayev University, Almaty, Kazakhstan. E-mail: m.akbarov@satbayev.university; ORCID ID: https//orsid.org/0000-0002-4272-8038*

Baltabay Tamerlan — *4th year student of the Department of Metallurgy and Mineral Processing, O.A. Baikonurov Mining and Metallurgical Institute, Satbayev University, Almaty, Kazakhstan. Email: t.baltabay@satbayev.university*

Introduction

In the context of global growth in industrial production and raw material consumption, the issue of natural resource depletion is becoming increasingly pressing. The world's reserves of many strategically important metals, including vanadium and molybdenum, are limited. At the same time, vast amounts of technogenic waste are generated annually, containing residual quantities of valuable elements that remain unutilised and are disposed of in landfills, thereby adding to the environmental burden.

According to geological survey estimates, easily accessible reserves of vanadium and molybdenum are diminishing, and the concentrations of these elements in primary ores are decreasing. As a result, the costs of extraction and processing are rising, and

the economic efficiency of traditional technologies is declining. This situation is driving the shift toward a circular economy, in which waste is viewed not as a burden but as a potential resource [1].

The integrated processing of secondary resources, such as metallurgical slags, fly ash, spent catalysts, and technological sludges, not only enables the recovery of strategically important metals into the production cycle but also reduces the volume of industrial waste. This approach addresses two key challenges simultaneously: ensuring resource security and mitigating environmental risks.

Vanadium and molybdenum are among the strategically important metals widely used across various industrial sectors. Their unique properties make them indispensable in metallurgy, the chemical and energy industries, as well as in high-tech sectors of the economy.

In recent years, global vanadium consumption has been steadily increasing due to the growing worldwide production of structural, stainless, and speciality steels. Beyond the metallurgical and chemical industries, vanadium and its compounds are also extensively used in nuclear and hydrogen energy applications and in the production of vanadium redox flow batteries.

The primary application of vanadium lies in the production of alloyed steels. The addition of vanadium significantly enhances the strength, wear resistance, and thermal stability of steel. Due to these properties, vanadium-containing alloys are widely used in construction, mechanical engineering, pipeline manufacturing, and the production of railway rails. Vanadium is also utilised in the production of armoured steels for the defence industry [[2], [3]].

In addition, vanadium pentoxide (V_2O_5) is used as a catalyst in the production of sulphuric acid and in various oxidation processes in the chemical industry. In recent years, increasing attention has been paid to the use of vanadium in the energy sector—particularly in vanadium redox flow batteries (VRFB), which are regarded as promising energy storage systems for renewable energy sources [4].

Molybdenum is primarily used as an alloying element in materials designed to operate under high temperatures and aggressive environments. It enhances strength, heat resistance, corrosion resistance, and wear resistance. Molybdenum-containing alloys are widely applied in the aerospace industry, power generation, the oil and gas sector, and nuclear energy.

A significant portion of molybdenum is used in the form of sulphides as catalysts in hydrotreating and hydrocracking processes in the petrochemical industry. Additionally, molybdenum compounds are utilised in the production of pigments, specialised lubricants, semiconductors, and glass enamels.

The limited availability of natural sources of vanadium and molybdenum, the high costs associated with their extraction, and geopolitical risks related to supply chains underscore the strategic importance of these metals. Both elements are included in the list of critical raw materials in several countries, including the European Union, the United States, and China.

Modern metallurgy and energy production generate substantial volumes of technogenic waste, which, despite the completion of the main production cycle, still contain residual amounts of valuable components, including vanadium and molybdenum. These waste materials are considered secondary resources that can be processed to obtain marketable products.

The most promising types of secondary raw materials for the extraction of vanadium and molybdenum include:

Fly ash and ash-slag waste: These are formed during the combustion of coal, fuel oil, and oil sludge at thermal power plants (TPPs). Such waste often contains vanadium in the form of oxides or complex compounds, particularly when the burnt fuel had a high content of vanadium and sulphur. In the ash from fuel oil combustion, vanadium concentrations can reach 5–10% [[5], [6], [7]].

Metallurgical slags: By-products of pig iron, steel, and alloy production. In converter slags and ferrovanadium slags, vanadium is typically present in the form of oxides or ferrites, with concentrations ranging from 1% to 15%. Some slags also contain molybdenum, especially when molybdenum-bearing ores have been processed.

Spent catalysts: Catalysts used in the oil refining and chemical industries often contain molybdenum and vanadium in the form of sulphides and oxides. After their operational lifespan ends, these materials become waste suitable for secondary processing. The molybdenum content in such catalysts can reach 10–20%, while vanadium content may be up to 5% [[8], [9]].

Sludges, filtrates, and dust residues: These are generated during filtration, wet gas scrubbing, and ore beneficiation processes. These materials often have a fine-grained structure, which facilitates subsequent metal recovery when properly pretreated.

Secondary resources represent a significant source of vanadium and molybdenum, with concentrations in certain waste streams comparable to—or even exceeding—those found in primary ores. Efficient processing of such materials could offer a sustainable alternative to conventional mining.

Classification of Secondary Resources Containing Vanadium and Molybdenum

The use of secondary resources is no longer merely an alternative—it has become a key strategic direction in modern metallurgy. In the coming years, metallurgists face the challenge of significantly reducing the energy and material intensity of production processes [10]. A critical solution to this challenge lies in the integration of secondary resources into various metallurgical technologies. The most effective results can be achieved when waste materials are returned to the very processes in which they were generated. When this is not feasible, such waste should be efficiently repurposed for other applications under economically favourable conditions.

Thermal Power Generation and Fuel Combustion. The combustion of solid fuels (coal, fuel oil, and petroleum) produces fly ash and ash-slag residues in which metal-containing components of the original raw materials accumulate. A significant quantity of vanadium is found in the waste from thermal power plants, particularly those burning fuel oil. The V_2O_5 content in such residues averages between 15% and 20% [11]. Another important source of secondary vanadium raw materials is spent catalysts from sulphuric acid production, which contain 5–10% V_2O_5. Additionally, the mining and beneficiation of vanadium-bearing ores generate massive volumes of tailings, classified as secondary vanadium resources, with V_2O_5 content up to 1%. Molybdenum can also be present in combustion residues, particularly when coal with high levels of mineral inclusions is used.

Metallurgical Slags and Dust Residues. During steelmaking, ferroalloy production, and the processing of vanadium- or molybdenum-bearing ores, a significant portion of these elements transfers into by-products such as slags, dust, and filtration sludges. For instance, the vanadium content in converter slags can reach 10–15%, depending on the ore composition and the specific technology employed [12]. These types of waste are generated in large volumes and accumulate over time at industrial sites, making them highly attractive for secondary processing and metal recovery.

Oil Refining and Chemical Industry. The widespread use of vanadium and molybdenum is largely due to their catalytic properties. These elements are key components of industrial catalysts employed in processes such as hydrotreating, hydrocracking, and desulfurisation of crude oil and petroleum products. Once their service life ends, these catalysts become highly concentrated waste materials: the molybdenum content can reach 10–20%, and vanadium up to 5–8% [13]. This makes them a particularly valuable type of secondary raw material.

Ore Beneficiation and Processing. During the processing of molybdenum- and vanadium-bearing ores, tailings, sludges, and spent solutions are generated, often retaining a substantial portion of valuable metals. This is mainly due to incomplete recovery of these elements during flotation, leaching, and filtration processes [14]. The presence of fine particles and chemically bound forms of Mo and V complicates their extraction, but modern technologies increasingly allow for efficient recovery even from such complex waste streams.

Vanadium and molybdenum enter secondary raw material flows from a wide range of industrial sources. Their further processing and extraction not only help to address the shortage of strategic metals but also contribute to reducing the accumulation of environmentally hazardous waste [15].

Technologies for Processing Vanadium- and Molybdenum-Containing Waste

As previously mentioned, technogenic waste from vanadium production includes sludges, ash, slags, and other solid residues containing oxides of vanadium, molybdenum, iron, aluminium, and other elements. The concentration of valuable components varies depending on the production technology and the characteristics of the original raw materials. The following key approaches are used for vanadium extraction from such waste:

- Hydrometallurgical Methods: These include both alkaline and acid leaching, which allow vanadium to be converted into a soluble form. For example, leaching with alkaline solutions such as sodium hydroxide (NaOH) or potassium hydroxide (KOH) is effective for processing slags with high vanadium content. Studies have shown that using sulphuric acid (H_2SO_4) at concentrations of 45–50 g/L, combined with pre-grinding of the material to a particle size of 0.1 mm, significantly enhances the efficiency of vanadium extraction, enabling a high degree of solubility [16].

In a study on the hydrometallurgical processing of molybdenum-bearing industrial products from the Shatyrkul-Zhaysan ore cluster, experiments were conducted on atmospheric leaching using nitric acid in both single-stage and two-stage counter-current modes to optimise molybdenum recovery and minimise acid consumption. The most effective conditions for single-stage leaching were found to be a nitric acid concentration of 300 g/L and a sulphuric acid concentration of 100 g/L at 90 °C for 2 hours, resulting in a molybdenum recovery rate of 98.8%. The two-stage leaching process further improved efficiency, achieving a recovery rate of 94.3% using solutions with lower residual acidity and redox potential. Additionally, the solvent extraction stage was optimised using the molybdenum-specific extractant CYANEX® 600 and the diluent Elixore 205, based on the initial leach solution composition. The final product was commercial-grade calcium molybdate with a molybdenum content of 46.83%. This study demonstrated a successful method for producing market-grade calcium molybdate from copper-molybdenum ores, achieving high molybdenum recovery, reducing acid consumption, and minimising harmful emissions [17].

- Pyrometallurgical Methods: These include roasting and smelting processes. For example, roasting slags with alkaline additives at temperatures of 930–950 °C can achieve vanadium recovery rates of up to 30% [8].

While such methods are effective for preliminary vanadium concentration, they are associated with high energy consumption.

- Sorption Technologies: The use of ion-exchange resins and sorbents allows for the efficient extraction of vanadium from liquid waste streams. These methods are particularly advantageous for treating low-concentration solutions or for final purification steps in hydrometallurgical processes.

The methods for extracting molybdenum from technogenic waste are largely similar to those used for vanadium. Hydrometallurgical approaches, particularly leaching followed by precipitation, are considered the most promising. Specifically, acid leaching followed by the precipitation of molybdenum in the form of ammonium molybdate has proven effective in achieving high recovery rates [18].

Bacterial Leaching (Bioleaching): Bioleaching is an environmentally friendly method for metal extraction using microorganisms—typically bacteria such as *Acidithiobacillus ferrooxidans* or *Acidithiobacillus thiooxidans*—which convert metal-containing compounds into water-soluble forms. This approach reduces the use of aggressive chemical reagents and significantly lowers energy consumption.

Bioleaching strategies applied to the treatment of spent hydrodesulfurization catalysts highlight the considerable potential of microbe-driven biocycling for metal recovery. This method offers key advantages, including low capital and operating costs, reduced energy and reagent consumption, and mild operating conditions with minimal emissions. Bacteria such as *A. ferrooxidans* and *A. thiooxidans* play a critical role in metal dissolution through various mechanisms, including direct and indirect oxidation, as well as sulphur, thiosulphate, and polysulphide oxidation pathways. Similarly, fungi such as *Aspergillus niger* and *Penicillium simplicissimum* contribute to metal recovery through processes such as acidolysis, complexolysis, redox reactions, and bioaccumulation. In addition to factors such as pulp density, pH, and particle size, the toxicity of metals to microbial cultures is identified as one of the most significant parameters affecting metal mobilisation in bioleaching systems. Therefore, the use of adapted microbial strains is critical to reducing metal toxicity, enhancing microbial growth, and improving the overall efficiency of bioleaching processes [19].

The development of a technology for the integrated processing of technogenic waste from vanadium production, with the extraction of vanadium and molybdenum, represents an important step toward more sustainable and environmentally friendly production. These technologies not only offer economic benefits but also contribute to the conservation of natural resources, making them extremely valuable in the context of today's world [[20], [21], [22], [23], [24], [25]].

Table 1 – Analysis of Main Methods for Extracting Vanadium (V) and Molybdenum (Mo) from Secondary Resources, Including Hydrometallurgical and Pyrometallurgical Techniques:

Method	Type	Applicability	Advantages	Disadvantages	Recoverable Forms of V and Mo
Alkaline Leaching	Hydrometallurgy	Power plant ash, slags, spent catalysts	High selectivity for vanadium; mild conditions	Low molybdenum recovery; requires solution purification stage	$NaVO_3$, Na_2MoO_4
Acid Leaching (H_2SO_4, HCl, HNO_3)	Hydrometallurgy	Catalysts, sludges, slags	Suitable for simultaneous extraction of V and Mo	High corrosivity, formation of toxic gases	$VOSO_4$, MoO_3, $(NH_4)_2MoO_4$
Ammonium Leaching	Hydrometallurgy	Spent catalysts, ores	High selectivity for Mo (as ammonium salts)	Low vanadium solubility; long leaching time	$(NH_4)_2MoO_4$
Roasting with Na_2CO_3 or NaOH + Leaching	Hydro- and Pyrometallurgy	Slags, ash, ores	Conversion of V and Mo into soluble forms; high efficiency	High energy consumption, dust pollution	$NaVO_3$, Na_2MoO_4
Sulphidation + Leaching	Pyrometallurgy	Concentrates, slags	Enhanced Mo recovery as sulphides	Requires high temperatures; difficulty in selective separation	MoS_2 (with further processing), V_2O_5
Oxidative Smelting	Pyrometallurgy	Alloy steel waste, slags	Oxidises V and Mo into volatile or soluble compounds	High temperatures, high energy costs	V_2O_5, MoO_3
Sorption/Ion Exchange from Solutions	Physicochemical	Post-leaching solutions	High selectivity; purification of solutions	Requires pre-treatment of solution, expensive sorbents	V(V), Mo(VI)
Solvent Extraction with Organic Reagents	Physicochemical	Post-acid leaching solutions	Separation of V and Mo; high selectivity	Multi-stage process, organic waste generation	Organic complexes of V and Mo

- **Environmental and Economic Aspects of Involving Secondary Resources in Processing**

- The reuse of waste generated during vanadium production to extract valuable components such as vanadium and molybdenum represents a promising path toward improving production profitability and minimising environmental harm. Successful processing experiences in Kazakhstan and other countries demonstrate that modern recycling methods can yield significant economic and environmental benefits. Further progress requires new research and development aimed at improving processing technologies, enhancing their environmental safety, and creating universal solutions applicable to various types of waste.

- **Environmental Significance: Reduction of industrial waste volumes.** Ash, slags, dust residues, and spent catalysts are traditionally landfilled or stockpiled, occupying space and causing long-term environmental burdens. Their processing reduces the need for disposal sites and decreases soil, air, and water pollution.

- Prevention of toxic component leaching. Vanadium and molybdenum in industrial waste can transform into water-soluble forms and leach into groundwater. Recovering these elements minimizes the risks of bioaccumulation and toxic effects on the environment.

- **Reduction of carbon footprint.** Metal production from secondary raw materials requires significantly less energy than extraction from primary ores, contributing to lower greenhouse gas emissions.

- **Economic Efficiency:**

- **Increased recovery of valuable materials.** Integrated processing enables the extraction not only of the target element (e.g., vanadium) but also of associated components such as iron, nickel, cobalt, sulphur, and others. This significantly enhances the overall value of processing and the profitability of the project.

- **Reduced dependence on imported raw materials.** Vanadium and molybdenum are classified as critical materials in many countries. Utilising domestic secondary sources strengthens raw material security and the resilience of the metallurgical sector.

- **Creation of new sectors in the waste recycling industry.** Entire industries focused on processing catalysts, slags, and ash are emerging, creating jobs and driving technological innovation at the intersection of metallurgy, chemistry, and environmental science.

Table 2 – Comparison of Main Methods for Extracting Vanadium (V) and Molybdenum (Mo) from Technogenic Feedstock Based on Efficiency, Environmental, and Economic Criteria

Method	Feedstock Type	V/Mo Recovery, %	Environmental Impact	Economic Efficiency	Comments
1. Alkaline Leaching	Slags, catalysts	V: 85–95%Mo: up to 98%	Moderate (alkaline effluents require neutralisation)	High (reagents are available, moderate energy consumption)	Simple, suitable for oxidised forms
2. Acid Leaching (H_2SO_4, HCl, HNO_3)	Slags, ash, catalysts	V: 80–95%Mo: 70–90%	Low (acidic effluents, corrosion)	High (inexpensive reagents)	Versatile, but low selectivity
3. Ammonium Leaching ($(NH_4)_2CO_3$, NH_4OH)	Catalysts, slags	V: 65–90%Mo: 80–95%	High (ammonia volatilises but can be captured)	Moderate (ammonium salts are more expensive)	Selective for Mo, forms complex salts
4. Roasting with Na_2CO_3 or NaOH + Leaching	Ash, slag, catalysts	V: 90–98%Mo: 90–99%	Low (high emissions and energy consumption)	Moderate (requires furnaces and additional equipment)	Suitable for hardly soluble phases
5. Sulphidation + Leaching	Molybdenum concentrates, catalysts	Mo: 80–95%V: 40–70%	Moderate (sulfur-containing emissions)	Moderate	Works better for Mo than for V
6. Oxidative Smelting (with $NaNO_3$, CaO)	Slags, ash	V: 85–95%Mo: 70–90%	Low (NO_x and CO_2 emissions)	Low (high energy consumption)	For complex matrices, but costly
7. Sorption / Ion Exchange	Leach solutions	V/Mo removal efficiency: >95%	High (closed-loop system, no liquid effluents)	Moderate (mixed sorbents are more expensive)	Reusable, high selectivity
8. Solvent Extraction with Organic Reagents	Leach solutions	V: up to 99.9%, Mo: 90–99%	Moderate (organic solvent vapors)	Moderate to high	High selectivity, but requires many stages

The integrated processing of vanadium- and molybdenum-containing waste is not only a way to improve the efficiency of metallurgical processes but also a powerful tool for the environmental modernisation of industry. A powerful and efficient tool like this integrated processing is essential [1]. It enables the simultaneous resolution of pollution issues, reduces dependence on natural resources, and fosters the creation of sustainable economic models within the framework of the green transition [26].

The ores of the Greater Karatau region represent a valuable but currently untapped source of rare and rare earth elements (REEs), even though technology is developing rapidly in the last 20 years [27]. To develop an integrated processing technology for the black shale ore, a series of chemical, X-ray phase, infrared, mineralogical, X-ray spectral, and electron microscopic studies were conducted. Rare and especially rare earth elements in the ore are present in various minerals as inclusions within a siliceous-carbonaceous matrix. This explains the failure of previously proposed processing methods, which resulted in either incomplete recovery of valuable components or uneconomical processes. New approaches are required to achieve more complete extraction. A method has been proposed for the preliminary treatment of the raw black shale ore by roasting with $(NH_4)_2SO_4$ in the presence of concentrated H_2SO_4, followed by leaching of the calcine with a dilute H_2SO_4 solution. Optimal conditions for each stage were determined. Kinetic studies of REE extraction from the sulphate calcine under the most favourable conditions showed maximum recovery rates of U – 98%, V – 92%, Mo – 89%, and REEs – 78%. The rate constant and effective activation energy for vanadium leaching, as a representative of rare and rare earth metals, were calculated. The process is diffusion-limited. After leaching valuable components, the remaining calcine can be used in a froth flotation enrichment process to extract carbon-containing material and subsequently as part of a charge for ferrosilicon production. The solution obtained from leaching the original calcine can be used for sorption recovery of U, Mo, V, and REEs [27, 28].

The authors of [29] proposed a technological scheme (Figure 1) for the processing of technogenic waste through integrated extraction of vanadium, molybdenum, and nickel, achieving a recovery rate of 87%. Meanwhile, during electrochlorination lasting 12 hours, the recovery rate of nickel was slightly lower—58%.

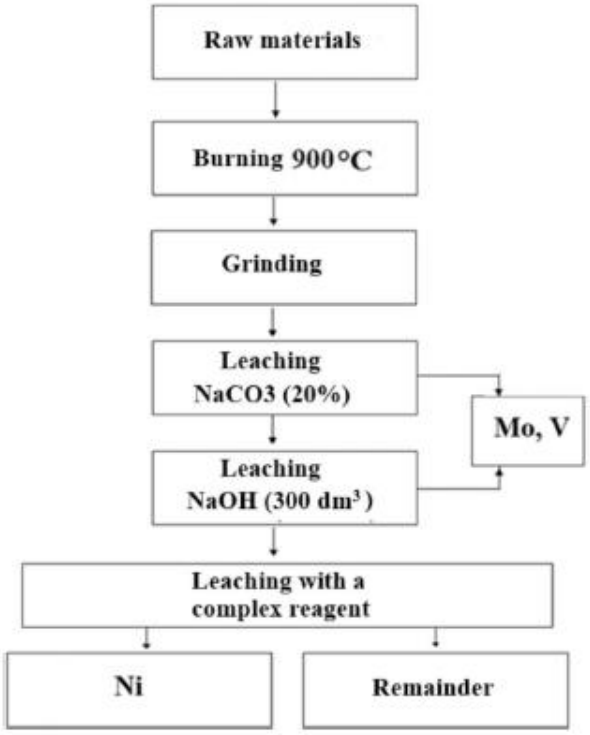

Figure 1 – Technological Flowchart for the Processing of Technogenic Waste with Integrated Extraction of Vanadium, Molybdenum, and Nickel

Conclusion

In the context of depleting high-grade natural ores and growing demand for strategic metals, the use of technogenic raw materials as an alternative source of vanadium and molybdenum is becoming increasingly relevant. Metallurgical slags, ash, spent catalysts, and other secondary resources not only contain high concentrations of valuable components but also pose a potential environmental threat when stored long-term or disposed of improperly.

The analysis shows that integrated waste processing technologies make it possible not only to efficiently extract vanadium and molybdenum but also to recover valuable by-products such as iron, nickel, sulphur, aluminosilicates, and others. This significantly enhances the economic viability of processing and helps reduce the environmental burden.

The most promising approaches are combined flowsheets that integrate pyrometallurgical, hydrometallurgical, and biotechnological methods. Their application should consider the specific waste composition, the chemical form of the metals, the level of contamination, and the final processing objectives. Particular attention must be given to the

environmental safety of all stages of the technological process.

The development and implementation of such technologies align with the goals of sustainable development, resource conservation, and the transition to a circular economy. This enables the creation of closed production cycles and the effective integration of waste recycling into existing industrial systems.

CRediT author statement: **S. Yulusov, Y. Merkibayev:** Methodology, formal analysis, investigation, Data writing, Original draft preparation, writing–review and editing; **M.Sarsembayeva, A.Khabiyev, H.Retnawati, M.Akbarov**: Data curation, Reviewing and Editing; **T.Baltabay:** Investigation.

Conflicts of Interest. On behalf of all authors, the correspondent author declares that there is no conflict of interest.

Gratitude: This research was funded by the Science Committee of the Ministry of Science and Higher Education of the Republic of Kazakhstan (grant No. AP19676107).

Cite this article as: Yulusov SB, Sarsembayeva MR, Khabiyev AT, Retnawati H, Merkibayev YS, Akbarov MS, Baltabay TY. Innovative approaches to the processing of vanadium- and molybdenum-containing technogenic waste. Kompleksnoe Ispolzovanie Mineralnogo Syra = Complex Use of Mineral Resources. 2027; 340(1):95-105. https://doi.org/10.31643/2027/6445.10

Құрамында ванадиий және молибдені бар техногендік қалдықтарды өңдеудің инновациялық тәсілдері

[1]Юлусов С.Б., [1]Сарсембаева М.Р., [1]Хабиев А.Т., [2]Retnawati H., [1*]Меркибаев Е.С., [1]Әкбаров М.С., [1]Балтабай Т.Е.

[1] Сәтбаев университеті, Алматы, Қазақстан
[2]Йогьякарта мемлекеттік университеті, Индонезия

Мақала келді: *17 шілде 2025*
Сараптамадан өтті: *15 тамыз 2025*
Қабылданды: *26 қыркүйек 2025*

ТҮЙІНДЕМЕ

Мақалада өнеркәсіптің түрлі салаларында ванадий мен молибденді тұтыну бағыттары қаралды, бұл олардың стратегиялық маңыздылығы мен шикізатпен тұрақты қамтамасыз етудің өсіп келе жатқан қажеттілігін көрсетеді. Металлургиялық қождарды, күлдерді, пайдаланылған катализаторлар мен өнеркәсіптік процестердің басқа да қалдықтарын қоса алғанда, осы элементтердің табиғи және техногендік шығу көздері талданды. Қоршаған ортаға уытты әсер етуі мүмкін ванадий мен молибден қосылыстарының жиналуына байланысты экологиялық қауіптерге ерекше назар аударылады. Минералдық-шикізат базасын ұтымды пайдалану және бастапқы шикізаттан металдарды алудың тиімділігін арттыру үшін өнеркәсіп айналымына қайталама ресурстарды тарту қажеттігі атап көрсетілді. Өңделетін материалдың құрамын, технологиялық жағдайлардың ерекшеліктерін, сондай-ақ жекелеген тәсілдердің шектеулері мен кемшіліктерін ескере отырып, ванадий мен молибденді алудың қолданыстағы химиялық және гидрометаллургиялық әдістеріне шолу жасалды. Бірнеше құнды компоненттерді алуды қамтамасыз ететін және айналмалы экономикаға көшуге ықпал ететін қалдықтарды кешенді қайта өңдеудің перспективалылығына баса назар аударылды.

Түйін сөздер: *ванадий, молибден, күл-қож қалдықтары, металлургиялық шлактар, сүзгі, гидрометаллургиялық әдістер, пирометаллургиялық әдістер, бактериялық шаймалау.*

Авторлар туралы ақпарат:

Юлусов Султан Балтабаевич — *Юлусов Сұлтан Балтабайұлы PhD докторы, Ө.А. Байқоңыров атындағы Тау-кен-металлургия институтының Металлургия және пайдалы қазбаларды өңдеу кафедрасының доценті, Сәтбаев университеті, Алматы, Қазақстан. Email: s.yulussov@satbayev.university; ORCID ID: https://0000-0001-8044-4186*

Сарсембаева Маржан Рахатовна — *Металлургия және пайдалы қазбаларды өңдеу кафедрасының PhD докторанты, О.А. Байқоңыров атындағы тау-кен металлургия институты, Сәтбаев университеті, Алматы, Қазақстан. Email: m.sarsembayeva@satbayev.university; ORCID ID: https://orcid.org/0009-0007-2315-3009*

Хабиев Алибек Талгатбекұлы — *Ph.D докторы, ассоц. профессор, Академик У.А. Жолдасбеков атындағы Механика және машинатану институты, Алматы, Қазақстан. E-mail: alibek1324@mail.ru; ORCID ID: https://orcid.org/0000-0001-9397-2367*

Heri Retnawati — *Профессор, Йогьякарта мемлекеттік университеті, Индонезия. Email: heri_retnawati@uny.ac.id; ORCID ID: https://orcid.org/0000-0002-1792-5873*

Меркибаев Ерик Серикович	*Ph.D. докторы, Металлургия және пайдалы қазбаларды байыту кафедрасының аға оқытушысы, Ө.А. Байқоңыров атындағы Тау-кен-металлургия институты, Сәтбаев университеті, Алматы, Қазақстан. Email: y.merkibayev@satbayev.university; ORCID ID: https://orcid.org/0000-0003-3869-6835*
Әкбаров Мерей Сәбитұлы	*Техника ғылымдарының магистрі, Металлургия және пайдалы қазбаларды байыту кафедрасының инженері, Ө.А. Байқоңыров атындағы Тау-кен металлургия институты, Сәтбаев университеті, Алматы, Қазақстан. E-mail: m.akbarov@satbayev.university; ORCID ID: https//orsid.org/0000-0002-4272-8038*
Балтабай Тамерлан	*Металлургия және пайдалы қазбаларды өңдеу кафедрасының 4 курс студенті, О.А. Байқоңыров атындағы тау-кен металлургия институты, Сәтбаев университеті, Алматы, Қазақстан. Email: t.baltabay@satbayev.university*

Инновационные подходы к переработке техногенных отходов, содержащих ванадий и молибден

[1]Юлусов С.Б., [1]Сарсембаева М.Р., [1]Хабиев А.Т., [2]Retnawati H., [1*]Меркибаев Е.С., [1]Акбаров М.С., [1]Балтабай Т.Е.

[1]Satbayev University, Almaty, Kazakhstan
[2]Джокьякартский государственный университет, Индонезия

Поступила: *17 июля 2025*
Рецензирование: *15 августа 2025*
Принята в печать: *26 сентября 2025*

ABSTRACT

В статье рассмотрены направления потребления ванадия и молибдена в различных отраслях промышленности, что подчёркивает их стратегическую значимость и растущую потребность в устойчивом обеспечении сырьём. Проанализированы источники этих элементов как природного, так и техногенного происхождения, включая металлургические шлаки, золы, отработанные катализаторы и другие отходы промышленных процессов. Отдельное внимание уделено экологическим рискам, связанным с накоплением соединений ванадия и молибдена, способных оказывать токсическое воздействие на окружающую среду. Подчёркнута необходимость вовлечения вторичных ресурсов в промышленный оборот для рационального использования минерально-сырьевой базы и повышения эффективности извлечения металлов из первичного сырья. Приведён обзор существующих химических и гидрометаллургических методов извлечения ванадия и молибдена, с учётом состава перерабатываемого материала, особенностей технологических условий, а также ограничений и недостатков отдельных подходов. Сделан акцент на перспективность комплексной переработки отходов, обеспечивающей извлечение нескольких ценных компонентов и способствующей переходу к циркулярной экономике.

Keywords: ванадий, молибден, золошлаковые отходы, металлургические шлаки, фильтрат, гидрометаллургические методы, пирометаллургические методы, бактериальное выщелачивание.

Информация об авторах:

Юлусов Султан Балтабаевич	*PhD, ассоциированный профессор кафедры Металлургии и обогащения полезных ископаемых, Горно-металлургический институт имени О.А. Байконурова, Satbayev University, Almaty, Kazakhstan. Email: s.yulussov@satbayev.university; ORCID ID: https://0000-0001-8044-4186*
Сарсембаева Маржан Рахатовна	*PhD докторант кафедры Металлургии и обогащения полезных ископаемых, Горно-металлургический институт имени О.А. Байконурова, Satbayev University, Almaty, Kazakhstan. Email: m.sarsembayeva@satbayev.university; ORCID ID: https://orcid.org/0009-0007-2315-3009*
Хабиев Алибек Талгатбекович	*Доктор Ph.D., ассоц. профессор, Институт механики и машиноведения имени академика У.А. Джолдасбекова, Алматы, Казахстан. E-mail: alibek1324@mail.ru; ORCID ID: https://orcid.org/0000-0001-9397-2367*
Heri Retnawati	*Профессор, Джокьякартский государственный университет, Индонезия. Email: heri_retnawati@uny.ac.id; ORCID ID: https://orcid.org/0000-0002-1792-5873*
Меркибаев Ерик Серикович	*PhD, старший преподаватель кафедры 'Металлургии и обогащения полезных ископаемых, Горно-металлургический институт имени О.А. Байконурова, Satbayev University, Almaty,Kazakhstan. Email: y.merkibayev@satbayev.university; ORCID ID: https://orcid.org/0000-0003-3869-6835*
Акбаров Мерей Сәбитұлы	*Магистр технических наук, инженер кафедры Металлургия и обогащения полезных ископаемых, Горно-металлургический институт имени О.А. Байконурова, Satbayev University, Алматы, Казахстан. E-mail: m.akbarov@satbayev.university; ORCID ID: https//orsid.org/0000-0002-4272-8038*
Балтабай Тамерлан	*Студент 4 курса кафедры Металлургии и обогащения полезных ископаемых, Горно-металлургический институт имени О.А. Байконурова, Satbayev University, Almaty, Kazakhstan. Email: t.baltabay@satbayev.university*

References

[1] Ashraf B, Mohamed M El-SS, Mohamed M. Zaky A, Saeed H, Sami G, Eskander H Recovery of vanadium and nickel from heavy oil fly ash (HOFA): a critical review. RSC Advances. 2023; 13:6327-6341.

[2] Nertil X, Francesco F Extraction and Recovery of Metals from Spent HDS Catalysts: Lab- and Pilot-Scale Results of the Overall Process. 2023; 13(7):1254.

[3] Xu W, Hou X Q, Shi Y, Z Zhang W, Gu Y F, Feng CG, Volodymyr K. Correlation between the microstructure and corrosion behaviour of copper/316 L stainless-steel dissimilar-metal welded joints. Corrosion Science. 2021; 191:109729. https://doi.org/10.1016/j.corsci.2021.109729 .

[4] Dikanbayeva K, Auyeshov AP, Satayev MS, Arynov KT, Yeskibayeva ChZ. Researching of sulfuric acid leaching of magnesium from serpentines. News of the National Academy of Sciences of the Republic of Kazakhstan, Series of Geology and Technical Sciences. 2021; 5(449):32-38. https://doi.org/10.32014/2021.2518-170X.95

[5] Chepushtanova TA, Merkibayev YS, Mamyrbayeva KK, Sarsenbekov T, & Mishra B. Mechanism and technological results of sulfidation roasting of oxidized lead compounds. Kompleksnoe Ispolzovanie Mineralnogo Syra= Complex use of mineral resources. 2025; 332(1):119-132.

[6] Silin KM Hahn, Gursel D, Kremer D, Gronen L, Stopic S, Friedrich B, Wotruba H. Mineral processing and metallurgical treatment of lead vanadate ores. Minerals. 2020; 10(2):197. https://doi.org/10.3390/min10020197.

[7] Mamyrbayeva KK, Kuandykova AN, Chepushtanova TA, Merkibayev YS. Review of technology for hydrometallurgical processing of lateritic nickel ores over the past 20 years in the world. Non-Ferr. Met. 2024; 13–21.

[8] Vohidov BR, Kaiumov OA. Issledovanie Sposoba Izvlechenia Vanadia Iz Tehnogennyh Othodov (Ovk-Otrabotannyi Vanadievyi Katalizator) [Research of the method for extraction of vanadium from technogenic waste (HVAC-Spent vanadium catalyst)]. Universum: tehnicheskie nauki:elektron. nauchn. jurn. [Universum: technical sciences: elektron. scientific. Journal]. 2023; 10(115). (in Russ.). https://7universum.com/ru/tech/archive/item/16140

[9] Churilov AE, Mukaev EG, Gorbunova AV. Vanadisoderjaşie resursy i himicheskie sposoby ih pererabotki [Vanadium-containing resources and chemical methods of their processing]. Obşie voprosy metalurgii [General issues of metallurgy]. 2017; 3(22):30-33. (in Russ.).

[10] Volkov Aİ, Stulov PE, Kologrieva UA. . İssledovanie tehnologicheskih svoistv i vozmojnostei pererabotki razlichnyh vidov vanadievogo syrä v Rosii [Research of technological properties and possibilities of processing of various types of vanadium raw materials in Russia]. Metallurgist [Metalurg]. 2024; 67:1379-1395. (in Russ.). https://doi.org/10.1007/s11015-024-01630-8

[11] Chepushtanova TA, Merkibayev YS, Mishra B, & Kuldeyev YI. Processing of the zinc-lead-bearing flotation middlings by sulfidizing roasting with pyrrhotites production by predicted properties. Non-Ferr. Met. 2022; 2:15-24.

[12] Makhotkina E.S., Shubina M.V. İzvlechenie vanadia iz şlaka prosesa ITMK3 [Extraction of vanadium from the slag of the ITMK3 process]. Aktuälnye problemy sovremennoi nauki, tehniki i obrazovania. Magnitogorsk: İzd-vo Magnitogorsk. gos. tehn. un-ta im. G.İ. Nosova [Actual problems of modern science, technology and education. Magnitogorsk: Publishing House of Magnitogorsk State Technical University. G.I. Nosov University]. 2013; 1: 168-171. (in Russ.).

[13] Liuyi R, Zhang Z, Zeng W, et al. Adhesion between nanobubbles and fine cassiterite particles. Intern J Mining Sci Technol. 2023; 33(4):503–509. doi:10.1016/j.ijmst.2022.09.

[14] Srivastava RR, Ilyas N, Chaerun SK. et al. Biological recycling of critical metals from spent hydrodesulfurization catalysts: a review. Environ Chem Lett. 2025. https://doi.org/10.1007/s10311-025-01849-0

[15] Chepushtanova TA, Yessirkigenov MI, Mamyrbayeva KK, Merkibayev ES, & Nikolosky A. Testing of the optimum extragent for solvent-extraction of Almaly deposit copper. Kompleksnoe Ispolzovanie Mineralnogo Syra = Complex Use of Mineral Resources. 2022; 323(4):77-83.

[16] Peng H. A literature review on leaching and recovery of vanadium. J. Environ. Chem. Eng. 2019; 7:103313. https://doi.org/10.1016/j.jece.2019.103313

[17] Gao F, Olayiwola AU, Liu B, et al. Review of Vanadium Production Part I: Primary Resources. Miner. Process. Extr. Metall. Rev. 2021; 42(3):466-488. https://doi.org/10.1080/08827508.2021.1883013

[18] Liu Y, Huang W, & Jiang T. Recovery of Valuable Elements from Molten Vanadium Slag Through High-Temperature Reduction. JOM. 2024; 76:4643-4652. https://doi.org/10.1007/s11837-024-06602-6

[19] Luo M, Xiang J, Huang Q, Zhang S, Liu Z. Recovery of Vanadium from Vanadium Slag by Roasting with CaO-MgO Composite Additive. In: Ouchi, T., et al. Rare Metal Technology 2023. TMS 2023. The Minerals, Metals & Materials Series. Springer, Cham. 2023. https://doi.org/10.1007/978-3-031-22761-5_28

[20] Ilyas S, Srivastava RR, Kim H, Cheema HA, Bhatti IA. Hydrometallurgical Extraction of Molybdenum and Rhenium from Molybdenite Flue Dust. In: Ouchi T, et al. Rare Metal Technology 2023. TMS 2023. The Minerals, Metals & Materials Series. Springer, Cham. 2023. https://doi.org/10.1007/978-3-031-22761-5_16

[21] Karimova L, Kairalapov Ye, Tussupbekova T, Oleinikova T, Makasheva G. Hydrometallurgical Processing Of Molybdenum Middlings From Shatyrkul-Zhaysan Cluster Ore. J. Min. Metall. Sect. B-Metall. 2024; 60(1):71-83.

[22] Xu YW, Hou XQ, Shi Y, Zhang WZ, Gu YF, Feng CG, Volodymyr K. Correlation between the microstructure and corrosion behaviour of copper/316 L stainless-steel dissimilar-metal welded joints, Corrosion Science. 2021; 191:109729. https://doi.org/10.1016/j.corsci.2021.109729

[23] Agapitov YE, Karimova LM, Khazhimukhametov TA, Meshkov EY, Bobyrenko NA. Development of a scheme for hydrometallurgical processing of high-sulphur copper sulphide concentrates, Scientific and Technical Bulletin of the Volga Region. 2019; 7:32-36.

[24] Rogozhnikov DA, Zakharyan SV, Dizer OA, Karimov KA. Nitric acid leaching of the copper-bearing arsenic sulphide concentrate of Akzhal, Tsvetnye Metally. 2020; 8. https://doi.org/10.17580/tsm.2020.08.02

[25] Retnawati H. Learning Trajectory of Item Response Theory Course Using Multiple Softwares. Olympiads In Informatics. 2017; 11(1):123-142. https://doi.org/10.15388/ioi.2017.10

[26] Lu Jun, Wang Shuize, Yu Hao, Wu Guilin, Gao Junheng, Wu Honghui, Zhao Haitao, Zhang Chaolei, Mao Xinping. Structure-property relationship in vanadium micro-alloyed TRIP steel subjected to the isothermal bainite transformation process. MSEA. 2023; 878:145208. https://doi.org/10.1016/j.msea.2023.145208

[27] Yulusov S, Sarsembayeva M, Surkova T, Yerik M, & Dronenko A. On the question of extracting valuable components from spent catalyst. Canadian Metallurgical Quarterly. 2025, 1-11.

[28] Kenzhaliyev BK, Surkova TY, Azlan MN, Yulusov SB, Sukurov BM, & Yessimova DM. Black shale ore of Big Karatau is a raw material source of rare and rare earth elements. Hydrometallurgy. 2021; 205:105733.

[29] Yulusov S, Sarsembayeva M, Surkova T, Yerik M, & Dronenko A. On the question of extracting valuable components from spent catalyst. Canadian Metallurgical Quarterly. 2025, 1-11.

Crossref
DOI: https://doi.org/10.31643/2027/6445.11
Metallurgy

Pyrolysis of copper telluride in a water vapour atmosphere

Nitsenko A.V., *Linnik X.A., Volodin V.N., Burabayeva N.M., Trebukhov S.A.

Institute of Metallurgy and Ore Beneficiation JSC, Satbayev University, Almaty, Kazakhstan

** Corresponding author emails: x.linnik@satbayev.university*

Received: *September 19, 2025*
Peer-reviewed: *September 27, 2025*
Accepted: *October 3, 2025*

ABSTRACT

This paper presents the results of exploratory studies on the feasibility of extracting tellurium from synthetic copper telluride and industrial tellurium–containing middlings using a vacuum-thermal method conducted in a water vapour atmosphere. It was determined that the thermal behavior of synthetic copper telluride follows an oxidation mechanism involving oxygen in a dry environment. The phase transformations occurring in the tellurium–containing industrial middlings are also comparable to those observed during oxidative-distillation roasting and vacuum-thermal processing in an inert atmosphere. The achieved degrees of extraction of copper telluride and tellurium-containing industrial middlings at a temperature of 1100 °C and a pressure of 1.3-2 kPa were 57.83 % and 94.89 %, respectively. The obtained residues are represented by copper oxide phases. At the same time, tellurium evaporates from the material and deposits on the walls of the condenser in the cold part of the reactor at temperatures below 400 °C. According to X-ray phase analysis, the condensate is represented by tellurium in the form of oxide.

Keywords: Telllurium, copper, vacuum, water vapour, evaporation

Information about authors:

Nitsenko Alina Vladimirovna — *Candidate of Technical Sciences, Head of the Vacuum Processes Laboratory of Institute of Metallurgy and Ore Beneficiation JSC, Satbayev University, Shevchenko str., 29/133, 050010, Almaty, Kazakhstan. Email: alina.nitsenko@gmail.com; ORCID ID: https://orcid.org/0000-0001-6753-0936*

Linnik Xeniya Alexandrovna — *Master of Technical Sciences, Junior Researcher of the Vacuum Processes Laboratory of Institute of Metallurgy and Ore Beneficiation JSC, Satbayev University, Shevchenko str., 29/133, 050010, Almaty, Kazakhstan. Email: x.linnik@satbayev.university, xenija_linnik@mail.ru; ORCID ID: https://orcid.org/0000-0002-0683-1409*

Volodin Valeriy Nikolaevich — *Doctor of Technical Sciences, Professor, Chief Researcher of the Vacuum Processes Laboratory of Institute of Metallurgy and Ore Beneficiation JSC, Satbayev University, Shevchenko str., 29/133, 050010, Almaty, Kazakhstan. Email: volodinv_n@mail.ru; ORCID ID: https://orcid.org/0000-0003-0116-1423*

Burabayeva Nurila Muratovna — *Candidate of Technical Sciences, Senior Researcher of the Vacuum Processes Laboratory of Institute of Metallurgy and Ore Beneficiation JSC, Satbayev University, Shevchenko str. 29/133, 050010, Almaty, Kazakhstan. Email: nuri_eng@mail.ru; ORCID ID: https://orcid.org/0000-0003-2183-2239*

Trebukhov Sergey Anatolyevich — *Candidate of Technical Sciences, Professor, Leading Researcher of the Laboratory of Vacuum Processes Institute of Metallurgy and Ore Beneficiation JSC, Satbayev University, Shevchenko str., 29/133, 050010, Almaty, Kazakhstan. Email: s.trebukhov@satbayev.university; ORCID ID: https://orcid.org/0000-0001-9708-0307*

Introduction

Tellurium is a promising material for industries such as power engineering, electrical engineering, medicine, glass production, and rubber manufacturing. Due to its low content in ores, tellurium is mainly extracted as a by-product [[1], [2], [3]]. Among the various tellurium-containing middlings (sludges, sublimates, dusts, slags, etc.), the key material is electrolytic copper sludges [[4], [5], [6]]. Due to the diverse phase composition of these sludges, traditional processing methods are complemented by new research aimed at finding more efficient technologies [[7], [8], [9], [10], [11], [12], [13]].

Industrial copper telluride obtained by the traditional method of precipitating tellurium from solution onto copper is characterized by a mixture of phases, including both non-stoichiometric ($Cu_{2-x}Te$)

and stoichiometric (Cu_2Te) compositions [[14], [15], [16], [17]], as well as a small amount of impurities.

The efficiency of traditional technology to process industrial copper telluride (oxidative-alkaline leaching) is about 80 % according to [16]. Therefore, developing a more effective method is an important direction. Studies are known that focus on improving the traditional method [[16], [18], [19]], as well as developing alternative pyrometallurgical approaches.

Pyrometallurgical methods have long been uncommon in both industrial practice and scientific research. This is since the decomposition of Cu_2Te is possible only at temperatures above 2704 °C [[20], [21]]. A significant reduction in temperature can be achieved by conducting the process under low pressure.

However, copper telluride has a low dissociation pressure: at 1780 °C, it is 0.7 kPa. Therefore, direct tellurium extraction via Cu_2Te decomposition is theoretically impossible.

Consequently, existing research on pyrometallurgical methods focuses on finding optimal conditions for tellurium extraction using reagents that lower the decomposition temperature of copper telluride. For example, paper [22] proposed using elemental sulfur, which replaces tellurium in copper telluride.

The technology is two-stage and involves pre-sulfidation of the tellurium–containing middlings followed by vacuum-thermal sublimation of elemental tellurium. The efficiency of tellurium extraction is 97 %. In paper [23], air oxygen was proposed as an oxidizer. This technology is also two-stage. Tellurium is extracted from the tellurium–containing middlings in oxide form, which is then subjected to thermal reduction. The efficiency of tellurium extraction is 98 %. Paper [24] considered the possibility of extracting tellurium in an inert atmosphere using the oxygen contained in the material itself. Tellurium was also extracted in oxide form, with an extraction efficiency of about 99 %.

These papers [[23], [24]] were based on the more favorable vapor pressure of tellurium oxide (TeO_2), which at 733 °C is about 0.02 kPa [[25], [26]]. However, it was found that during both oxidative distillation roasting and vacuum thermal processing, up to the evaporation temperature, tellurium oxide interacts with copper oxide. As a result, copper orthotellurate (Cu_3TeO_6) is formed, which is stable up to 880 °C [27].

It is known that in a water vapour atmosphere, the volatility of tellurium oxide increases due to the formation of the more volatile $TeO(OH)_2$ [[28], [29]], which upon condensation converts to tellurium dioxide [30].

In this regard, we conducted a study aimed at evaluating the effect of water vapour on tellurium extraction from tellurium–containing middlings. The results of the work are presented in the current article.

Experimental part. Materials

Synthetic Copper Telluride.

The study used synthetic copper telluride obtained by direct melting of the starting components in an evacuated quartz ampoule. For the synthesis, electrolytic copper chips (99.99 %) and elemental tellurium powder (99.98 %) were taken in stoichiometric amounts (49.92 wt.% % Cu and 50.08 wt.% % Te). The synthesis temperature was 1200 °C, with a heating rate of 2 °C/min up to the target temperature. The synthesis duration was 6 hours. The obtained alloys were slowly cooled in the furnace after the set holding time.

Phase analysis of the material was conducted using the ICDD PDF-2 database (relies 2023) and corroborated with literature data [[31], [32]]. Semi-quantitative phase analysis (Figure 1) showed that the main portion of the alloy consisted of the Cu_7Te_4 ($Cu_{1.75}Te$) phase at 85.1 %, while the $Cu_{0.664}Te_{0.336}$ ($Cu_{1.91}Te$) phase was present at 14.9 %. According to the literature, the primary phase corresponds to Cu_2Te.

Tellurium-Containing Middling.

Industrial copper telluride obtained at Kazakhmys Smelting LLP (Republic of Kazakhstan) was used as a tellurium-containing middling.

Copper telluride is an agglomerated material of malachite color, odorless, with a moisture content of 3%. The material composition is presented in Table 1. X-ray phase analysis (Figure 2) revealed a significant fraction of amorphous halo due to scattering from disordered phases. The crystalline part is represented by phases of non-stoichiometric copper telluride (Cu_7Te_4 – PDF 00-057-0196, $Cu_{1.79}Te$ – PDF 01-082-9896) and copper hydroxysulfates ($Cu_5(SO_3)_2(OH)_6{\cdot}5H_2O$ – PDF 00-041-0007, $Cu_3(SO_4)(OH)_4$ – PDF 00-007-0407, $Cu_4(SO_4)(OH)_6{\cdot}H_2O$ – PDF 01-083-1410, $Cu_6SO_4(OH)_6$ – PDF 00-043-1458). The presence of the latter can be explained by insufficient washing of copper telluride from the $CuSO_4$ solution after the operation of tellurium cementation on copper from tellurous acid.

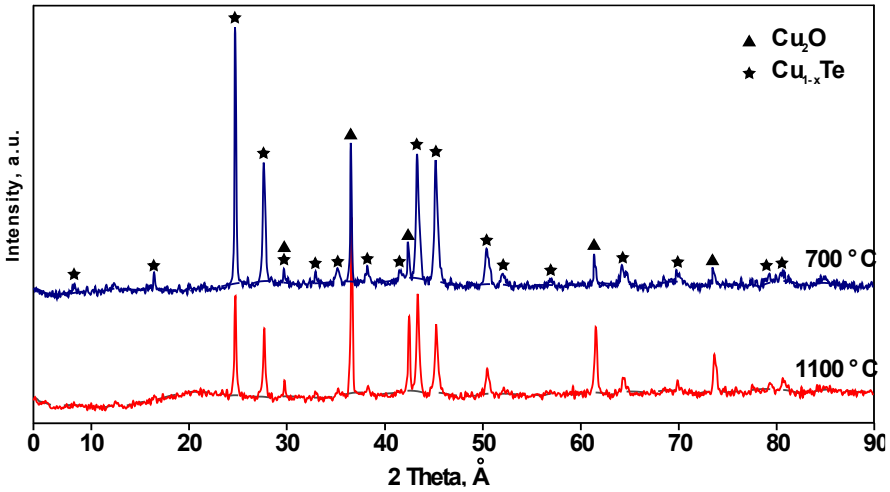

Figure 1 - Diffractogram of synthetic copper telluride

Table 1. Composition of the tellurium-containing middling

Elemental composition, wt. %									
O	Al	Si	S	Cl	Cu	As	Te	Se	Pb
31.38	0.02	0.05	2.31	0.20	42.45	0.12	23.42	0.03	0.02

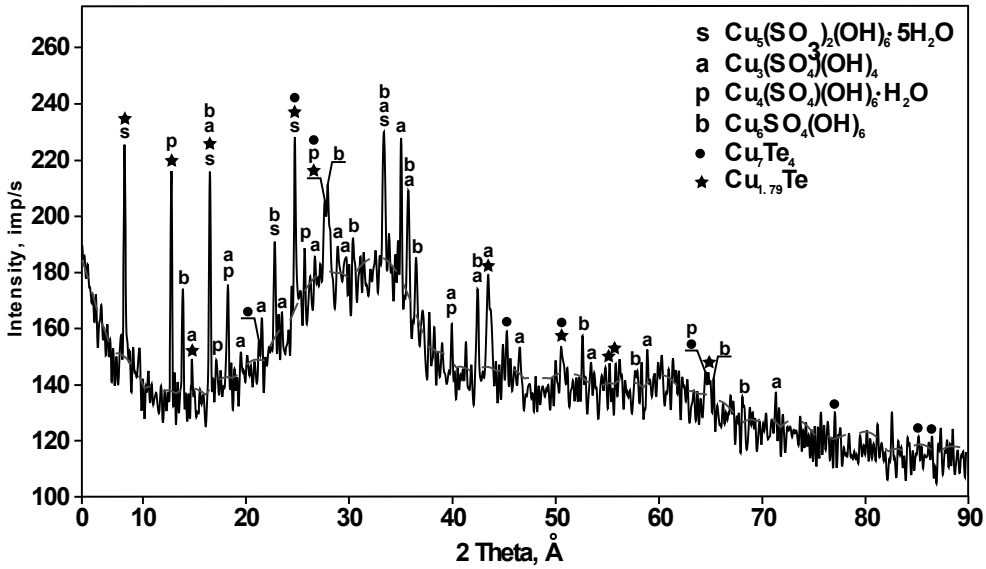

Figure 2 – X-ray diffraction pattern of the tellurium–containing middling from Kazakhmys Corporation L

Methodology

A laboratory setup with a horizontally arranged reactor was used for the study (Figure 3).

The setup consists of a Nabertherm electric furnace with a B–180 controller, a 2HB3-5DM UHL4 vacuum pump, and a quartz reaction vessel, in which a boat containing the sample of predetermined mass was placed. Additionally, a detachable porcelain condenser was mounted over the boat to collect the condensed material. A chromel–alumel thermocouple (thermoelectric transducer DTPK021-1.2/0.7) with a single-channel microprocessor-based measuring controller TRM1 was used to control the temperature in the reaction zone. The pressure was measured with a DCP 3000 vacuum gauge (Vacuubrand, Germany) with a VSP 3000 sensor (accuracy ±10 Pa). The sample was weighed before and after the experiment with a PA214C analytical balance (Ohaus-Pioneer) with an accuracy of ±0.1 mg.

Argon was used as the carrier gas saturated with water vapor in a flask filled with distilled water. The flask was placed in a thermostat. Argon flow was

controlled using an RS-3A rotameter. Two desiccators were installed, represented by Tishchenko bottles filled with alumogel, to dry the exhaust gases.

The experimental procedure was as follows. The copper telluride sample was loaded into an alumina boat. The boat was then placed into the detachable (longitudinal) alumina condenser. The condenser was in turn placed into the quartz reactor. The prepared reactor was placed in the preheated furnace so that the sample was located in the isothermal zone. The reactor was connected to the vacuum system and the water vapor supply system. The vacuum pump was turned on, and the argon flow was set. The water vapor flow into the reaction chamber was regulated by adjusting the thermostat temperature. The water flow rate was determined by weighing the flask before and after the experiment. The start of the experiment was defined as the moment when the target pressure and temperature values, recorded by the monitoring thermocouple, were reached. The gas supply and evacuation systems were turned off at the end of the experiment. The reactor was removed from the furnace and allowed to cool in air. The obtained calcination products were weighed and analyzed.

Characterization. The study of the material composition was performed by X–ray fluorescence analysis using a wavelength-dispersive spectrometer Axios 1kW (PANalytical, Netherlands) with an accuracy of ±5 %.

For phase composition identification, X–ray diffraction analysis was performed using a D8 Advance diffractometer (Bruker, Germany), Cu-Kα radiation. The phase composition was determined using the ASTM database (reference database of diffraction data PDF-2 rel. 2023 of the International Centre for Diffraction Data (ICDD, USA)).

Results and discussion

Experiments with the synthetic material were performed under the following conditions: temperature 700–1100 °C, pressure 1.3 kPa, duration 10–60 min, humidity 0.5–1 %. The degree and rate of oxidation were determined based on CuO, where O = 20.2 %. The results are presented in Table 2.

As can be seen, exposure of synthetic copper telluride to water vapor significantly increases the degree of tellurium evaporation (up to 58%) compared to the process conducted in an inert atmosphere (0.5–2 %) [33]. A positive effect on tellurium extraction is observed with increasing duration and temperature of the process, while increasing the argon flow rate from 5.21 to 32.7 L/h has little effect on the degree of tellurium evaporation from synthetic copper telluride. At the same time, the degree of oxidation of copper telluride itself shows an almost linear dependence on the duration and temperature of the process. It should be noted that decreasing the water vapor flow rate promotes longer interaction between copper telluride and oxygen.

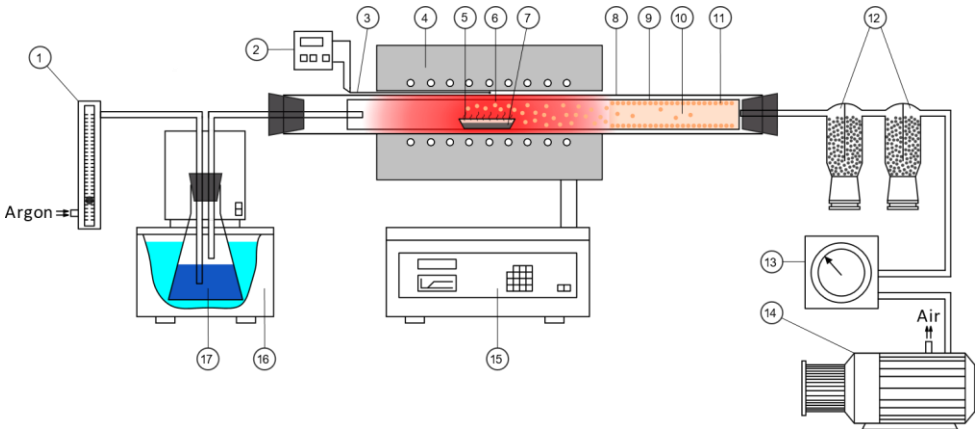

1 – rotameter; 2 – temperature controller in the reaction zone; 3 – control thermocouple; 4 – electric furnace; 5 – boat; 6 – isothermal zone; 7 – sample; 8 – reactor; 9 – detachable condenser; 10 – condensation zone; 11 – condensate; 12 – desiccators; 13 – aneroid barometer; 14 – vacuum pump; 15 – furnace controller; 16 – thermostat; 17 – flask with distilled water

Figure 3 - Installation diagram of the pyrolysis setup in a water vapor atmosphere

Table 2 – Dependence of tellurium extraction from synthetic copper telluride and the degree of copper telluride oxidation on key process parameters

Experiment No.	Temperature, °C	Ar Flow Rate, L/h	Time, min.	Te Content in Residue		Te Evaporation Degree, %	Cu_2Te Oxidation Degree, %
				%	g		
1	700	13.0	60	40.76	1.2746	11.4857	32.8218
2	700	13.0	30	41.26	1.3071	9.2280	26.6337
3	700	13.0	10	43.99	1.3600	5.5529	20.1485
4	900	13.0	60	40.60	1.1798	18.0669	35.0495
5	900	13.0	30	41.29	1.2434	13.6552	28.1040
6	900	13.0	10	43.23	1.3103	9.0069	22.6436
7	1100	13.0	60	28.34	0.7004	51.3615	38.7178
8	1100	13.0	45	30.42	0.8223	42.8991	34.5050
9	1100	13.0	30	34.58	0.9548	33.6977	31.6337
10	1100	13.0	10	41.63	1.2260	14.8638	24.2475
11	1100	32.7	60	30.93	0.8077	43.9115	35.00
12	1100	5.21	60	24.57	0.6073	57.8266	56.58

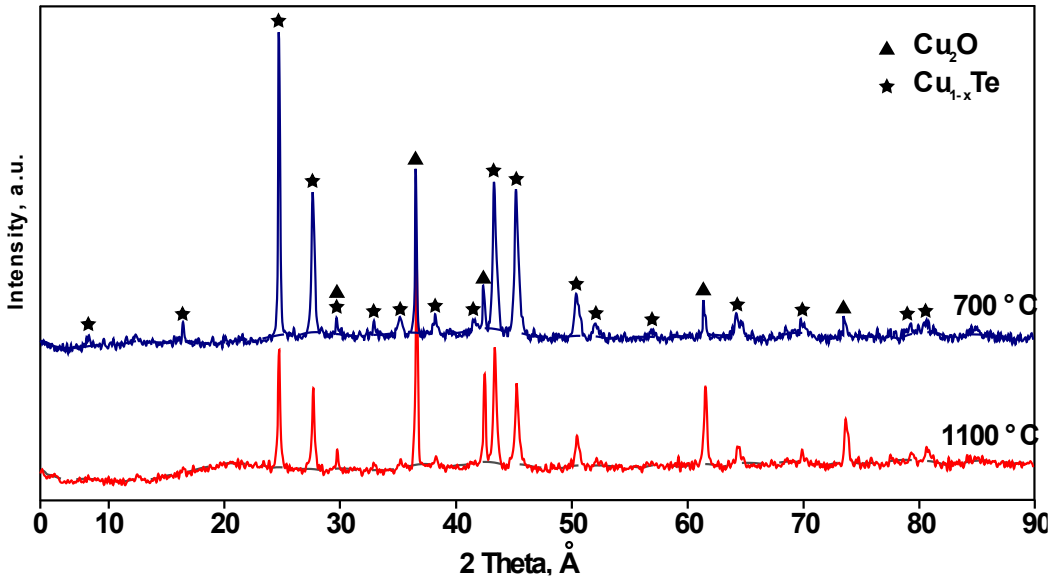

Figure 4 – Diffractograms of residues obtained at 700 °C and 1100 °C

Based on the experimental data, the dependence of the average rate of tellurium evaporation and copper telluride oxidation on temperature is described by equations (1) and (2), respectively:

$$\lg V = -2{,}103.3/T - 2.0838, \quad \text{where } E_{app.\,act.} = 40.27 \text{ kJ/mol} \qquad (1)$$

$$\lg V = -234.56/T - 3.5017, \quad \text{where } E_{app.\,act.} = 4.49 \text{ kJ/mol} \qquad (2)$$

Analysis of the phase composition of the obtained residues revealed, among the crystalline phases, the presence of copper oxide and unreacted copper telluride in varying ratios (from 18.9 to 58.0 wt. % Cu_2O). A typical X-ray diffraction pattern is shown in Figure 4. As seen in the figure, the diffractogram contains an amorphous halo, indicating the presence of compounds with a disordered structure in the residues. Based on literature data [[24], [34], [35]], it can be assumed that the amorphous phase consists of copper tellurates and/or tellurites formed during the interaction of oxidized copper and tellurium, as well as tellurium oxide. The phase composition of the residues is presented in Table 3.

Table 3 – Phase composition of residues

Experiment No.	Content of Crystalline Phases, wt. %		Degree of Amorphousness, %
	Cu_2O	$Cu_{2-x}Te$	
1	19.8	80.2	34.4
2	42.7	57.3	39.4
3	56.4	43.6	40.6
4	32.0	68.0	49.3
5	18.9	81.1	30.6
6	22.4	77.6	34.8
7	58.0	42.0	39.4
8	38.5	61.5	37.5
9	42.2	57.8	36.6
10	25.9	74.1	35.7
11	44.7	55.3	31.5
12	46.6	53.4	37.4

Table 4 – Dependence of tellurium extraction from industrial copper telluride on main process parameters

Temperature, °C	Ar Flow Rate, L/h	Time, min.	Te Content in Residue		Te Evaporation Degree, %
			%	g	
700	13.0	60	25.075	0.52	0
700	13.0	30	24.879	0.52	0
700	13.0	10	23.71	0.52	0
900	13.0	60	7.201	0.14	71.87
900	13.0	30	15.13	0.31	39.49
900	13.0	10	21.896	0.47	8.74
1100	13.0	60	6.228	0.09	83.21
1100	13.0	30	10.979	0.16	67.91
1100	13.0	10	22.031	0.39	22.65
1100	32.7	60	6.552	0.09	81.67
1100	5.21	60	2.211	0.03	94.89

Experiments with the tellurium–containing middling were performed under the following conditions: temperature 700–1100 °C, pressure 2 kPa, duration 10–60 min, humidity 0.5–1 %. The results are presented in Table 4 and Figure 5.

As follows from the obtained data, at 700 °C no tellurium evaporation from the industrial telluride occurs, which is associated with the formation of the most stable copper orthotellurate Cu_3TeO_6, stable up to 900 °C. Cu_3TeO_6 is the decomposition product of phase X, the identification of which is complicated due to the absence of the necessary compound card in the PDF-2 database (2023 edition). Considering the probable composition of phase X – $Cu_{0.37}Te_{0.26}O_{0.76}S_{0.084}$ – and the absence of formation of the aforementioned phases during oxidation of the synthetic telluride, the following can be assumed. Phase X is formed during the oxidation of the industrial telluride, due to the interaction of decomposition products of copper hydroxysulfates with oxidized copper and tellurium. This phase subsequently decomposes to Cu_3TeO_6. In contrast, during the oxidation of the synthetic material, the tellurium extraction process proceeds without the formation of the sulfur-containing phase X and, consequently, without formation of copper orthotellurate, following the oxidation mechanism described in [34]. At 900 °C, the formation of

orthotellurate is observed within the first 10 min and is completely decomposed over the next 20 min of the experiment. At 1100 °C, only crystalline copper oxides are identified in the obtained residues. The maximum tellurium extraction reaches 94.89 % under the following conditions: temperature – 1100 °C, pressure – 15 mm Hg, process duration – 60 min, carrier gas flow rate – 5.21 L/h, humidity – 0.7 % (with evaporated water temperature 27 °C).

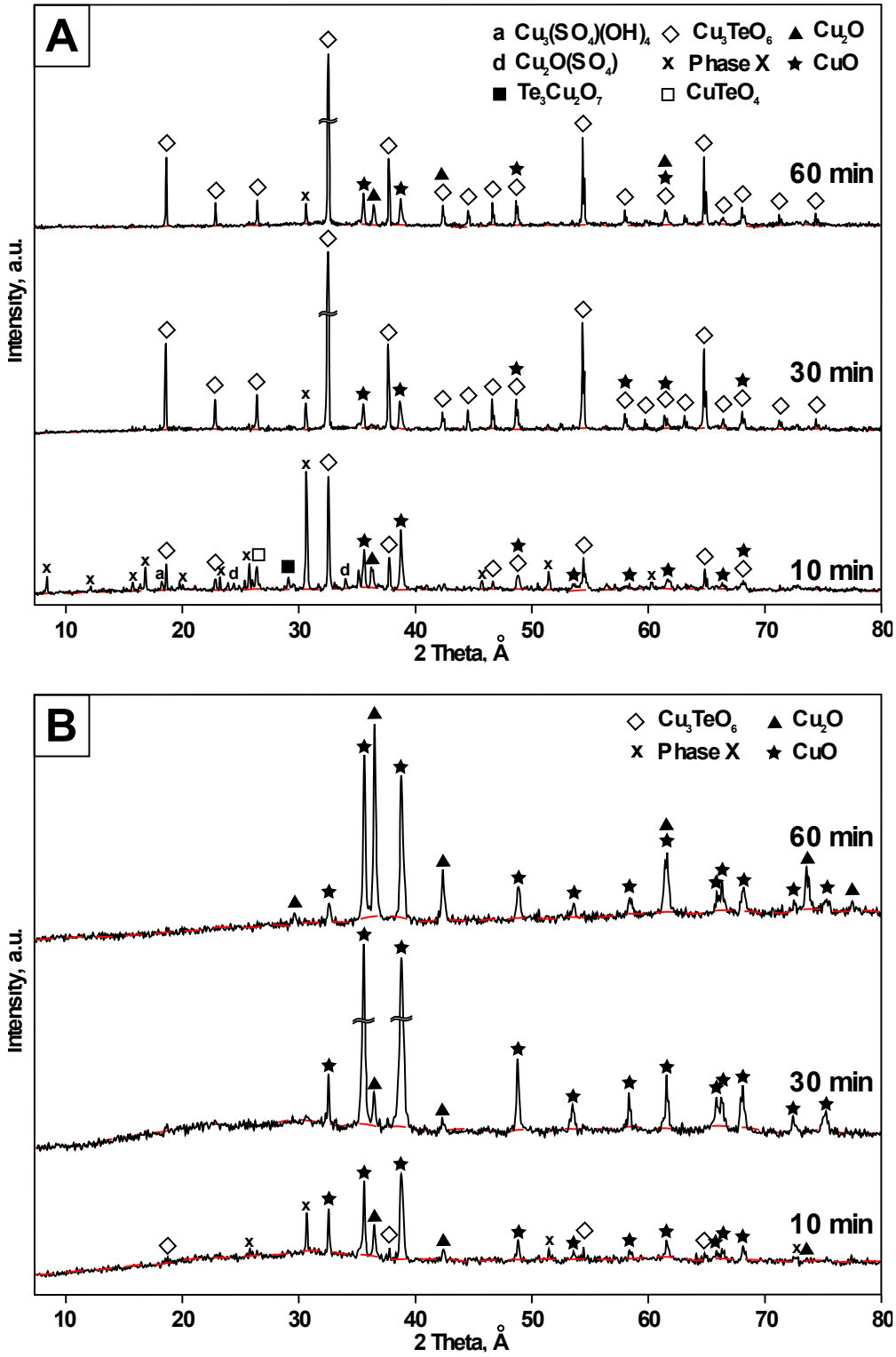

Figure 5 – Phase composition of residues obtained at 700 (a) and 900 (b) °C

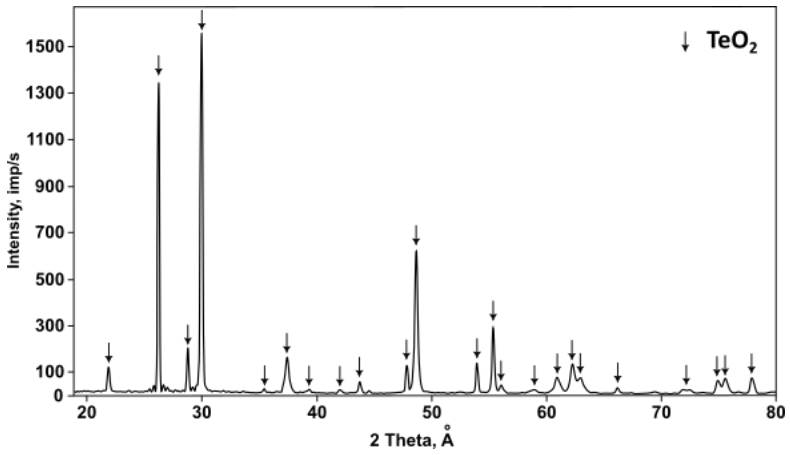

Figure 7 – XRD of the tellurium-containing condensate

Based on the experimental data, the dependence of the average tellurium evaporation rate on temperature is described by equation (3):

$$\lg V = -10{,}184/T + 4.5259, \quad \text{where } E_{app.\,act.} = 194.96 \text{ kJ/mol} \qquad (3)$$

During the roasting process, tellurium evaporated from the tellurium-containing by-product and deposited on the walls of the corundum condenser. The obtained condensate is a dense fine-crystalline white powder (Figure 6). Determination of the deposition conditions established that the vapor–gas phase condensed in the "cold" part of the reactor at temperatures below 600 °C. X-ray diffraction analysis (Figure 7) showed that the deposited condensate is represented by a monophasic tellurium oxide (TeO_2). Further processing of such a condensate to obtain elemental tellurium does not present technological difficulties. It can be carried out by carbothermal reduction in vacuum at moderate temperatures.

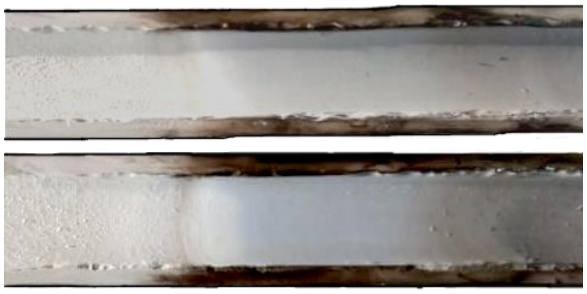

Figure 6 – Photo of the deposited condensate

Conclusion

Thus, the conducted set of studies demonstrated the feasibility of tellurium extraction from synthetic copper telluride and industrial tellurium-containing middling using a vacuum-thermal method conducted in a water vapour atmosphere. The thermal behavior of synthetic copper telluride follows the oxidation mechanism known from literature data. The behavior of the tellurium-containing middling is similar to that previously described for oxidative-distillation roasting and vacuum-thermal processing in an inert atmosphere. The achieved tellurium extraction values for synthetic copper telluride and tellurium-containing middlings were 57.83 % and 94.89 %, respectively, at a temperature of 1100 °C and pressure of 1.3–2 kPa. Incomplete oxidation of the synthetic material is apparently due to the insufficient amount of oxygen supplied by the water vapor flow. The obtained condensate is represented by the TeO_2 phase. The tellurium-containing condensate serves as a raw material for the production of elemental tellurium using well-known technologies, such as carbothermal reduction.

Funding: The research was funded by the Science Committee of the Ministry of Science and Higher Education of the Republic of Kazakhstan (Grant AP 19576910).

Conflict of interest. The corresponding author declare that there is no conflict of interest.

CRediT author statement: **A. Nitsenko**: Data Curation, Writing – original draft preparation, Conceptualization, Visualization, Investigation, Project administration; **X. Linnik, N. Burabayeva**: Data Curation, Writing –original draft preparation; Writing – Review & Editing; **V. Volodin, S. Trebukhov**: Methodology, Writing –original draft preparation, Writing – Review & Editing. All authors have read and agreed to the published version of the manuscript.

Cite this article as: Nitsenko AV, Linnik XA, Volodin VN, Burabayeva NM, Trebukhov SA. Pyrolysis of copper telluride in a water vapour atmosphere. Kompleksnoe Ispolzovanie Mineralnogo Syra = Complex Use of Mineral Resources. 2027; 340(1):106-116. https://doi.org/10.31643/2027/6445.11

Мыс теллуридінің сулы бу атмосферасындағы пиролизі

Ниценко А.В., Линник К.А., Володин В.Н., Бурабаева Н.М., Требухов С.А.

Металлургия және кен байыту институты АҚ, Сәтбаев университеті, Алматы, Қазақстан

Мақала келді: *19 қыркүйек 2025*
Сараптамадан өтті: *27 қыркүйек 2025*
Қабылданды: *3 қазан 2025*

ТҮЙІНДЕМЕ

Жұмыста су буының атмосферасында жүргізілетін вакуумды-термиялық әдісті қолдана отырып, синтетикалық мыс теллуридінен және құрамында теллур бар өнеркәсіптік ортадан теллур алу мүмкіндігін анықтау бойынша барлау зерттеулерінің нәтижелері берілген. Синтетикалық мыс теллуридінің жылулық әрекеті құрғақ ортада оттегінің қатысуымен тотығу механизміне сәйкес келетіні анықталды. Құрамында теллур бар аралық өнімде орын алатын фазалық өзгерістер де тотығу-дистилляциялық күйдіру және инертті атмосферадағы вакуум-термиялық үрдіс кезінде сипатталғандармен салыстыруға болады. 1100 °С температурада және 1,3-2 кПа қысымда мыс теллуридті және құрамында теллур бар өнеркәсіп өнімдерін алу дәрежесінің қол жеткізілген мәндері сәйкесінше 57,83 және 94,89 %-ды құрады. Алынған қалдықтар мыс оксидтерінің фазаларымен ұсынылған. Бұл жағдайда теллур материалдан буланып, конденсатордың қабырғаларында реактордың суық бөлігінде 400 °С-тан төмен температурада тұндырылады. Рентгендік фазалық талдауға сәйкес конденсат теллурмен оксид түрінде ұсынылған.

Түйін сөздер: теллур, мыс, вакуум, су буы, буландыру.

Авторлар туралы ақпарат:

Ниценко Алина Владимировна — *Техника ғылымдарының кандидаты, Металлургия және кен байыту институты АҚ, Вакуумдық процестер зертханасының меңгерушісі, Satbayev University, 050010, Шевченко көшесі 29/133, Алматы, Қазақстан. Email: alina.nitsenko@gmail.com; ORCID ID: https://orcid.org/0000-0001-6753-0936*

Линник Ксения Александровна — *Техника ғылымдарының магистрі, Металлургия және кен байыту институты АҚ, Вакуумдық процестер зертханасының кіші ғылыми қызметкері, Satbayev University, 050010, Шевченко көшесі 29/133, Алматы, Қазақстан. Email: x.linnik@satbayev.university, xenija_linnik@mail.ru; ORCID ID: https://orcid.org/0000-0002-0683-1409*

Володин Валерий Николаевич — *Техника ғылымдарының докторы, профессор, Металлургия және кен байыту институты АҚ, Вакуумдық процестер зертханасының бас ғылыми қызметкері, Satbayev University, 050010, Шевченко көшесі 29/133, Алматы, Қазақстан. Email: volodinv_n@mail.ru; ORCID ID: https://orcid.org/0000-0003-0116-1423*

Бурабаева Нурила Муратовна — *Техника ғылымдарының кандидаты, Сәтбаев университеті, Металлургия және кен байыту институтының аға ғылыми қызметкері, Алматы, Қазақстан, 050010, Шевченко көшесі 29/133, Алматы, Қазақстан. Email: nuri_eng@mail.ru; ORCID ID: https://orcid.org/0000-0003-2183-2239*

Требухов Сергей Анатольевич — *Техника ғылымдарының кандидаты, профессор, Металлургия және кен байыту институты АҚ, Вакуумдық процестер зертханасының жетекші ғылыми қызметкері, Satbayev University, 050010, Шевченко көшесі 29/133, Алматы, Қазақстан. Email: s.trebukhov@satbayev.university; ORCID ID: https://orcid.org/0000-0001-9708-0307*

Пиролиз теллурида меди в атмосфере водяного пара

Ниценко А.В., Линник К.А., Володин В.Н., Бурабаева Н.М., Требухов С.А.

АО Институт металлургии и обогащения, Satbayev University, Алматы, Казахстан

Поступила: *19 сентября 2025*
Рецензирование: *27 сентября 2025*
Принята в печать: *3 октября 2025*

АННОТАЦИЯ

В работе приведены результаты поисковых исследований по определению возможности извлечения теллура из синтетического теллурида меди и промышленного теллурсодержащего промпродукта вакуум-термическим способом, проводимым в атмосфере водяного пара. Определено, что термическое поведение синтетического теллурида меди подчиняется механизму окисления с участием кислорода в сухой среде. Фазовые преобразования, происходящие в теллурсодержащем промпродукте также сопоставимы с описанными при окислительно-дистилляционном обжиге и вакуум-термическом процессе в инертной атмосфере. Достигнутые значения степени извлечения теллурида меди и теллурсодержащего промпродуктов при температуре 1100 °С и давлении 1,3-2 кПа составляли 57,83 и 94,89 %, соответственно. Полученные остатки представлены фазами оксидов меди. При этом теллур испаряется из материала и осаждается на стенках конденсатора в холодной части реактора при температурах ниже 400 °С. По данным рентгенофазового анализа конденсат представлен теллуром в виде оксида.

Ключевые слова: теллур, медь, вакуум, водяной пар, испарение.

Ниценко Алина Владимировна	***Информация об авторах:*** *Кандидат технических наук, заведующая лабораторией вакуумных процессов АО Института металлургии и обогащения, Satbayev University, 050010, ул. Шевченко, 29/133, Алматы, Казахстан. Email: alina.nitsenko@gmail.com; ORCID ID: https://orcid.org/0000-0001-6753-0936*
Линник Ксения Александровна	*Магистр технических наук, младший научный сотрудник лаборатории вакуумных процессов АО Института металлургии и обогащения, 050010, ул. Шевченко, 29/133, Алматы, Казахстан. Email: x.linnik@satbayev.university, xenija_linnik@mail.ru; ORCID ID: https://orcid.org/0000-0002-0683-1409*
Володин Валерий Николаевич	*Доктор технических наук, профессор, главный научный сотрудник лаборатории вакуумных процессов АО Института металлургии и обогащения, Satbayev University, 050010, ул. Шевченко, 29/133, Алматы, Казахстан. Email: volodinv_n@mail.ru; ORCID ID: https://orcid.org/0000-0003-0116-1423*
Бурабаева Нурила Муратовна	*Кандидат технических наук, старший научный сотрудник лаборатории вакуумных процессов АО Института металлургии и обогащения, Satbayev University, 050010, ул. Шевченко, 29/133, Алматы, Казахстан. Email: nuri_eng@mail.ru; ORCID ID: https://orcid.org/0000-0003-2183-2239*
Требухов Сергей Анатольевич	*Кандидат технических наук, профессор, ведущий научный сотрудник лаборатории вакуумных процессов АО Институт металлургии и обогащения, Satbayev University, 050010, ул. Шевченко, 29/133, Алматы, Казахстан. Email: s.trebukhov@satbayev.university; ORCID ID: https://orcid.org/0000-0001-9708-0307*

References

[1] Wang X, Forssberg KSE. The Chemistry of Cyanide-Metal Complexes in Relation to Hydrometallurgical Processes of Precious Metals. Mineral Processing and Extractive Metallurgy Review. 1990; 6(1–4):81–125. https://doi.org/10.1080/08827509008952658

[2] Haque KE. Gold Leaching from Refractory Ores—Literature Survey. Mineral Processing and Extractive Metallurgy Review. 1987; 2(3):235–253. https://doi.org/10.1080/08827508708952607

[3] Chibesa M, Nakhaei F, Alagha L. Surface Chemistry and Activation of Pyrite in Flotation: Enhancing Critical Minerals Recovery. Mineral Processing and Extractive Metallurgy Review. 2025; 1–23. https://doi.org/10.1080/08827508.2025.2518970

[4] Koizhanova A, Kenzhaliyev B, Magomedov D, Erdenova M, Bakrayeva A, Abdyldaev N. Hydrometallurgical studies on the leaching of copper from man-made mineral formations. Kompleksnoe Ispolzovanie Mineralnogo Syra = Complex Use of Mineral Resources. 2024; 330(3):32–42. https://doi.org/10.31643/2024/6445.26

[5] Chen A, Peng Z, Hwang J-Y, Ma Y, Liu X, Chen X. Recovery of Silver and Gold from Copper Anode Slimes. JOM. 2015; 2:493–502. https://doi.org/10.1007/s11837-014-1114-9

[6] Mahmoudi A, Shakibania S, Mokmeli M, Rashchi F. Tellurium, from copper anode slime to high purity product: A review paper. Metallurgical and Materials Transactions B. 2020; 51:2555–2575. https://doi.org/10.1007/s11663-020-01974-x

[7] Liu G, Wu Yu, Tang A, Pan D, Li B. Recovery of scattered and precious metals from copper anode slime by hydrometallurgy: A review. Hydrometallurgy. 2020; 197:105460. https://doi.org/10.1016/j.hydromet.2020.105460

[8] Mastyugin SA, Naboichenko SS. Processing of copper-electrolyte slimes: Evolution of technology. Russian Journal of Non-Ferrous Metals. 2012; 53:367–374. https://doi.org/10.3103/S1067821212050070

[9] Xing WD, Lee MS. Leaching of gold and silver from anode slime with a mixture of hydrochloric acid and oxidizing agents. Geosystem Engineering. 2017; 20(4):216–223. https://doi.org/10.1080/12269328.2017.1278728

[10] Xiao L, Wang YL, Yu Y, Fu GY, Han PW, Sun ZHI, Ye SF. An environmentally friendly process to selectively recover silver from copper anode slime. Journal of Cleaner Production. 2018; 187:708–716. https://doi.org/10.1016/j.jclepro.2018.03.203

[11] Ding Y, Zhang S, Liu B, Li B. Integrated process for recycling copper anode slime from electronic waste smelting. Journal of Cleaner Production. 2017; 165:48–56. https://doi.org/10.1016/j.jclepro.2017.07.094

[12] Kenzhaliyev BK, Trebukhov SA, Volodin VN, Trebukhov AA, Tuleutay FKh. Selenium extraction out of metallurgical production middlings. Kompleksnoe Ispolzovanie Mineralnogo Syra = Complex Use of Mineral Resources. 2018; 307(4):56–64. https://doi.org/10.31643/2018/6445.30

[13] Kenzhaliyev BK, Trebukhov SA, Nitsenko AV, Burabayeva NM, Trebukhov AA. Determination of technological parameters of selenium recovery from metallurgical production middlings in a vacuum distillation unit. International Journal of Mechanical and Production Engineering Research and Development. 2019; 9(6):87–98.

[14] Shibasaki T, Abe K, Takeuchi H. Recovery of tellurium from decopperizing leach solution of copper refinery slimes by a fixed bed reactor. Hydrometallurgy. 1992; 29:399–412. https://doi.org/10.1016/0304-386X(92)90024-T

[15] Nitsenko AV, Burabaeva NM, Tuleytay FK, Seisembaev RS, Linnik XA, Azlan MN. Study of physical and chemical properties of tellurium-containing middlings. Kompleksnoe Ispolzovanie Mineralnogo Syra = Complex Use of Mineral Resources. 2020; 315(4):49–56. https://doi.org/10.31643/2020/6445.36

[16] Xu L, Xiong Y, Song Y, Zhang G, Zhang F, Yang Y, Hua Z, Tian Y, You J, Zhao Z. Recycling of copper telluride from copper anode slime processing: Toward efficient recovery of tellurium and copper. Hydrometallurgy. 2020; 196:105436. https://doi.org/10.1016/j.hydromet.2020.105436

[17] Nitsenko AV, Linnik KA, Tuleutay FH, Burabayeva NM, Seisembayev RC. Fiziko-himicheskaya harakteristika tellursoderzhashchego promprodukta TOO «Kazahmys Smelting» [Physical and chemical characterization of tellurium-containing industrial product of Kazakhmys Smelting LLP]. Teoriya i tekhnologiya metallurgicheskogo proizvodstva = Theory and technology of metallurgical production. 2021; 3:10–16

[18] Zhang H, Li Z, Yang Y, Zha G, Xu B, Liu D, Yang B, Jiang W. Advances in tellurium recovery and purification: A comprehensive review of separation methods and emerging technologies. Resources, Conservation and Recycling. 2025; 215:108160. https://doi.org/10.1016/j.resconrec.2025.108160

[19] Xu L, Xiong Y, Zhang G, Zhang F, Yang Y, Hua Z, Tian Y, You J, Zhao Z. An environmental-friendly process for recovery of tellurium and copper from copper telluride. Journal of Cleaner Production. 2020; 272:122723. https://doi.org/10.1016/j.jclepro.2020.122723

[20] Weissburd SE. Fiziko-himicheskie svojstva i osobennosti stroeniya sul'fidnyh rasplavov [Physical and chemical properties and structure peculiarities of sulfide melts]. Metallurgy: Moscow, Russia, 1996. (in Russ.).

[21] Dutchak YaI, Korenchuk NM, Korenchuk SV. Issledovanie davleniya para i termodinamicheskiy analiz splavov sistemy Cu_2S–Cu_2Te [Study of vapor pressure and thermodynamic analysis of alloys of the system Cu_2S–Cu_2Te]. Izvestiya AN SSSR. Neorganicheskie materialy = Proceedings of the Academy of Sciences of the USSR. Inorg. Materials. 1975; 11(2):201–203. (in Russ.).

[22] Li Zh, Deng J, Liu D, Jiang W, Zha G, Huang D, Deng P, Li B. Waste-free separation and recovery of copper telluride slag by directional sulfidation-vacuum distillation. Journal of Cleaner Production. 2022; 335:130356. https://doi.org/10.1016/j.jclepro.2022.130356

[23] Nitsenko AV, Volodin VN, Linnik XA, Tuleutay FKh, Burabaeva NM. Distillation recovery of tellurium from copper telluride in oxide form. Russian Journal of Non-Ferrous Metals. 2022; 63(3):284–291. https://doi.org/10.3103/S1067821222030105

[24] Nitsenko AV, Linnik XA, Volodin VN, Trebukhov SA, Tuleutay F. Behavior of Technical Copper Telluride During Vacuum Thermal Treatment. Mineral Processing and Extractive Metallurgy Review. 2025; 1–16. https://doi.org/10.1080/08827508.2025.2555366

[25] Plyushchev VE, Stepina SB, Fedorov PI. Khimiya i tekhnologiya redkikh i rasseyannykh elementov [Chemistry and technology of rare and scattered elements]: textbook for universities. Edited by K.A. Bolshakov. Moscow: graduate School. 1976; 3:320. (in Russ.).

[26] Chizhikov DM, Shchastlivyi VP. Tellur i telluridy [Tellurium and Tellurides]. Collet's Publishers Ltd.: London. 1970. (in Russ.).

[27] Zhu X, Wang Zh, Su X, Vilarinho PM. New Cu_3TeO_6 ceramics: phase formation and dielectric properties. ACS Applied Materials and Interfaces. 2014; 6:11326–11332. https://doi.org/10.1021/am501742z

[28] Konings RJM, Cordfunke EHP, Smit-Groen V. The vapour pressures of hydroxides II. $TeO(OH)_2$ The Journal of Chemical Thermodynamics. 1990; 22(8):751-756. https://doi.org/10.1016/0021-9614(90)90066-Y

[29] Malinauskas AP, Gooch Jr JW, Redman JD. The Interaction of Tellurium Dioxide and Water Vapor. Nuclear Applications and Technology. 1970; 8(1):52–57. https://doi.org/10.13182/NT70-A28633

[30] A Chemical Perspective on the Tellurium Source Term in the Context of Severe Nuclear Power Plant Accidents, Department of Chemistry and Chemical Engineering, Chalmers University Of Technology, Gothenburg, Sweden. 2020. https://research.chalmers.se/publication/518849/file/518849_Fulltext.pdf (accessed on 12 May 2025)

[31] Qiu Y, Ye J, Liu Y, Yang X. Facile rapid synthesis of a nanocrystalline Cu_2Te multi-phase transition material and its thermoelectric performance. RSC advances. 2017; 7:22558–22566. https://doi.org/10.1039/C7RA02145C

[32] He Y, Zhang T, Shi X, Wei S-H, Chen L. High thermoelectric performance in copper telluride. NPG Asia materials. 2015; 7:1-7. https://doi.org/10.1038/am.2015.91

[33] Nitsenko AV, Linnik XA, Volodin VN, Tuleutay FKh, Bakhytuly N. Pyrolysis of synthetic copper telluride in an inert atmosphere. Kompleksnoe Ispolzovanie Mineralnogo Syra = Complex Use of Mineral Resources. 2025; 335(4):67-77. https://doi.org/10.31643/2025/6445.41

[34] Kukleva TV, Fedorova TB, Vishnyakov AV, Kovtunenko PV. Features of low-temperature oxidation of copper(i) telluride. Inorganic Materials. 1988; 24:1469–1471.

[35] Nitsenko A, Linnik X, Volodin V, Tuleutay F, Burabaeva N, Trebukhov S, Ruzakhunova G. Phase Transformations and Tellurium Recovery from Technical Copper Telluride by Oxidative-Distillate Roasting at 0.67 kPa. Metals. 2022; 12:1774. https://doi.org/10.3390/met12101774

Crossref
DOI: 10.31643/2027/6445.12
Metallurgy

Effect of Complex Alloying on the Phase Composition and Thermal Characteristics of Al–Fe–Si Aluminum Alloys

Andreyachshenko V.A.

Abylkas Saginov Karaganda Technical University, Karaganda, Kazakhstan

Corresponding author email: v.andreyachshenko@ktu.edu.kz

Received: *September 8, 2025*
Peer-reviewed: *September 26, 2025*
Accepted: *October 3, 2025*

ABSTRACT

This study presents a comprehensive analysis of phase formation in Al–Fe–Si aluminum alloys with the addition of ten industrially significant alloying elements (Mg, Cu, Ni, Mn, Cr, Zn, Ti, Zr, V, Be), performed using thermodynamic modeling via the Thermo-Calc software package. Phase formation was investigated and compared in a commercial alloy (Al98–Fe1–Si1) and an intermetallic alloy (Al60–Fe33–Si7) under both individual and synergistic alloying conditions. The thermal characteristics (liquidus, solidus, and α- and β-transformations) and phase constituents were analyzed across a broad temperature range (0–1200 °C). It was found that the alloying elements exert diverse effects on phase stability and alloy structure, with intermetallic systems exhibiting greater thermal stability. Particular attention was given to the formation of the matrix phase and the influence of synergistic alloying on phase equilibria and the potential emergence of new stable compounds. The results provide a basis for targeted alloy design, including the use of secondary aluminum, to develop materials with tailored properties for transportation and mechanical engineering applications.

Keywords: Al-Fe-Si, ThermoCalc software, intermetallic phases, phase equilibrium, synergistic alloying.

Andreyachshenko Violetta Alexandrovna

Information about author:
PhD, associate professor, Head of the Testing Laboratory Engineering Profile Comprehensive Development of Mineral Resources, Abylkas Saginov Karaganda Technical University, N. Nazarbayev Ave., 56, Karaganda, Kazakhstan. E-mail: v.andreyachshenko@ktu.edu.kz; ORCID ID: https://orcid.org/0000-0001-6933-8163

Introduction

The modern development of the metal products industry requires the creation of new materials with enhanced performance characteristics, cost-effective production, and compatibility with advanced manufacturing technologies. In the context of increasing demand for lightweight, durable, and wear-resistant materials—particularly in the aerospace and automotive sectors—aluminum alloys remain among the most promising candidates due to their low density, excellent corrosion resistance, high electrical conductivity, and adequate mechanical properties [[1], [2], [3], [4], [5]].

Significant improvements in mechanical and operational properties are often achieved through additional processing techniques aimed at critical grain refinement [[6], [7], [8], [9], [10]]. However, to meet the desired performance levels, costly alloying additions—primarily rare-earth elements—are still commonly used, which significantly increases the overall production cost [[11], [12], [13], [14], [15]].

In this regard, the exploration of alternative alloying strategies aimed at improving the performance of aluminum alloys without relying on scarce and expensive elements is of particular relevance. A promising approach involves studying the ternary Al–Fe–Si system, incorporating alloying elements frequently present as impurities in aluminum alloys, which could potentially be used for the targeted modification of phase composition [[16], [17], [18], [19], [20]].

Special attention is drawn to the potential formation of the intermetallic Al_8Fe_2Si phase, which possesses a highly symmetric crystal structure. This opens new pathways for developing intermetallic aluminum-based composite materials with a unique combination of strength and ductility [[21], [22], [23], [24], [25]].

Despite growing global scientific interest in Al–Fe–Si alloys [[26], [27], [28], [29], [30]], data on the influence of impurity and secondary alloying elements on their structure and properties remain limited. Particularly important is the comparative investigation of phase formation in conventionally

alloyed commercial aluminum grades and intermetallic-based materials.

This study provides a detailed investigation into phase formation mechanisms under various alloying conditions and analyzes the features of phase evolution depending on composition and thermal treatment regimes.

Accordingly, the present research is aimed at establishing a scientific basis for the alloying of aluminum intermetallic composites, enabling the design of materials with tailored properties without the use of costly alloying components. The results obtained are of interest for the development of high-reliability products intended for operation under harsh conditions and may serve as a foundation for designing new structural materials for transport and mechanical engineering applications.

Objective of the study: To compare phase formation and identify its key features in a commercial aluminum alloy and an intermetallic Al–Fe–Si alloy through thermodynamic modeling of the phase composition, using the most commonly encountered alloying elements in aluminum systems.

Experimental part

Thermodynamic modeling was carried out using the Thermo-Calc software package (version 2024a) with the TCS Al-based Alloys (TCAL8.2) database. Main modeling stages:

1. Definition of alloy compositions. At this stage, two types of alloys were studied: the commercial alloy Al_{98}–Fe_1–Si_1, alloyed both stepwise and synergistically with 10 impurity elements (Mg, Cu, Ni, Mn, Cr, Zn, Ti, Zr, V, Be, Sc). The concentrations of alloying elements varied from 0.003 to 5.4 wt.%, introduced at the expense of aluminum content. In the case of synergistic alloying, the aluminum concentration was 81.77 wt.%. For comparison, alloying of the intermetallic alloy Al60–Fe33–Si7 with the same elements as in the commercial alloy was also studied. As a result of synergistic alloying, the aluminum concentration decreased to 43.77 wt.% (Table 1).

2. System creation in Thermo-Calc. The modeling process was implemented using the Graphical Mode (TCG) module. A system project was created for the multiphase Al–Fe–Si–X system, where the alloying elements and their mass fractions were added. For individual alloying, one alloying element was added to the base system at a time; for synergistic alloying, all elements were added simultaneously. For comparison, diagrams for the base system without additives were also constructed.

Table 1 - Alloying conditions

Individual alloying, wt%	Synergistic alloying, wt%
Cu4.2	Cu4.2 Mg4.2 Mn0.9 Cr0.21 Zn5.4 Ni0.84 Ti0.12 V0.09 Zr0.27 Be0.003
Mg4.2	
Mn0.9	
Cr0.21	
Zn5.4	
Ni0.84	
Ti0.12	
V0.09	
Zr0.27	
Be0.003	

3. Setting modeling parameters. All calculations were performed under the following conditions:

- Calculation type: Equilibrium Calculation;
- Temperature range: from 1200 °C to 0 °C;
- Temperature step: 50 °C;
- Pressure: 1 atm (standard).

4. Calculation and construction of polythermal sections. After running Thermo-Calc, the equilibrium phase composition at each temperature step was calculated. Polythermal sections were built using the Plot Renderer module. The X-axis represents the volume fraction of the phase, and the Y-axis represents temperature (°C). The graph displays curves of the forming phases with a legend.

5. Interpretation of the obtained diagrams. Phases were identified, and phase transformation temperatures were evaluated. At temperatures above the liquidus, the system is completely liquid. Cooling leads to the sequential precipitation of phases: for the commercial alloy, FCC_A1 is the first to form, followed by θ and others; for the intermetallic alloy, the primary phase is θ or Al_7Cu_4Ni, followed by AlFeSi, Laves, and others.

The final phase composition at room temperature determines the performance properties.

6. Hardness testing of the alloyed intermetallic alloys was carried out using a Wilson VH1150 Vickers hardness tester. The chemical composition of the investigated alloys was determined using an Olympus Vanta Element S X-ray fluorescence (XRF) analyzer.

Results and Discussion

The obtained results on the influence of alloying/impurity elements on the phase composition and, consequently, on the resulting

properties indicate that the characteristics of phase transformations are highly sensitive to the aluminum content in the alloy.

When transitioning to an intermetallic state, the activity of individual elements and the thermodynamic conditions for phase formation change. Not all elements present in industrial alloys are capable of dissolving in the base phase constituents. The introduced elements form compounds with one (or several) of the base alloy components, thereby shifting the phase equilibrium and promoting the binding or, conversely, the precipitation of other elements.

The effect of individual alloying on the phase transformation temperatures of aluminum alloys is presented in Table 2, which shows the calculated temperatures of the liquidus ($\boldsymbol{T_L}$), solidus ($\boldsymbol{T_S}$), and the start ($\boldsymbol{T_{st}}$) and end ($\boldsymbol{T_{end}}$) of α- and β-phase transformations for both commercial (com) aluminum alloys and intermetallic (int) systems modified by the addition of various alloying elements (Cu, Mg, Mn, Cr, Ni, Zn, Ti, V, Zr, Be). The temperatures are given in degrees Celsius (°C).

Analysis of the data makes it possible to trace both the general effect of alloying on the thermodynamic behavior of the system and the specific influence of individual elements.

In commercial alloys (T_L^{com}), a predominant decrease in the liquidus temperature is observed compared to the base alloy without alloying (650 °C). The most significant reductions are noted with the addition of Mg (630 °C), Zn (641 °C), and Mn (630 °C), indicating their strong ability to lower the melting onset temperature. Conversely, Be increases T_L^{com} to 740 °C—the highest value among all elements—which may be attributed to the formation of high-melting-point compounds between Be and aluminum.

T_S^{com} also decreases with the addition of most elements. The most pronounced decrease in solidus temperature is observed with Mg (546 °C) and Zn (596 °C), indicating a widening of the solidification interval and a potential deterioration in casting properties. Higher T_S^{com} values are found with Cr (626 °C) and Ni (615 °C).

For intermetallic alloys (T_L^{int}), the liquidus temperature remains virtually unchanged (1070 °C) with most alloying elements, except for Zn, where it increases to 1100 °C, suggesting the formation of stable intermetallic compounds with higher melting points. In intermetallic systems (T_L^{int}), the range of values is broader – from 399 °C with Zn to 680 °C with Cr. Thus, intermetallic systems alloyed with Cr exhibit the most thermally stable solid state, while Zn drastically reduces the end temperature of solidification, which may indicate the presence of low-temperature eutectics.

Given the particular interest in the α-phase in the intermetallic alloy, the effect of alloying on its formation and transformation into the low-temperature β-phase was also analyzed.

The onset temperature of α-phase formation in commercial alloys ($T_{st}^{com}\boldsymbol{\alpha}$) varies within the range of 600–629 °C. A significant reduction is observed with Mg (600 °C), reflecting its impact on lowering the thermal stability of the α-phase. The addition of Mn, Cr, and Ni suppresses α-phase formation in this temperature region. $T_{st}^{int}\boldsymbol{\alpha}$ in intermetallic alloys demonstrates higher values – from 650 °C (Zn) to 769 °C (baseline and some alloying compositions). This indicates the thermal stability of the α-phase in the intermetallic matrix and the weak influence of most alloying elements, except Zn and Mg, which noticeably lower the α-transformation onset temperature.

The α-phase transformation end temperature ($T_{end}^{com}\boldsymbol{\alpha}$) ranges from 572 °C (with Mg) to 629 °C (without alloying), indicating a narrowing of the α-phase stability interval with alloying. Meanwhile, in intermetallic alloys, the lower boundary of α-phase stability remains almost unchanged for all additions – around 446–450 °C, except for Zn (462 °C). This may suggest the thermodynamic stability of the α-phase in intermetallic systems regardless of composition.

The onset temperature of β-phase transformation in commercial alloys ($T_{st}^{com}\boldsymbol{\beta}$) shows a broader variation – from 550 °C (Ni) to 612 °C (unalloyed), reflecting the differing thermodynamic activity of alloying elements, with Ni significantly reducing β-phase stability. $T_{st}^{int}\boldsymbol{\beta}$ remains nearly identical across all systems, at 446–462 °C, indicating low sensitivity of this phase to the type of alloying in intermetallic compositions.

Thus, individual alloying reveals that the addition of alloying elements exerts diverse effects on phase transformation temperatures. Mg and Zn exhibit the strongest lowering effect on liquidus and solidus temperatures, while Be and Cr contribute to their increase. Intermetallic systems overall demonstrate greater phase stability compared to commercial alloys, particularly with respect to the α- and β-phases. Zn emerges as the most sensitive element affecting the thermal characteristics of both the liquidus/solidus and the phase transformations, especially in intermetallic compounds. Certain elements (e.g., Ni and Mg) can significantly narrow the phase stability temperature intervals, which must be taken into account in the

design of heat-resistant and castable aluminum alloys.

Multicomponent system modeling was subsequently performed to assess the mutual influence of the considered elements. Although the simultaneous presence of all alloying elements in an alloy is unlikely, the investigation of such a system is crucial for a deeper understanding of the synergistic alloying effect, particularly in identifying the potential formation of new phases resulting from interactions among impurity/alloying elements within an aluminum or intermetallic matrix.

At the same time, similar individual alloying effects in commercial and intermetallic alloys result in different base phases under synergistic alloying conditions. In the commercial alloy, the matrix is primarily a solid solution of aluminum, whereas in the intermetallic alloy, the θ-phase serves as the main matrix.

Analysis of polythermal sections enables conclusions to be drawn about the nature of phase transformations, crystallization features, phase composition and stability from the liquid state down to 0 °C, as well as predictions of the service properties of the resulting materials.

Figure 1 presents the polythermal sections for two alloys with different base element compositions: the commercial alloy Al_{98}–Fe_1–Si_1 and the intermetallic alloy Al_{60}–Fe_{33}–Si_7, each synergistically alloyed with ten of the most common impurity elements. The X-axis shows the volume fraction of all phases, while the Y-axis represents temperature (°C). Each colored curve corresponds to the phase fraction of one of the stable or metastable phases in the system, depending on the temperature. This allows for tracing the sequence of phase transformations upon cooling and quantifying the phase distribution.

The polythermal sections demonstrate fundamental differences in phase formation mechanisms depending on the chemical composition: from matrix α-Al systems to structures saturated with intermetallic phases.

For the Al_{98-ni}–Fe_1–Si_1–nX_i alloy, the initial melting point (liquidus) is ~660 °C—above which only the liquid phase exists. Upon temperature reduction, the first phase to crystallize is FCC_A1, a solid solution of alloying elements in aluminum with an FCC lattice. The volume fraction of solid aluminum remains in the range of ≈70–80% upon further cooling down to room temperature. Thus, the aluminum matrix is retained as the primary phase, while intermetallics play a secondary role.

Below ~600 °C, a wide range of secondary phases emerges. The alloy exhibits the presence of $AL_{13}Fe_4$ (θ), $AL_{15}Si_2M_4$ (where M = Mn, Cr, Ti), $AL_5Fe_2Si_2$, and $AL_{18}Mg_3Ti_2$, primarily forming below 600 °C. Additionally, phases such as AL_7Cu_4Ni, AL_2Cu_C16, ALZr_D023, FEB_B27 (ZrSi), T_PHASE ($Al_2Mg_3Zn_3$), S_PHASE (Al_2CuMg), and Laves phases (C14_LAVES) are detected, indicating complex alloying, enrichment of the structure with various intermetallic inclusions, and complex multiphase eutectic crystallization. These phases form in small volume fractions and within narrow temperature intervals.

Of particular note is the formation of a cubic αC phase involving manganese and chromium atoms—an effect not observed in alloys individually alloyed with Mn or Cr. Overall, the phase structure indicates heterogeneity, but the high volume fraction of ductile aluminum matrix is preserved. This ensures good workability and impact toughness, although local strengthening and embrittlement may occur in areas with concentrated intermetallics.

For the Al_{60-ni}–Fe_{33}–Si_7–nX_i alloy, an intermetallic composition is considered, characterized by a significantly lower aluminum content (60 wt.%) and elevated Fe and Si content. The liquidus temperature of the intermetallic alloy is substantially higher, reaching ~1100 °C, corresponding to the presence of a large fraction of high-melting phases.

The first crystallizing phase is $AL_{13}Fe_4$ (a binary intermetallic compound), which constitutes a major part of the solid phase between 1000 and 700 °C. In contrast to the commercial alloy, the FCC phase is virtually absent, indicating replacement of the aluminum matrix with rigid intermetallic formations.

At ~400–800 °C, the dominant phases are Al_7Cu_4Ni, FeSi_B20, BCC_B2, the θ-phase, and a family of AlFeSi_T phases (τ_3, τ_7, τ_8, τ_9). These phases result from Fe–Si interactions within the aluminum matrix and play a key role in forming the intermetallic framework. The presence of FeSi_B20 further confirms the Fe-rich nature of the structure. The θ-phase occupies up to 70% of the volume in the 400–700 °C range, indicating high material hardness and brittleness.

Below 400 °C, numerous minor-volume phases appear, including Laves phases (C14, C15, C36), $AL_{13}Fe_{4\#2}$, $AL_5Mn_6Si_7$, and other complex structures. Of note is the presence of rigid Laves-type intermetallics, pointing to stabilizing elements within the structure. The $AL_{13}Fe_{4\#2}$ phase differs from the θ-phase by a higher content of dissolved elements, including silicon, and partial substitution of Fe atoms.

Table 2 – Effect of alloying on phase transformation temperatures

Alloying element	Indicator									
	T_L^{com}	T_L^{int}	T_S^{com}	T_S^{int}	$T_{st}^{com}\alpha$	$T_{st}^{int}\alpha$	$T_{end}^{com}\alpha$	$T_{end}^{int}\alpha$	$T_{st}^{com}\beta$	$T_{st}^{int}\beta$
-	650	1070	612	629	629	769	586	446	612	446
Cu	640	1070	546	665	600	665	572	447	572	447
Mg	630	1060	585	600	-	720	-	446	-	446
Mn	649	1070	626	680	-	762	-	450	-	462
Cr	695	1070	615	629	-	769	-	446	550	446
Ni	649	1070	606	641	621	753	606	446	606	446
Zn	641	1100	596	399	616	650	597	462	598	462
Ti	667	1070	612	630	629	767	585	446	611	446
V	652	1070	612	629	629	767	585	446	611	446
Zr	740	1070	615	629	629	769	578	446	603	446
Be	652	1070	611	620	629	768	586	446	611	446

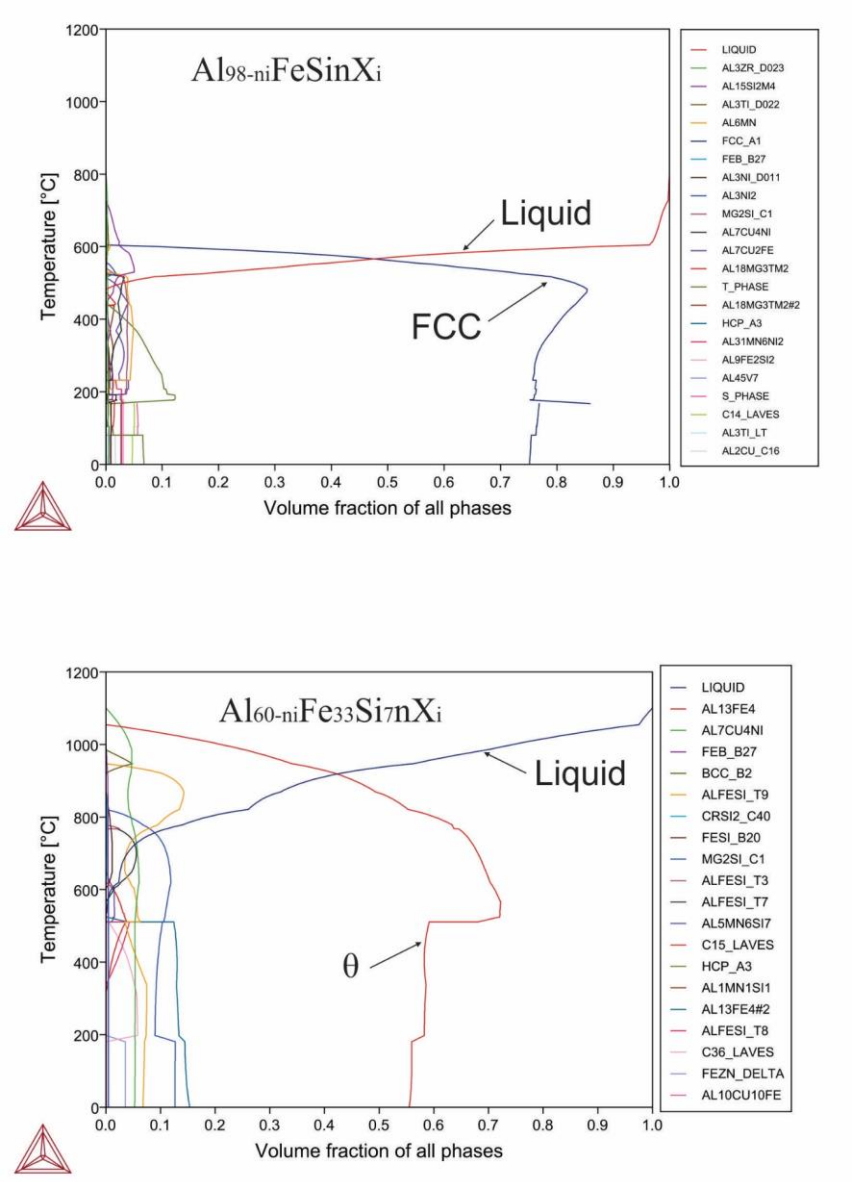

Figure 1 - Polythermal cutting of aluminum alloys with synergistic alloying

This system is dominated by intermetallic compounds across the entire temperature range, with almost complete absence of α-Al (FCC) and a wide stability range of the θ-phase. This indicates high stiffness and thermal stability but low plasticity. Such a structure is suitable for heat-resistant and wear-resistant materials but not for wrought (deformable) alloys.

When all investigated alloying elements are simultaneously introduced into the intermetallic alloy, the aluminum concentration decreases to 43.77 at.%, which is significantly lower than that in the commercial alloy (81.77 at.%). This reduction in the aluminum base has a critical impact on the phase composition: in none of the systems is the formation of the α-phase observed.

Moreover, in the intermetallic alloy, even the cubic α-modifications stabilized by Cr and Mn additions are absent. No formation of the low-temperature β-phase is observed either. In the commercial alloy, the β-phase originates from the cubic α-phase as a product of phase transformation, but the transition temperature is anomalously low—around 200 °C—confirming its metastable nature. The total volume fraction of all secondary phases is approximately 25%.

Upon the addition of magnesium under complex alloying conditions, the formation of Laves-type intermetallic phases is observed. In the commercial alloy, the hexagonal phase $MgZn_2$ appears. In the intermetallic system, two different modifications are formed: cubic $MgCu_2$ and hexagonal $MgNi_2$, indicating magnesium's active participation in the formation of highly stable structures.

Despite the overall reduction in aluminum content, no significant increase in mutual interaction between the alloying elements is observed in the intermetallic alloy. In the commercial variant, nearly all compounds form with aluminum, with the exception of Laves phases. In contrast, the intermetallic alloy shows a tendency toward the formation of intermetallics between the alloying elements and iron.

In the commercial alloy, the synergistic effect is particularly evident in the formation of ternary intermetallic compounds involving impurity atoms. Notable phases include $Al_2Mg_3Zn_3$, Al_2CuMg, and $Al_{18}Mg_3(Cr, Mn, Ti)_2$, reflecting complex interactions between the base and alloying components.

Under conditions of limited aluminum availability in the intermetallic system, new phases form, such as Al_7Cu_4Ni, along with compounds based on the Al–Fe–Si system. This indicates a shift in chemical equilibrium toward more complex intermetallic compounds involving copper, iron, and nickel.

It is important to emphasize the high chemical reactivity of Cu, Mg, and Ni, which promotes the formation of stable binary and ternary phases. However, it is the available aluminum content that ultimately determines the final phase composition and the direction of interactions. The total fraction of all phases, excluding the main matrix composed of θ and θ′-modifications, reaches 30%.

In the intermetallic alloy, the earliest crystallizing phase is Al_7Cu_4Ni, followed by the formation of the θ-phase upon undercooling by approximately 40 °C. In the temperature range of 500–600 °C, the θ-phase content exceeds 70%. At around 510 °C, coexistence of the θ-phase with impurities in the structure is observed, indicating the formation of its substitutional modifications. As a result, at room temperature, the material consists predominantly (≈70%) of the θ-phase with a variable elemental composition. The solidus temperature is 485 °C for the commercial alloy and 533 °C for the intermetallic alloy.

Interestingly, many elements that typically tend to form silicides lose the ability to independently form such phases under complex alloying conditions and remain in dissolved form. Exceptions include: Cr-silicide (observed only in the intermetallic system), as well as silicides of Mg and Zr. Beryllium appears as a separate phase, along with copper intermetallics and a Fe–Zn compound.

Key differences between the commercial and intermetallic alloys based on analysis of polythermal sections:

The commercial alloy retains the FCC_A1-type aluminum matrix, ensuring high ductility and good processability. Intermetallic phases are secondary and do not dominate the overall structure.

In the intermetallic alloy, α-Al is absent, and the matrix is formed by $AL_{13}Fe_4$ and ALFeSi (τ) intermetallics, which crystallize directly from the melt. This imparts increased hardness and heat resistance, but reduces formability.

The commercial alloy exhibits a more complex phase structure with numerous local phases, including compounds of Cu, V, Zr, and other elements, while the intermetallic alloy's structure is simplified, focused on forming a highly stable framework.

The onset temperature of crystallization for the intermetallic alloy (~850 °C) is significantly higher

than that of the commercial alloy (~650 °C), indicating direct formation of the intermetallic θ-phase from the melt.

The presence of Laves phases in the intermetallic system enhances resistance to thermal and chemical exposure, but also increases brittleness.

The practical significance of the obtained results lies in their potential to predict the performance characteristics of real-world alloys. Moreover, the findings of this study may serve as a fundamental basis for selecting alloying strategies in the design of new aluminum-based alloys, including intermetallic systems, particularly in the context of synergistic alloying.

The temperature-dependent phase formation behavior under the influence of alloying elements enables control over the thermal stability of alloy properties and facilitates the development of optimized heat treatment regimes aimed at achieving target microstructures and performance characteristics.

To validate the obtained results, hardness tests were conducted on both commercial and alloyed intermetallic aluminum systems. For instance, in the intermetallic alloy with the nominal composition $AlFe_{33.59}Si_{5.18}Mn_{1.574}Ni_{0.19}$ (wt.%), the microhardness of the intermetallic phases reached 756 HV1. In contrast, the alloy with the composition $AlFe_{29.5}Si_{3.72}Mn_{0.18}Ni_{0.02}Cu_{0.02}$ (wt.%) exhibited a significantly lower microhardness of 450 HV1 for its intermetallic phases.

This difference in microhardness is primarily attributed to the presence of manganese, which promotes the coagulation of intermetallic phases and is capable of dissolving into the binary intermetallic θ-phase through partial substitution of iron atoms, thereby stabilizing the θ_2-phase.

Meanwhile, in the commercial alloy, the microstructure is dominated by a FCC aluminum solid solution with a typical microhardness in the range of 130–135 HV1.

Conclusions

Using thermodynamic modeling methods, phase diagrams were obtained for aluminum alloys containing 1 wt.% Fe and 1 wt.% Si, as well as for the intermetallic Al–Fe–Si system alloyed with 10 industrially significant elements. The influence trends of each alloying addition on thermal characteristics and phase formation mechanisms were established.

It was found that increasing the volume fraction of the α-phase is not achievable through the addition of any of the investigated elements, regardless of their nature or concentration. The primary effect of alloying additions is manifested through the shift of phase transformation temperatures and the formation of alternative stable phases.

It was demonstrated that copper, nickel, and magnesium tend to form stable binary and ternary compounds. Their combined addition leads to the formation of Laves-type phases. In the intermetallic alloy, an increase in the amount of θ-phase was observed in each case, including modifications of its stoichiometry due to partial dissolution of impurities.

The obtained data enable targeted alloying strategies aimed at optimizing alloy properties, including the use of secondary (recycled) aluminum. These results hold practical value for the development of new composite materials and for interpreting the microstructure of industrial aluminum alloys.

Conflict of interest. On behalf of all authors, the corresponding author declares that there is no conflict of interest.

Acknowledgements. This research is funded by the Science Committee of the Ministry of Science and Higher Education of the Republic of Kazakhstan. Grant No. AP19675471 “Development of technology for the synthesis of composite ceramic materials of the AlxFeySi system using the additive method”

Cite this article as: Andreyachshenko VA. Effect of Complex Alloying on the Phase Composition and Thermal Characteristics of Al–Fe–Si Aluminum Alloys. Kompleksnoe Ispolzovanie Mineralnogo Syra = Complex Use of Mineral Resources. 2027; 340(1):117-126. https://doi.org/10.31643/2027/6445.12

Al-Fe-Si жүйесінің алюминий қорытпаларының фазалық құрамы мен температуралық сипаттамаларына кешенді легирлеудің әсері

Андреященко В.А.

Әбілқас Сағынов атындағы Қарағанды техникалық университеті, Қарағанды, Қазақстан

Мақала келді: *8 қыркүйек 2025*
Сараптамадан өтті: *26 қыркүйек 2025*
Қабылданды: *3 қазан 2025*

ТҮЙІНДЕМЕ

Жұмыста Thermo-Calc бағдарламалық пакетін қолдану арқылы термодинамикалық модельдеу арқылы жүзеге асырылатын, он өнеркәсіптік маңызы бар легірлеуші элементтердің (Mg, Cu, Ni, Mn, Cr, Zn, Ti, Zr, V, Be) қосылған Al–Fe–Si жүйесінің алюминий қорытпаларындағы фазалардың түзілуінің жан-жақты талдауы берілген. Жеке және синергиялық легирленген коммерциялық қорытпадағы (Al98–Fe1–Si1) және интерметалдық қорытпадағы (Al60–Fe33–Si7) фазаның түзілуі зерттеліп, салыстырылады. Қорытпалардың температуралық сипаттамаларын (сұйықтық, солидус, α- және β-түрлендірулер) және фазалық құрамдастарды салыстыру кең температуралық диапазонда (0–1200°C) жүргізіледі. Легірлеуші элементтер қорытпалардың фазалық тұрақтылығына және құрылымына көп бағытты әсер ететіні анықталды, интерметалдық жүйелер жоғары термиялық тұрақтылықты көрсетеді. Негізгі фазаның түзілуіне, сонымен қатар синергетикалық легирлеудің фазалық тепе-теңдікке әсері мен жаңа тұрақты қосылыстардың түзілу мүмкіндігіне ерекше көңіл бөлінеді. Алынған нәтижелер көліктік және машина жасау үшін белгіленген қасиеттері бар материалдарды жасау үшін қайталама алюминийді қолдануды қоса алғанда, алюминий қорытпаларының легірленуін мақсатты бақылауға мүмкіндік береді.

Түйін сөздер: Al-Fe-Si, ThermoCalc бағдарламалық қамтамасыз ету, интерметалдық фазалар, фазалық тепе-теңдік, синергиялық легирлеу.

Андреященко Виолетта Александровна

Автор туралы ақпарат:
PhD, қауымдастырылған профессор, Минералдық шикізат қазбаларды кешенді игеру инженерлік бейіндегі сынақ зертханасының басшысы, Әбілқас Сағынов атындағы Қарағанды техникалық университеті, Н. Назарбаев даңғылы, 56, Қарағанды, Қазақстан. Email: v.andreyachshenko@ktu.edu.kz; ORCID ID: https://orcid.org/0000-0001-6933-8163

Влияние комплексного легирования на фазовый состав и температурные характеристики алюминиевых сплавов системы Al–Fe–Si

Андреященко В.А.

Карагандинский технический университет имени Абылкаса Сагинова, Караганда, Казахстан

Поступила: *8 сентября 2025*
Рецензирование: *26 сентября 2025*
Принята в печать: *3 октября 2025*

АННОТАЦИЯ

В работе представлен комплексный анализ фазообразования в алюминиевых сплавах системы Al–Fe–Si с добавлением десяти промышленно значимых легирующих элементов (Mg, Cu, Ni, Mn, Cr, Zn, Ti, Zr, V, Be), проведённый методом термодинамического моделирования с использованием программного комплекса Thermo-Calc. Исследовано и сопоставлено фазообразование в коммерческом сплаве (Al98–Fe1–Si1) и в интерметаллидном сплаве (Al60–Fe33–Si7) при индивидуальном и синергетическом легировании. Проведено сравнение температурных характеристик (ликвидуса, солидуса, α- и β-превращений) и фазовых составляющих сплавов в широком температурном диапазоне (0–1200 °C). Установлено, что легирующие элементы оказывают разнонаправленное влияние на фазовую стабильность и структуру сплавов, причём интерметаллические системы демонстрируют более высокую термостабильность. Особое внимание уделено формированию фазы основы, а также влиянию синергетического легирования на фазовое равновесие и возможность образования новых устойчивых соединений. Полученные результаты позволяют целенаправленно управлять легированием алюминиевых сплавов, в том числе с использованием вторичного алюминия, для создания материалов с заданными свойствами для транспортного и машиностроительного применения.

Ключевые слова: Al-Fe-Si, программное обеспечение ThermoCalc, интерметаллидные фазы, фазовое равновесие, синергетическое легирование.

Андреященко Виолетта Александровна

Информация об авторе:
PhD, ассоциированный профессор, руководитель испытательной лаборатории инженерного профиля Комплексное освоение ресурсов минерального сырья, Карагандинский технический университет имени Абылкаса Сагинова, пр. Н. Назарбаева, 56, Караганда, Казахстан. Email: v.andreyachshenko@ktu.edu.kz; ORCID ID: https://orcid.org/0000-0001-6933-8163

References

[1] Padalko AG, Pyrov MS, Karelin RD, Yusupov VS, Talanova GV. Barothermal Treatment, Cold Plastic Deformation, Microstructure and Properties of Binary Silumin Al–8 at % Si. Russ. Metall. 2021, 1155–1164. https://doi.org/10.1134/S0036029521090123

[2] Becker H, Thum A, Distl B, Kriegel MJ, Leineweber A. Effect of melt conditioning on removal of Fe from secondary Al-Si alloys containing Mg, Mn, and Cr. Metallurgical and Materials Transactions A. 2018; 49:6375-6389. https://doi.org/10.1007/s11661-018-4930-7

[3] Arbeiter J, Vončina M, Volšak D, Medved J. Evolution of Fe-based intermetallic phases during homogenization of Al–Fe hypoeutectic alloy. Journal of Thermal Analysis and Calorimetry. 2020; 142(5):1693-1699. https://doi.org/10.1007/s10973-020-10161-8

[4] Lee JY, Heo H, Kang N, Kang CY. Microstructural Evolution of Reaction Layer of 1.5 GPa Boron Steel Hot-Dipped in Al-7wt% Ni-6wt% Si Alloy. Metals. 2018; 8(12):1069. https://doi.org/10.3390/met8121069

[5] Khan MH, Das A, Li Z, Kotadia HR. Effects of Fe, Mn, chemical grain refinement and cooling rate on the evolution of Fe intermetallics in a model 6082 Al-alloy. Intermetallics. 2021; 132:107132. https://doi.org/10.1016/j.intermet.2021.107132

[6] Kocich R, Kunčická L. Optimizing Structure and Properties of Al/Cu Laminated Conductors via Severe Shear Strain. J. Alloys Compd. 2023; 953:170124. https://doi.org/10.1016/j.jallcom.2023.170124

[7] Wang C, Yu F, Zhao D, Zhao X, Zuo L. Microstructure Evolution of Al-15% Si Alloy during Hot Rolling. Philos. Mag. Lett. 2018; 98:456–463. https://doi.org/10.1080/09500839.2019.1573332

[8] Cepeda-Jiménez CM, García-Infanta JM, Zhilyaev AP, Ruano OA, Carreño F. Influence of the Supersaturated Silicon Solid Solution Concentration on the Effectiveness of Severe Plastic Deformation Processing in Al–7wt.% Si Casting Alloy. Mater. Sci. Eng. A. 2011; 528:7938–7947. https://doi.org/10.1016/j.msea.2011.07.016

[9] Andreyachshenko VA. Finite element simulation (FES) of the fullering in device with movable elements. Metalurgija. 2016; 55(4):829-831.

[10] Naizabekov AB, Andreyachshenko VA, Kliber J, Kocich R. Tool for realization several plastic deformation. In: 22th International Conference on Metallurgy and Materials METAL; Brno, Czech Republic. 2013, 317-321.

[11] Belov NA, Alabin AN, Matveeva IA, Eskin DG. Effect of Zr additions and annealing temperature on electrical conductivity and hardness of hot rolled Al sheets. Trans. Nonferrous Met. Soc. China. 2015; 25:2817-2826. https://doi.org/10.1016/S1003-6326(15)63907-3

[12] Jiang H, Li S, Zhang L, He J, Zheng Q, Song Y, et al. The influence of rare earth element lanthanum on the microstructures and properties of as-cast 8176 (Al-0.5 Fe) aluminum alloy. Journal of Alloys and Compounds. 2021; 859:157804. https://doi.org/10.1016/j.jallcom.2020.157804

[13] Chen Y, Xiao C, Zhu S, Li Z, Yang W, Zhao F, et al. Microstructure characterization and mechanical properties of crack-free Al-Cu-Mg-Y alloy fabricated by laser powder bed fusion. Additive Manufacturing. 2022; 58:103006. https://doi.org/10.1016/j.addma.2022.103006

[14] Zhu H, Li J. Advancements in corrosion protection for aerospace aluminum alloys through surface treatment. International Journal of Electrochemical Science. 2024; 19(2):100487. https://doi.org/10.1016/j.ijoes.2024.100487

[15] Fan T, Ruan Z, Zhong F, Xie C, Li X, Chen D, et al. Nucleation and growth of L12-Al3RE particles in aluminum alloys: A first-principles study. Journal of Rare Earths. 2023; 41(7):1116-1126. https://doi.org/10.1016/j.jre.2022.05.018

[16] Wang T, Chen C, Ma J, Wei S, Xiong M, et al. Influence of Si on the intermetallic compound formation in the hot-dipped aluminide medium carbon steel. Materials Characterization. 2023; 197:112700. https://doi.org/10.1016/j.matchar.2023.112700

[17] Sersour Z, Amirouche L. Effect of Alloying Additions and High Temperature T5-Treatment on the Microstructural Behavior of Al–Si-Based Eutectic and Hypo-Eutectic Alloys. Int. J. Met. 2022; 16:1276–1291. https://doi.org/10.1007/s40962-021-00676-7

[18] Alemdag Y, Karabiyik S, Mikhaylovskaya AV. Kishchik, M.S.; Purcek, G. Effect of Multi-Directional Hot Forging Process on the Microstructure and Mechanical Properties of Al–Si Based Alloy Containing High Amount of Zn and Cu. Mater. Sci. Eng. A. 2021; 803:140709. https://doi.org/10.1016/j.msea.2020.140709

[19] Tsaknopoulos K, Walde C, Tsaknopoulos D, Cote DL. Evolution of Fe-Rich Phases in Thermally Processed Aluminum 6061 Powders for AM Applications. Materials. 2022; 15(17):5853. https://doi.org/10.3390/ma15175853

[20] Zhang X, Wang D, Li X, Zhang H, Nagaumi H. Understanding crystal structure and morphology evolution of Fe, Mn, Cr-containing phases in Al-Si cast alloy. Intermetallics. 2021; 131:107103. https://doi.org/10.1016/j.intermet.2021.107103

[21] Fang CM, Que ZP, Fan Z. Crystal chemistry and electronic structure of the β-AlFeSi phase from first-principles. Journal of Solid State Chemistry. 2021; 299:122199. https://doi.org/10.1016/j.jssc.2021.122199

[22] Que Z, Fang C, Mendis CL, Wang Y, Fan Z. Effects of Si solution in θ-Al13Fe4 on phase transformation between Fe-containing intermetallic compounds in Al alloys. Journal of Alloys and Compounds. 2023; 932:167587. https://doi.org/10.1016/j.jallcom.2022.167587

[23] Wang M, Guo Y, Wang H, Zhao S. Characterization of Refining the Morphology of Al–Fe–Si in A380 Aluminum Alloy Due to Ca Addition. Processes. 2022; 10(4):672. https://doi.org/10.3390/pr10040672

[24] Xia X, Chen M, Lu Y-J, Fan F, Zhu C, Huang J, Deng T, Zhu S. Microstructure and Mechanical Properties of Isothermal Multi-Axial Forging Formed AZ61 Mg Alloy. Trans. Nonferrous Met. Soc. China. 2013; 23:3186–3192. https://doi.org/10.1016/S1003-6326(13)62851-4

[25] Kocich R. Effects of Twist Channel Angular Pressing on Structure and Properties of Bimetallic Al/Cu Clad Composites. Mater. Des. 2020; 196:109255. https://doi.org/10.1016/j.matdes.2020.109255

[26] Asadikiya M, Yang S, Zhang Y, Lemay C, Apelian D, Zhong Y. A Review of the Design of High-Entropy Aluminum Alloys: A Pathway for Novel Al Alloys. J. Mater. Sci. 2021. 56: 12093–12110. https://doi.org/10.1007/s10853-021-06042-6

[27] Aranda VA, Figueroa IA, González G, García-Hinojosa JA, Alfonso I. Study of the microstructure and mechanical properties of Al-Si-Fe with additions of chromium by suction casting. Journal of Alloys and Compounds. 2021; 853:157155. https://doi.org/10.1016/j.jallcom.2020.157155

[28] Pang N, Shi Z, Wang C, Li N, Lin Y. Influence of Cr, Mn, Co and Ni Addition on Crystallization Behavior of Al13Fe4 Phase in Al-5Fe Alloys Based on ThermoDynamic Calculations. Materials. 2021; 14(4):768. https://doi.org/10.3390/ma14040768

[29] Hemachandra M, Mamedipaka R, Kumar A, Thapliyal S. Investigating the Microstructure and Mechanical Behavior of Optimized Eutectic Al Si Alloy Developed by Direct Energy Deposition. J. Manuf. Process. 2024; 110:398–411. https://doi.org/10.1016/j.jmapro.2024.01.002

[30] Cheng W, Liu CY, Ge ZJ. Optimizing the Mechanical Properties of Al–Si Alloys through Friction Stir Processing and Rolling. Mater. Sci. Eng. A. 2021; 804:140786. https://doi.org/10.1016/j.msea.2021.140786

МАЗМҰНЫ
СОДЕРЖАНИЕ
CONTENTS

ENGINEERING AND TECHNOLOGY

EARTH SCIENCES

METALLURGY

Техникалық редакторлар:
Г.К. Қасымова, Н.М.Айтжанова, Т.И. Қожахметов

Компьютердегі макет:
Г.К. Қасымова

Дизайнер:
Г.К. Қасымова, Н.М.Айтжанова

“Металлургия және кен байыту институты” АҚ
050010, Қазақстан Республикасы, Алматы қаласы, Шевченко к-сі, 29/133

Жариялауға 03.10.2025 жылы қол қойылды

Технические редакторы:
Г.К. Касымова, Н.М. Айтжанова, Т.И. Кожахметов

Верстка на компьютере:
Г.К. Касымова

Дизайнер:
Г.К. Касымова, Н.М.Айтжанова

АО “Институт металлургии и обогащения”
050010, г. Алматы, Республика Казахстан. ул. Шевченко, 29/133

Подписано в печать 03.10.2025 г.

Technical editors:
G.K. Kassymova, N.M. Aitzhanova, T.I. Kozhakhmetov

The layout on a computer:
G.K. Kassymova

Designer:
G.K. Kassymova, N.M. Aitzhanova

“Institute of Metallurgy and Ore Beneficiation” JSC
050010, Almaty city, the Republic of Kazakhstan. Shevchenko str., 29/133

Signed for publication on 03.10.2025